Joint European Research Infrastructure network for Coastal Observatory – Novel European eXpertise for coastal observaTories - **JERICO-NEXT**	
Deliverable title	JRAP Synthesis and contribution to the strategy for the future
Work Package Title	WP 4
Deliverable number	D4.5
Description	This document reports on the work achieved within the six Joint research Activity Projects achieved within the WP4 of JERICO-NEXT. It also present the experience gained during these projects and their contributions to the definition of a future strategy for European Coastal Observing.
Lead beneficiary	CNRS
Lead Authors	Antoine Grémare, Ingrid Puillat, Bengt Karlson, Felipe Artigas, Luca Nizzetto, Anna Rubio, Lauri Laakso, Baptiste Mourre
Contributors	All JRAPs' participants
Submitted by	Antoine Grémare
Revision number	V5
Revision Date	22/09/2019
Security	Consortium Only (Public when final)

History			
Revision	**Date**	**Modification**	**Author**
V1	23/04/2019	Table of Contents	Grémare
V2	19/07/2019	JRAPs' contributions (first draft)	JRAP leaders
V3	25/08/2019	revision of JRAPs' contributions	JRAP leaders
V4	17/09/2019	Full text (first draft)	Grémare
V5	22/09/2019	Full text (final revision)	JRAP leaders

Approvals				
	Name	**Organisation**	**Date**	**Visa**
Coordinator	Patrick FARCY	IFREMER	30/09/2019	PF
WP Leader	Ingrid Puillat	IFREMER	24/09/2019	IP

Table of Contents

Nota

In the following pages, the European Coastal Research Infrastructure will be named JERICO-RI, the project funded in the framework of the FP7 JERICO-FP7 (2011-2015) and the one funded within H2020 JERICO-NEXT (2015-2019)

1. Executive summary

Six Joined Research activity Projects (JRAPS have been achieved within JERICO-NEXT. These projects have been set up to tackle some of the complex technical and scientifical issues associated with the implementation of Coastal Ocean Observing over a wide range of environmental conditions and spatiotemporal scales. The topics of these projects have been defined in relation with some of the Marine Strategy Framework Directive:

- **JRAP 1**: Biodiversity of plankton, harmful algal blooms and eutrophication,
- **JRAP 2**: Monitoring changes in microbenthic biodiversity, assessing potential environmental controls and functional consequences
- **JRAP 3**: Occurrence of contaminants in Northern coastal waters and biological responses
- **JRAP 4**: 4D characterization of trans-boundary hydrography and transport
- **JRAP 5**: Coastal carbon fluxes and biogeochemical cycling
- **JRAP 6**: Operational oceanography and forecasting

In its first part, this document reports the work led in the framework of the JRAP activities during the whole JERICO-NEXT project. Itn its second part, it also shows how the experience gained from JRAP activities contributed to the elaboration of the JERICO-RI science strategy, which is presented in JERICO-NEXT **D1.2**.

JRAP 1 explored different automated or semi-automated innovative approaches for improving the temporal and spatial resolution of phytoplankton observations based on different plarforms: research cruises, fixed platforms, moorings and/or ships of opportunity. Based on seven different research actions, it clearly showed how the combination of these techniques allowed to reach new insights into the functional diversity and photosynthetic status of phytoplankton communities in different environmental and hydrological conditions (i.e., from oligotrophic and mesotrophic to eutrophic conditions, and from brackish to saline systems). JRAP 1 nevertheless also identified gaps and underlined the necessity in continuing technological developments to improve the resolution and understanding of phytoplankton dynamics, in connection with the requirements of environmental managing at a regional, national and international level.

JRAP 2 tackled three main questions: (1) Do alternative techniques provide sound surrogates for the classical analysis of benthic macrofauna composition? (2) Irrespective of the nature of the disturbance, does the relationship between disturbance intensity and benthic diversity follow the same pattern? and (3) What are the functional consequences of a benthic macrofauna diversity loss on ecosystem functioning? JRAP 2 supported the ability of surface and sediment profile imaging and 16S rRNA metabarcoding of benthic microfauna in detecting the impact of disturbance gradients on benhic diversity. JRAP 2 also showed that the effects of disturbance on benthic diversity are not necessarily gradual and may result from non *a priori* identified disturbance sources. The functional consequences of biodiversity loss were assessed in only one of the four actions achieved by JRAP 2. Results showed no clear effect of benthic macrofauna species richness on sedimented organic matter remineralization.

JRAP 3 tackled four main questions: (1) Can existing integrative sampling methods (i.e. passive samplers) be effectively used in combination with existing CRI to obtain reliable data on marine chemical pollution? (2) Can CRI be used to support exploratory monitoring of marine pollution to identify new chemical contaminants? (3) Can the drivers of spatial distribution of chemical contaminants in coastal waters be assessed using data from infrastructure sensors and spatial analyses? and (4) Is there a co-variance between contaminant signals and biological responses? JRAP 3 results suggested that passive samplers were able to report expected gradients of variability in measured concentrations and could now be routinely used to address monitoring of chemical pollution in coastal areas. They also confirmed the benefit of using FerryBox based sampling to carry out monitoring of contaminants in coastal water. JRAP 3 reported no simple overall correlation between the levels of detected chemicals and the distance of the sampling sites to the coast. JRAP 3, however, developed a specific spatial analysis allowing for correlating an index of anthropic impact with measured contaminant concentrations. JRAP 3 results at last showed the concordance between selected microbial molecular markers of hydrocarbon pollution and the sum of 29 Persistant Aromatic Hydrocarbons, which highlighted the possibility of using chemical and molecular biomarkers to retrieve information of pollution influence on microbial community assemblages.

JRAP 4 tackled three main questions: (1) Can we use JERICO infrastructures to study the 4D shelf/slope circulation and transports and their time variability? (2) What is the impact of the ocean transport on the distribution of floating and dissolved matter? and (3) How can we maximize the impact of the JERICO-RI for the assessment of coastal transport? JRAP 4 showed the benefit of new high-resolution observations through new deployments (including HF radars and innovating moorings) for the upgrading of current coastal observatories. It successfully tested several HF radar data advanced processing and analysing procedures. JRAP 4 successfully performed several *ad-hoc* experiments to quantify the impact of ocean transport on the distribution of biological quantities and pollution. JRAP 4 finally underlined the interest of Observing System Simulation Experiments to optimize existing coastal ocean observing network and to better design future observatories.

JRAP 5 tackled three main questions: (1) What kind of role European Coastal Ocean and Marginal Seas have on the marine carbon system? (2) What is the role of biological activity on marine carbon uptake or release? and (3) How should the integrated C-cycle monitoring be organized in coastal regions? JRAP 5 showed the high regional variability and regional differences in pCO_2 dynamics between areas, which could either constiture a carbon sinks or sources. Based on a limited number of stations and VOS routes, JRAP 5 concluded that biological activity had a significant role on the marine carbon balance. At last, JRAP 5 stressed the need for better coordination between coastal carbonate system observations, with frequent instrument comparisons.

JRAP 6 tackled four main questions through the implementation of coastal model assessment studies and observing system experiments in different areas of European coastal waters: (1) How accurate are our ocean models in coastal areas? (2) How could we improve these models? (3) What is the impact of coastal observations on the model performance after data assimilation? and (4) What would be the impact of potentially future additional observations? Overall, models were found to be able to properly reproduce the spatio-temporal scales of sea surface current variability. However, JRAP 6 also identified gaps in the performances of current hydrodynamical models. JRAP 6 evaluated the sensitivity of model results to the horizontal resolution, model parameters, surface forcing or to the treatment of open boundary conditions, providing solutions to improve them. Observing System Experiments allowed evaluating the positive impact of the assimilation of glider, FerryBox, fixed moorings and HF radar observations on model performances. Observing System Simulation Experiments were also performed to evaluate the impact of future observing systems. Overall, and considering the specificities of coastal situations in European waters, Overall, JRAP6 was able to demonstrate the usefulness of JERICO-NEXT coastal observations in distinct environments, leading to an improvement of the understanding and of the performance of high-resolution numerical models implemented in the coastal European ocean.

Through the gains of experience generated within its six JRAPs, WP4 contributed to the five pillars of the JERICO-RI scientific strategy, namely:

- **Pillar 1:** Developping innovative technologies for Coastal Ocean Observing and modelling
- **Pillar 2:** Enhancing integrated Coastal Ocean Monitoring
- **Pillar 3:** Interfacing with other ocean observing initiatives operating at different spatiotemporal scales
- **Pillar 4:** Fostering societal impact for a larger community of stakeholders
- **Pillar 5:** Establishing observing objectives, strategy and implementation at the regional level

Pillar 1: All JRAPs clearly confirmed that the development of innovative technologies constitutes a major key point for the future of Coastal Ocean Observing. They more specifically showed that Technology Readiness Levels differ between disciplines and recommended to carry out specific developments for better balancing the disciplinary scope of (semi)automated observations. JRAPs also underlined the necessity of developing multidisciplinary platforms to enhance the emergence of holistic observation. They stressed the importance of modelling in addressing the spatial heterogeneity and temporal dynamics of physical processes taking place in the Coastal Ocean and the strong interest in putting a focus on the development of biological/biogeochemical models and on their coupling with physical models.

Pillar 2: JRAPs identified the harmonization of observations as a key issue for Coastal Ocean Observing. They however also acknowledged limitations and plead for for the definition of an optimal threshold between

homogenization and the consideration of regional specificities while designing a future European Coastal Ocean Observing infrastructure. They more specifically pinpointed that such a threshold is likely to differ according to the nature of tackled environmental issues. The implementation of multidisciplinarity within the different JRAPs was overall considered as unsatisfactory. Two ways forward were identified: (1) developing new multidisciplinary platforms allowing for high frequency data acquisition, and (2) *a priori* optimizing monitoring strategies. It was also stressed that a threshold should be reached between an *a priori* optimization (which is necessary based on current knowledge) and a certain degree of ability to detect the impact of non-foreseen changes/processes when designing future monitoring strategies.

Pillar 3: All JRAPs involved tight interactions with other observing initiatives consisting in observing infrastructures and/or research projects. The interactions with other observing initiatives proved satisfactory. They were, nevertheless, facilitated by the small spatiotemporal scales addressed by most JRAPs and it is anticipated that future interactions operating at larger scales would benefit a strong coordination of monitoring strategies. The interactions with research projects sometimes proved odd and should be defined over a long-term perspective as well.

Pillar 4: Addressed topics clearly varied both within and between JRAPs. This heterogeneity refers both to the nature (i.e., fundamental vs applied) and the spatial scale (i.e., from the local to the pan-european level) of addressed issues. Overall, it was stressed that such a diversity should clearly be taken in consideration while designing a future pan-European Coastal Ocean Observing infrastructure and suggested that stakeholders should be deeper involved in the definition of the products derived from Coastal Ocean Observing so that they become better suited in tackling their concerns.

Pillar 5: Most JRAPs were implemented at a sub regional spatial scale and their designs mostly consisted of complementary actions achieved at different sites representative of a large set of environmental conditions and issues. This structuration showed clear limitation relative to the implementation of the first four pillars of the JERICO-RI strategies. It was therefore suggested that the systems and tools developed within JERICO-NEXT could become part of regional systems and most JRAPs therefore recommanded the design and implementation of a future Coastal Ocean Observing insfrastructure as a network of Augmented Regional Coastal Observatories.

2. Introduction

Within the WP4 "Valorisation through apllied joint research" of JERICO-NEXT, the JERICO-RI community has set up six pilot Joined Research Activity Projects to tackle some of the complex technical and scientifical issues associated with the implementation of Coastal Ocean Observing over a wide range of environmental conditions and spatiotemporal scales. The topics of these projects are as follows:

- **JRAP 1**: Biodiversity of plankton, harmful algal blooms and eutrophication,
- **JRAP 2**: Monitoring changes in microbenthic biodiversity, assessing potential environmental controls a and functional consequences
- **JRAP 3**: Occurrence of contaminants in Northern coastal waters and biological responses
- **JRAP 4**: 4D characterization of trans-boundary hydrography and transport
- **JRAP 5**: Coastal carbon fluxes and biogeochemical cycling
- **JRAP 6**: Operational oceanography and forecasting

They address key scientific questions together with major environmental issues and/or policy requirements (e.g. a subset of the descriptors considered by the Marine Strategy Frameword Directive).

The present document first **reports on the work achieved** in the framework of these six Joint research Activity Projects **during the whole JERICO-NEXT** program. **This** item **is addressed separately for each Joint Research Activity Project**.

The present document also **synthetises the practical experience gained** from their implementation and **lists** a series of **propositions for a future monitoring strategy** of the European Coastal Ocean. **These** two items **are first addressed separately** within each JRAP **and then synthetised** for the whole WP4.

3. JRAP 1: Biodiversity of plankton, harmful algal blooms and eutrophication

Contributors
Bengt Karlson, Malin Mohlin, **SMHI, Sweden**
Felipe Artigas, Arnaud Louchart, Morgane Didry, Fabrice Lizon, Guillaume Wacquet, **CNRS-ULCO&UL, France**
Michael Brosnahan, **WHOI, USA**
Pascal Claquin, **CNRS-UC, France**
Véronique Créach, **Cefas, UK**
Elisabeth Debusschere, Jonas Moltermans, Lennert Tyberghien, Klaas Deneudt, **VLIZ, Belgium**
Reinhoud De Blok, Wim Veyverman, **U Gent, Belgium**
Weinke Eikrem, **NIVA, Norway**
Jacco Kromkamp, **NIOZ, Netherlands**
Alain Lefebvre, **IFREMER, France**
Klas O. Möller, Jochen Wollshläger, **HZG, Germany**
Grant Prischer, Bernard Stewart, **CSIR, South Africa**
Machteld Rijkeboer, Hedy Aardema, Arnold Veen, **RWS, Netherlands**
Jukka Seppälä, Pasi Ylöstalo, Suvi Rytövuori, Timo Tamminen, Petri Maunula, Jani Ruohola, Sirpa Lehtinen, Kaisa Kraft, Seppo Kaitala, **SYKE, Finland**
Lars Stemmann, **CNRS-UPMC, France**
Melilotus Thyssen, Pierre Marrec, Gélrald Grégori, **CNRS –AMU, France**

3.1. Topic and specific objectives

JRAP 1 aimed at giving a new approach of the dynamics of phytoplankton blooms, supporting the Marine Strategy Framework Directive (MSFD) requirements concerning mainly Descriptors 1-marine biodiversity and 5-eutrophication although, non-indigenous species (Descriptor 2) and food webs (Descriptor 4) were also relevant. Phytoplankton are the main primary producers in marine systems, at the direct interface between non-living (inorganic and organic) matter and food webs at higher trophic levels (which they support). As such they are key actors of biogeochemical cycles and, in some occasions (depending on diversity and physiological conditions), can represent a threat to marine life and/or human health by being responsible of noxious events (harmful algal blooms). Harmful Algae have effects on tourism (e.g. by algal toxins in aerosols affecting tourists on beaches and by accumulations of scums on beaches). Harmful Algal Blooms (HAB) also affect aquaculture and fisheries. Algal toxins may accumulate in bivalves posing a threat to human health. Other harmful algae cause fish mortalities affecting fish farming and sometimes fisheries.

Phytoplankton blooms can take place at different spatial and temporal scales, from local to regional (and larger), from hours to days (weeks and sometimes even months). To study these episodes and understanding their determinism, there is a need to perform observations at higher spatial and temporal resolution than current monitoring carried out in coastal systems. Innovative automated approaches allow to quantify and characterize phytoplankton diversity changes (at taxonomical and/or functional level) and physiological state (photosynthetic parameters) in (almost) real time both *in vivo* and *in situ*, and at a high frequency i.e., (from seconds to minutes or hours), when coupled to automated environmental continuous monitoring on board research vessels, ships of opportunity and/or fixed stations or moorings.

In this context, the main objectives of JRAP 1 were:

- To enhance the understanding of the dynamics of algal blooms by combining data on phytoplankton distribution, abundance and diversity with chemical and physical oceanographic data,
- To apply novel *in vivo/in situ* or *ex situ* automated or semi-automated methods to address phytoplankton diversity, abundance, biomass and photosynthesis parameters in marine coastal systems, with a focus on harmful algae and eutrophication,
- To assess their potential for complementing traditional methods, which are based on discrete water sampling and labour-intensive laboratory microscope work, in addressing questions related to the of phytoplankton

changes in space and time at regional, meso- and sub-mesoscale, as well as to address the timing and extension of phytoplankton blooms (including HABs).

- To formulate inputs for science strategy related to the JERICO-RI and recommendations for its further development.

3.2. Overall structuration and strategy

Most coastal areas of Europe have problems with harmful algal blooms, biotoxin producing algae and/or algal toxins in shellfish. Comparable studies where originally planned in at least four European seas corresponding to four selected sites of different ecological status:

- An enclosed brackish system (the Baltic Sea) submitted to eutrophication pressure in which a multiscale assessment of cyanobacterial was carried out combining FerryBox data gathered in regular Ferry line crossings, dedicated cruises and automated fixed station, at high spatial and temporal resolution,
- A transition system (fjord-strait-shelf system) (Skagerrak-Kattegat-Oresund), dealing with strong stratification and harmful algal blooms producing toxins killing fish (as *Pseudo-chatonnella*) also combining continuous recording on Ferry lines, dedicated cruises and mooring
- Marginal and shelf seas well mixed or partially stratified (eastern English Channel – southern North Sea) also submitted to eutrophication from major rivers and dealing with diatoms and *Phaeocystis globosa* blooms (big organic matter accumulation, i.e. foam in the littoral area), in which the main issue was to follow the timing and spatial distribution of diatoms and *Phaeocystis globosa* blooms
- An open mainly oligotrophic system (the Ligurian Sea and Western Mediterranean) where picoplankton dominates, were a Ferry line was instrumented with both chemical-physical and phytoplankton sensors

The coupling between phytoplankton and physical structures (eddies, upwelling) was also explored in other shelf area systems featuring different characteristics such as the southern Bay of Biscay and the Benguela Current (DAFF, Republic of South Africa). The initial idea was to address different ecosystems for which the temporal scales of phytoplankton booms are often approximately a few weeks (or less), but with different temporal and spatial scales according to the area considered. Therefore, we have focused on periods when blooms were expected in each area, with a fine spatial and temporal resolution.

3.3. Achieved actions

3.3.1. Sampling campaigns.

Sampling campaigns were carried out on research vessels and/or on merchant vessels (including ferries) equipped with flow-through FerryBox systems, as well as on fixed platforms. Figure 3.1 gives an overview of the main cruises and fixed sites.

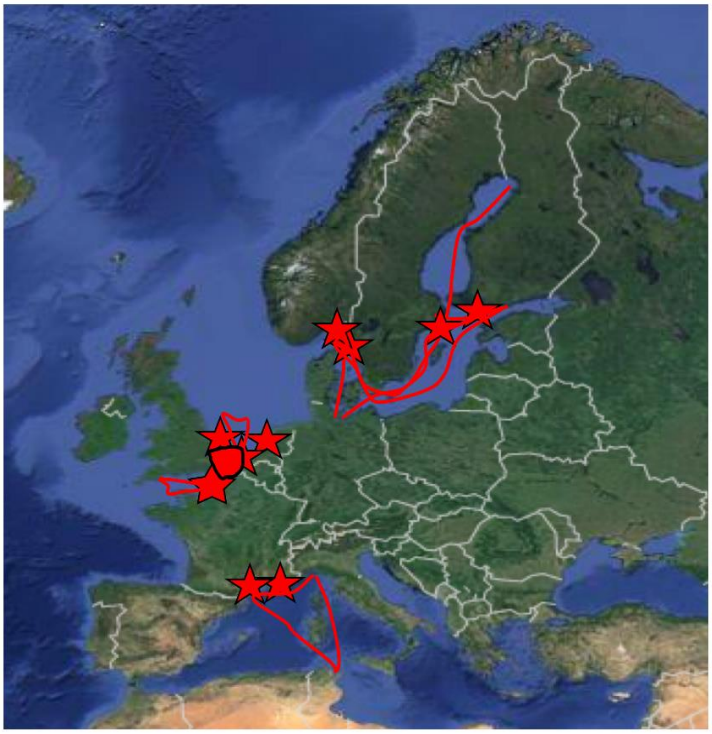

Figure 3.1: *Map showing the locations of main field campaigns carried out in JRAP 1. Stars represent fixed systems while lines represent cruises with research vessels or FerryBox systems on merchant vessels (e.g. ferries). Not all activities are represented on the map, see Table 1.1. for details.*

3.3.2. Variables/parameters.

Novel optical sensors were evaluated as part of the work in WP3, task 1, then, were applied in different marine systems (**Table 3.1**) in the frame of WP4.1 (JRAP 1) in order to characterize phytoplankton taxa, size classes, pigmentary groups, functional types as well as photosynthetic parameters In a wide range of coastal marine systems of different structure and trophic status and anthropogenic impact, from semi-enclosed to open seas. An overview of the sensing approaches used is shown in **Figure 3.2**.

Two *in vivo* approaches and five automated techniques were implemented in order to address taxa, size classes, pigmentary and functional groups distributions, in terms of cell/colony abundance or in terms of pigment contents/contributions to total chlorophyll fluorescence (proxy of phytoplankton biomass):

- Single-cell (single-particle) approach, including image in-flow (Imaging Flow CytoBot, FlowCAM and *in situ* imaging techniques (UVP5), as well as image and optical characterization *in flow* by pulse shape-recording flow cytometry (PSFCM, CytoSense/Sub)
- Bulk approach, including in-flow spectrophotometry (HyAbs, PsiCAM), targeted fluorometry (chlorophyll, phycoerytrhin or phycocyanin fluoroometers, multispectral fluorometry (AlgaeOnlineAnalyzer, Fluoroprobe), profiling *in situ* multi-spectral fluorometry (Fluoroprobe, Multi-Exciter), as well as multispectral/variable/active fluorometry on discrete samples (PhytoPAM), in-flow (FRRf FastOcean2) and profiling (FRRf FastOcean 3).

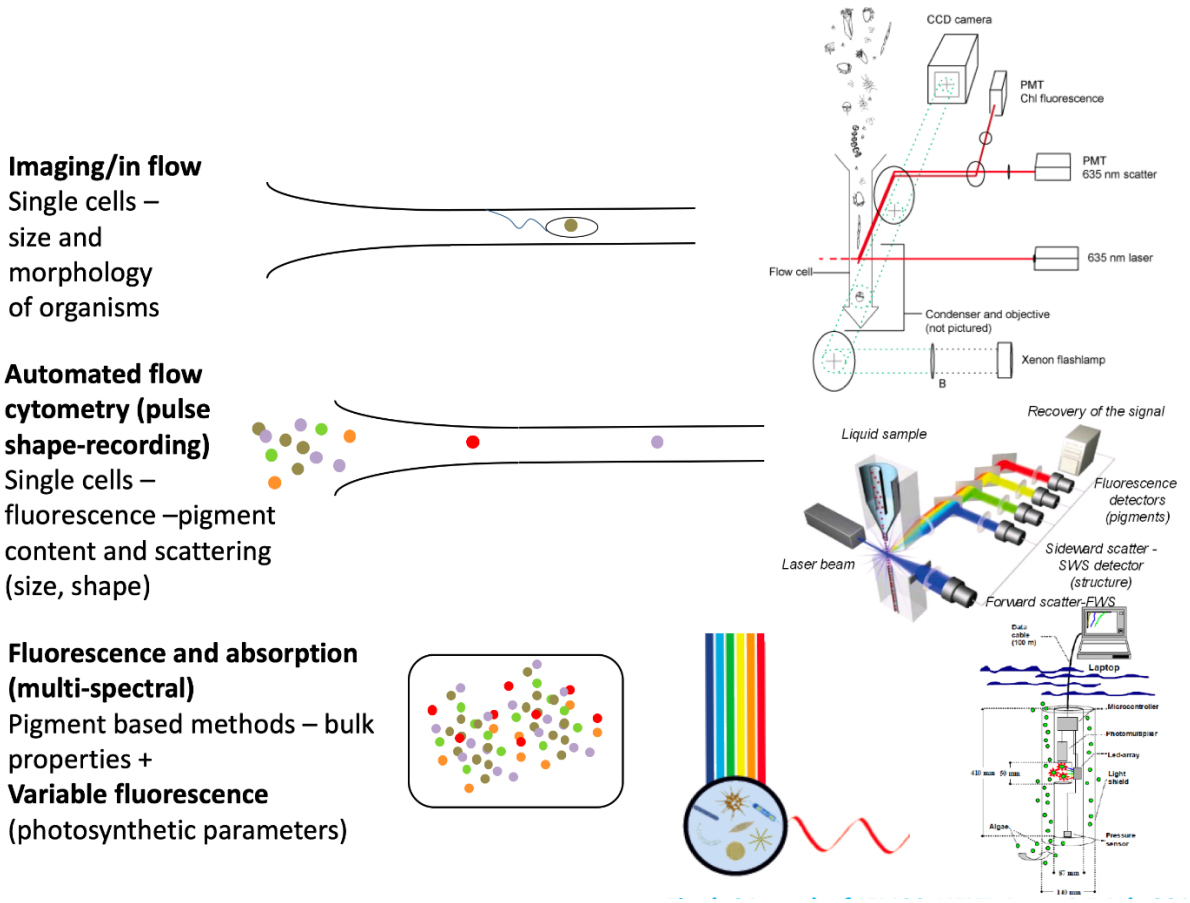

Figure 3.2: *Approaches for the observation of phytoplankton* in vivo, in situ *and in near real time*

3.3.3. Data analysis.

Different automated analytical tools were tested and improved during the project, for moving towards better automated treatment of sensors' raw data: classification, discrimination and estimation of abundance, biomass, pigment content, size and other properties of phytoplankton functional groups or taxa (see JERICO-NEXT D3.2). Moreover, other sets of methods allowed us to characterize the different water masses and to address the dynamics and spatial variability, at fine scales, of phytoplankton communities of common characteristics (for more details, see the Channel North Sea of D4.4; Lefebvre & Poisson-Caillault, 2019).

Table 3.1: *Instruments on board the different ferrybox systems, cruises or field stations with numbers of acquisitions and measurement types (C: continuous recording in surface or sub-surface waters; P: Profiles (casts) in the water column; D: Discrete measurements in (sub)-surface or along the water-column). Crosses indicate measurements with the corresponding device with no detailed information on numbers of samples*

Observatory/ Ferrybox/ Cruise	Period	CTD	PSFCM (C)	PSFCM (D)	Plankton Imager	PhytoPAM (stations)	FluoroProbe /Multiexciter (C)	FluoroProbe/ Multiexciter (P)	FB	Chl. fluor.	Phycocyanin fluor.	Nut	FRRf2 (C)	FRRf3(P)
*Le Carthage	2016-2017		X (CNRS-MIO)						x					
*Finmaid Ferry	2016				FlowCAM				x	x	x			
*TransPaper	2015-2017										x			
***VLIZ	2016	22	(VLIZ) (RWS)		CytoSense (RWS + VLIZ)	15 (3 depths per station)	1057	14		x		X		
***RWS	2016	x	(RWS)	x	CytoSense (RWS)	18	4353		x	x		X		
**Tångesund observatory	2016	x		x	Imaging Flow cytobot SMHI	x	x	x					x	
*Le Carthage	2016		X (CNRS-MIO)						X					
***Nephrops TV Survey	2016	X	X		X				X	X		X		
***CEFAS Pelagic Fish	2016	X	X		X				X	X		X		
**SMILE Buoy	2016 - 2017												x	
***CEFAS	2017	X	X		X				X	X		X		

**Utö observatory	2017 - 2018				Imaging FlowCytobot		x		x	x		x	x	
**Kosterfjord Buoy	2018	x								x				
**Huvudskär E Buoy											x			
***PHYCO	2017	46	1064 (CNRS-LOG)	197	CytoSense (CNRS-LOG)	46 (surface) 48 (bottom)	AOA (IFREMER)	47	x	48 (surf.) 48 (bottom)		48	x	37
***VLIZ	2017	44	641 (CNRS-LOG) (VLIZ) (RWS)	106	CytoSense (CNRS-LOG, RWS, VLIZ)	25 (surface) 25 (bottom)		27						19
***RWS	2017	19	322 (CNRS-LOG) (RWS)	61	CytoSense (CNRS-LOG, RWS)	18 (surface) 15 (bottom)	4194		x					17
*Silja Serenade Ferry	2017 - 2018								x	x	x			
***SMHI Aranda cruise	2017	30	783 (CNRS-LOG)	246	CytoSense (CNRS-LOG) FlowCAM (SMHI) UVP5 (CNRS-LOV)	19 103 (many depths per station)	5415	16	x		x		x	16
***Pelrad	2017	22	136 (CNRS-LOG)		CytoSense (CNRS-LOG)		781	17		22 (surf.) 22 (bottom)		22	x	6
***ETOILE	2017	25	859 (CNRS-LOG)	117	CytoSense (CNRS-LOG)		10638	15						

*Ferry box systems.

One merchant vessel and two ferries in the Baltic Sea were operated continuously during the JERICO-NEXT project. They were all equipped with sensors for phycocyanin and chlorophyll fluorescence. The ferry Le Carthage was operated continuously part of the project.

**Fixed platforms, buoys or observatories. The Tångesund observatory was operated for 12 months with Imaging Flow Cytobot used during approximately 12 weeks. The Utö observatory was operated continuously during The SMILE buoy was operated continuously during part of the project.

***Cruises with research vessels, length usually around one week.

Explanations of selected acronyms: PSFCM = Pulse Shape Recording Flow Cytometer, FB = FerryBox, chl. Fluorescence = chlorophyll f *in vivo* fluorescence, FRRf = Fast Repetition Rate Fluorometer, Nut = Inorganic nutrients

3.4. Main results

Hereby we present some significant results of the implementation of (semi-)automated approaches and techniques for monitoring phytoplankton temporal and spatial variability and dynamics at fine spatial and temporal scales, in selected coastal marine systems.

3.4.1. The Baltic Sea current monitoring.

The Baltic Sea is a eutrophic coastal sea characterized by a low salinity and strong anthropogenic pressures. Phytoplankton community has a clear seasonality, with strong spring blooms of diatoms and dinoflagellates, followed by early summer minimum period with low abundance of phytoplankton. In mid/late summer, massive blooms of filamentous N-fixing cyanobacteria are typical for the area. Occasionally, other blooms (e.g. dinoflagellates) are observed during summer months. The fast-growing picoplankton has also important role in BGC-cycles of the Baltic Sea during summer. In this context, the actions carried out within JRAP 1 were as follows:

- *Baltic Sea 1.* Monitoring phycoeryhtrin fluorescence in the Baltic Sea using ferrybox system. May 2016-September 2016.
- *Baltic Sea 2.* Tests with emerging optical sensors for phytoplankton research at Utö. Spring 2017-spring 2018.
- *Baltic Sea 3.* Continuous measurements at ferrybox Silja Serenade for filamentous cyanobacterial blooms between Helsinki and Stockholm. Spring 2017- summer 2018.
- *Baltic Sea 4.* Continuous measurements at Tavastland Ferrybox (formerly TransPaper) between Lübeck and Kemi.
- *Baltic Sea 5.* The Huvudskär E- oceanographic buoy. Measurements of bio-optical parameters etc.

Baltic Sea 1. Phycoerythrin (PE) is a spectrally diverse pigment, especially suited to harvest blue/green light at greater water depths. In the Baltic Sea PE has a characteristic absorption maximum around 566 nm with fluorescence emission at 578 nm, and picocyanobacteria have been considered as main source of PE signal (Seppälä et al 2005). We installed two commercial PE fluorometers in a ferry Finnmaid, as part of Algaline flowthrough system, from May 2016 until end of year 2016. Samples for detailed laboratory analysis of PE containing cells were taken using automated water sampler onboard, and PE-containing cells were counted using epifluorescence microscopy and FlowCAM. Additional spectral fluorescence and absorption measurements were performed, targeting to quantification of PE in different size-fractions. Details of the study are given in Rytövuori (2017).

PE fluorescence showed seasonally distinct spatial structures (**Figure 3.3**). During the early summer the signal was related to abundance of ciliate *Mesodinium rubrum*, while in late summer it was closer related to picocyanobacteria. Occasional increases of PE fluorescence were observed due to upwelling, which was explained by the uplift of PE rich deeper phytoplankton populations. Based on these measurements, it seems clear that PE fluorescence originated from various organisms. Thus, PE fluorescence signal needed to be analysed along with other phytoplankton group-specific data to get insight in pelagic phytoplankton biodiversity and functionality. As a follow-up of this study, operational monitorings of PE fluorescence were in the ferries Finnmaid and Silja Serenade, and at the profiling buoy at Utö. Recent observations from these platforms (2017-19) show similar results as in 2016, indicating locally high abundances of *M. rubrum* in spring.

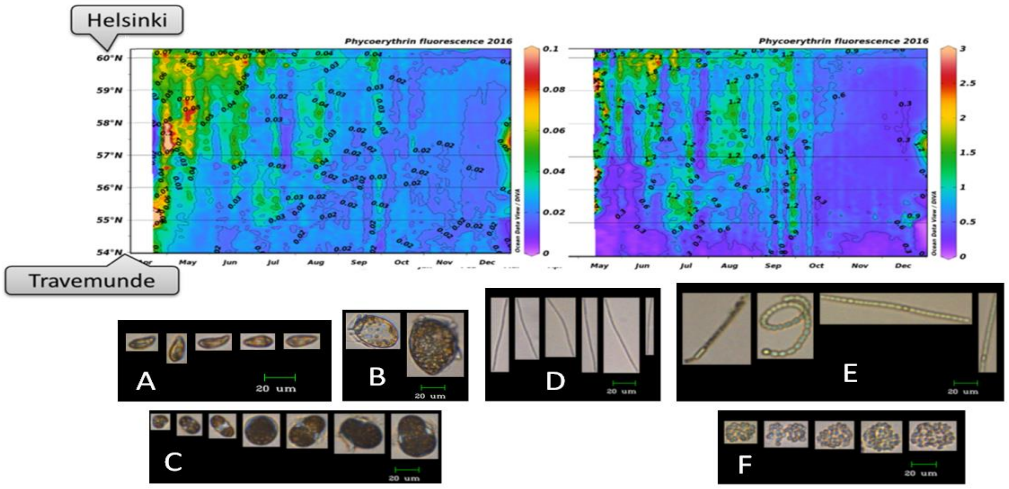

Figure 3.3: *Variability in phycoerythrin fluorescence in 2016, along a ferry transect between Helsinki and Travemünde. Two commercial fluorometers were used; Trios MicroFlu Red (left) and Chelsea Unilux PE (right). In the lower panel representative images of the cells identified to contain phycoerythrin, according to FlowCAM analysis: A – cryptophytes; B – dinoflagellates Dinophysis spp.; C – ciliate Mesodinium rubrum; D – cyanobactreria Oscillatoriales; E – cyanobactreria Nostocales; F – cyanobacteria Chroococcales.*

<u>*Baltic Sea 2.*</u> Various emerging optical sensors were tested at the Utö station from April 2017 to March 2018. A flowthrough system provided water from 5 m depth using underwater pump, pumped through 300 m to reach the measuring hut where it was distributed to a stationary FerryBox system.

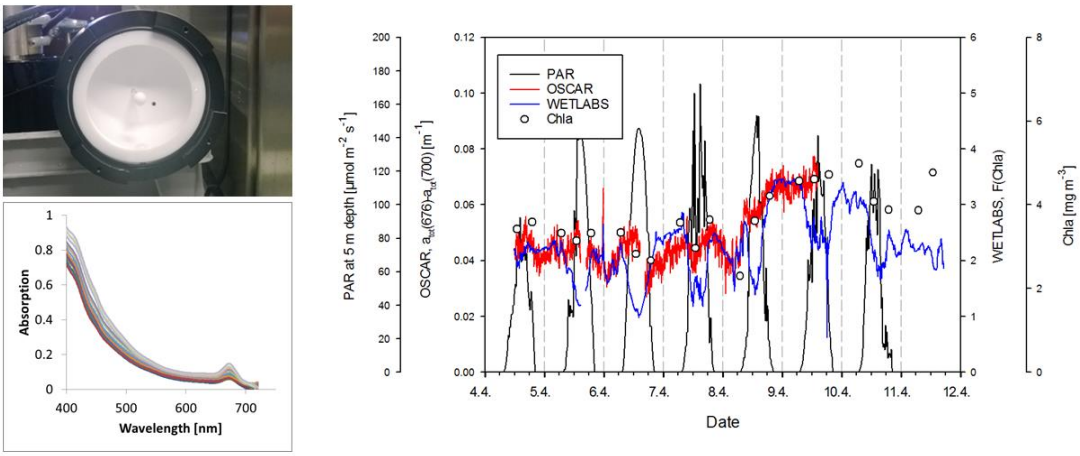

Figure 3.4: *Integrating cavity spectrophotometer Oscar (Upper Left), some absorption spectra collected at Utö station in April 2017 (Lower Left) and continuous measurement of light (PAR, black line), Chlorophyll a fluorescence with WETLABS fluorometer (blue line), showing decrease of fluoresce at noon, proxy of Chlorophyll a concentration calculated from the absorption red peak of the OSCAR spectrophotometer (red line) and laboratory measurements of Chlorophyll a (open circles) (Right).*

Various sensors were tested, two of them highlighted in this report.

- Integrating cavity spectrophotometer (OSCAR, Trios Gmbh) measures total absorption of the water samples, and the contribution of various optically active compounds may be retrieved from the signal. The results from Uto station, showed that the absorption-based estimation of Chlorophyll a

(calculated as peak height of Chlorophyll a absorption band at 676 nm) correlated strongly with analytical measurements of Chlorophyll *a* concentration (**Figure 3.4**). In turn, fluorescence-based measurements showed decline in response during sunny conditions due to non-photochemical quenching. Thus, the absorption-based method would yield much better estimation of Chlorophyll *a* concentration than fluorescence-based method. This is however compromised by much higher need for sensor maintenance in the absorption method, and automated systems for cleaning and calibration need still to be developed (Wollschläger et al. 2019).

- Fast Repetition Rate fluorometry (FRRf) provides assessment of the photo-physiological status of phytoplankton and allow for an estimation of the primary productivity. However, the conversion factor between electron transport rate (measured with e.g. FRRf fluorometer) and carbon fixation rate (measured using carbon isotope) is showing a large variability, hindering the use of optical FRRf measurement as a substitute of isotopic methods. In Utö station, in 2017, we studied the variability of the conversion factor during four one-week campaigns. The observed variability was from 4 to 18 (mol e^- mol C^{-1}). In spring, the variability was much less than during other seasons and close to the theoretical minimum value of 4. Values higher than 4 indicate that part of the light energy gained by primary reactions of photosynthesis are used for other processes than carbon fixation. Our results indicate that the observed variability in the conversion factor is not related to the time of the day (i.e. light), but rather to phytoplankton community composition and maybe also to the availability of nutrients (**Figure 3.4**).

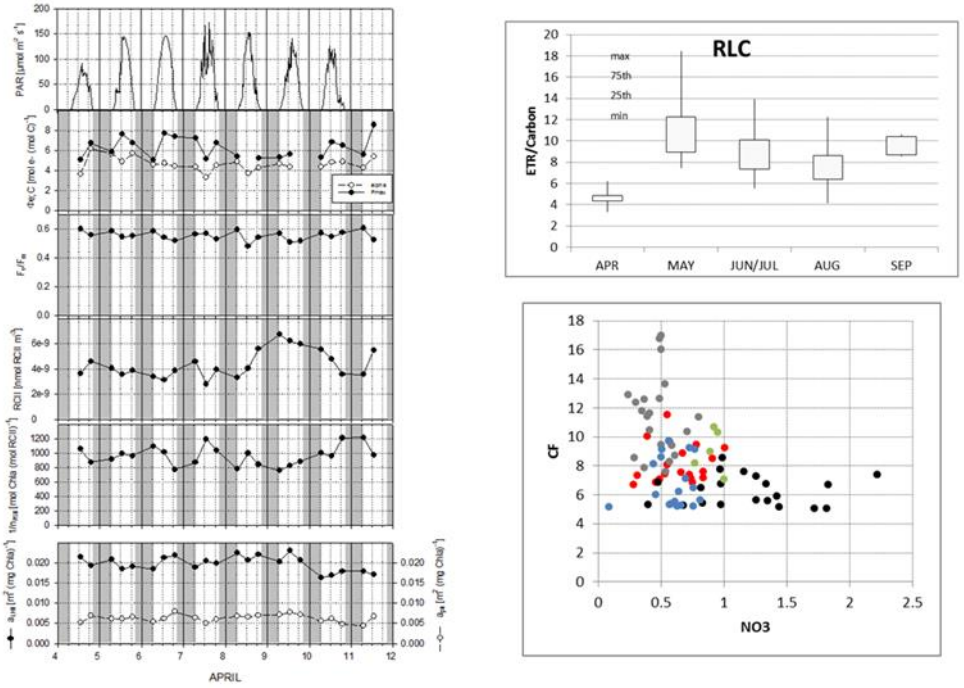

Figure 3.4: *Fluorescence induction measurements during the intensive measurement period at Utö, in April 2017 showing values of Irradiance, conversion factor between electron transport rate and rate of carbon fixation, efficiency factor for photosystem II, number of reaction centers, size of reaction centers and absorption cross-section (from top to down, Left). Conversion factor varied seasonally (Upper Right) and was partly related to the amount of inorganic nutrients, thus to the physiological state of cells (Lower Right).*

Baltic Sea 3. Monitoring of cyanobacteria has been carried out by SYKE since 2005, using ferrybox monitoring of phycycyanin (PC) fluorescence (Seppälä et al 2007). The results are used to assess the state of the water basins and also to inform authorities and public on the algal bloom situations. The combined measurements with Imaging FlowCytobot (IFCB) and PC fluorescence allowed to study, with high number of observations, how these different biomass indices are related (**Figure 3.5**). For the cyanobacterial bloom period in 2018, the IFCB classifiers for the major bloom forming species (*Aphanizomenon flosaquae* and *Dolichospermum* spp.) were carried out following Sosik and Olson (2007), and the biomass of these major species were calculated using observed dimensions of

filaments. *Nodularia spumigena*, typically dominant species during these blooms, was observed only in very small quantities. The measured PC fluorescence correlated with the biomass of filamentous cyanobacteria. Such validation allowed analysing how the optical signatures develop during the bloom, and which technologies are best suited in bloom detection. Results show the tight coupling of PC fluorescence and biomass of filamentous cyanobacteria, with slight shifts showing higher biomass-specific fluorescence during the early bloom (maybe due to highly pigmented cells). Results promote the conversion of fluorescence records to biomass estimates, making them more user-friendly for studying algae situation, and also more usable to satellite and ecosystem model validation.

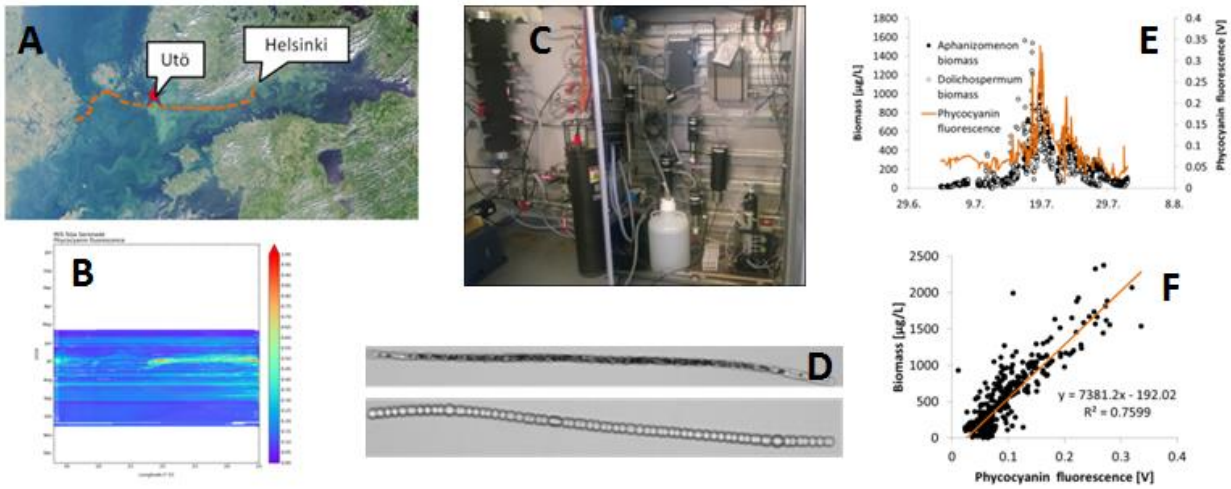

Figure 3.5: *(A) Satellite image with cyanobacterial bloom (ESA Copernicus Sentinel data 16.7. 2018, processed by SYKE) and location of Utö station and cruise track of Silja Serenade (orange dashed line). (B) Phycocyanin fluorescence observations by Silja Serenade, showing the highest cyanobacterial abundance in mid-Jjuly, east of Utö station. (C) photo of Utö station sensors in flow-through system. (D) Imaging FlowCytobot images of Aphanizomenon flosaquae and Dolichospermum spp.. (E) Temporal variability of phycocyanin fluorescence and biomass of Aphanizomenon flosaquae and Dolichospermum spp. measured with IFCB. (F) Relationship between phycocyanin fluorescence and biomass of filamentous cyanobacteria, as estimated by IFCB.*

3.4.2. Baltic and Skagerrak/Kattegat straits - Aranda cruise.

The Aranda cruise investigated the Baltic Sea, and the Kattegat and Skagerrak on July 2017, 10th – 17th. Thirty stations were investigated (18 for JERICO-NEXT). Sixteen profiles were carried out with the FRRf3 andthe FluoroProbe. UVP5 casts were carried out at each station. The FlowCam was also used but due to broken cuvette it was not possibleto process all samples. The main objectives were:

- To investigate the vertical and horizontal distribution of cyanobacteria
- To characterize phytoplankton with an *in situ* multispectral fluorometer (Fluoroprobe),
- To display an automated pulse shape-recording flow cytometer (CytoSense) for in-flow continuous recording on surface waters a well as on discrete samples at different depths
- To use a discrete/in-flow image analysis (FlowCAM).
- To investigate the vertical and horizontal distribution of zooplankton using the in situ imaging with a UVP5
- To test PhytoPAM on discrete samples for addressing photosynthetic parameters.
- To test *in situ* Fast Repetition Rate fluorometry (FFRf) for photosynthetic parameters

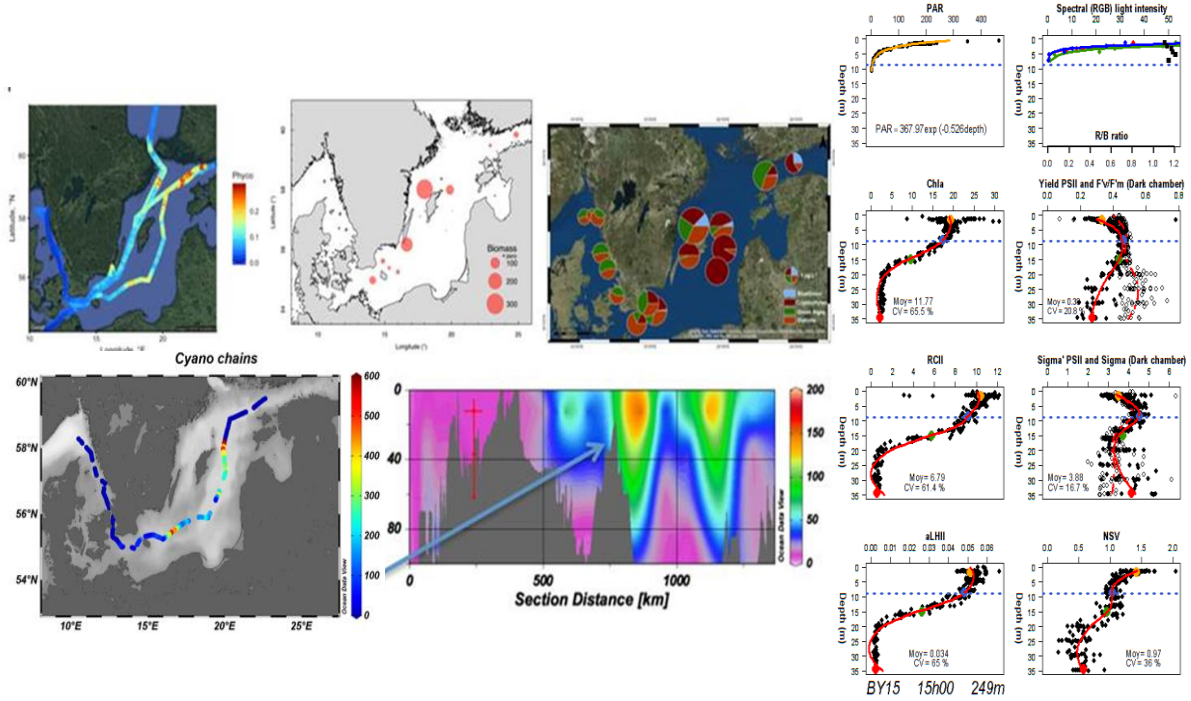

***Figure 3.6**: Results from the Aranda cruise (July 2017). Top left: Phycocyanin fluorescence from Aranda cruise and from the ferrybox system on merchant vessel Tavastland during the same week. Top middle: the biomasse of* Nodularia spumigena *based on microscopy counts and contribution of pigmentary groups to total chlorophyll based on multi-spectral fluorescence (Fluoroprobe). Bottom left: abundance of cyanobacterial filaments from automated pulse shape-recroding flow cytometry (CytoSense) during the first transect, corresponding to stations used for Bottom middle: distribution of Nodularia spumigena-lyke cyanobacteria colonies based on in situ imaging (UVP5). Right: FRRF vertical profile at station BY15, displaying light intensity and quality (λ for blue, green and red wavebands); the effective and pseudo-maximum PSII quantum yield (YPSII and F'v/F'm rel. unit), absorption cross section of PSII (σ ' and σ PSII in nm2.PSII-1), photoinhibition (NSV rel. unit), reaction centre concentration (RCII in nmol PSII.m-3), absorption coefficient of PSII light harvesting (aLHII in m-1) with Euphotic Depth (blue line) and Chla (mg.m-3) vertical profiles. CV mean coefficient of vertical variation (%).*

Sensors deployements were successful. Horizontal and vertical gradients were characterized (**Figure 3.6**). Single-cells to large filaments of cyanobacteria were observed mostly in surface waters of the Baltic and we could also track their distribution in the water column both from fluorescence and in situ imaging, whereas deep diatom/dinoflagellate accumulations were observed in the Skagerrak/Kattegat. This spatio-temporal heterogenity was also observed through changes in photosynthetical parameters within the water column or across the horizontal gradient.

3.4.3. Skagerrak-Kattegat area: the Tångesund harmful algal bloom study.

The Tångesund observatory was established in summer 2016. It included an oceanographic buoy, a sub-surface mooring and a raft with advanced instrumentation. An automated underwater microscope, the Imaging FlowCytobot (IFCB), was used during a study of harmful algal blooms from August to October 2016. Data was collected autonomously from six depths and displayed in near real time on the internet. Water sampling was carried out weekly. Phytoplankton abundance and composition, chlorophyll *a*, inorganic nutrients and other parameters were measured in the laboratory.

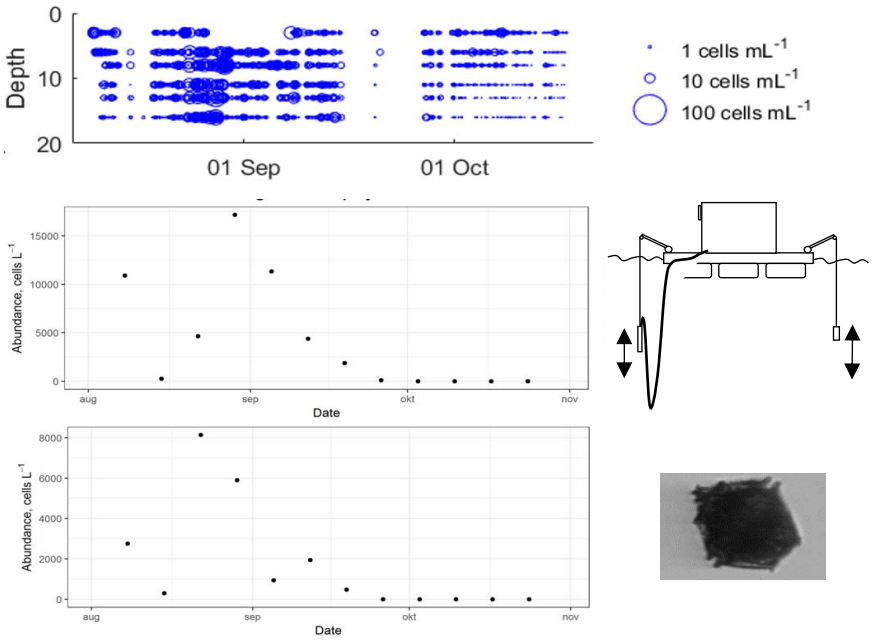

Figure 3.7: *The abundance of* Lingulodinium polyedrum *at Tångesund, Sweden August to October 2016. Results from Imaging Flow Cytobot with high temporal resolution at six depths (up) and microscopic counts at 5m (center) and 15m depth (bottom) at selected dates.*

The results of the analysis of IFCB made it possible to characterize the dynamics of a toxic dinoflagellate bloom *(Lingulodinium polyedrum)* during late summer and beginning of fall (**Figure 3.7**). It was possible to detect the setting of the bloom starting from surface waters in August and extending to deep waters by end of August. These high frequency measurements targeting a single period stressed the importance of considering both the high frequency monitoring of coastal systems at least during particular sensitive periods (i.e. HAB development) and also to take into account stratification through the assessment of vertical profiles (as confirmed during the Aranda summer cruis, see above).

3.4.4. North Sea phytoplankton seasonal dynamics and productivity.

In 2017, four cruises were undertaken in the Dutch EEZ using the RV Zirfaea (RWS), aiming at measuring the different phases in the annual phytoplankton bloom cycle: the spring bloom (April), the end of the bloom phase (May), the clear water phase with probable high grazing rates and when production is driven by nutrient regeneration (June), and the late summer bloom phase (August). FRRf and flow cytometry data were gathered during these cruises which were part of the regular water quality monitoring program (called MWTL-program). Data from this MWTL monitoring program are used for several purposes, amongst reporting for the Marine Strategy Framework Directive and OSPAR assesments. Phytoplankton total abundance, red fluorescence and community composition showed high spatial heterogeneity in the Dutch North Sea from April to August 2017 (**Figure 3.8**, Aardema et al., 2018). The relative abundance of picophytoplankton was generally higher offshore and in the Northern part of the area. The pico-red group was always dominant even though they contributed less to total red fluorescence. The pico-*Synechococcus* group showed a strong numerical presence offshore in April and in most of the Dutch North Sea in June. The nano-red group was often a dominant group, both in terms of cell abundance and contribution to total red fluorescence. The nano-cryptophytes were never dominant in terms of abundance, but contributed significantly to the total red fluorescence in Northern offshore regions. Notwhistanding micro phytoplankton represented always less than 10% of the total cell numbers, they sometimes dominated the total red fluorescence, mostly in coastal regions (**Figure 3.8**).

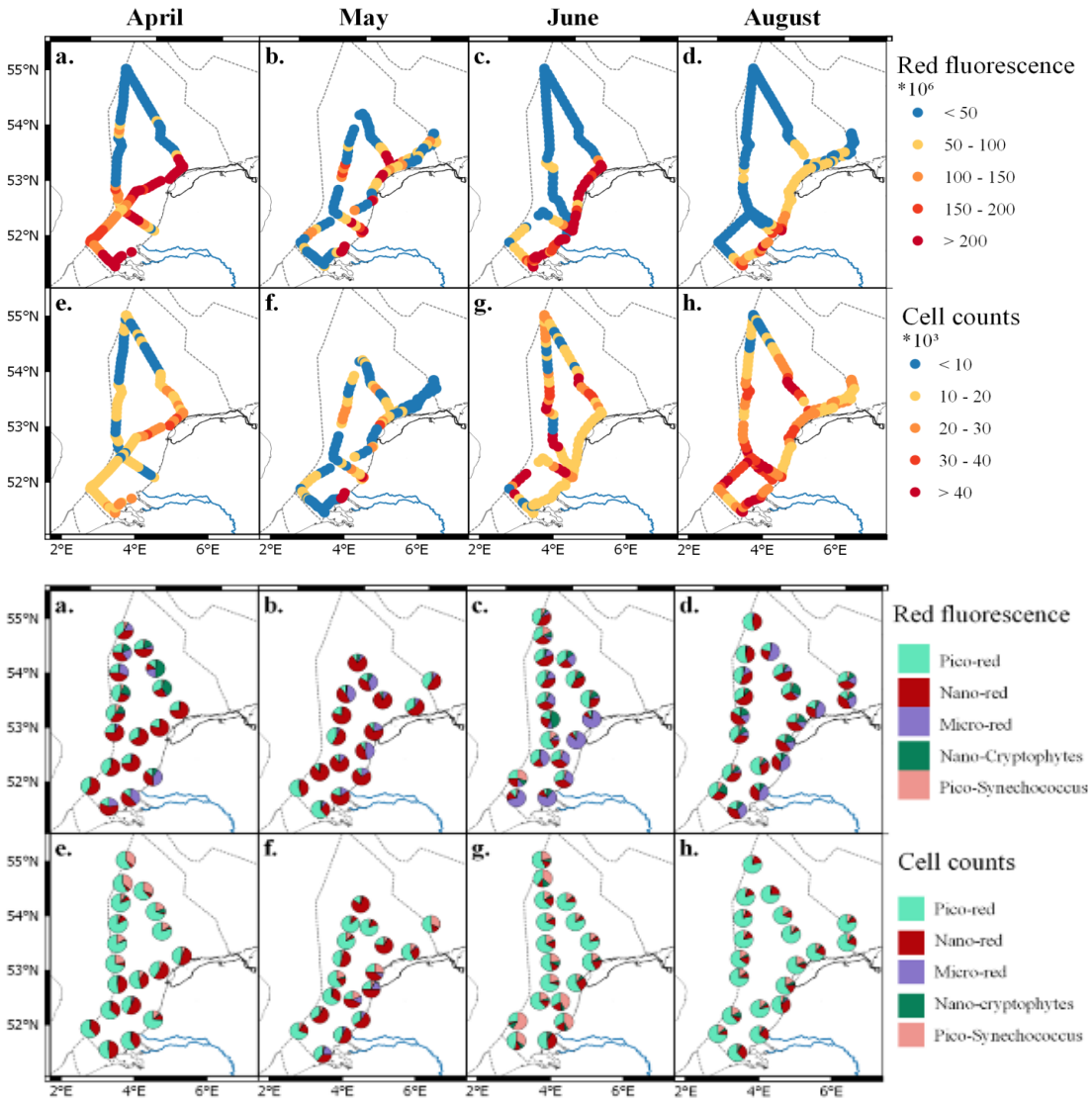

Figure 3.8: *Use of automated Flow Cytometry to address phytoplankton spatial and temporal distribution in the southern North Sea (RWS cruise, Aardema et al., 2018). From top to bottom : Total Red Fluorescence (proxy of chl a), Cell counts, Contribution of each of the 5 cytometry classes to total reed fluorescence and to total cell count.*

Photo-pyhsiological parameters were addressed and gross primary productivity was estimated. It ranged from minimum values in June to peak productivities recorded in the coastal zone in May (**Figure 3.9**). Spatial variability in the three selected FRRF was limited during April, especially in the case of Fv/Fm and σPSII. In the Northern part Fv/Fm > 0.6, and in the Southern part, Fv/Fm >0.5. σPSII showed little variability. Interestingly, In May low Fv/Fm-values were observed, most likely resulting from nutrient limitation. High spatial variability clearly demonstrated that extrapolation from single measurements to larger spatial scales might induce wrong conclusions. The σPSII v values approximately doubled in May. Ek also showed a strong spatial variability with values in the Southern part (70km offshore) being much lower than those close to the shore. In June and August Fv/Fm recovered (high values) mostly everywhere, but changes in σPSII were limited.

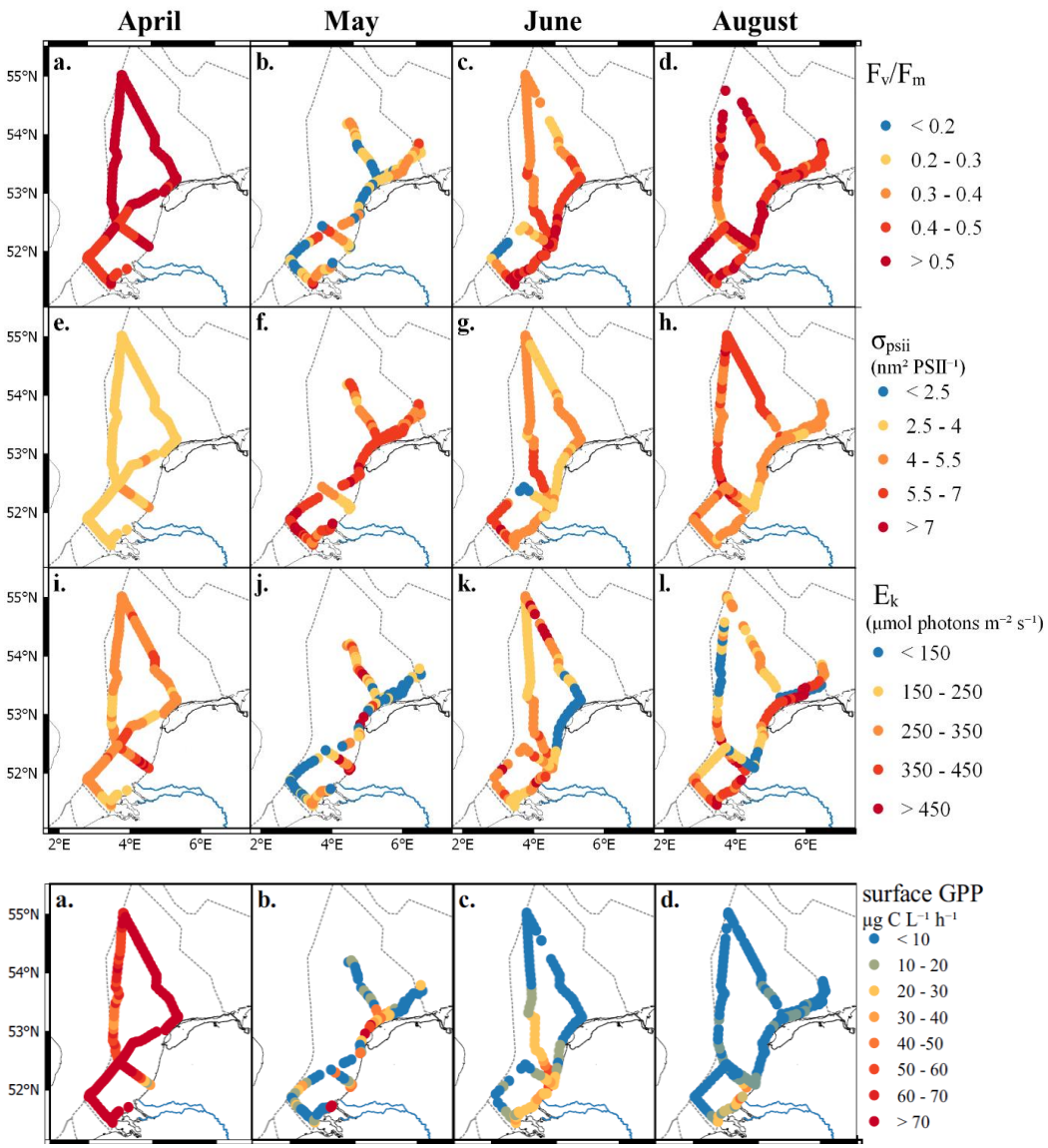

Figure 3.9: *Maps of the photophysiological parameters Fv/Fm (a-d), σPSII (e-h; in nm² PSII⁻¹), Ek (i-l; in µmol photons m⁻² s⁻¹) and Surface primary productivity values in the Dutch EEZ (assuming 6 electrons are needed to fix a CO_2 molecule) per month (from left to right: April, May, June and August).*

This recovery could not be explained by an increase in nutrient concentrations as they were still potentially limiting in most areas. More likely is that the algae acclimated to the low nutrient conditions and Fv/Fm recovered. This has been observed before (Kruskopf & Flynn 2006) and shows that Fv/Fm can only be used as indicator of nutrient limitation when the cells are in the initial phase of nutrient limitation causing unbalanced growth conditions, a situation, which occurs when the spring bloom terminates as the phytoplankton use up most of the nutrients.

Surface production values in April were high compared to the other months, but they were also high at the offshore stations. In June and August primary production increased again, but mostly in the Southern coastal regions. Productivity remained low in the Northern End of the Dutch EEZ after cessation of the spring bloom.

3.4.5. Eastern English Channel – Strait of Dover - southern North Sea.

The Eastern English Channel is characterized by eutrophic and mixing conditions. Spring blooms are dominated by diatoms (including the genus *Pseudo-nitzshia* which can produce toxins) and the haptophyte *Phaeocystis*

globosa (responsible for accumulation of high amounts of organic matter/foam), and are characterised by a succession of these two groups. Our main objective was to follow and address phytoplankton distribution and dynamics during the phytoplankton spring bloom development from the Eastern Channel towards the North Sea. Three research cruises (PHYCO - CNRS-LOG, Lifewatch-VLIZ and RWS), from April 20 to May 19, 2017) were carried out from eastern English Channel to the southern North Sea at an interval of one week, in order to follow the progression towards the North of the *Phaeocystis globosa* bloom from late April to mid-May 2017.

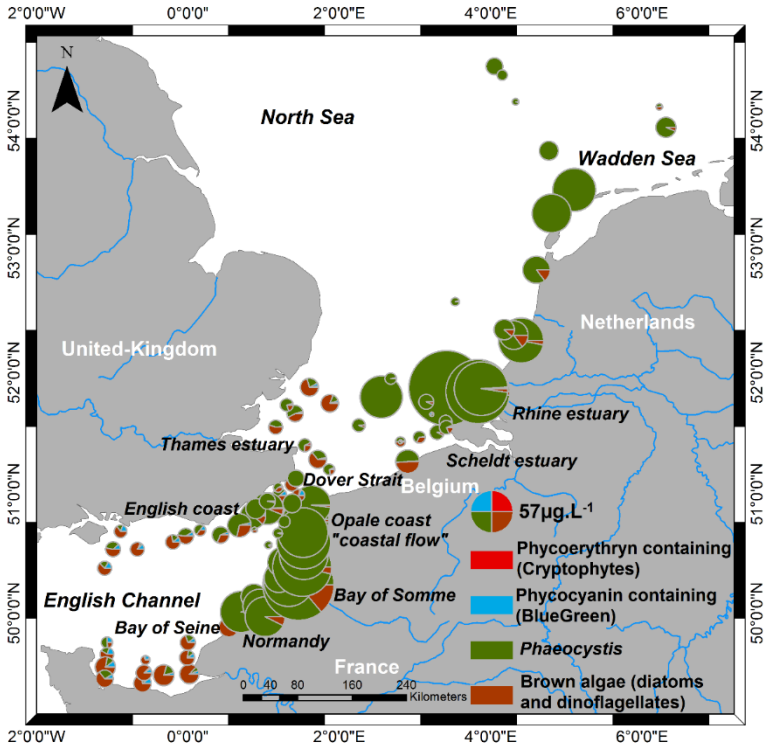

Figure 3.10: *Chlorophyll a equivalents (total and per group, right) addressed by multispectral groups fluorometry (AOA and Fluoroprobe bbe Moldaenke): discrimination of 4 pigmentary groups (Haptophytes, brown algae, phycocyanin and phytcoerythrin)*

The multi-spectral fluorometer Fluoroprobe (bbe Moldaenke) revealed the heterogeneity of up to 4 phytoplankton spectral (pigmentary) groups (**Figure 3.10**): BlueGreen algae (phycocyanin containing), Brown algae, *Phaeocystis globosa* (thanks to the implementation of a dedicated fingerprint for Haptophytes; Houliez et al., 2012) and Cryptophytes (Phycoerythrin containing). It was possible then to estimate the absolute and relative contribution of each group to total chlorophyll *a* equivalents. *P. globosa* was dominant in brackish coastal waters except in the Thames estuary and the Bay of Seine, where brown algae (mainly diatoms) dominated. Highest concentrations of chlorophyll *a* were reported around brackish waters from the Bay of Somme to the Dutch estuaries. Moreover, the high frequency acquisition performed by automated pulse shape-recording flow cytometers made it possible to detect and characterise the patchiness of phytoplankton groups (here, two potential HAB micro-algae, *Phaeocystis globosa* and *Pseudo-nitzschia* spp.; **Figure 3.11**) at sub-mesoscale from the Eastern English Channel to the Southern North Sea (Louchart et al., *in rev)*.

Through the three spring cruises (**Figure 3.12**), waters under direct brackish influence were dominated by nanophytoplankton groups (and microphytoplankton), whereas offshore waters and other coastal waters were dominated by picophytoplankton (*Synechococcus*-like and Picoeukaryotes) and coccolitophore-like (Nano-SWS). As already noticed in previous cruises (Bonato et al., 2015), eukaryotic nanophytoplankton groups were dominant in the eastern English Channel, especially in the brackish waters (i.e. “Coastal flow”) as well as off most French, English, Belgian and Dutch estuaries, whereas eukaryotic picophytoplankton groups were mostly dominant along the English coast and offshore waters of the southern North Sea. Alternance of low-high abundance (fig. 1.12) and

low-high total red fluorescence (autofluorescence of the chlorophyll *a*) evidenced spatio-temporal patches of abundance and chlorophyll *a* concentration which all occured often along the cruise, revealing large amplitude of both phytoplankton variables. Despite a dominance of eukaryotic nanophytoplankton in terms of abundance, the contribution of microphytoplankton to the total red fluorescence was the highest (data not shown, but see D4.4).

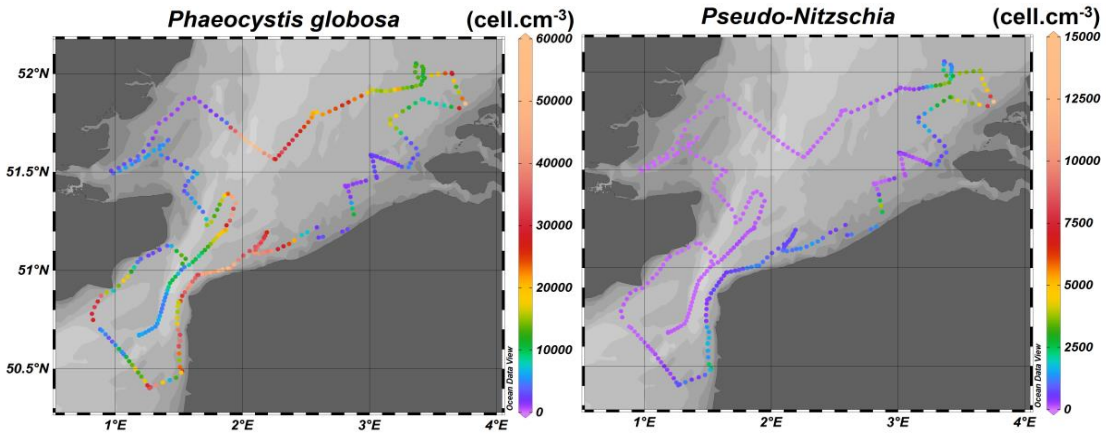

Figure 3.11: *Spatial distribution of* ***Phaeocystis globosa*** *and* ***Pseudo-nitzchia*** *spp. characterized from the eastern English Channel to the southern North Sea, during the Lifewatch- VLIZ -cruise (May 2017). Louchart et al., accepted*

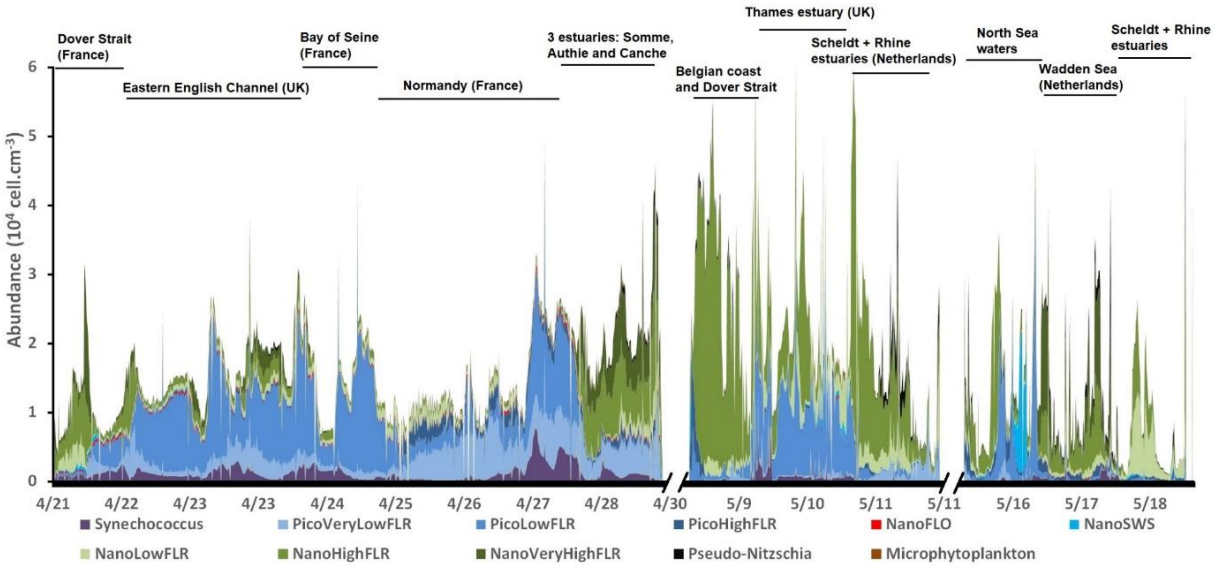

Figure 3.12: *Continuous recording of phytoplankton functional groups by automated pulse shape-recording flow cytometry during the spring bloom development from South to North: PHYCO (CNRS-LOG), Lifewatch (VLIZ) and RWS cruises (April-May 2017)- Louchart et al., in prep.*

In 2017 more than 125 FRRf profiles were performed in mixed waters as well as in stratified waters off the Thames, Schelde and Rhine estuarine waters, in parallel to light quality measurements (red-blue and green light ratio). FRRf measurements were related to changes into taxon physiology on which a variability was superimposed due to fast photoregulation, photoacclimation occuring at more or less daily time scale and stress due to high light and low nutrient concentrations. Even though not representing a real productivity index because light was different for all sampling stations, the JVPII photosynthetic parameter (Oxborough et al., 2012) was integrated over the whole water column and showed interesting differences between sampled areas (**Figure 3.13**).

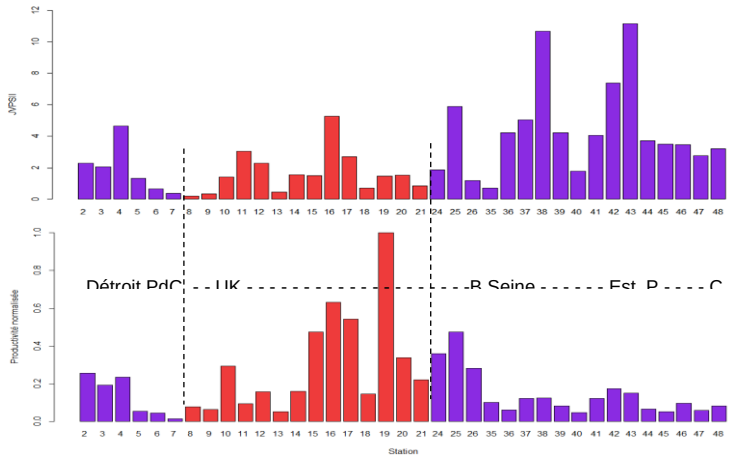

Figure 3.13: *FRRf vertically integrated JVPII photosynthetic parameter (e-.m^{-3}.s^{-1}), total and normalized by Chla, during the PHYCO cruise (April 2017).*

Figure 3.14 shows that the physiological data obtained from the profiling APD system in the water column are also well suited to globally discriminate against water bodies sampled during a large-scale spatial campaign (here the VLIZ cruise in spring 2017 in the south bight of the North Sea) even if it is well known that physiological parameters display daily cycles (see JERICO-NEXT **D3.2**, results of continuous recording in sub-surface waters). The box-plots of vertically measured data for the effective quantum efficiency (Fq'/Fm') display clear differences in medians and in distributions (interquartile ranges) between the waters of the Strait of Dover, the Thames influence area and the Dutch estuaries.

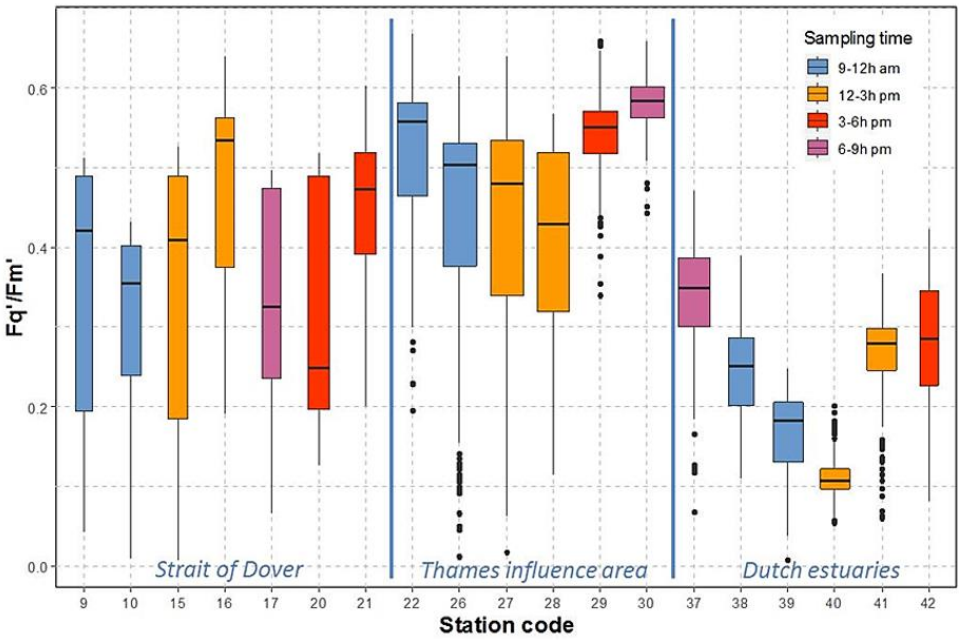

Figure 3.14*: Boxplots of effective quantum efficiency for all data measured in the water column by the FRRf APD system at 19 sampling stations, during the VLIZ cruise (May 2017)*

Mean values also significantly differed between the three areas. In addition, there was no relationship between these data distributions (box-plots) and the sampling time (cf. boxplot colour code) which is here considered as an indicator of the duration of illumination experienced by the cells. This duration could theoretically control phytoplankton physiology at the daily scale and so the extent of the vertical distribution of physiological parameters.

This lack of sampling time effect is probably due to the fact that these distributions integrate all measurements made over the ntire water column (i.e., over the whole euphotic layer), so that changes would be integrated.

3.4.6. Western English Channel – Celtic Seas Fisheries cruises.

As a part of multidisciplinary studies carried on for several years in Celtic Sea, Western Channel and North Sea, CEFAS aimed at estimating the contribution of the different phytoplankton functional types alongside with physical, biogeochemical parameters and other biological compartments including zooplankton, fish, and mammals (**Figure 3.15**). Measurements were carried on the RV Cefas Endeavour using a 4H-Jena FerryBox and a Cytosense automated pulse shape-recording flow cytometer (Cytobuoy b.v., Woerden, NL).

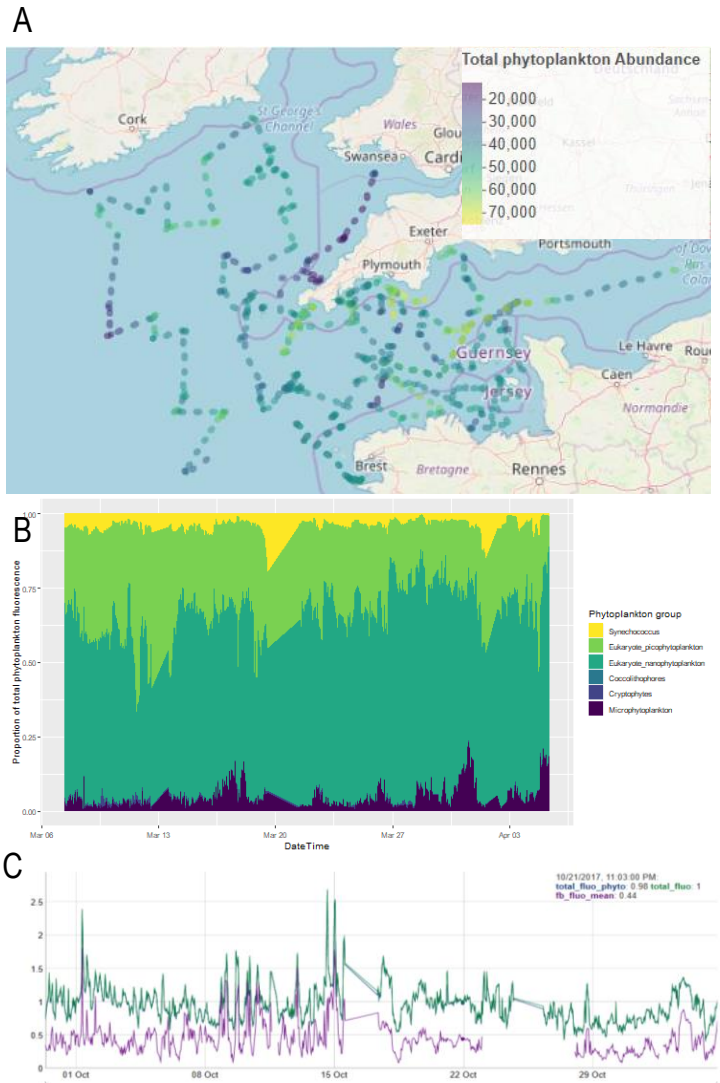

Figure 3.15: *Abundance (A), and relative contribution of the functional types (B) to the total fluorescence (C) of phytoplankton during the The International Bottom Trawl Survey in March 2017.*

Automated phytoplankton monitoring was also implemented during some French fisheries cruises as the CAMANOC cruise (mid-September-mid-Ocober 2014) from Celtic Seas and Western English Channel (WEC) to the Eastern English Channel (EEC) and the Bay of Seine (BOS). Continuous recording evidenced thermo-haline structures as fronts and gradients conditioning the distribution of phytoplankton groups defined by automated pulse shape-recording flow cytometry (CytoSense). As an example, *Synechococcus* spp. (picocyanobacteria) abundance showed great patchiness by and between frontal systems (**Figure 3.16**). At the opposite size class, microphytoplankton showed also higher abundance by the thermal front (Louchart et al., *in revision*).

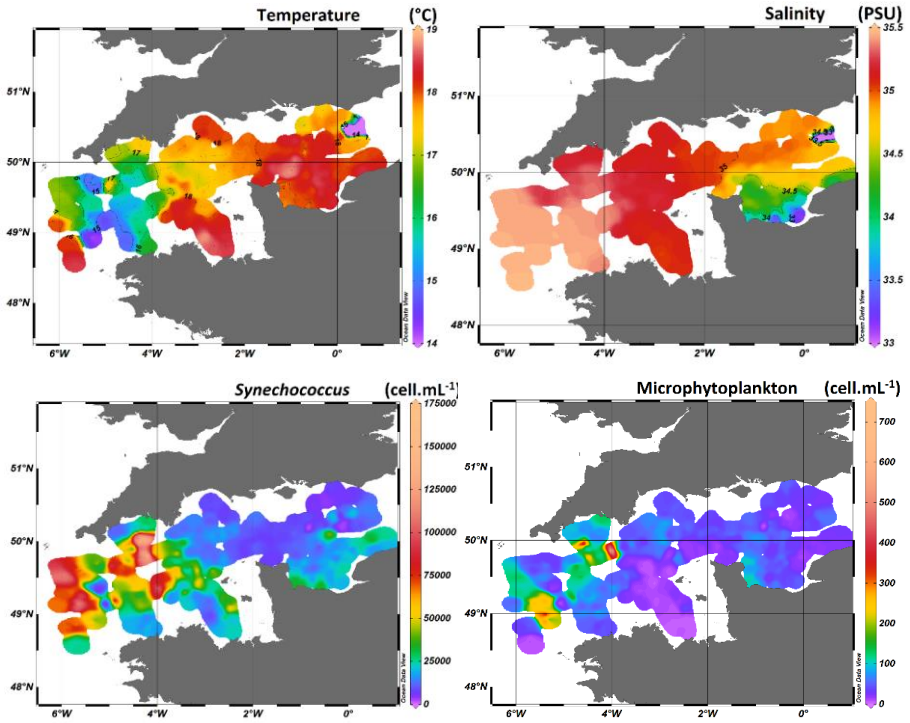

Figure 3.16: *Spatial distributions of temperature (A), salinity (B),* Synechococcus*-like (picocyanobacteria; C) and microhytoplankton (D) addressed by automated pulse shape-recording flow cytometry during the CAMANOC cruise (IFREMER, September-October 2014).*

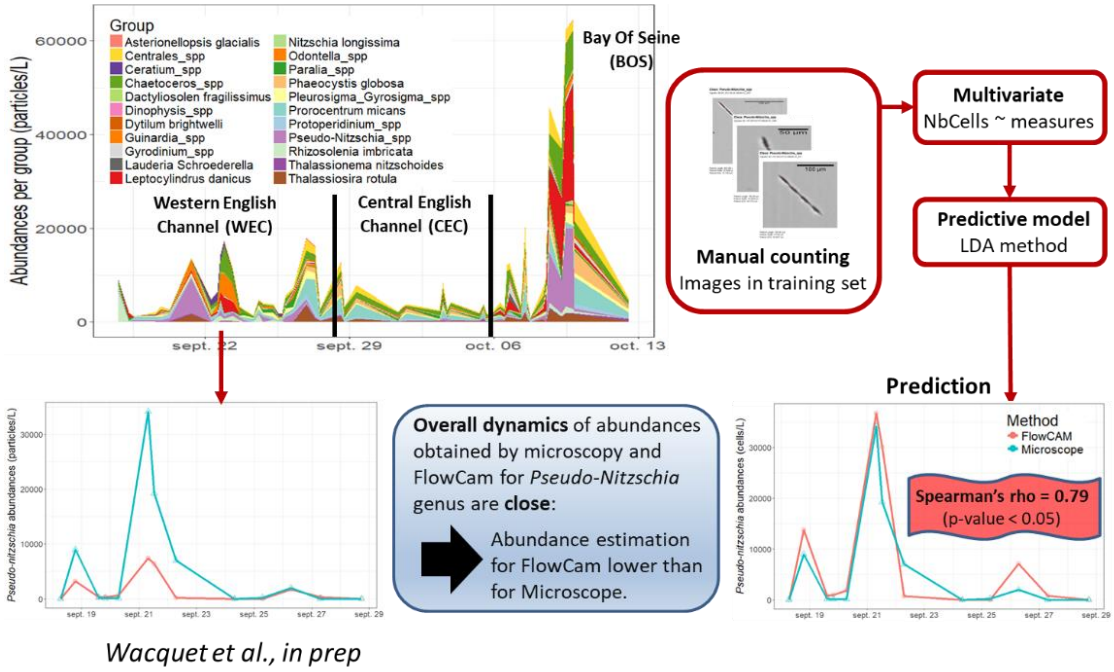

Figure 3.17: *Example of the application of an automated discrimination and classification tool (ZooPhytoImage) to charcaterize the spatial phytoplankton abundance per taxa during the CAMANOC cruise ("Thalassa" R.V., Sept-Oct 2014).*

Moreover, different semi-automated tools were applied to the *in vivo* image dataset acquired with the FlowCam instrument during the CAMANOC cruise in order to evaluate their operational ability to monitor the diversity of samples for the microphytoplankton, and especially to detect, track and count the most frequent potentially harmful

algae found in this area at that period, like species belonging to *Pseudo-nitzschia*, *Dinophysis*, *Prorocentrum* and *Phaeocystis* genera (Wacquet et al., *in rev*). A distribution of these target groups was computed which highlighted different sub-regions in the English Channel during the late summer-fall transition (**Figure 3.17**).

3.4.7. Western Mediterrranean.

In the frame of both JERICO-NEXT and the A*MIDEX CHROME project (leader, CNRS MIO), a ferrybox (4H JENA) coupled with an automated flow cytometer (Cytobuoy b.v.) was installed onboard of the "Le Carthage" (Compagnie Tunisienne de navigation). This ship crossed the Western Mediterranean Sea from Marseille to Tunisia and from Tunisia to Genova 4 times a week. The project, in collaboration with the Institut des Sciences de la Mer de Tunisie (C.Sammari), yealded to two succesfull coupling (March 2016 and October-January 2016-2017). Improvements of combined phytoplankton and hydrological data observation from a fully sub mesoscale analysis system were possible thanks to a continuous flowthrough of seawater and a succession of sensors. The adaptation of the Ferrybox system was possible to resolve the meso scale distribution of phytoplankton functional groups to to the speed of the ship. A total of 400 samples, i.e.80 samples per crossing, were collected. Results concerned the period between the end of fall to the mid-winter conditions (**Figure 3.18**), where the decrease of surface temperature related to deepening of the mixed layer depth follows a north-south gradient. The increase of fluorescence could be linked to the first steps of the Mediterranean spring blooms, with sooner and higher values of chlorophyll a in the south (Fluorescence values (u.a.)). The automated flow cytometry resolved *Prochlorococcus, Synechococcus*, picoeukaryotes, nanoeukaryotes and microeukaryotes. Thanks to this unique high resolution coverage, a focus can be done on the impact of strong wind events occuring at the Bonifacio strait, east of Corsica (41-42 °N), known to trigger upwellings, generating increases in phytoplankton. Picoeukaryotes and nanoeukaryotes groups reacting are typical of Mediterranean Sea dominant groups.

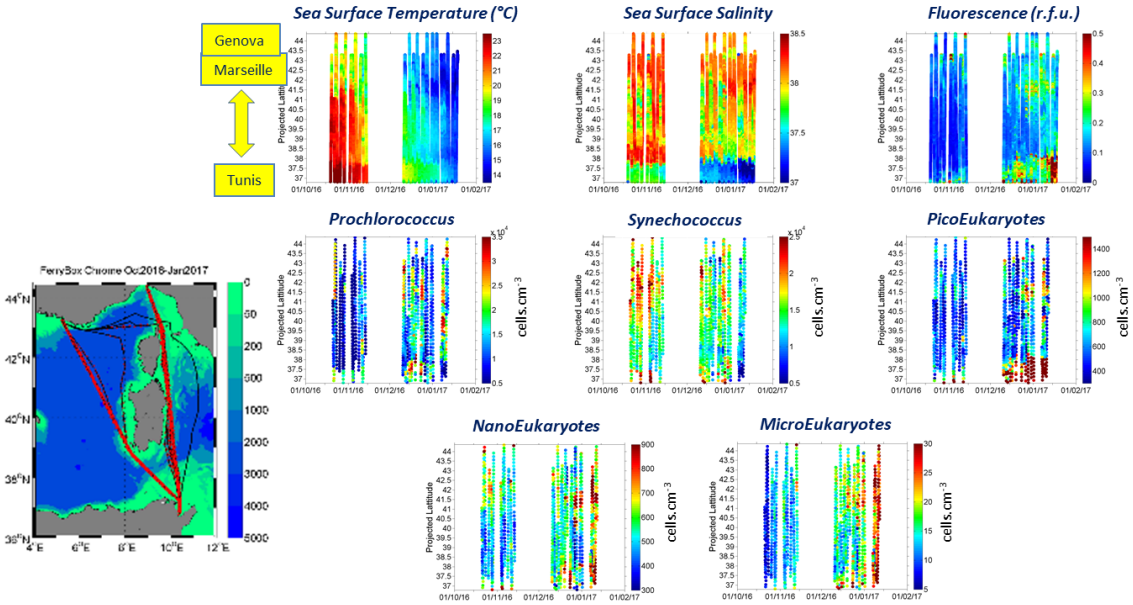

Figure 3.18: *Ferry (Cartaghe) routes and results of the four-month continuous recording of sub-surface waters with an automated flow cytometer (CytoSense).*

3.5. Main inputs relative to initial specific objectives

A combination of automated tools made it possible to address both taxonomical and functional diversity (including size-classes and pigmentary groups, but also optically defined groups) of phytoplankton. A comparison of the advantages and weaknesses of both automated and reference techniques was made in JERICO-NEXT Deliverable **D3.1** and is shown again hereby (**Table 1.2**). Moreover, we also explored and implemented different techniques of variable/active fluorescence in order to address photosynthetic properties of living cells in-flow or *in*

situ in order to estimate phytoplankton productivity (both potential and current) and to complete the study of phytoplankton dynamics in different marine coastal ecosystems.

Table 3.2: *Overview of methods for observing phytoplankton biomass, abundance and biodiversity. Not all methods were used in JERICO-NEXT*

Method	Biodiversity	Biomass estimates	Functional groups	Sample throughput	Level of automation	Horizontal coverage
Light microscopy	Good	Good	Good	Low	Low (automated water sampling is available)	Low
Fluorescence microscopy	Medium	Medium	Medium-Good	Low	Low	Low
Electron microscopy	Very good	Medium	Low	Very low	Low	Low
Flow cytometry	Low-Medium	Medium	Good	Hiigh	Semi-automated on research vessels and/or in fixed stations	Medium (Ferrybox)
Imaging flow cytometry	Medium-Good	Medium-Good	Good	Medium	Semi-automated on research vessels and/or in fixed stations	Medium (FerryBox)
Gene probes	Medium (only a limited number of species)	Low-Medium	Medium	Medium	Semi-automated (ESP)	Low-medium
Barcoding	Good	Low	Medium	Medium	Automated sampling an preservation in development	Low-medium
Chlorophyll a analyses (water sampling)	-	Medium	-	Low-Medium	Low (automated water sampling is available)	Low-Medium
HPLC-analysis of photosytnhtetic pigments	Low-medium	Medium	Medium (pigment groups)	Low	Low (automated water sampling is available)	Low
In vivo fluorescence methods based on the fluorescence of photosynthetic pigments	Low-Medium	Medium	Low-Medium	High	High	High
Methods based on the absorbance of photosynthetic pigments	Low-Medium	Medium	Low-Medium	High	High	Medium-high
Satellite remote sensing (ocean colour-reflectance of photosynthetic pigments	Low	Medium	Low	High	Yes	High (during cloud free conditons)

The main conclusion from the results gathered within JRAP 1 is that it is highly recommended to include estimates of phytoplankton diversity (both taxonomical and functional), abundance, biomass and productivity in automated coastal ocean observing systems:

- Automated tools for *in vivo* observation of phytoplankton abundance and diversity in near real time are being implemented in a more or less autonomous way, depending on the characteristics of platforms and of techniques, giving new insights into their dynamics and spatial variability, at fine scales.
- Mono- or Multispectral techniques allow to follow the distribution of different phytoplankton pigmentary groups as green, blue-green, red and brown algae or other groups discriminated by their pigment content.
- Imaging in-flow systems (and, to some extent, *in situ* imaging for bigger particles) give information at the genus and, when possible, at the species level.

- Functional groups based on size and pigment content are discriminated by automated pulse shape-recording flow cytometry (see also **Table 3.3**) to at least four main categories
  - ✓ Phototrophic pico-eukaryotes
  - ✓ Phototrophic cyanobacteria
  - ✓ Phototrophic nano-eukaryotes
  - ✓ Phototrophic micro-eukaryotes
- Harmful Algal Blooms can be monitored using automated methods - early warnings are feasible
- Theres is still a need for sharing best practices for the use and analysis of data from multispectral fluorometers as well as for the calibration of fluorometry measurements to be able to build inter comparible databases.
- Photosynthetic status of phytoplankton can be addressed *in vivo* in real time and high frequency. There is still need to share best practices and to build a common database.
- There is a need for further development of joint image database for improving the already developed classifiers for automated species/genus identification.
- There is a need to strengthen collaboration between users of automated pulse shape-recording flow cytometry in shared databases (including optical fingerprints) for improving the already developed classifiers for phytoplankton functional groups.
- One instrument/method does not solve all problems, which means that a particular combination of methods is required depending on the nature of phytoplankton blooms to be tracked and the ecological and hydrodynamic characteristics of the considered coastal marine ecosystem.

***Table 3.3**: Main phytoplankton functional groups based on automated pulse shape-recording flow cytometry*

Cluster	Length FWS	Standardized name (BODC)	Phytoplankton functional group
Pico-Synecho	<3.3µm	*Synechococcus*	*Synechococcus* (pico-cyanobacteria)
Pico-Red	<3µm	Eukaryote picophytoplankton	Autotrophic Pico-eukaryotes (Chlorophytes, Chrysophytes, Prasinophytes, etc.)
Nano-Red	[20 - 3µm]	Eukaryote nanophytoplankton	Small diatoms, dinoflagellates, haptophytes, Prasinophytes, Chlorophytes, etc.
Nano-Crypto	[20 - 3µm]	Cryptophytes	Cryptophytes
Nano-Cocco	[20 - 3µm]	Coccolithophores	Coccolithophores
Micro-Red	>20µm	Microphytoplankton	Autotrophic micro-eukaryotes (Diatoms, dinoflagellates, colonial haptophytes, etc.)

An important aspect is that natural variability can be better resolved using the novel automated methods. This means that averages of the conditions of whole sea basin can be based on hundreds or thousands of samples instead of a handful that is the case suing traditional microscope-based methods. It also means that temporal variability can be resolved in a much higher detail than earlier. Algal blooms have a duration of on or a few weeks. The traditional monthly sampling misses most blooms while frequent automated sampling will observe most of them. The temporal variability is thus much better resolved and meaningful averages can be calculated.

Moreover, automated techniques can give new insights into phytoplankton dynamics and diversity by considering both pico and nanoplankton, usually ignored or misregarded by traditional methods, as well as physiological status and potential productivity, most of the times lacking in current monitoring programmes. Moreover, functional groups were addressed according to their optical features, mostly corresponding to functional traits that need further consideration in ecological studies. .

3.6. Analysis of the experience gained

3.6.1. Developing innovative technologies for coastal ocean observing and modelling.

Within JRAP 1, we implemented different automated or semi-automated approaches for improving the temporal and spatial resolution of phytoplankton observations based on different plarforms: research cruises, fixed platforms, moorings and/or ships of opportunity. The objective was to gain new insights into the functional diversity and photosynthetic status of phytoplankton communities in different environmental and hydrological conditions.

Innovative techniques were explored, inter compared and, for some of them, improved, in order to apply the most standardized operational procedures as possible. The diversity of tested sensors sometimes complicated the obtention of comparable results. Nevertheless, during some inter comparison exercises or joint implementation, we succeeded in producing such results, which led to common characterizations of the taxonomical and functional diversity of phytoplankton natural communities from different regions and marine ecosystems (i.e., from oligotrophic and mesotrophic to eutrophic conditions, and from brackish to saline systems).

Analytical developments on already existing and commercial or on recently developed software tools, made it possible to consider common applications for the three main methodological approaches considered: single-cell/colony images (automated imaging inflow and/or *in situ* acquisition, single-cell/colony optical profiles and features (automated pulse shape-recording flow cytometry) and bulk fluorescent or absorption properties of inflow and/or *in situ in vivo* sampling.

Coastal areas see large gradients in phytoplankton biomass, diversity and also physiological conditions. A clear protocol was set up for both in-flow continuous recording of photosynthetic parameters (for which some extra measurements are still to be done in parallel on filtered water) and on profiling systems. When automated underway measurements are made, they require adjustment of instrument sensitivity and adjustment of the LED output used to generate the fluorescence induction curves. Fortunately, the FastOcean sensor, in contrast to its predecessors, have an inbuild routine to so that these settings (autoPMT and autoLED) are optimized during the operation.

Some gaps are however still to be considered, and there is a clear need in continuing the work initiated before and within JERICO-NEXT and to open the improvements to the whole coastal observation community in order to improve the resolution and understanding of phytoplankton dynamics, in connection with the requirements of environmental managing at a regional, national and international level. A first challenge consists in improving automation of techniques and sensors to allow for longer lasting measurements. Analytical tools need also to be pull out to the status of being available to the whole community, which requires to provide support to their use and rationales for their selection, which should clearly result both from the question to be tackled and the characteristics (including previous knowledge regarding phytoplankton diversity and variability) of the considered system.

3.6.2. Establishing observing objectives, strategy and implementation at the regional level.

The spatial scale addressed by JRAP 1 concerned from local (fixed platforms or moorings in the Baltic, the Skagerrak, the North Sea, the Channel) to regional (Eastern-Channel-Southern North Sea, Skagerrak-Kattegat) and whole seas (Baltic Sea, North Sea, English Channel, Western Mediterranean Sea) scales.The three approaches made it possible to test the implementation of automated techniques to answer local, regional and whole seas questions about phytoplankton fine spatial and temporal distribution and dynamics and to test the limits of the use of the different types of techniques to address these main questions in the different systems, at the different time and spatial scales considered.

Moreover, based on the use of high resolution and multivariate data generated by automated techniques, new numerical methodologies make it possible to define eco-hydrodynamic regions from large to small spatial scales (hundreds of meters). This ecoregion approach will facilitate transboundary collaborations for a better integrated, harmonized and standardized definition of monitoring strategies. Beyond the improvement of scientific knowledge within contrasted environments, this will support, for example, the MSFD Good Ecological Assessment and the OSPAR (but also HELCOM and Barcelona Convention) Common Procedures implementation

3.6.3. ***Enhancing integrated coastal ocean monitoring and interfacing with other ocean observing initiatives operating at different spatiotemporal scales.***

JRAP 1 has benefited, in some regions as the Skagerrak-Kattegat, the Baltic, the North Sea, and to a lesser extent in the Southern Bay of Biscay and the Cretan Sea, of physical (JRAP 4) and/or chemical/physical (JRAP 5) ongoing measurement campaigns recording physical properties and currents together with chemistry, pCO_2 exchanges and/or phytoplankton diversity and dynamics. Integration proved difficult within the framework of JERICO-NEXT because disciplinary consortia first needed to be strengthened. Even though some new combinations (as pCO_2 and single-cell phytoplankton analysis were initiated (Marrec et al., 2018), one way forward clearly consists in strengthening these links within local, regional and international monitoring strategies, combining physical-chemical and biological assessment (i.e. hydrodynamics, pCO_2 exchanges, phytoplankton diversity and productivity), wider exploring of microbial and plankton diversity (i.e. by the application of molecular methods) and pelagic-benthic coupling.

JRAP 1 represent an example of the implementation of automated novel technologies in different coastal marine systems and different platforms, providing new information on phytoplankton dynamics, spatial variability and functional groups that are being used within the EU MSFD in order to support discussions on their application to Pelagic Habitats and Food Webs indicator calculation and on their possible implementation into national monitoring programs, particularly for Descriptor 1 Pelagic Habitats and Descriptor 5 Eutrophication + links with Hydrological conditions (D7) and Food Webs (D4)). JERICO-NEXT JRAP 1 experience was also used to support discussions about the general monitoring strategy in the whole English Channel and southern bight of the North Sea, discussions and common work that was started within the INTERREG IVA "2 Seas" DYMAPHY project (2010-2014) and which continued and was extended during JERICO-NEXT. Existing monitoring systems combined with very promising perspectives from JERICO-NEXT allowed regional scientific teams (Institutes, Universities, National Research Councils) to propose a new step towards an integrated (Biology/Biogeochemistry/Physics) monitoring program in the different areas. Moreover, OSPAR, HELCOM and Barcelona conventions of regional seas are, to some extent and taking into consideration their own particularities, also supporting new approaches for monitoring the ecological status of coastal and open seas as well as transition (estuarine) waters as well as regional and national environmental and water agencies.

3.7. Proposition of a future monitoring strategy for the topic

It should be stressed that one monitoring strategy does not cover all aspects of monitoring of phytoplankton dynamics, biodiversity and harmful algal blooms. In the following partly different strategies are therefore proposed depending on the goal of the monitoring.

Phytoplankton and harmful algal blooms are not evenly distributed in time and space. Resolving the variability fully is not feasible due to costs and limitation in technology. Different strategies are needed in different sea areas due to regional conditions. The following general strategy is recommended:

- Maintain and further develop existing long-time series that include phytoplankton abundance, diversity and biomass, from weekly to monthly sampling and addressed by reference techniques (microscopy, pigments). These time series are essential to follow and understand effects of climate change and other long-term effects of anthropogenic activities.
- Incorporate automated phytoplankton observations in FerryBox systems (in both research vessels and ships of opportunity as ferry lines) and fixed platforms (dry or immerge d) in all European coastal seas. This should be a part of regional ocean observing systems contributing to UNESCO-IOC Global Ocean Observing System and the UN Decade of Ocean Science for Sustainable Development.
- Investigations of total biomass of phytoplankton:
  - ✓ Combine measurements of chlorophyll *a*-based multispectral absorption with chlorophyll *a* from water samples. Rationale: Results from PSICAM (commercial version Trios OSCAR) show a strong

correlation with chlorophyll a from water samples analysed in the laboratory after filtering samples. Disadvantage: multispectral absorption instruments requires frequent cleaning
- ✓ Combine measurements of chlorophyll *a,* based on chlorophyll *a* fluorescence with chlorophyll *a* extracted from water samples. Rationale: chlorophyll fluorometers are relatively low coast and can be deployed on multiple platforms if anti fouling measures are properly used and if fluorometry is calibrated with an external source of fluorescence.
- ✓ Use automated *in situ* imaging systems to measure cell volume to calculate total biomass.
- ✓ Use automated pulse shape-recording flow cytometry to measure total red fluorescence (chl. fluorescence) of the whole size spectra of phytoplankton an define the contribution of each size/pigmentary fraction to total signal. Explore other ways of addressing phytoplankton biomass from optical signals (Haraguchi et al., 2018) and/or DNA content-derived C (Owen, Ph.D. Thesis).
- ✓ Reference samples: traditional microscopy with analyses of taxa at the species level and measurements of cell volumes, at least for micro- and the biggest fraction of nanophytoplancton.
- ✓ Combine the results from a-e with satellite remote sensing

➢ Phytoplankton diversity and non-indigenous species
- ✓ Use a combination of methods based on morphology (imaging), optical signatures (automated flow cytometry) and genes
- ✓ Automated or manual water sampling
- ✓ Light microscopy (reference samples and continuation of long time series)
- ✓ Imaging in flow methods for automated analyses of abundance and diversity
- ✓ Automated pulse shape-recording flow cytometry for optical characterisation and discrimination (abundance, size, status)
- ✓ Metabarcoding of selected genes for analysis of diversity (note: this only gives relative abundance of genes)
- ✓ Electron microscopy on selected samples, e.g. for quality control and identification of non-indigenous species
- ✓ Combine both bottle sampling with phytoplankton nets (20µm mesh) in order to gather also species that do not bloom and which are less concentrated than the usual cells and which can represent non indigenous potentially invasive species.

➢ Functional groups
- ✓ Use automated flow cytometry for discriminating phytoplankton groups based on size and pigmentation, as well as on other optical properties (see **Table 1.3**)
- ✓ Use automated imaging in flow or *in situ* systems for discriminating organisms at the species or genus level – aggregate data to functional groups according to size and algal group, e.g. dinoflagellates, diatoms, cyanobacteria, haptophytes, other flagellates, etc.
- ✓ Functional groups based on fluorescence of different pigments has value, especially for in estuarine and coastal sea areas. Phycocyanin fluorescence is a useful proxy for certain cyanobacteria. Phycoerythrin fluorescence is a proxy for some other cyanobacteria but also for the photosynthetic cilate *Myrionecta rubra* (*Mesodinium rubrum*).

➢ Harmful Algal Blooms (HABs)
- ✓ HABs observations should include identification of species, see item IV.
- ✓ HABs warning systems must produce in near real time to be meaningful
- ✓ Low biomass HABs (e.g. causing shellfish toxicity) are most often observed by manual microscope analyses of water samples. They can be observed using automated *in situ* imaging systems. In parallel, molecular methods are in development and may be useful tools in the future
- ✓ High biomass HAB (as well as some phytoplankton functional types defined from optical properties) can be observed using a combination of *in situ* observations and remote sensing

➢ Phytoplankton photosynthesis and primary productivity
- ✓ The results of JRAP 1 clearly show the potential of in-flow automated measurements of primary production based on FRRF or similar active fluorescence based measurements.
- ✓ On the other hand, there is a need to also consider the vertical dimension of primary productivity even though automation is not possible and there.

- ✓ The FRRF method allows absolute estimates of photosynthetic electron transport. To be transformed into primary productivity, there is a need to define the electron requirement for C-fixation ($\Phi_{e,C}$). The issue is that not all electrons produced in PSII are used for C-fixation (some electrons are used for other assimilatory purposes like the reduction of nitrate or sulphate).
- ✓ Values < 10 are normally observed for the coastal seas, thus for the areas examined by the JERICO-NEXT campaigns. For investigation of $\Phi_{e,C}$ samples were taken during the cruises, but they have to be analysed yet. The ultimate goal is to predict $\Phi_{e,C}$ based on abiotic factors and biotic factors obtained from flow cytometry.
- ✓ To obtain the most accurate estimation of the photosynthetic quantum efficiency in-flow measurements, there is a need to avoid any non photosynthetical quenching (NPQ). This is one of the topics of the SCOR working group 156 On "Active Chlorophyll fluorescence for autonomous measurements of global marine primary productivity"
- ✓ Carrying out good blanks is a pre-requisite to avoid background fluorescence of dissolved organic matter, but difficult to do on automated systems, especially when using ships-of-opportunity.
- ✓ Even with very precise ETR estimates the relationship with measured C-fixation rates will contain noise, due to the inherent "problems" of the C14 (or C13) method. Therefore, one might consider that FRRF give true estimates of gross photosynthesis, so even in the absence of conversion to C-units it can be used to estimate change in primary production thus to estimate changes in the potential carrying capacity of an aquatic ecosystem.

3.8. References

Aardema, H. M., Rijkeboer, M., Lefebvre, A., Veen, A., and Kromkamp, J. C. (2018) High resolution *in situ* measurements of phytoplankton photosynthesis and abundance in the Dutch North Sea, *Ocean Sci. Discuss., https://doi.org/10.5194/os-2018-21.*

Bonato S., Christaki U., Lefebvre A., Lizon F., Thyssen M. & Artigas L.F. (2015) High spatial variability of phytoplankton assessed by flow cytometry, in a dynamic productive coastal area, in spring: the eastern English Channel. *Estuarine Coastal and Shelf Science*, 154: 214-223.

Haraguchi, L., Jakobsen, H., Lundholm, N., & Carstensen, J. (2017) Monitoring natural phytoplankton communities: A comparison between traditional methods and pulse-shape recording flow cytometry. Aquatic Microbial Ecology, 80(1), 77-92

Kruskopf M, Flynn KJ. 2006. Chlorophyll content and fluorescence responses cannot be used to gauge reliably phytoplankton biomass, nutrient status or growth rate. New Phytologist 169:525-536

Lefebvre A. and Poisson-Caillault E. (2019) High resolution overview of phytoplankton spectral groups and hydrological conditions in the eastern English Channel using unsupervised clustering. Marine Ecology Progress Series, 608, 73-9.

Louchart A., Lizon F., Lefebvre A., Didry M., Schmitt F.G. and Artigas L.F. Phytoplankton distribution at sub-mesoscale across frontal systems during the summer-fall transition in the English Channel revealed by high-frequency automated flow cytometry. *In revision for Continental Shelf Research*

Louchart A., de Blok R., Debuschere E., Gómez F., Lefebvre A., Lizon F., Mortelmans J., Rijkeboer M., Deneudt K., Veen A., Wacquet G., Schmitt F.G. and Artigas L.F. Automated techniques to follow the spatial distribution of *Phaeocystis globosa* and diatom spring blooms in the English Channel and North Sea. *In revision for Proceedings of the ICHA 2018, Nantes.*

Marrec, P., Grégori, G., Doglioli, A. M., Dugenne, M., Della Penna, A., Bhairy, N., Cariou, T., Hélias Nunige, S., Lahbib, S., Rougier, G., Wagener, T., and Thyssen, M. (2018) Coupling physics and biogeochemistry thanks to high-resolution observations of the phytoplankton community structure in the northwestern Mediterranean Sea, Biogeosciences, 15, 1579–1606, https://doi.org/10.5194/bg-15-1579-2018.

Owen, K. Flow cytometruc investifation of the size spectrum of North Sea phytoplankton communities (2014) Doctoral thesis, University of East Anglia.

Oxborough K, Moore CM, Suggett DJ, Lawson T, Chan HG, Geider RJ. (2012) Direct estimation of functional PSII reaction centre concentration and PSII electron flux on a volume basis: a new approach to the analysis of Fast Repetition Rate fluorometry (FRRf) data. Limnology and Oceanography-Methods 10:142-154

Rytövuori S. (2017) Detection of picocyanobacteria and other algae containing phycoerythrin pigment in the Baltic Sea. MSc Thesis, University of Helsinki, *in Finnish*. http://urn.fi/URN:NBN:fi:hulib-201705174155

Seppälä J., P. Ylöstalo. and H. Kuosa (2005) Spectral absorption and fluorescence characteristics of phytoplankton in different size fractions across the salinity gradient in the Baltic Sea. International Journal of Remote Sensing 26, 387-414

Seppälä J., P. Ylöstalo, S. Kaitala, S. Hällfors, M. Raateoja and P. Maunula (2007) Ship-of-opportunity based phycocyanin fluorescence monitoring of the filamentous cyanobacteria bloom dynamics in the Baltic Sea. Estuarine, Coastal and Shelf Science, 73, 489-500.

Sosik H.M. and R.J. Olson (2007) Automated taxonomic classification of phytoplankton sampled with imaging-in-flow cytometry. Limnol Oceanogr Methods 5: 204-216

Wacquet G., Lefebvre A., Blondel C., Grosjean P., Neaud-Masson N., Belin C. Artigas L.F. Combination of machine learning methodologies and imaging-in-flow systems for the automated detection of Harmful Algae. *In revision for Proceedings of the ICHA 2018, Nantes.*

Wollschläger J., R. Röttgers, W. Petersen and O. Zielinski (2019) Stick or dye: evaluating a solid standard calibration approach for point-source integrating cavity absorption meters (PSICAM*). Frontiers in Marine Science*, https://doi.org/10.3389/fmars.2018.00534

3.9. Abreviations

AOA: Algae Online Analyzer
CTD: Conductivity-Temperature-Depth sensor
ETR: Electron Transport Rate
FB: FerryBox
FRRf: Fast Repetition Rate fluorometer
HAB: Hamful Algal Blooms
MSFD: Marine Strategy Framework Directive
PSFCM: Pulse Shape-Recording Flow Cytometry
Phyto-PAM: Phytoplankton Pulse Amplitude Modulated sensor
WFD: Water Framework Directive

4. JRAP 2: Monitoring changes in macrobenthic biodiversity. Assessing potential environmental controls and functional consequences

Contributors
Antoine Grémare, Bruno Deflandre, sabine schmidt, Frédéric Garabétian, Christophe Fontanier, Nicolas Lavesque, Pascal Lebleu, Hervé Deriennic, Guillaume Bernard, hélène Moussard Rémi Sinays, Bastien Lamarque, **CNRS-UB, France**
Jacques Grall, Vincent Le Garrec, Gabin Droual, Alizé Bouriat, Marion Maguer, Erwan Amice, Thierry Le Bec, Emilie Gossteffan, Isabelle Bihannic, **CNRS-UBO, France**
Antoine Carlier, **IFREMER, France**
Christos Arvanitidis, Christina Pavloudi, **HCMR, Greece**

4.1. Topic and specific objectives.

One of the major challenges of today's science consists in identifying the causes of current diversity loss and the interaction linking biodiversity and ecosystem functioning (Naeem et al. 1994, Naeem & Li 1997, Naeem & Hahn 2000, Naeem & Wright 2003). Marine ecosystems are among the most productive on earth (Poore & Wilson 1993). Their role in controlling major biogeochemical cycles is well acknowledged so as their contribution to human food sources (Costanza et al. 1997). Coastal ecosystems contribute for about half of the mineral carbon fixed by the world's ocean and for about 90% of the remineralization achieved in marine sediments (Wollast 1998). Their biodiversity is now clearly at threat due to a large variety of disturbances including eutrophication (Diaz & Rosenberg 1995), contaminantion (Dauvin 1998), overfishing (Pauly et al. 1998, Jackson et al. 2001) and habitat loss (Short & Wyllie-Echeverria 1996). Benthic species especially suffer from those disturbances because of their low mobility (Solan et al. 2004). The analysis of the species composition of benthic macrofauna is therefore classically used as an indicator of the ecological quality status (ECOQ) of benthic habitats due to its response to a large variety of disturbances. There is therefore an increasing need for the assessment of benthic diversity due to the increasing awareness of its decline and the rise of corresponding remediation procedures (including both the Water Framework Directive (WFD) and the Marine Strategy Framework Directive (MSFD) as far as coastal seas are concerned).

The collection, preparation and analysis of samples in view of benthic macrofauna composition assessments involve long and tedious procedues (i.e., sieving, manual sorting, species determination based on morphological criteria requiring specific and currently declining expertise). Overall, this clearly limits the number of samples that can be processed both in terms of time and money. Such a monitoring at the European scale would require an effort exceeding by far available time and financial capacities. There is therefore a strong need for identifying new methodologies and/or proxies of benthic macrofauna composition. Several methodological developments including the use of imaging and molecular techniques have been recently developed to infer benthic biodiversity and biogeochemical processes at a lower cost. Some of these developments have been achieved within the JERICO and JERICO-NEXT projects (Romero-Ramirez et al 2013 & 2016). There is however still a clear need for surveys comparing the benthic diversity assessments obtained using these new approaches and the classical one.

An approach in view of monitoring the consequences of changes in benthic diversity on the ECOQ of benthic habitats is to: (1) assess the relationship linking disturbance intensity, benthic diversity and ECOQ, (2) monitor disturbance intensity, and (3) use it as a proxy. In coastal seas, this approach is complicated by the spatial heterogeneity and the strong temporal dynamics of both disturbances and benthic communities. It requires to develop approaches allowing for a sound assessment of spatio-temporal changes in disturbance intensity, and to articulate the monitoring of benthic fauna composition with those of changes in the nature and the intensity of the main postulated disturbance.

According to the MSFD, benthic processes are also key constituents in defining a good ECOQ, which raises the question of the relationship between benthic diversity and ecosystem functions. This is classically tackled through *ex situ* experiments during which the same function is measured within different species assemblages differing in species richness. This approach has led to rather erratic results (Emmerson et al. 2001), partly because of the low number of species and individuals that can be manipulated. Moreover, the experimental approach lies in

the fact that it does not allow for the proportion of the natural variance of the function that is effectively due to changes in biodiversity (i.e., relative to environmental changes taking place in the field). An alternative consists in carrying out comparative field measurements of benthic diversity and function and to derive their relationship based on the hierarchical approach put forward by Zajac & Whitlatch (1985) to infer the determinism of soft bottom secondary succession.

Within this general framework, JRAP 2 was aiming at tackling three main questions:

- **Q1**: Do alternative techniques (i.e., both metabarcoding and imaging techniques) provide sound surrogates for the classical analysis of benthic macrofauna composition?
- **Q2**: Irrespective of the nature of the disturbance, does the relationship between disturbance intensity and benthic diversity follow the same pattern?
- **Q3**: What are the functional consequences of a benthic macrofauna diversity loss on ecosystem functioning?

4.2. Overall structuration and strategy

The strategy put forward by JRAP 2 to tackle these questions was based on the achievements of 4 research actions corresponding to 4 different ecological contexts including the nature of the main postulated disturbance (**Figure 4.1**):.

- The impacts of spatio-temporal changes in continental inputs originating from the Gironde River on benthic diversity and functioning were studied in the West Gironde Mud Patch. (**Action 1**)
- The impact of spatio-temporal changes in clam dredging intensity on the structuration of maerl beds and the composition of the hosted benthic fauna was studied in the Bay of Brest. (**Action 2**)
- The impact of spatial changes in the abundance and the vitality of an invasive species (the slipper limpet *Crepidula fornicata* was studied in the Bay of Brest as well. (**Action 3**)
- The impact of a sewage output on benthic microbial community composition was studied in the Heraklion Gulf. (**Action 4**)

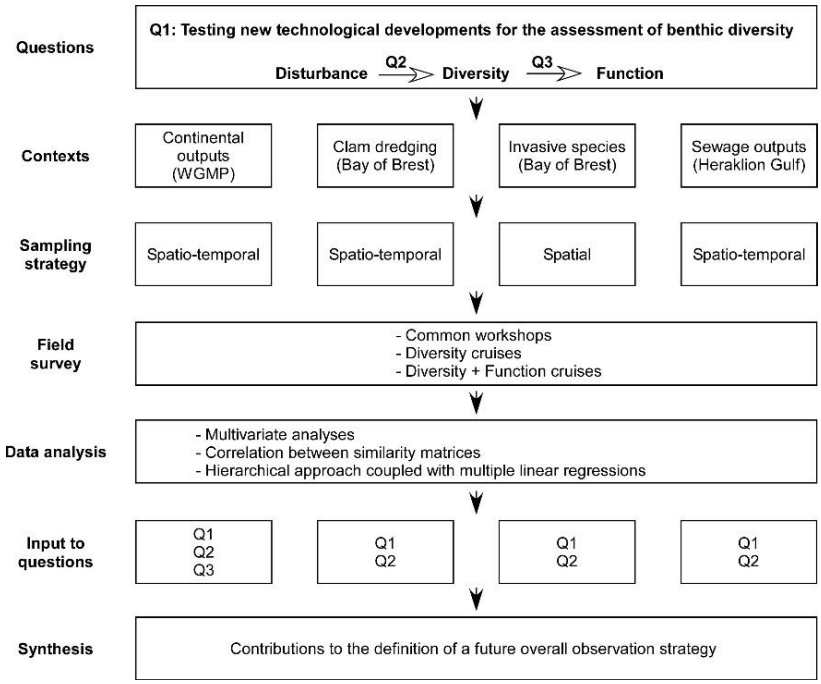

***Figure 4.1**: Presentation of the overall structuration and strategy of JRAP 2.*

All four actions allowed for field-testing of recent technological developments (sediment imaging and metabarcoding).

4.3. Achieved actions

Overall, thirteen cruises were achieved during JRAP 2. The sampling plan of each action and the overall time schedule are presented in **Figure 4.2**.

4.3.1. West Gironde Mud Patch.

Four seasonal cruises were achieved within the West Gironde Mud Patch between October 2016 and April 2018, which allowed covering the whole annual cycle of water flows from the Gironde Estuary. During these cruises, 4 to 8 stations located along two inshore-offshore transects were sampled. This allowed for sampling 4 of the 5 stations located along the Northern transect during the 4 seasonal cruises (station 8 being sampled only during 3 out 4 cruises). During each seasonal cruise, we assessed: (1) macrobenthic diversity (abundance and biomass per species), (2) sediment profile images (15 per station), (3) surface sediment characteristics (Particulate Organic Carbon (POC), Chlorophyll *a* and phaeophytin *a* concentrations), and (4) total (through *ex situ* incubations) and diffusive (through oxygen microprofiling) oxygen fluxes at each sampled station. These data were later compared with similar ones collected in July 2010 by Massé *et al* (2016) at three stations of the Northern transect. In addition, the June 2018 cruise was specifically dedicated to the mapping of the mud patch. It involved the sampling of 32 stations and the assessments of surface sediment characteristics, and sediment profile images only.

4.3.2. Bay of Brest Dredging.

The analysis from Marine Traffic data allowed for the mapping of clam dredging pressure in the Bay of Brest during the 2012-2016 fishing seasons at a spatial resolution of 50 m x 50 m. These data were used to locate 10 stations in order to cover the whole pressure gradient. These stations were monitored for macrobenthic diversity (abundance per species) during 5 cruises, which took place between January 2016 and May 2017. Since fishing season lasts between mid-October and early March, this allowed to the partial cover of the 2016 and the total cover of the 2017 fishing seasons. During the June 2016 cruises 10 photos of 0.1 m² frames placed at the seafloor were taken by scuba divers and later used to assess epibenthic megafauna (numbers per taxa at the lowest tractable taxonomic level). Moreover, during the May 2017 cruise, 15 sediment profile images were collected at each station and analyzed (penetration, interface rugosity, maerl vitality).

4.3.3. Bay of Brest Invasive species.

The 'Pagure-2' towed underwater video system developed within JERICO-NEXT was used to quantitatively assess the taxonomic composition of macrobenthic epifauna along several gradients with differences in the abundance and vitality of the invasive slipper limpet *Crepidula fornicata*. The cruise took place during April 2018 and the 'Pagure-2' was deployed on four different areas of the Bay of Brest, representing different stages of slipper limpet proliferation dynamics (high-density live *Crepidula* bed; low-density live *Crepidula* bed; dead *Crepidula* bed). In each area, about 4 (~500m long) profiles were achieved during which both continuous video and still images (every 10 sec) were collected. quantitative data of biodiversity of epibenthic compartment (matrices of taxa's densities x Stations) was gained by estimating densities of each encountered taxon, based on video (megafauna) and still image (macrofauna) recordings. Slipper limpet coverage and vitality were assessed using a semi-quantitative approach based on the analysis of still images. For each profile, these analyses were achieved for subsets of images presenting similar characteristics in terms of combination of slipper limpet abundance (coverage percentage) and vitality (ratio of the numbers of live *vs* dead individuals).

4.3.4. Heraklion Gulf.

Sampling was initially planned to consist of four spatial surveys to account for temporal changes in both sewage outputs and natural variability in the composition of benthic communities. The cruises were planned for October 2016, July 2017, January 2018 and April 2018. The highest sewage output was expected in summer due to the increasing number of tourists in Heraklion during that season. However, there was a deviation from this original sampling plan: the R/V Philia, which was used for the first two cruises, was unavailable afterwards due to engine malfunction. The two last cruises were therefore cancelled. Five stations located along a predefined gradient starting from the sewage outfall (close to the shore and at shallow depth) until a control station at 200-meter depth where no effect of the sewage outfall should be detected were sampled during both cruises. At each station, we

assessed: (1) macrobenthic diversity (through both classical morphological analysis and eDNA metabarcoding), and (2) microbenthic diversity (through 16S rRNA metagenomics).

4.3.5. Data analysis.

A large set of data analysis procedures was used. Two biotic indices (e.g. B_{val} and BBC:A) to infer the Ecological Quality (ECOQ) of benthic habitats based on macro and microfauna, respectively. B_{val} is based on the measure of the deviation from the composition of macrofauna between the considered station and a reference one known/supposed to feature a good ECOQ. BBC:A is computed as the ratio of the relative abundances of Bacteroidetes+Bacilli+Clostridia and Alphaproteobacteria (Wu et al 2010) . We used the Benthic Habitat Quality index (BHQ) to infer ECOQ from the characteristics of sediment profile images. This index is mostly based on the numbers and sizes of biogenic structures present on sediment profile images (Nilsson and Rosenberg 1997). All three univariate indices were used to tackle **Q1** and **Q2**. 2D scatter plots (together with simple regression models whenever appropriate) were used to infer the relationships between disturbance intensity and a set of dependent variables describing the responses of benthic fauna (**Q2**). We used several types of multivariate techniques including non Metric Multi Dimensional Scaling (nMDS), hierarchical clustering and correlation analysis between similarity matrices to: (1) describe and compare the pattern put forward by classical taxonomic approach and both sediment imaging and metabarcoding (**Q1**), and (2) infer the response of benthic fauna to disturbance (**Q2**). At last, we used ascendant multiple linear regression models following a hierarchical approach to assess the gains in the amount of variance in both DOU and TOU explained when incorporating species richness to models already including temperature, organic matter availability and benthic macrofauna quantity as dependent variables (**Q3**).

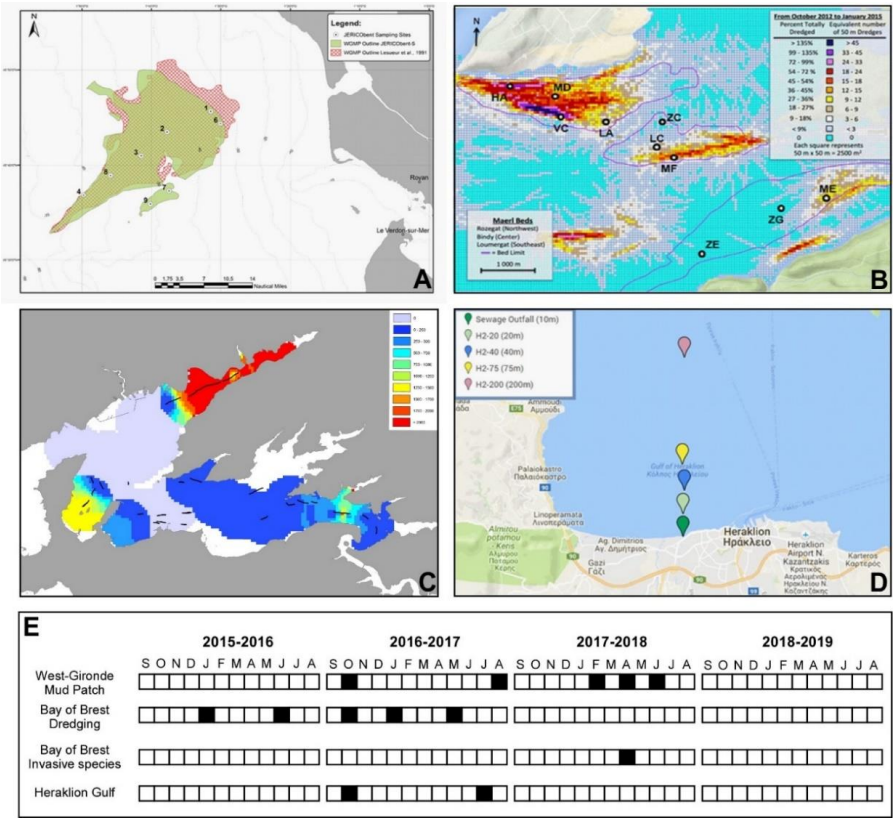

***Figure 4.2**: Maps showing the stations and video profiles sampled within the 4 actions (A; West Gironde Mud Patch, B: Bay of Brest Dredging, C: Bay of Brest Invasive species, D: Heraklion Gulf) constitutive of JRAP 2 and the overall schedule of achieved cruises (E).*

4.4. Main results

4.4.1. West Gironde Mud Patch.

The June 2018 cruise put in evidence a clear inshore-offshore gradient in surface sediment characteristics with the occurrence of coarser surface sediment at the shallowest stations (**Figure 4.3A**) and a regular increase in POC concentration with increasing depth (**Figure 4.3B**).

Multivariate analyses of the sediment profile images collected during the same cruise allowed for the identification of two main groups of stations in tight relationship with station depth (**Figure 4.4A**). The values of the BHQ derived from these characteristics tended to increase with depth. They were indicative of a Bad/Moderate ECOQ at shallow stations and of a Good or even High ECOQ at deep stations (**Figure 4.5**).

The nMDS performed on the total set of macrofauna composition data recorded during all four seasonal cruises also clearly showed the existence of a clear inshore-offshore gradient (from the right to the left in **Figure 4.4B**). In spite of clear temporal differences between cruises as indicated by the dispersion of sampling dates along the vertical dimension of the first plane of the nMDS, this gradient was clearly apparent during all cruises.

The nMDS presented in **Figure 4.6** is also based on macrofauna compositions recorded during all WGMP JRAP 2 cruises. However, it also includes data collected during July 2010 at stations 1, 3 and 4. This analysis shows major differences in benthic fauna composition between the July 2010 and the October 2016 cruises then followed by a tendency of the evolution of benthic macrofauna composition toward initial (i.e., 2010) situations. This trend was observed at all 3 stations but the magnitude of corresponding temporal changes was much higher at deep stations (i.e., stations 3 and 4).

The results of the hierarchical analyses aiming at assessing the potential importance of benthic macrofauna in controlling these fluxes shows that the inclusion of this variable only merely improves the description of spatiotemporal changes in either DOU (**Figure 4.7A**) or TOU (**Figure 4.7B**).

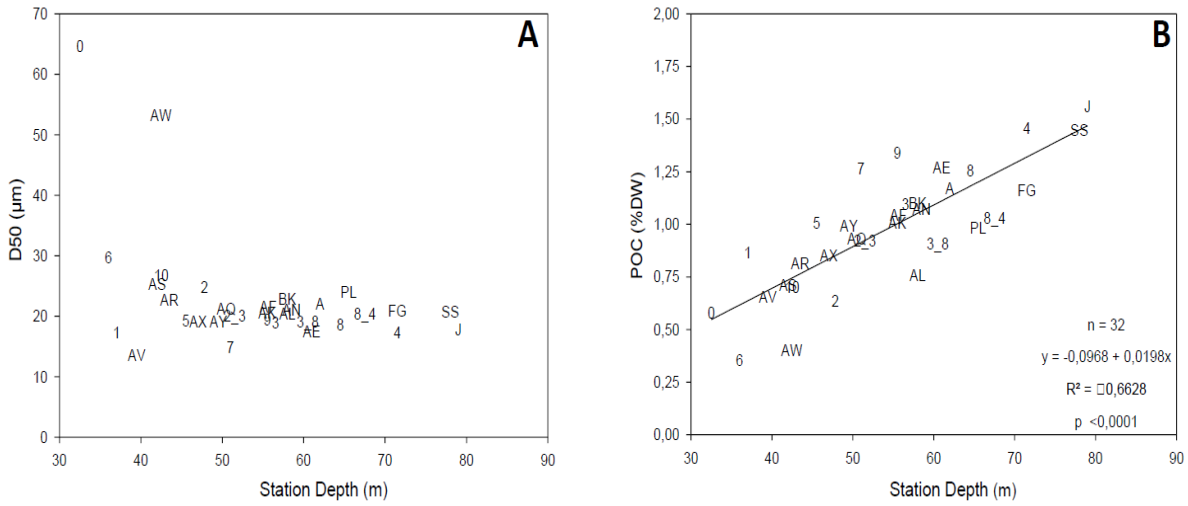

***Figure 4.3**: Relationships between station depth and: (A) surface sediment median diameter (D50), and (B) Particulate Organic Carbon (POC) concentrations. Results are from the June 2018 cruise.*

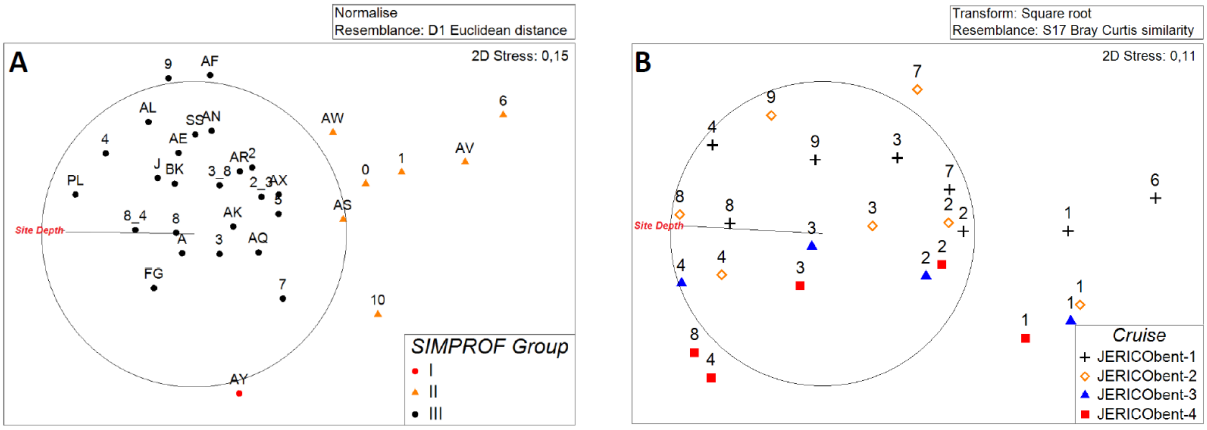

***Figure 4.4**: Non Metric Multi-Dimensional Scaling analyses of: (A) sediment profile images during the June 2018 cruise and (B) benthic macrofauna species abundances during all 4 seasonal cruises. Vectors in A and B, panels represent the Pearson correlation, coefficients between station depth and coordinates in the nMDS first plan.*

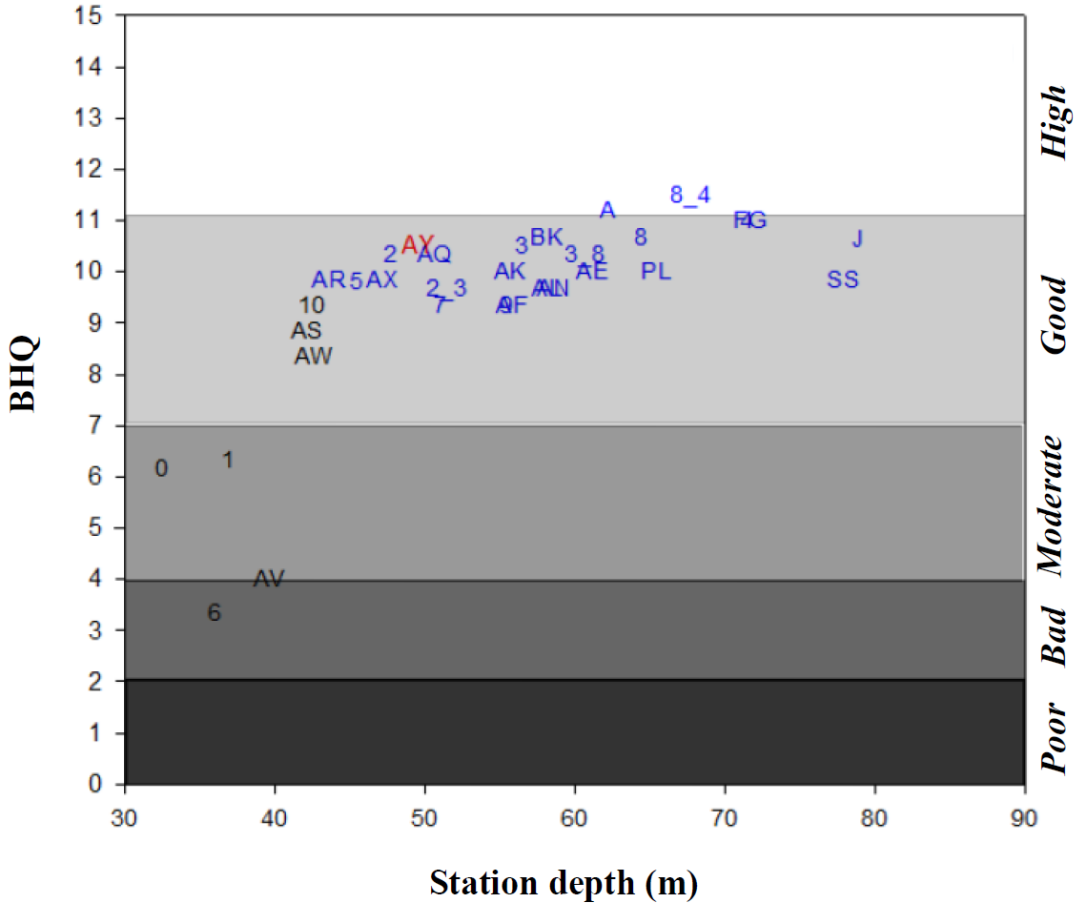

***Figure 4.5**: Relationships between station depth and the values of the Benthic Habitat Quality Index (BHQ). Results are from the June 2018 cruise. Levels in the shade of grey are indicative of derived Ecological Quality Status.*

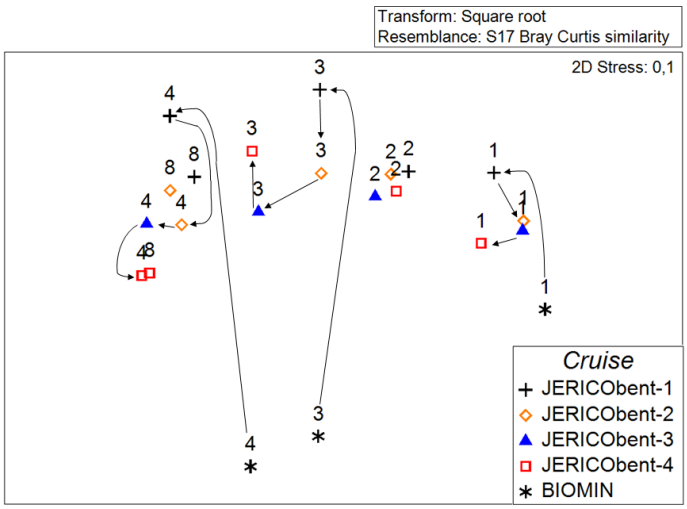

***Figure 4.6**: Non Metric Multi-Dimensional Scaling analysis of benthic macrofauna genus abundances during all 4 seasonal JRAP 2 cruises and during the Massé et al (July 2010) cruise for stations 1, 3 and 4. The temporal "trajectories" of these 3 stations are indicated by the black arrows.*

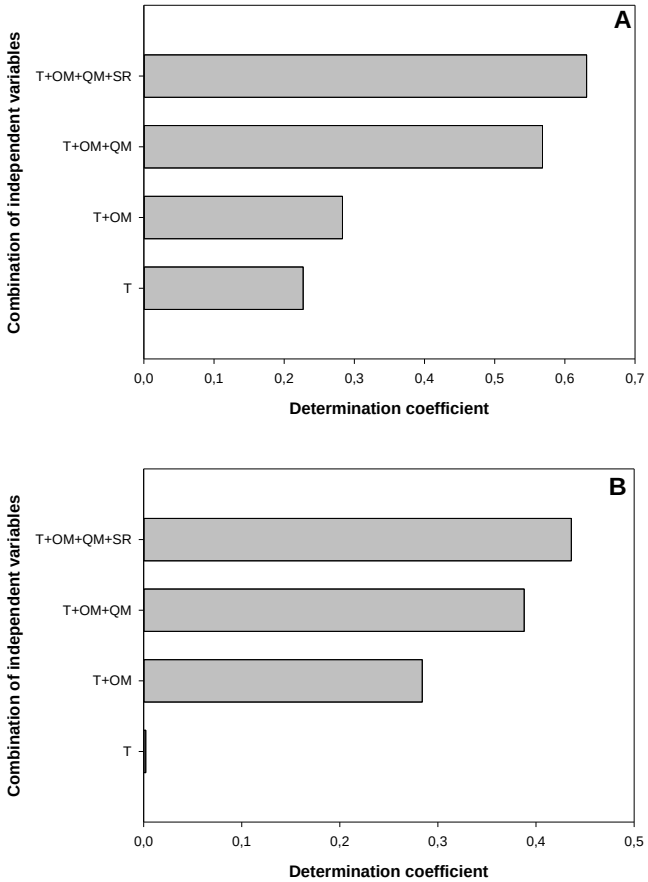

***Figure 4.7**: Results of the hierarchical analyses aiming at assessing the impact of benthic macrofauna species richness on (A) DOU and (B) TOU. See text for details.*

4.4.2. Bay of Brest dredging.

Dredging pressure was highly variable through time and space during the period under study (**Figure 4.8**). Some stations (e.g. ZG, ZE and ZC) were (almost) not dredged and considered as controls. The pressure between dredged stations was highly variable. The season 2015-2016 was by far the one during which dredging was most intensive (especially at stations LA, MD and HA).

The nMDS performed on the total set of macrofauna composition data clearly discriminated the control station from the impacted stations along its vertical dimension (**Figure 4.9A**). Conversely, there was no clear trend related to differences in pressure intensity among dredged stations. Spatial heterogeneity appeared higher between control stations than between dredged ones. Finally, there was a clear shift between the January 2016 to January 2017, and the May 2017 cruises. This shift did concern the whole set of stations (i.e., both control and impacted ones), which suggested that it was probably not attributable to dredging. In fact, it resulted from differences in sieving procedures (i.e., between the May 2017 and the 4 other cruises), which restricted the analysis of temporal changes in benthic fauna composition to the January 2016-January 2017 time period.

The nMDS performed on the characteristics of sediment profile images collected during June 2016 also discriminated control and impacted stations (**Figure 4.9B**). This discrimination indeed tightly correlated with the 2012 to 2017 cumulated fishing pressure as indicated by the positioning of this vector in the first plane of the nMDS. Interestingly, stations VC and MF seemed to represent intermediate states of habitat degradation as shown by their position in this plane.

The nMDS performed on the composition of benthic macrofauna during June 2016 and May 2017 (i.e., immediately after the 2015-2016 and 2016-2017 dredging seasons) are shown in **Figures 4.9B** and **4.9C**, respectively. Both analyses showed the same pattern: (1) a clear discrimination between control and impacted stations, and (2) a higher heterogeneity in control than in impacted stations. Moreover, in both cases, station MF seemed to present an intermediary state of degradation consistent with the fact that it suffered from only low dredging pressure during the 2015-2016 and 2016-2017 fishing seasons (**Figure 4.8**).

The concordance of the patterns resulting from the analysis of benthic macrofauna composition, sediment profile images and benthic megafauna was further assessed by testing the significance of the between similarity matrices resulting from the analysis of these three sets of parameters. For benthic macrofauna and sediment profile images, this was achieved for the May 2017 cruise. For benthic macrofauna and megafauna compositions, this was achieved for the June 2016 cruise. The correlations were significant (ρ=0.451 and p=0.013) and almost significant (r=0.298 and p=0.058), respectively).

The relationships between cumulated dredging pressures and maerl vitality, and Bval values based on macrofauna compositions (May 2017 and June 2016) and megafauna composition (June 2016) are shown in **Figures 4.10A-D**. They all show the same pattern with a clear (and almost binary) response of these four indices to dredging intensity.

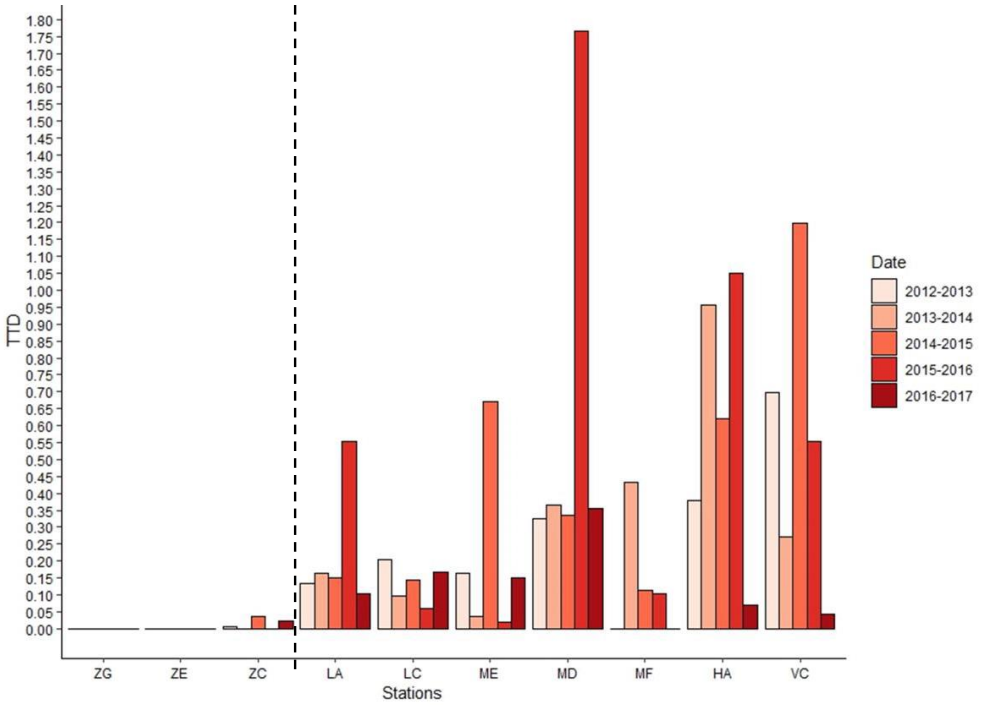

Figure 4.8: *Temporal changes in dredging pressure at each studied station from 2012 to 2017. The dotted line represents the distinction between control and impacted stations.*

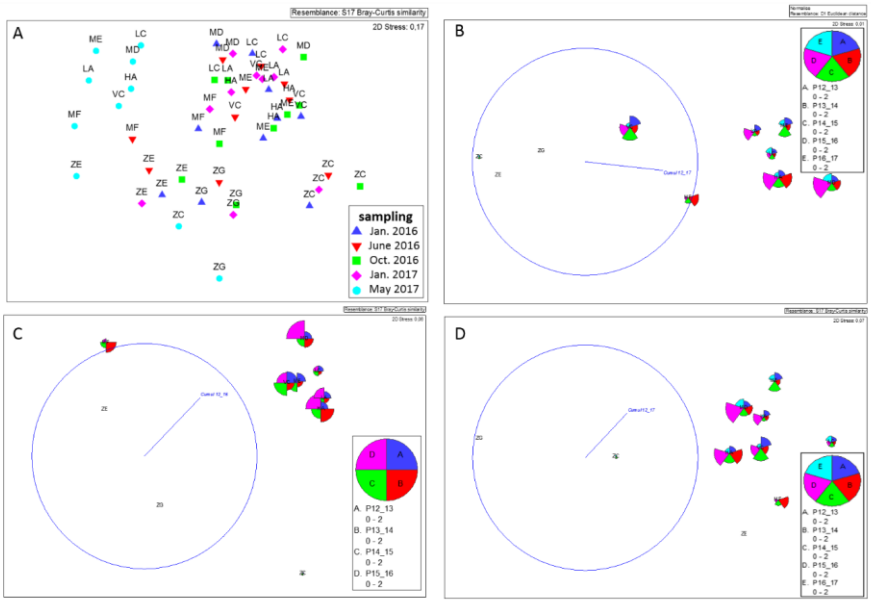

Figure 4.9*: Non Metric Multi Dimensional Scaling analysis of: (A) macrofauna community composition over the whole survey (i.e., all 5 cruises); (B) parameters measured on Sediment Profile Images (rugosity, penetration depth, live/dead ratio); (C) macrofauna community composition in grabs during June 2016; (D) macrofauna community composition in grabs during May 2017. Bubble size represent the intensity of dredging calculated at a given station and for each fishing season from 2012 to the sampling year. Vectors in B, C and D panels represent the Pearson correlation, coefficients between cumulated dredging pressures and station coordinates in the nMDS 2D first plan.*

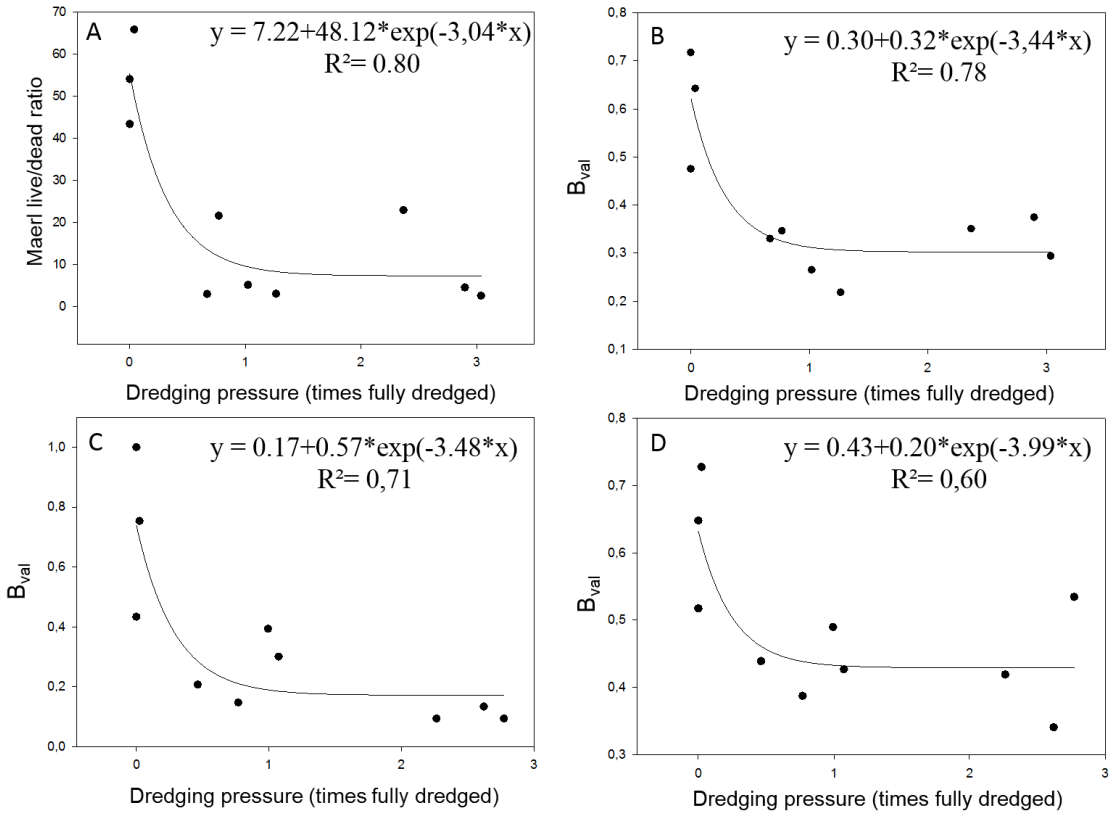

***Figure 4.10**: Relationships between dredging pressures and: (A) maerl vitality (measured in May 2017 through Sediment Profile Imaging), (B) Benthoval biotic index (BVal) based on benthic macrofauna composition in grabs during May 2017 , (C) Benthoval biotic index (BVal) based on benthic macrofauna composition in grabs during May 2016, (D) Benthoval biotic index (BVal) based on benthic megafauna during June 2016.*

4.4.3. Bay of Brest Invasive species.

Imagery data (video recording and still images) were acquired on a total of 32 profiles distributed in four main areas in the Bay of Brest. This corresponds to ca 500 min of video recordings and 3000 still images. Image analysis is still under progress and the results of only a subset of the data (5 profiles; still images; 2 zones) are presented below.

Examples of still images are shown in **Figure 4.11**. Their visual analysis shows clear differences between living and dead slipper limpet beds. From a quantitative standpoint, and based on currently available data, epibenthic macrofauna composition clearly differed between the two zones (**Figure 4.12**). The between-profile within zone heterogeneity was higher within Zone 1 than Zone 2, which probably resulted from the fact that Zone 1 encompassed a longer portion of an estuarine gradient. Overall, the variability in epibenthic macrofauna composition between zones correlated much better with slipper limpet vitality (**Figure 4.12B**) than coverage (**Figure 4.12A**). Differences between profiles were still apparent when image subsets were identified based on combinations of slipper limpet coverage and vitality (**Figure 4.13**). However, within profile heterogeneities were then almost equivalent between Profile 1 (located in Zone 1) and Profile 2 (located in Zone 2). In both cases, slipper limpet coverage and vitality both clearly contributed to within profile heterogeneities in epibenthic macrofauna composition between subsets of images (**Figures 4.13A** and **4.13B**, respectively).

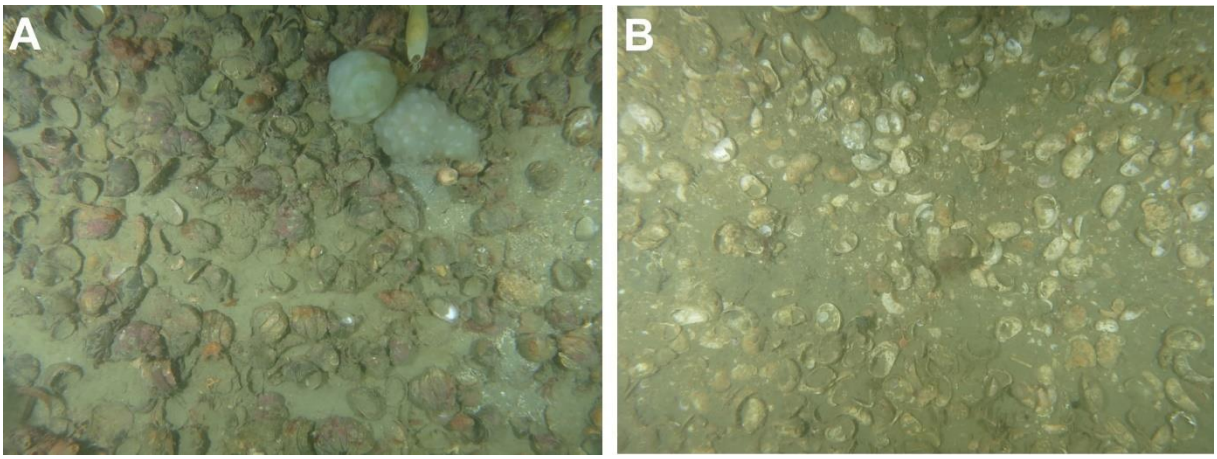

***Figure 4.11**: Examples of still images collected using the 'Pagure 2' towed video system. (A): Living slipper limpet bed. (B): Dead slipper limpet bed.*

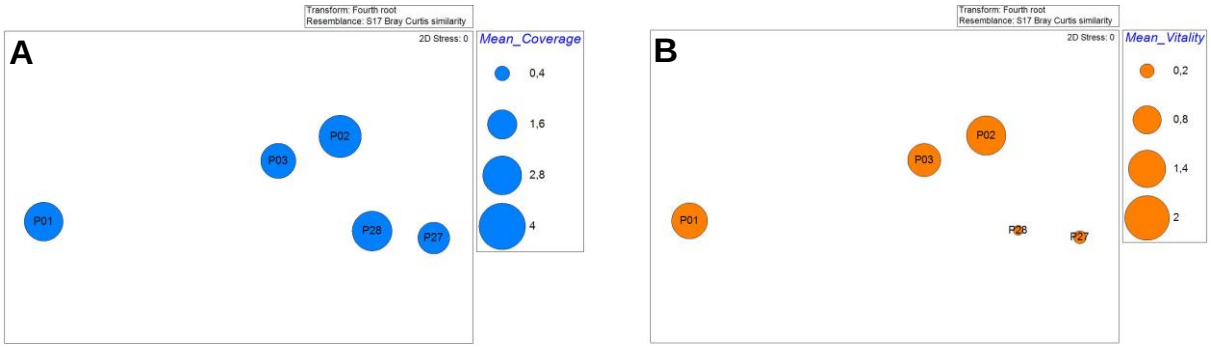

***Figure 4.12**: Non Metric Multi Dimensional Scaling analysis of benthic macrofauna composition within still images collected along 5 profiles. Bubble plots correspond to slipper limpet coverage (A) and vitality (B)*

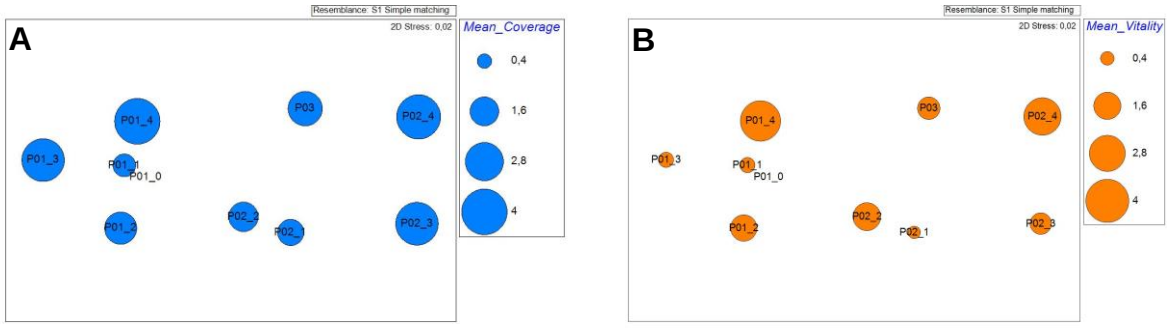

***Figure 4.13**: Non Metric Multi Dimensional Scaling analysis of benthic macrofauna composition within still images collected for different combinations of slipper limpet coverage and vitality and along three profiles. Bubble plots correspond to slipper limpet coverage (A) and vitality (B).*

4.4.4. Heraklion Gulf.

Multivariate analyses (i.e., hierarchical clustering and Non Metric Multi Dimensional Scaling) of surface sediment physicochemical parameters during the October 2016 (**Figure 4.14**) result in the grouping of intermediate stations while the shallowest (H2_10) and the deepest (H2_200) ones are separated. This reflects habitat variability of the sampling stations, with the intermediate ones being classified as "infralittoral sandy mud", H2_75 as "Mediterranean biocoenosis of muddy detritic bottoms" and the last one (H2_200) as "Facies of sandy muds with *Thenea muricata*".

Bacterial compositions derived from relative abundances of Operational Taxonomic Units (OTUs) obtained through 16S rRNA metabarcoding follow the same pattern. (**Figure 4.15A** and **4.15B**). However, this pattern was not conserved when clustering was based on OTU presence/absence (**Figure 4.15C**). The inshore-offshore gradient was characterized by a clear decrease in the values in the BBC:A ratio from the inner station, which is closer to the sewage outfall, to the outermost station, which is expected not to be impacted by the sewage (**Figure 4.15D**). Conversely, benthic fauna composition did not correlate with the inshore-offshore gradient both when clustering were based with abundance (**Figure 4.16A**) or presence/absence data (**Figure 4.16B**).

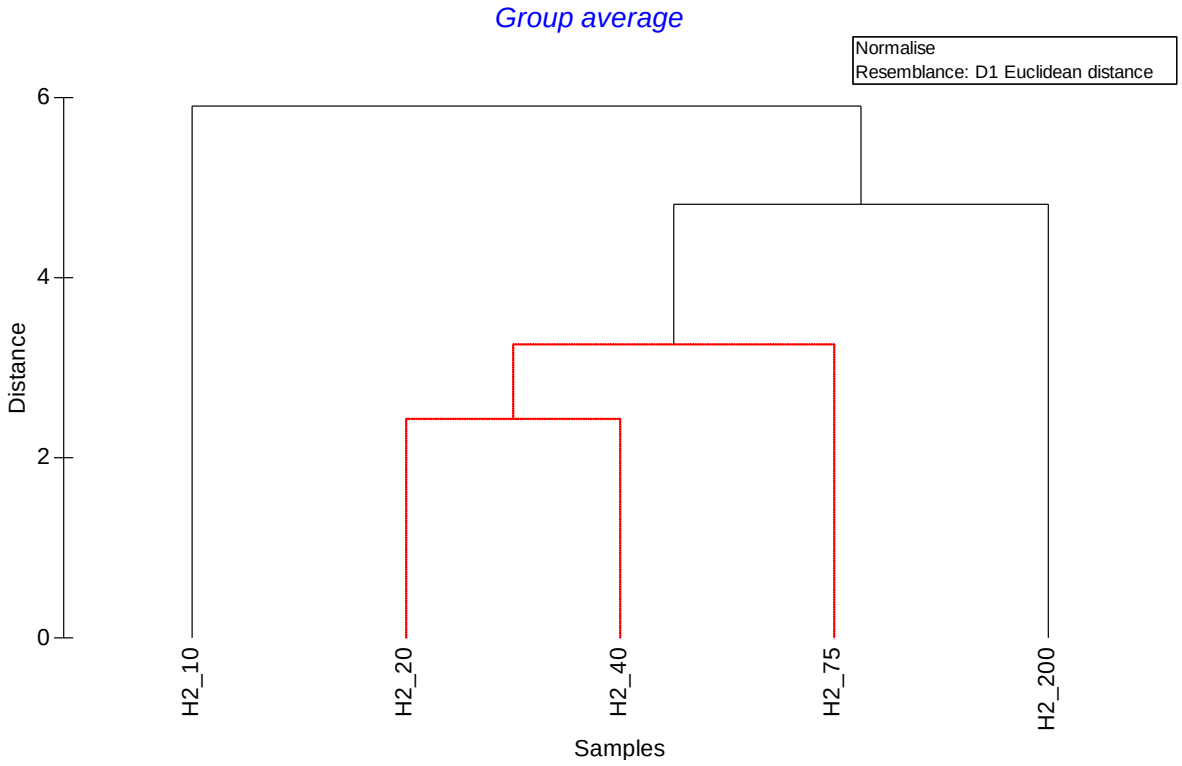

***Figure 4.14**: Hierarchical clustering of the sampling stations based on sediment physicochemical characteristics during the October 2016 cruise. Considered variables are temperature, pH, Eh, MD, σ1, Sk1, percentage of silt and clay, percentage of sand, Chlorophyll a, Phaeopigments, chloroplastic pigment equivalents, Particulate Organic Carbon. Figures following _ refer to the depth of the station. Black lines are indicative of significant differences (SIMPROF tests).*

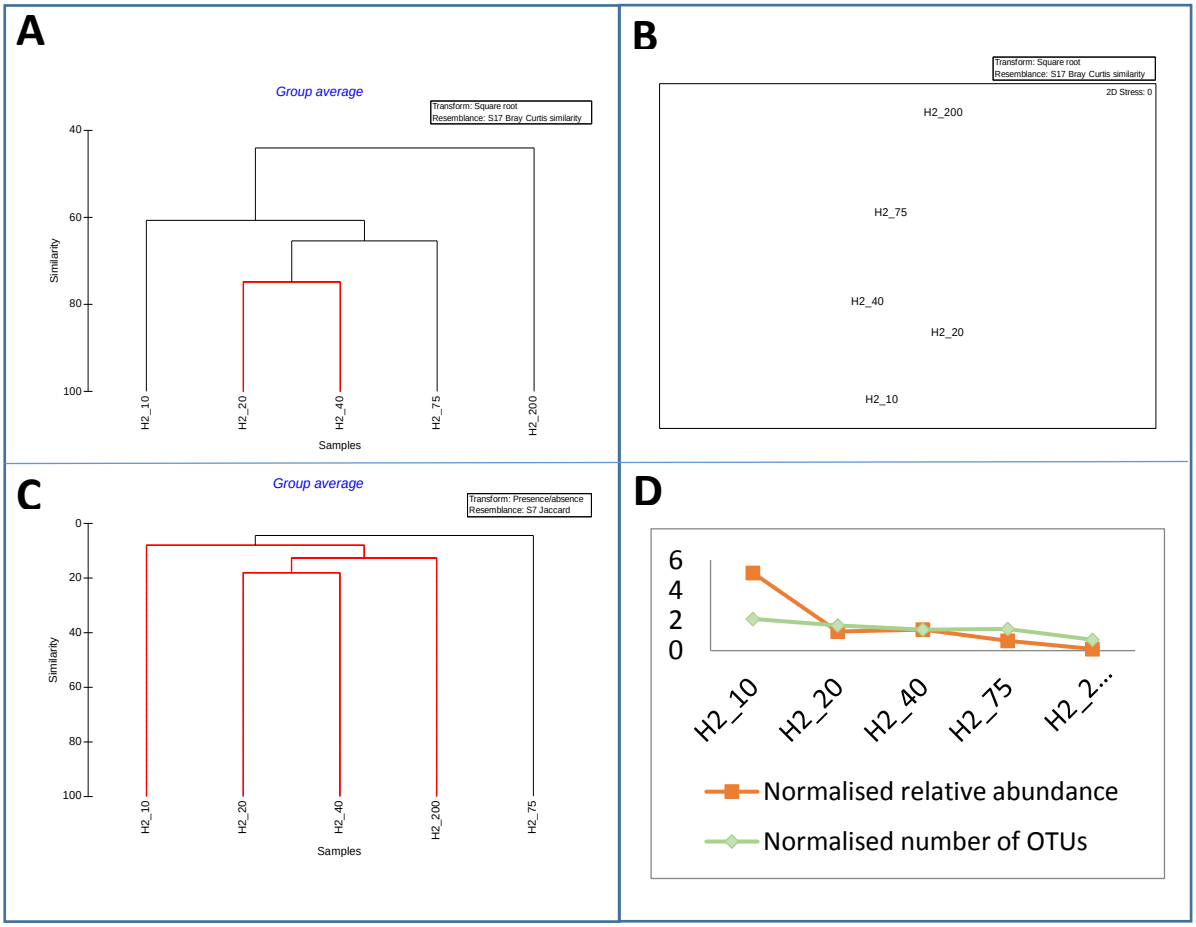

***Figure 4.15**: Hierarchical clustering of the 5 sampled stations based on relative abundance (A) and the presence/absence (C) of bacterial OTUs derived from 16S rRNA metabarcoding during the October 2016 cruise. Non Metric Multi Dimensional Scaling analysis of the relative abundance of bacterial OTUs, as derived from 16S rRNA metabarcoding during the October 2016 cruise (B). Changes in the values of the BBC:A ratio with depth during the October 2016 cruise (D). Black lines are indicative of significant differences (SIMPROF tests).*

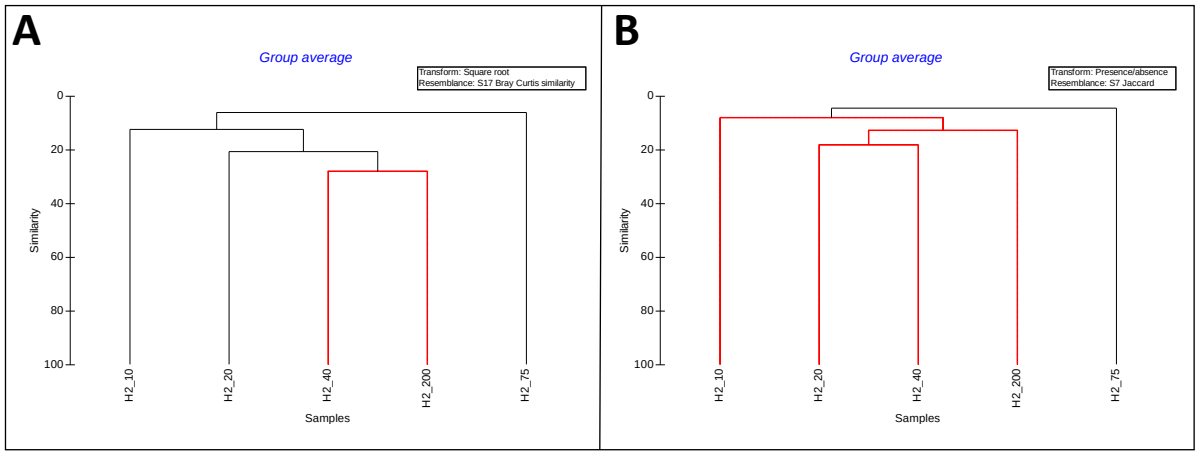

***Figure 4.16:** Hierarchical clustering of the five sampled stations based on the abundance (A) and the presence/absence (B) of benthic macrofauna. Black lines are indicative of significant differences (SIMPROF tests).*

4.5. Main inputs relative to initial specific objectives

4.5.1. Q1: Do alternative techniques (i.e., both metabarcoding and imaging techniques) provide sound surrogates for the classical analysis of benthic macrofauna composition?

There are several lines of evidences suggesting that sediment profile imaging may indeed constitute sound surrogate for the classical assessment of benthic macrofauna composition. During both the West Gironde Mud Patch and the Bay of Brest Dredging actions the analysis, the spatial patterns derived from these two approaches were indeed almost identical as similarity matrices either correlated significantly or almost significantly. This was also true for surface sediment imaging during the Bay of Brest Dredging action during which both the classical and the two imaging approaches moreover resulted in similar relationships between the intensity of disturbance and the value of B_{val}. As for the Bay of Brest Invasive species action, surface sediment imaging also proved efficient in depicting the effect of slipper limpet coverage and vitality in controlling epibenthic macrofauna composition.

Based on the results of the Heraklion Gulf action, the 16S rRNA metabarcoding of benthic microfauna seemed efficient in detecting the disturbance gradient resulting from a sewage output both through the analysis of overall benthic microfauna composition and through the computation of the BBC:A index. This supports using BCC:A as a community-based indicator to assess ecosystem health (Wu et al., 2010). This ratio is indeed expected to be lower in samples not impacted by fecal material, which corresponds to its decreasing trend long our inshore-offshore sampling gradient, suggesting that indeed there is a clear impact close to the Heraklion sewage outflow. Our results thus highlight the interest of using molecular methods (i.e. metabarcoding) as an alternative approach for analysing benthic microbial community composition both in terms of diversity and structure. Alternative techniques indeed capture only a small fraction of total microbial diversity.

4.5.2. Q2: Irrespective of the nature of the disturbance, does the relationship between disturbance intensity and benthic diversity follow the same pattern?

The most comprehensive assessment of the relationship between disturbance intensity and benthic fauna composition was achieved within the Bay of Brest dredging action due to the sound assessment of disturbance intensity through the analysis of AIS data. Results suggested that the effect of disturbance were not gradual but rather binary. This is probably resulting from: (1) the physical nature of the disturbance caused by dredging, (2) the constant renewal of this disturbance during the 5 dredging seasons covering the studied period, and (3) the low resilience of maerl beds.

Particle inputs from the Gironde River were initially thought to constitute the main disturbance for West Gironde Mud Patch Sediment. Based on JRAP 2 results, there are several lines of evidence suggesting that this is indeed not the case: (1) the organic carbon concentration of surface sediment is increasing offshore which suggests that the Gironde River is not the main source of particulate organic matter for the West Gironde Mud Patch, and (2) the magnitude of temporal changes in benthic macrofauna compositions tended to increase with depth as well which suggest that the factors driving those changes do not originate from the Gironde River. Evidences from the present study, supported by sedimentological literature data, suggest that local hydrodynamics and associated resuspension events are in fact the main source of disturbance and that they affect benthic macrofauna composition in two different ways in the shallower and deeper parts of the West Gironde Mud Patch. This pattern is likely related with the strong hydrodynamics in the inner part of the WGMP, which results in frequent transitory hydrosedimentary (i.e., sedimentation/resuspension) events (Jouanneau et al 1989), which preclude the development of a mature benthic macrofauna community penetrating deep in the sediment and indicative of a good ECOQ (Nilsson & Rosenberg 2000). Conversely, temporal changes at deeper stations appear related with much less frequent strong resuspension events, which are followed by secondary succession sequences.

At this stage, it is still difficult to tackle **Q2** for the Bay of Brest Invasive species and the Gulf of Heraklion actions since data acquisition is still in progress for these two actions. Already available results nevertheless show clear effects of the two considered disturbances. It is anticipated that establishing the shape of the relationship linking

disturbance intensity and benthic macrofauna composition will prove easier for the Bay of Brest Invasive species action since the relevant information is included in benthic macrofauna composition as well.

4.5.3. Q3: What are the functional consequences of a benthic macrofauna diversity loss on ecosystem functioning?

This issue was mostly tackled within the West Gironde Mud Patch Action through the assessments of both benthic macrofauna species diversity and oxygen fluxes at the sediment-water interface. Results suggest a significant contribution of the abundance of benthic macrofauna to both DOU and TOU but almost no effect of species richness on those fluxes, which are indicative of the mineralization of sedimentary organics. It should however be underlined that species richness is not the only pathway by which benthic macrofauna diversity could contribute to benthic oxygen fluxes, which could for example be controlled by the presence/abundance of key species. Moreover, a major methodological issue when assessing the relationships between oxygen fluxes and benthic macrofauna composition is the difference in the spatial scales associated with the measurements of associated variables. This clearly underlines the importance of pursuing technological developments allowing for the measurements of TOU over larger sediment surfaces as initiated during JERICO-NEXT.

4.6. Analysis of the experience gained

4.6.1. Developing innovative technologies for coastal ocean observing and modelling.

The technological developments tested within JRAP 2 mostly dealt with the assessment of benthic diversity *per se*. They first refer to benthic macrofauna through sediment imaging regarding both sediment profile (West Gironde Mud Patch and Bay of Brest Dredging actions) and surface (Bay of Brest Dredging and invasive species actions). Imaging techniques allow to get access to a degraded information (i.e., as compared to classical taxonomical analysis based on morphology) but on a larger number of combination of stations and sampling dates. For all JRAP 2 considered actions deployed imaging techniques allowed for the detection of: (1) of the effect of considered disturbances, and/or (2) patterns similar to those identified using the classical taxonomic approach. Results of the same kind were obtained for 16S rRNA metabarcoding, which proved efficient in detecting the gradient in benthic microfauna composition resulting from the Heraklion sewage output. A significant improvement being that this approach is accounting for total and not only cultivable bacteria. Overall JRAP 2 results thus support the use of imaging techniques and metabarcoding as surrogates for biodiversity assessments. Corresponding developments should now be pursued and the applicability of these techniques to other biological compartments assessed.

4.6.2. Establishing observing objectives, strategy and implementation at the regional level.

The spatial scales associated with the four disturbance sources tested within JRAP 2 actions were all clearly sub regional. This was especially apparent within the Bay of Brest Dredging action during which disturbance intensity was shown to drastically vary between 50x50m grids. Moreover, the effects of disturbances were superimposed to the natural spatial structuration of benthic communities and its temporal dynamics as for example put forward by the results of: (1) the spatial survey achieved within the West Gironde Mud Patch action, and (2) the 2017 shift in benthic fauna composition during the Bay of Brest dredging action. A last point to take into consideration is linked to the limitation of available technologies. Benthic observations are indeed almost exclusively punctual (i.e., both in space and time) and only seldom semi-automatized, which is restricting sampling. Overall, upscaling of benthic observations should therefore probably not necessarily be looked for at the whole regional scale (see also the section “Proposition of a future monitoring strategy for the topic”).

4.6.3. Enhancing integrated coastal ocean monitoring and interfacing with other ocean observing initiatives operating at different spatiotemporal scales.

As a biological compartment, the spatiotemporal dynamics of benthic fauna, including its diversity is clearly influenced by physico-chemical processes. There is thus a clear interest/necessity of interfacing its observations with those of other initiatives. The most comprehensive environment factor accounting for the spatial distribution of benthic macrofauna is sediment granulometry, which clearly pleas for the coupling of benthic observations with hydrosedimentary observations and/or modelling. Results of JRAP 2 nevertheless shows that such a coupling may

depend on the nature of the tackled environmental issue. Interfacing with: (1) the Gironde River observing (i.e., MAGEST network), (2) the project regarding the fate of Gironde River originating particles over the Bay of Biscay continental shelf (i.e., AMORAD), and (3) the national wave monitoring network (i.e., CANDHIS) were for example an evidence for the West Gironde Mud Patch Action. This was much less clear for other actions especially when disturbance intensity could be directly derived from available data (*Bay of Brest Dredging*) or from the benthic fauna matrix itself (*Bay of Brest Invasive species*). Moreover, the *West Gironde Mud Patch* action experimented some practical difficulties in its interaction with the two-above mentioned hydrosedimentary modelling initiatives. As for AMORAD, this was linked to differences in the time schedule of the two projects, which resulted in the non-availability of the AMORAD hydrosedimentary model within the JRAP 2 time framework. In the case of the CANDHIS Observation network, this resulted from a lot of missing observations which induced the necessity of using modelling to derive physical constraints acting on sediment (which here again was not practically feasible within the framework of JERICO-NEXT). Overall this underlines the necessity of coupling future observation of benthic fauna with other running observation initiatives (and not research projects) that are fully operational especially regarding their modelling components.

4.7. Propositions for a future monitoring strategy for the topic

Based on the outputs of the four actions of JRAP 2, the main propositions for a future monitoring of benthic fauna diversity are as follows:

- Pursue with the development and test of new technologies for the assessment of benthic: (1) fauna diversity, and (2) functions at appropriate spatiotemporal scales.
- Favor the development of integrated platforms allowing for the simultaneous (semi-automated) assessments of both diversity and functions.
- Do not limit tackled issues to large-scale long-term (i.e., academic) ones
- Identify environmental/scientific issues and associated spatiotemporal scales in tight interaction with a large variety of stakeholders.
- Adapt the monitoring strategy and associated data analysis procedures to those issues and scales through *a priori* interactions with stakeholders.
- Use a stratified approach (i.e., per community) to build the monitoring strategy. This implies to sample at least one control (i.e., relative to the main postulated disturbance(s)) station per community.
- Manage the possibility of detecting the effect of new (i.e., not *a priori* postulated) disturbance sources, which may for example require the monitoring of several control stations per community).
- Carry out preliminary tests for validating the use of alternatives (i.e., less costly in terms of manpower and money) to classical taxonomic approaches.
- Once achieved, use these alternatives (e.g., sediment imaging, metabarcoding…) to optimize monitoring strategies.
- Include the interfacing of the monitoring strategy with those of existing initiatives based on a conceptual model of the interactions linking considered parameters paying a particular attention to differences in spatial and temporal interactions.
- Favor the interactions with the initiatives including a modelling component.
- Develop interaction with other benthic fauna diversity observation providers to constitute large high quality data sets relevant to tackle long-term large-scale functions.
- Take advantage of future running monitoring actions to host further developments and specific research projects (e.g. development of new technologies, Development of niche models, development of new data analysis procedures, assessment of the link between diversity and ecosystem functions…).

4.8. References

Costanza R, D'Arge R, de Groot R, Farber S, Grasso M, Hannon B, Limburg K, Naeem S, O'Neill RV, Paruelo J, Raskin RG, Sutton P, van der Belt M (1997) The value of the world's ecosystem services and natural capital. Nature 387:253-260

Dahllöf, I. (2002) Molecular community analysis of microbial diversity. Current Opinion in Biotechnology, 13(3), 213-217.
Diaz RJ, Rosenberg R (1995) Marine benthic hypoxia: A review of its ecological effects and the behavioural responses of benthic macrofauna. Oceanography Marine Biology on Annual Review 33:245-303
Dauvin JC (1998) The Fine Sand *Abra alba* Community of the Bay of Morlaix Twenty Years after the Amoco Cadiz Oil Spill. Marine Pollution Bulletin 36:669-679.
Emmerson MC, Solan M, Emes C, Paterson DM, Raffaelli D (2001) Consistent patterns and the idiosyncratic effects of biodiversity in marine ecosystems. Nature 411:73-77
Jackson JB, Kirby MX, Berger WH, Bjorndal KA, others (2001) Historical overfishing and the recent collapse of coastal ecosystems. Science 293:629-638
Massé C, Meisterhans G, Deflandre B, Bachelet G, Bourrasseau L, Bichon S, Ciutat A, Jude-Lemeilleur F, Lavesque N, Raymond N, Grémare A, Garabetian F (2016) Bacterial and macrofaunal communities in the sediments of the West Gironde Mud Patch, Bay of Biscay (France). Estuarine, Coastal and Shelf Science 179: 189-200
Naeem S (2006) Expanding scales in biodiversity-based research: challenges and solutions for marine systems. Marine Ecology Progress Series 311:273-283
Naeem S, Hahn DR (2000) Producer-decomposer co-independency influences biodiversity effects. Nature 403:762-764
Naeem S, Li S (1997) Biodiversity enhances ecosystem reliability. Nature 390:162-165
Naeem S, Thompson LJ, Lawler SP, Lawton JH, Woodfin RM (1994) Declining biodiversity can alter the performance of ecosystems. Nature 368:734-737
Naeem S, Wright JP (2003) Disentangling biodiversity effects on ecosystem functioning: deriving solution to a seemingly insurmontable problem. Ecological Letters 6:567-579
Nilsson H, Rosenberg R (1997) Benthic habitat quality assessment of an oxygen stressed fjord by surface and sediment profile images. Journal of Marine Systems 11, 249–264
Nogales B, Lanfranconi MP, Piña-Villalonga JM, Bosch R (2011) Anthropogenic perturbations in marine microbial communities. FEMS Microbiology reviews, 35(2), 275-298.
Pauly D, Christensen V, Dalsgaard J, Froese R, Torres Jr F (1998) Fishing down marine food webs. Science 279:860-863
Stefani FO, Bell TH, Marchand C, Ivan E, El Yassimi A, St-Arnaud M, Hijri M (2015) Culture-dependent and-independent methods capture different microbial community fractions in hydrocarbon-contaminated soils. PLoS One, 10(6), e0128272.
Short FT, Wyllie-Echeverria S (1996) Natural and human-induced disturbance of seagrasses. Environmental Conservation 23:17-27
Romero-Ramirez A, Grémare A, Desmalades M, Duchêne JC (2013) Semi-automatic analysis and interpretation of sediment profile images. Environmental Modelling & Software 47: 42-54
Romero-Ramirez A, Grémare A, Bernard G, Pascal L, Maire O, Duchêne J.C. (2016) Development and validation of a video analysis software for marine benthic applications. Journal of Marine Systems 162, 4-17
Solan M, Cardinale BJ, Downing AL, Engelhardt KAM, Ruesink JL, Srivastava DS (2004) Extinction and ecosystem function in the marine benthos. Science 306:1177-1186
Stewart EJ (2012) Growing unculturable bacteria. Journal of Bacteriology, 194(16), 4151-4160.
Wollast R (1998) Evaluation and comparison of the globel carbon cycle in the coastal and in Open Ocean. In: Wollast R (ed) In The Sea: the global coastal ocean. John Willey & Sons, p 213-252
Wu CH, Sercu B, Van De Werfhorst LC, Wong J, DeSantis TZ, Brodie EL, ... Andersen GL (2010) Characterization of coastal urban watershed bacterial communities leads to alternative community-based indicators. PloS one, 5(6), e11285
Zajac RN, Whitlatch RB (1985) A hierarchical approach to modelling soft-bottom successional dynamics. In: Gills PE (ed) Proc 19th Europ Mar Biol Symp. Cambridge University Press, p 265-276

4.9. Abbreviations

BBC/A: Bacteroidetes+Bacilli+Clostridia / Alphaproteobacteria Ratio
BHQ: Benthic Habitat Quality Index

B_{val}: Benthoval Index
DOU: Diffusive Oxygen Uptake
ECOQ: Ecological Quality Status
JRAP: Joined Research Activity Project
MD: Median Diameter
MSFD: Marine Strategy Framework Directive

nMDS: Non Metric Multi Dimensional Scaling
OTU: Operational Taxonomic Unit
POC: Particulate Organic Carbon
σ_1: Standard Deviation$_1$
SIMPROF: Similarity Profile Test
Sk_1: Skewness$_1$
TOU: Total Oxygen Uptake
WFD: Water Framework Directive

5. JRAP 3: Occurrence of chemical contaminants in Northern coastal waters and biological responses

Contributors
Luca Nizzetto, **Norwegian Institute for Water Research, Norway**
Elisa Ravagnan, Catherine Boccadoro, **NORCE, Norway**
Anna Willstrand Wranne, Bengt Karlson, **SMHI, Sweden**
Anna Rubio, **AZTI, Spain**
Klaas Deneudt, **Flanders Marine Institute, Belgium**
Naomi Greenwood, **CEFAS, UK**
Joaoi Vitorino, **Instituto Hydrographico, Portugal**
Jon Albertsen, **Marine Institute, Norway**
Petra Prybilova, Miroslav Brumovsky, Ondra Sanka, **Research Centre for Toxic Compounds in the Environment, Czech Republic** (Contractor),

5.1. Topic and specific objectives.

Marine areas are indispensable for securing life-support services to humanity, through providing, among others: food, oxygen and climate regulation. With uprising human population size and increasing living standards, concern on human impacts on marine ecosystems structures and functioning is growing. Health of coastal environments is of particular concern because of especially intense interactions with human activities. The most acknowledge human-driven impacts include climate change (and, by reflex, ocean acidification, ocean warming and sea-level rise), eutrophication, hypoxia, overfishing and chemical pollution (Noone et al., 2013). Among these, chemical pollution is among the less understood and studied stressors.

Marine environments are exposed to a large number of chemical substances. During the Anthropocene, chemicals have become central to agriculture, medicine, personal and house care and virtually any type of industrial processes. Several of these substances have been identified as hazardous for the humans and the environment. Among them figure toxic metals (Braune et al., 2015; de Souza Machado et al., 2016; Naser, 2013; Pan and Wang, 2012), and several persistent organic pollutants (POPs) such as polychlorinated biphenyls (PCBs) and organochlorine pesticides (AMAP, 2004; Rigét et al., 2010; Wania and MacKay, 1996). These compounds have been found both in coastal, Open Ocean and other pristine marine areas, including the Arctic and Antarctic as a result of long-range transport from source areas.

Beyond these well studied marine contaminants, coastal environments are recipients of hundreds of chemical pollutants released to freshwater systems, or directly to the sea from domestic and industrial wastewater and agricultural runoff, veterinary and hospitals wastewater (aus der Beek et al., 2016; Dachs and Mejanelle, 2010; Noguera-Oviedo and Aga, 2016). While their potential number is in the order of several hundreds or thousands, most updated inventories are still largely incomplete. Hence, the building of realistic perspectives over the number and identity of coastal pollutants is seriously hindered. Marine coastal contaminants may be individually present in water at relatively low concentrations. However, research on the toxicity of chemical mixtures suggests that additive effects must be accounted as the most common mode of toxic action. It follows that current ignorance on chemical pollutant inventories in coastal environment hinder the formulation of a correct perception over the scale of their pressure and their potential impacts on biota and ecosystem services.

Building an adequate comprehensive understanding on the occurrence and distribution of the largest possible number of contaminants in coastal environments and the identification of aggregated measures of their impacts on the ecosystem is the way forward. This is however a difficult scientific and organizational task calling for a major monitoring and research effort. Through the Marine Strategy Framework Directive (MSFD) - Descriptor 8, The EU has taken action towards this challenge demanding countries to conduct an assessment of the ecological status of their coastal ecosystems and transitional marine waters with regards to chemical pollution (European Comission, 2008). In order to fulfill such a demand a rational use and further development of Coastal Research Infrastructures

(CRI) is the mandatory step for a future routine implementation of manageable and effective protection of coastal waters from chemical pollution.

Contaminants that are detected in environmental samples but that are not yet included in environmental protection acts are collectively referred to as “Contaminants of Emerging Concern” (CECs) and include, among others, pharmaceuticals for human and veterinary use, personal care products, artificial food additives, stimulants, several current use pesticides and several industrial contaminants.

Based on the above premises, JRAP 3 addressed the following questions:

- **Q1**: Can existing integrative sampling methods (i.e. passive samplers) be effectively used in combination with existing CRI to obtain reliable data on marine chemical pollution?
- **Q2**: Can CRI be used to support exploratory monitoring of marine pollution to identify new chemical contaminants?
- **Q3**: Can the drivers of spatial distribution of chemical contaminants in coastal waters be assessed using data from infrastructure sensors and spatial analyses?
- **Q4**: Is there a co-variance between contaminant signals and biological responses?

Furthermore, while addressing these questions, JRAP 3 addressed the following sub-tasks:

- Delivering best practices for the monitoring of chemical pollutants using existing coastal infrastructures
- Optimizing existing chemical sensor technology for use on fixed coastal monitoring infrastructures
- Providing guidelines for the implementation of future contaminant monitoring with specific regards to the adopted spatio-temporal resolution of observations

5.2. Overall structuration and strategy

The initial strategy to tackle these questions was conceived to fully exploit the potential of JERICO-NEXT coastal fixed and mobile infrastructures to carry out integrated monitoring of chemical pollution, water physical chemical parameters and biological signals (specifically, through the quantification of specific microbial biomarkers of pollution). The ambition was to carry out development and actions to empower the full use of the spatial resolution and multi-parameter observations provided by Jerico-RI especially along a transect linking the eastern North Sea-the Norwgian Sea and the Arctic. To our knowledge, this was the first time that such an analysis was conducted at continental scale using existing CRI including moorings and ships of opportunity. The strategy to tackle these questions included the following actions:

5.2.1. Action 1

A pan-European monitoring campaign; using passive samplers deployed on moorings in the Portuguese coast, Bay of Biscay, several locations of the North Sea, Kattegat, Skagerrak and Norwegian coasts; was conducted to tackle **Q1**. Passive samplers are accumulators that can be left in the field over a certain amount of time during which they passively takeup chemical substances and pollutants from the surrounding environment. They offer the advantage of providing pollutant concentrations averaged over long exposure times, and do not require power supply(Lohmann et al., 2012). Deployments of thses device have been carried so far mostly as part of focused scientific projects, during which dedicated infrastructures were temporarily installed, and deployment/collections occurred over consistent times in different locations through the work of specifically trained personnel.

Passive samplers are very sensitive tools. Sample contamination during field operation is unfortunately a common source of data uncertainty and error, which can frequently make monitoring results unreliable, unusable and misleading. To avoid such confounding factors, qualified and properly trained personnel has been required for field operations with passive samplers. When using passive sampling on multi-purpose CRI operated by personnel with no specific experience and training, during complex, multi-task field operations there is a serious chance of negatively affecting the quality of measurements from the passive samplers. Such a probability was never systematically assessed so far. Action 1 was conceived to support the development and test new operational

approaches to passive sampling for hydrophobic chemical pollutants from fixed Jerico CRI. This included the design of a new protective cage hosting silicon-base passive samplers to facilitate installation on different type of mooring by field staff with little or no experience in passive samplers. Such a device would enable the collection and delivery of reliable data under different logistic requirements and deployment times, as in the case of CRI operated by different countries/institute with different scheduled activities. During JRAP 3 proof of concept deployments in the Atlantic coast (Portugal), Bay of Biscay (Spain), North Sea (Belgium, UK), Kattegat (Sweden) and Skagerrak (Norway) were achived. The quality of retrieved data was analyzed looking at significance of obtained concentration data (e.g. by comparing measured contaminant level in the field with those of field blanks), analytical recovery performance, and the range and trends of observed variability in the measured concentration data.

5.2.2. Action 2.

A monitoring campaign using a set of FerryBox platforms (mobile platform) in the outflow of the Baltic (Oslo and Kiel transect), the North Sea, and the Norwegian Sea, was carried out to tackle **Q2** and **Q3**. Monitoring from multiple FerryBox units was conceived to demonstrate the capability of the FerryBox automatic water samplers (present on-board as part of the standard equipment) to enable large regional/continental scale monitoring of CECs and to facilitate the analysis of their spatial distribution in relationship to water biophysical parameters and source distribution gradients. The planned work focused on the occurrence, in coastal waters, of pharmaceuticals, antibiotics, personal care products, current used pesticides and food additives, many of which were never measured before in marine waters.

The main focus of Action 2 was to provide first-hand data on the occurrence and spatial distribution of a high number of new marine contaminants. The underlying rationale was that by performing observations along coastal transects with steep gradients of water properties and land-based source influences, the following issues could be addressed:

- Identifying possible covariant or causal relationships between the distribution of marine coastal pollutants and the main environmental gradients.
- Evaluating best monitoring strategies (e.g. in terms of spatial-temporal resolution) to be implemented in future campaigns where the same CRI could be used.

A inherent important focus for Action 2 was to prove the quality of obtained data using FerryBox (previously used only once in a pilot study focused on a single region) (Brumovsky et al., 2016a) of sampling through existing equipment installed on the FerryBox units. Several quality criteria must be fulfilled for a measurement of chemical pollution to be fully validated and accepted. These include: (1) significance of the measurement values (e.g. measured concentrations must be significantly higher than field blanks (i.e. negative controls)); (2) quantitative recovery of the chemical pollutants present in water (e.g. through the assessment of spiked samples analyses (i.e. positive controls)); and (3) the stability of the chemical substances present in the samples during the storage on board of the ship (i.e. through carrying out stability tests). The monitoring activity carried out as part of Action 2 were therefore conceived to demonstrate the fulfillment of these quality criteria, and ultimately the usefulness of CRI as resources to gather meaningful marine chemical pollution data.

5.2.3. Action 3.

A high spatio/temporal resolution campaign based on Ferrybox along the Oslo-Kiel transect focusing on the analysis of coupled chemical signals and biological responses was carried out to tackle **Q4**. **Q4** represents two fundamental issues for marine protection from chemical pollution: (1) can the diffuse burden of chemical pollutants present in mixtures in marine coastal waters affect the biological structures of marine ecosystems, and (2) can the measurement of biological data provide additional information to routine chemical coastal data observations? Such questions are difficult to address as ecosystems are simultaneously under the influence of a multitude of factors, including several types of anthropogenic stressors. In pelagic systems, this is even further complicated by the extreme dynamics of biological communities varying both temporally and spatially with high frequency as an effect, among other factors, of marine advection. An opportunity to scientifically tackle these questions is offered by using specific biomarkers as proxies of biological structures. During JRAP 3, we opted for studying the covariance

between a group of chemical pollutants (Polycyclic Aromatic Hydrocarbons (PAHs)) originating from the combustion or spills of fossil fuels and lubricants, and the quantification of microbial markers based on bacterial species and genes, which are specifically stimulated in the presence of hydrocarbons in the marine environment.

The goal of Action 3 was to quantify these specific organisms or genes and investigate the correlations between their abundance and the presence of hydrocarbon compounds in the environment. To our knowledge, this was the first time that such an exploratory exercise was carried out at this scale focusing on environments subject to background diffuse pollution (rather than in the case of extreme pollution events such as oil spills). The study had therefore a high-risk profile and was conceived as an exploratory exercise.

This overall scheme is summarized in **Figure 5.1**.

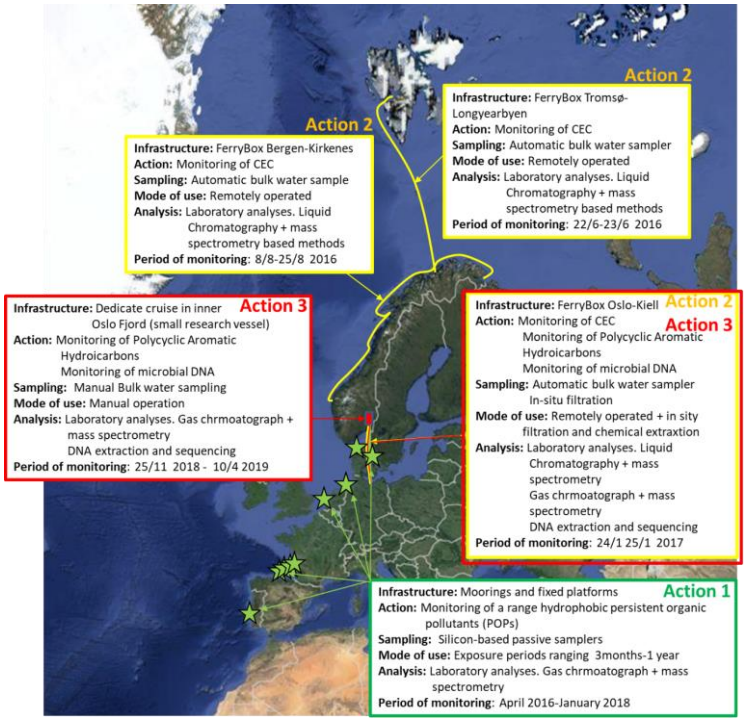

***Figure 5.1**. Overview of the structuration of the monitoring activities carried out within JRAP 3*

5.3. Achieved actions

In Action 1 we succesfully carried out 9 deployments (over a total of 12) of the newly designed passive sampling system (**Figure 5.2**) as described in **Table 5.1**.

5.3.1. Sampling

***Table 5.1:** Detailed information on Passive sampler successful deployments*

Country	Infrastructure	Latitude	Longitude	Operator	Time-Period
Portugal	Monican 1	39.52	-9.64	Instituto Hidrográfico	16/5-16/9 2016
Spain	Mendexa	43.21	-2.26	AZTI	21/2-3/4 2017
Spain	Mendexa	43.21	-2.26	AZTI	21/2 2017 - 8/1 2018
Spain	Mendexa	43.21	-2.26	AZTI	19/6 – 1/8 2017
Spain	Donostia	43.33	-2.26	AZTI	10/3 - 5/12 2017
Belgium	Thornton Bank	51.34	2.59	VLIZ	1/6 – 1/10 2016
Belgium	Bligh Bank	51.42	2.48	VLIZ	1/6 – 1/10 2016
Norway	Torungen Lighthouse	58.4	8.83	MI	13/2 – 8/5 2017
Sweden	Tångesund_SMHI_MOS	58.04	11.29	SMHI	15/4 2016 – 15/4 2017

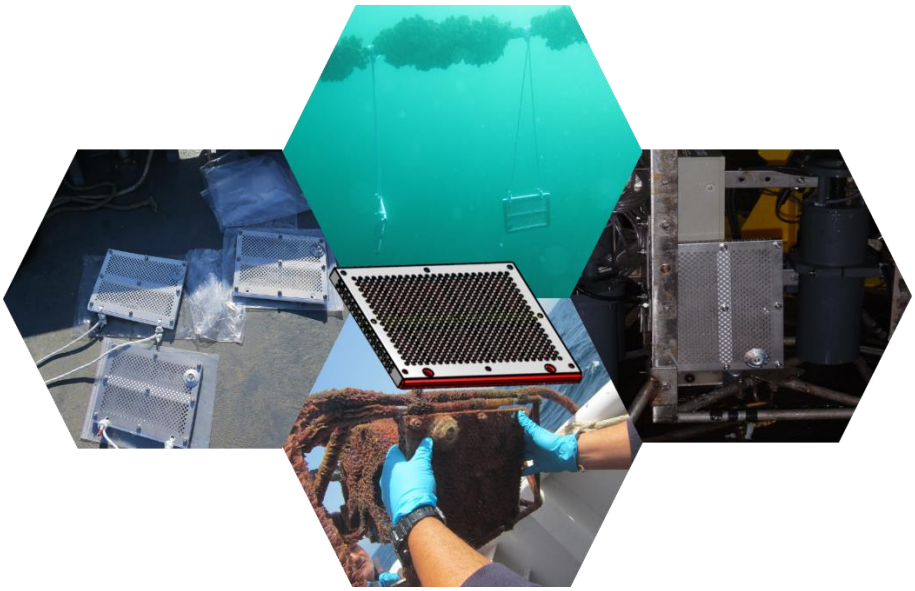

Figure 5.2: *The Jerico Passive sampler concept and images from field deployments*

In Action 2 We conducted three cruises using FerryBox lines as illustrated in **Figure 5.1**. The campaigns took place in three distinct periods: June 2016 on the Tromsø-Longyearbyen line, August 2016 on the Bergen-Kirkenes line and January 2017 on the Oslo-Kiell line.

A significant deviation from the original monitoring plan was introduced. The monitored transect was extended to the Barents Sea and the Arctic. This addition allowed covering remote marine areas, to extend the gradient of anthropic influence and capture contamination of pristine open ocean areas (as opposed to impacted coastal waters). The Tromsø-Longyearbyen transect substituted an additional campaign in the central North Sea. Monitoring the Central North Sea would have provided redundant information with the results from the Oslo-Kiell transect. Both areas indeed suffer from high anthropic impacts. In addition, the central North sea was the study areas of previous research activity on contaminants, including one conducted by the Jerico network in 2015 (Brumovsky et al., 2016a). The deviation introduced in the monitoring plan therefore clearly resulted in a better design to tackle **Q2** and **Q3**.

The whole monitored transect obtained by combining the three campaigns covers an important advection system linking mid-latitude areas in the North Sea to the Arctic, through the Atlantic Coastal Current and the Norwegian Coastal current. One of the scopes of JRAP 3 was to address the potential for marine long-range transport of chemical substances with different properties. The transect covered by the Jerico CRI used during the present study clearly represents an ideal design for tackling this scientific issue.

Sampling carried out during Action 2 was conducted using FerryBox automatic water samples installed as a standard equipment on each unit. In order to validate the measurements, we routinely deployed negative and positive controls, and we addressed the stability of the targeted substances during on board storage through the duration of the sampling campaign. This was necessary to assess whether degradation of the substances after the sampling could affect measurements results, and to validate collected data. The sampling method and sample analyses were previously described by (Brumovsky et al., 2016a).

In Action 3, we conducted a main cruise using the Oslo-Kiell FerryBox. This cruise was conceived to maximize the spatio/temporal resolution in surveying a regional transect. Considering the limitations and the conditions for the chemical sampling, we obtained hourly samples for the analyses of PAHs and biomarkers (corresponding to a spatial resolution of about 1 sample every 25 nautical miles). This sampling frequency was set to increase resolution along transient areas where water properties (or estimated anthropic impact/influence) present maximum variability. A challenge was to identify geographical clusters, which had likely been chronically exposed to high levels of

petroleum contaminants due to the coastal industrial activity, high frequency of shipping activity and highly active harbour areas. Provisionally these areas were assumed to be harbour areas, estuarine areas, areas with intense marine traffic, presence of industry along the coast… We also conducted samplings inside the Inner Oslo Fjord area focusing on a local scale in costal zones known to be chronically exposed to hydrocarbons due to intensive boat traffic and industrial activity.

5.3.2. Parameters

The focus of this task was to simultaneously gather information on distribution of PAHs and of microbial biomarkers from organisms specialized in using oil-related pollution as a source of energy. Samples for molecular biology analysis were collected consistently with those for chemical pollution, filtered through a 0.2 µm filter and frozen at -80°C before further analyses. DNA analysis was conducted using qPCR assays for the quantification on microbial communities and specific organisms. Markers and methods developed in WP3 Task 3.4 (molecular and microbial markers) of JERICO-NEXT were deployed during the present study.

Table 5.2 lists the chemical substances targeted during the study along with the biological parameters and water biophysical parameters recorded during cruises.

Table 5.2. *List of chemical, biological and physical parameters monitored in JRAP 3*

	Chemical parameters	Biological parameters	Physical parameters
Action 1	**Polychlorinated Biphenyls (PCBs):** PCB 28, PCB 52, PCB 101, PCB 118, PCB 153, PCB 138, PCB 180 **Organochlorine Pesticides:** Pentachlorobenzene, Hexachlorobenzene, GammaHCH, BetaHCH, opDDE, ppDDE, opDDD, ppDDD, opDDT, ppDDT **Polybrominated diphenyl Ethers (PBDE):** BDE28, BDE 47, BDE 66, BDE100, BDE 99, BDE 85, BDE 154, BDE 153, BDE 183 **Polycyclic Aromatic Hydrocarbons (PAHs):** Naphtalene, Biphenyl, Acenaphthylene, Acenaphthene, Fluorene, Phenantrene, Antracene, Fluoranthene, Pyrene, Retene, Benzo-b-fluorene, Benzonapthothiophene, Benzo-ghifluoranthene, Cyclopenta-cd-pyrene, Benzo-a-anthracene, Triphenylene, Chrysene, Benzo-b-fluoranthene, Benzo-j-fluoranthene, Benzo-k-, fluoranthene, Benzo-e-pyrene, Benzo-a-pyrene, Perylene, Indeno-123cd-pyrene, Dibenzo(ah)anthracene, Dibenzo(ac)anthracene, Benzo-ghi-perylene, Anthanthrene, Coronene		Water Temperature, salinity, turbidity, current velocity
Action 2	**Pharmaceuticals:** atenolol, caffeine, carbamazepine, clofibric acid, diclofenac, hydrochlorothiazide, ibuprofen, ketoprofen, naproxen, paracetamol, sulfamethoxazole **Personal care products:** DEET, triclocarban, triclosan. **Artificial sweeteners:** acesulfame, saccharin and sucralose. **Current Use Pesticides:** Acetochlor, Alachlor, Atrazin, Azinfos-metyl, Carbaryl, Carbendazim, Dimetachlor, Dimetoate, Diuron, Fenitrothion, Fenoxaprop ethyl ,	Chlorophyll a fluorescence	Water Temperature, salinity, turbidity, current velocity

	Fenpropimorph, Florasulam, Fluroxypyr, Fonofos, Chlorpyrifos, Chlorsulfuron, Chlortoluron, Isoproturon, Malathion, Metamitron, Metazachlor, Metolachlor, Metribuzin, Methyl Parathion, Pendimethalin, Phosmet, Pirimicarb, Prochloraz, Propiconazole, Pyrazon, Simazine, Tebuconazole, Temefos, Terbufos, Terbutylazine, Acesulfam, Cyklamat sodny, Sacharin, Aspartam, Sukraloza, Neohesperidin dihydr.		
Action 3	**Polycyclic Aromatic Hydrocarbons (PAHs):** Naphtalene, Biphenyl, Acenaphthylene, Acenaphthene, Fluorene, Phenantrene, Antracene, Fluoranthene, Pyrene, Retene, Benzo-b-fluorene, Benzonapthothiophene, Benzo-ghifluoranthene, Cyclopenta-cd-pyrene, Benzo-a-anthracene, Triphenylene, Chrysene, Benzo-b-fluoranthene, Benzo-j-fluoranthene, Benzo-k-, fluoranthene, Benzo-e-pyrene, Benzo-a-pyrene, Perylene, Indeno-123cd-pyrene, Dibenzo(ah)anthracene, Dibenzo(ac)anthracene, Benzo-ghi-perylene, Anthanthrene, Coronene	Chlorophyll a fluorescence, Microbial markers of petroleum contamination (Oleispira, Colwellia, petroleum degrading genes).	Water Temperature, salinity, turbidity, current velocity

5.3.3. Data analysis.

A large set of specific data analysis procedures was used. Based on data from Action 1, we tackled Q1 by checking performance of the newly designed silicon-based passive samplers along a set of basic quality assurance and control criteria. Method detection limits were calculated based on field blank results. A measurementfor a given substance was assumed valid if it exceeded three times the standard deviation of the level of the substance in the field blanks. Analytical recoveries from passive samplers were determined through the analyses of spiked internal standards. Passive sampler sampling rates were estimated through the use of performance reference compounds (i.e., analytical chemical standards deliberately added to the passive samplers prior to deployment in the field). By measuring their diffusion out from the sampler to the marine waters, an estimation of the diffusion rate of the different targeted substances can be achieved. The calculations were performed as described in previous papers through a commonly accepted model (Allan et al., 2009; Vrana et al., 2005). Data analysis conducted in JRAP 3 focused in particular on the assessment of measurement quality and on a qualitative comparison between results from different regions. We compared observed variability of measured concentrations against *a priori* based on previous experience with the deployment of similar passive samplers over subregional scales. We expected the variability between impacted and less impacted areas to vary for the different compounds between 1 and 2 order(s) of magnitude.

We tackled **Q2** and **Q3** based on data collected during Action 2. An assessment of data quality was carried out based on a thorough assessment of method detection limits, through the use of adequate field blanks, analytical recovery assessment and stability tests carried out on the full set of targeted chemical substances. Procedures and chemical analyses related to this specific task are described in previous studies where these chemical pollutants were measured in marine waters(Brumovsky et al., 2016a, 2016b; Brumovský et al., 2017a). The assessment of spatial gradients and correlation of chemical pollutant concentrations with bio-physical and geographical parameters were conducted using non-parametric correlation (Spearman). Only compounds with detection frequency >30% were used.

An original spatial analysis was carried out to generate data on potential anthropic influence to individual sampling points. For pesticide contaminants, the influence of riverine runoff (and therefore salinity) was evident (See result section). This was less clear for the group of substances originating from municipal wastewater (namely, pharmaceuticals, personal care products and artificial food additives). An Index of Potential Anthropic Influence (IPAI) was therefore elaborated. This index was based on the distance of sampling points from an aggregated measure of all wastewater emission points in coastal areas. In order to geolocalize municipal wastewater discharge points and weight their contributions as emitting sources a Geographical Information System (GIS) dataset of population distribution in Europe (Center for International Earth Science Information Network, CIESIN) was used

as one of the IPAI model inputs together with a dataset of wastewater discharge points throughout Europe. Emission of contaminants are in fact expectedly proportional to the human population draining in a given point source. In case of inland discharges, the estuary point of the main draining river was considered as the reference source point. Direct discharge points to coastlines were mapped from the position of coastal municipal wastewater drains throughout all Europe. Furthermore, the topographic information regarding coastline surrounding the emission point was included to influence source strength. This was done as dilution in enclosed coastlines (e.g. inside bays or fjords) expectedly occur at a lower rate then in more exposed areas, due to mixing and marine advection. Therefore, a weighting operator, linearly proportional to the percentage of land within a circular range of 10 km surrounding discharge points, was included to influence source contributions. Finally, the overal distance of the source point from the sampling point was considered. Overall, IPAI corresponded to a proxy of the probability of detecting a given substance at a certain distance from the coastal discharge point. A two-dimensional kernel density function was used to estimate IPAI. This function approximated a probabilistic normal distribution function with the maximum value, obviously, at the source point and the shape influenced by a parameter defining the variance. We defined this parameter as the search radius representing the standard deviation of the normal distribution. As the probability of detecting a contaminant at a given point in marine surface water depends on the simultaneous contribution of all sources, the values of the kernel density functions from each source point calculated to any given sampling point of the monitoring were summed to obtain the IPAI value. The correlation between IPAI values and monitoring results was assessed using a non-parametric regression model. To define the spatial range (SR) of a substance (i.e. the value of the search radius for which the correlation coefficient between IPAI and the monitoring data is maximized). SR was conceived to represent a specific descriptor of the inherent behaviour of a given substance in marine water. SR can be seen as a property depending essentially on the contaminants physical chemical characteristics useful to predict the ability of the substance to undergo long-range transport. Further explanation and details on this analysis are included in the discussion section.

Finally we tackled **Q4** based on the data collected during Action 3. Data of contaminants genetic biomarkers were checked for normality and outliers. Data were centered and reduced to account for differences in relative abundances of microorganisms while preserving their correlations. Multivariated (e.g. Principal Component Analysis) and correlation analyses were then carried out.

5.4. Main results

5.4.1. Action 1.

Nine out of 12 deployments of the newly designed passive sampling system were successfully achieved. In three cases, samples went lost: one sampler in Portugal was lost at sea during deployment, while 2 samplers from England went lost during logistics on land. From the retrieved and analysed samples, we could detect most of the targeted relevant substances above the detection limits and within an expected range of variability. Data from different locations showed in fact variability that was contained within 1-2 order(s) of magnitude.

Figure 5.3 summarizes the quality of results. It shows the level of contaminants detected in the samples in comparison with those found in field and laboratory blanks. The recovery performances of two intentionally added contaminants through spiking (PCB 29 and PCB 185 not found in the environment) are also reported. Effective sampling rates of the passive samplers were derived from reference depuration compounds. From case to case differences in sampling rates were observed. On average, sampling rates were 20 $L.d^{-1}$ ranging for individual deployments between 4 and 50 $L.d^{-1}$ (**Figure 5.3**).

Figures 5.4 and **5.5** show the measured distribution of POPs, and PAHs observed in coastal European waters through the use of silicon-based passive samplers on fixed CRI.

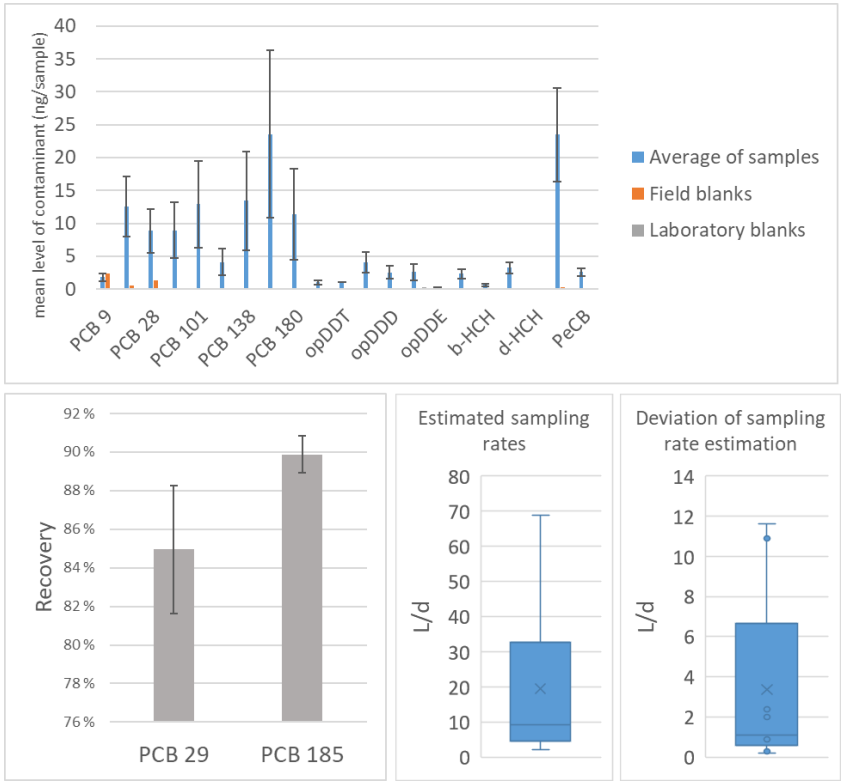

Figure 5.3: *Quality assurance and control results. The upper panel shows the level of different contaminants measured in the samples (Mean + standard errors) in comparison with the levels measured in the field and laboratory blanks. The lower panel (left) shows the results of recovery performance of the analytical method measured through the use of two representative recovery standards. The lower panels on the right show results for estimated effective sampling rates (through the use of performance reference compounds spike to the sampler prior deployment) and their deviations.*

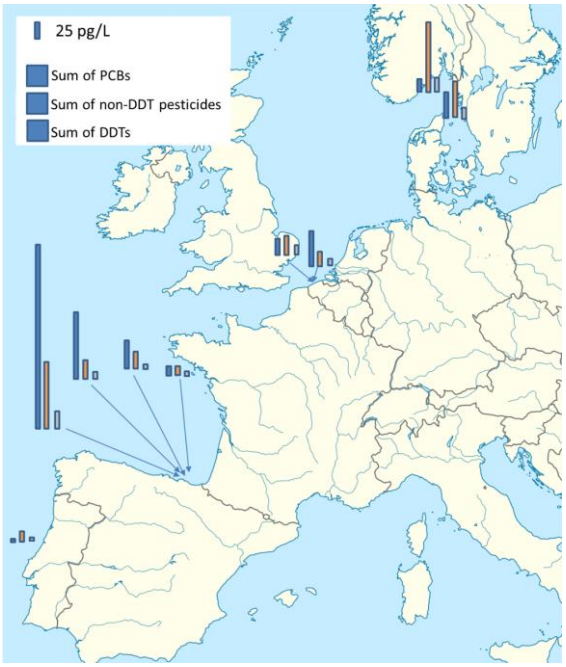

Figure 5.4: *Distribution of selected POPs observed from the deployment of silicon passive samplers on fixed CRI in JERICO-NEXT adjusted for effective sampling rates of silicon passive samplers during individual depolyments.*

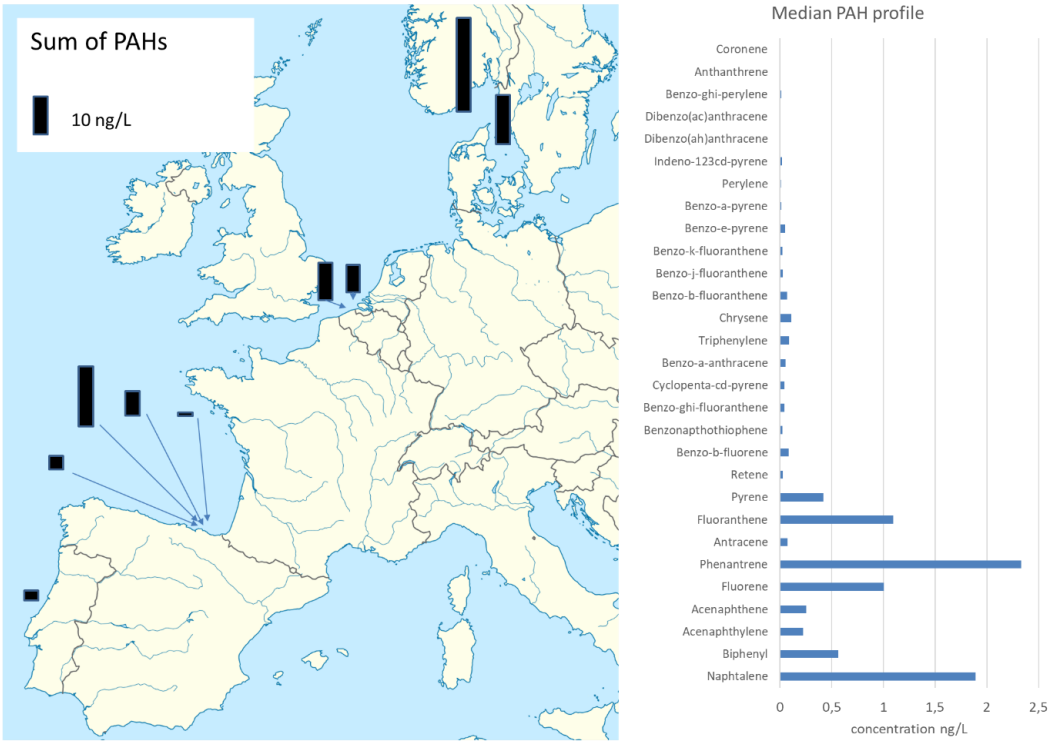

Figure 5.5: *Distribution of PAHs observed from the deployment of silicon passive samplers on fixed CRI. On the right the median composition of the PAH mixture measured in the different locations is depicted.*

In all samples (with the exclusion of those from the Basque Country), the concentration of polybrominated diphenyl ethers (PBDE) were determined. These are banned flame retardants often used as additives in plastic that have endocrine disrupting properties on vertebrates. Results are shown in **Figure 5.6**.

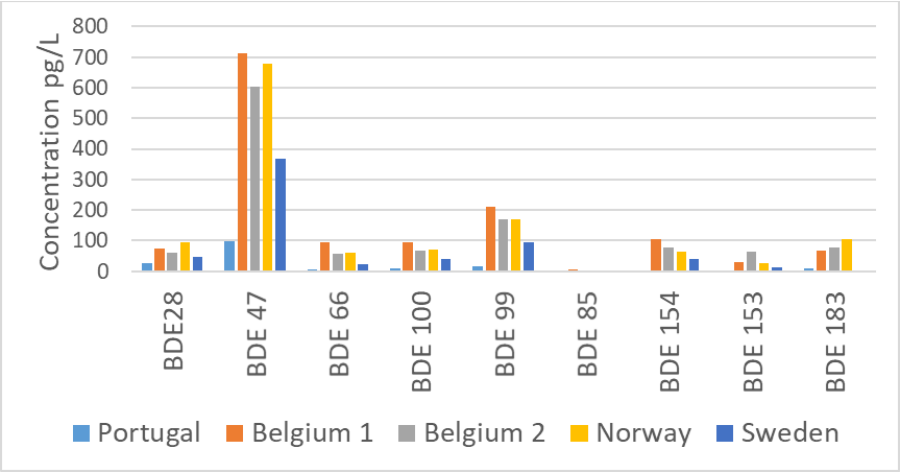

Figure 5.6: *Concentration of selected PBDEs from the deployment of silicon-based passive samplers.*

In the case of the Basque country deployments, monitoring with a higher resolution was conducted. In this case, four passive samplers were deployed at two different sites of the southeastern Bay of Biscay. Three of them were located in the aquaculture facilities of Mendexa, whilst the fourth one was fixed to a buoy in Donostia. The passive

sampler deployments on te fixed platforms delivered data that enabled the characterization of water contamination profile and the assessment of the main seasonal fluctuation. Detailed results are shown in **Figure 5.7**.

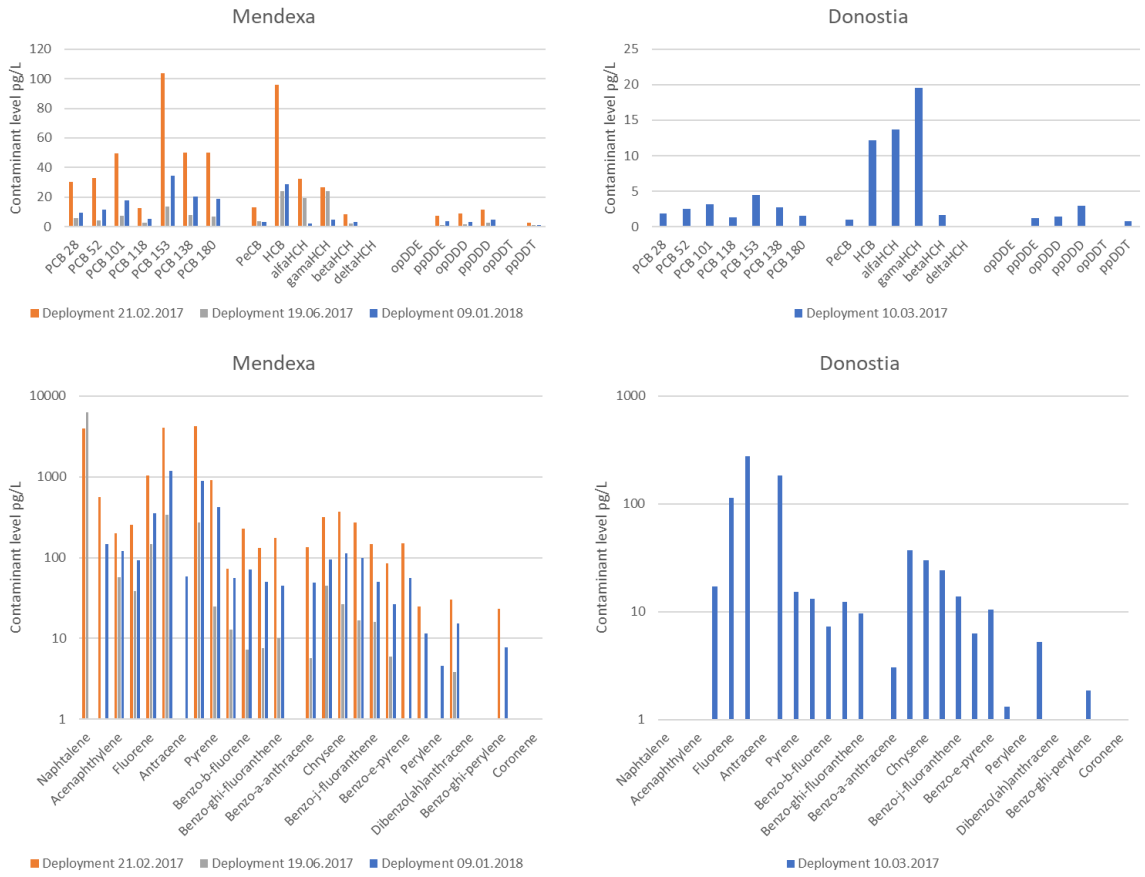

Figure 5.7: *Results of the analyses of passive samplers deployed in the Bay of Biscay during 2017-2018.*

As a general overview of the results, most of the deployments were successfull. Quality criteria were matched with the majority of targeted compounds being quantified at level well above the limit of detections derived from field blank results. Excellent recoveries were obtained for the two tested standards (PCB 29 and PCB 185), which accounted for of range physical-chemical properties covering most of the other targeted substances. Effective sampling rates were successfully estimated using the performance reference compounds and showed a pronounced variability across different deployments, possibly reflecting heterogeneous conditions of temperature, salinity and marine advection.

We observed a variability in measured concentrations across different locations essentially varying within 1-2 orders of magnitude for each individual compound. This is in line with *a priori* expectations. The deployment carried out in offshore Atlantic waters provided the lowest observed concentrations for all compounds, and coastal samples were more contaminated than offshore ones.

More insights on the capability of these devices in reporting spatial and temporal changes in contaminant concentrations can be obtained by looking at the deployments carried out in the Basque Country where the monitoring was carried out at higher resolution, including redeployments of samples in the same location over different periods. Measurements provided consistent information on the contamination profile, with the relative proportion of different contaminants substantially maintained between locations and across deployments during

different seasons. The main axis of variability was represented by time. In Mendexa, winter and early spring concentrations tended to be higher than in summer for most compounds, which here again was expected. The targeted contaminants were prevalently hydrophobic volatile substances with the atmosphere serving as major source (Gioia et al., 2008; Lohmann et al., 2009). Lower temperatures favour partitioning of these compounds, present as gases in the atmosphere, towards the water. PCBs were the most abundant group of POPs regulated under the Stockholm Convention. Hexachlorobenzene was the must abundant chlorinated pesticide. All DDT congeners were below 10 pg.L^{-1}, with a contamination profile dominated by methabolites such as p,p'DDE and p,p'DDDn reflecting the influence of secondary sources (e.g. old burden of contaminants volatilizing from soils and depositing in seawater, or released from sediments) re-emitting "aged" pesticides.

5.4.2. Action 2

Quality of measurements. Based on the results of field blanks (i.e. negative controls) detection limits were quantified for individual compounds ranging 0.005–17.50 ng/L. These allowed meaningful detection of several substances in marine coastal areas and open sea. The highest detection limit was observed for caffeine due to high levels in the field blanks, likely because of on-board contamination. Except for caffeine, all other targeted substances had detection limits below 1 ng.L^{-1}. Traces of several compounds, including caffeine, diclofenac, paracetamol, DEET and acesulfame, were measured in field blanks. These were generally higher than the levels measured in procedural blanks (i.e. negative controls processed to access the sample contamination originating from the chemical laboratory). Low levels of diclofenac, DEET and sucralose were consistently detected in procedural blanks. The occurrence of traces of the compounds in field and procedural blanks had a limited effect on the quality of the measurements and on the significant detection of most of targeted water contaminants.

The recovery test based on the application of spiked positive controls provided satisfactory results too. Recoveries of all compounds were in the range 50–120 %, except for acesulfame, which reached lower values (34±8 %). Relative standard deviations among replicated (n=7) recovery tests were <20 %.

The stability test indicated that the recovery of most of targeted substances in the spiked sample was >65%, except for saccharin (34%), triclosan (44%), triclocarban (48%) and caffeine (54%). These results provide a conservative estimate of compounds stability since analytes were present in the spiked matrix in the sampler for the full duration of the cruise. It is important to note that the losses during stability tests may be due to both degradation and partitioning (sorption/volatilization) of the substances.

Because quality criteria were satisfactory fulfilled no recovery correction were applied to quantitative results.

Observed Levels and distribution of contaminants of emerging concern (CEC) in European coastal waters. Forteen out of 17 targeted CECs were detected in the presented study at least once in the Northern European and Arctic seawaters. These included: 4 anti-inflammatory drugs (diclofenac, ibuprofen, ketoprofen, and naproxen), the three artificial sweeteners, a β-blocker (atenolol), a stimulant (caffeine), an anticonvulsant (carbamazepine), an analgesic (paracetamol), an antibiotic (sulfamethoxazole), an insect repellent (DEET) and an antimicrobial agent (triclosan). **Table 5.3** summarizes detection frequencies of targeted chemicals in seawater samples, including different sections of the sampled transect. The antilipidemic clofibric acid, the diuretic hydrochlorothiazide and the antimicrobial agent triclocarban were present below their detection limits in all samples.

Out of the detected chemicals, carbamazepine, naproxen, sulfamethoxazole, DEET and sucralose were found above the detection limits at more than 50% sampling sites (**Figure 5.8**). The antiepileptic carbamazepine was detected in 100% of samples in the range 0.02–1.01 ng.L^{-1}. The second most frequently detected contaminant was the artificial sweetener sucralose found at 86% sites at levels 0.82–15.29 ng.L^{-1}. Naproxen, DEET and sulfamethoxazole were found at 74%, 68% and 56% sites at levels 0.03–0.78, 0.63–51.54 and 0.11–0.45 ng.L^{-1}, respectively

For most targeted CECs, detection frequency was highest in the Skagerrak-Kattegat transect and Oslo Fjord. Detection frequencies decreased from South to North reflecting the postulated distribution of sources of

wastewater-related-pollution. Maximum contaminant levels were frequently detected in the Kattegat-Skagerrak-Oslofjord transect (e.g. for carbamazepine, sucralose and sulfamethoxazole). Saccharin was detected in this area at surprisingly high concentrations ranging 3.01–285.15 ng.L^{-1}. The maximum detected concentrations of other contaminants ranged typically from 0.1 to 1 ng.L^{-1} and were mostly recorded in this same coastal area.

As for pesticides, the ubiquitous distribution of some herbicides such as atrazine and simazine was observed (**Figure 5.9**). These are highly persistent photosynthetic inhibotors toxic to primary producers at low concentrations. Interestingly, for most detected current use pesticides, a correlation with water salinity was observed. The correlation, however, in most cases held when only the results from the meridional part of the transect (Oslo-Kiel transect) were considered. When the entire dataset was included, a simple bi-variate regression model could not capture the distribution of these compounds.

Table 5.3: *Detection frequencies of targeted chemicals*

.

	Detection frequency (%)			
	Overall	**Baltic outflow (BO)**	**Norwegian West Coast (NWC)**	**Barents Sea (BS)**
Pharmaceuticals				
Atenolol	12	35	0	0
Caffeine	14	18	15	10
Carbamazepine	100	100	100	100
Clofibric acid	0	0	0	0
Diclofenac	4	6	0	5
Hydrochlorothiazide	0	0	0	0
Ibuprofen	12	18	15	5
Ketoprofen	18	53	0	0
Naproxen	74	53	92	80
Paracetamol	34	29	62	20
Sulfamethoxazole	56	100	62	15
Personal care products				
DEET	68	6	100	100
Triclocarban	0	0	0	0
Triclosan	4	0	0	10
Food Additives				
Acesulfame	28	82	0	0
Saccharin	34	100	0	0
Sucralose	86	94	100	70

.

Only few studies have focused on monitoring CEC (including pharmaceutical, personal care products and artificial food additives) in coastal and marine waters. As a results the distributions and behaviors of these compunds are yet poorly understood (Arpin-Pont et al., 2016; Gaw et al., 2014)(Borecka et al., 2015a; Gros et al., 2012; Klosterhaus et al., 2013a; Magnér et al., 2010; Munaron et al., 2012a; Nödler et al., 2014a; Vidal-Dorsch et al., 2012; Weigel et al., 2004). Environmental occurrence of pharmaceuticals is of special concern since these compounds are designed to be bioactive at very low concentrations and, hence, could pose a risk to ecosystems even at low concentrations.These compounds were often detected in coastal and estuarine areas but dat for

transitional waters and offshore areas are still largely lacking. Carbamazepine is ubiquitous in the freshwater compartment (Hughes et al., 2013) and has been detected at low levels even in offshore water in the North Sea, the Adriatic Sea and the Mediterranean Sea (Brumovský et al., 2017b, 2016; Loos et al., 2013; Weigel et al., 2001). Carbamazepine is one of the most frequently reported pharmaceuticals in environmental samples including biota (Gaw et al., 2014). Results of Activity 2 confirm the broad distribution of this substance highlighting the trends of marine water concentrations along a large-scale trans-regional transect

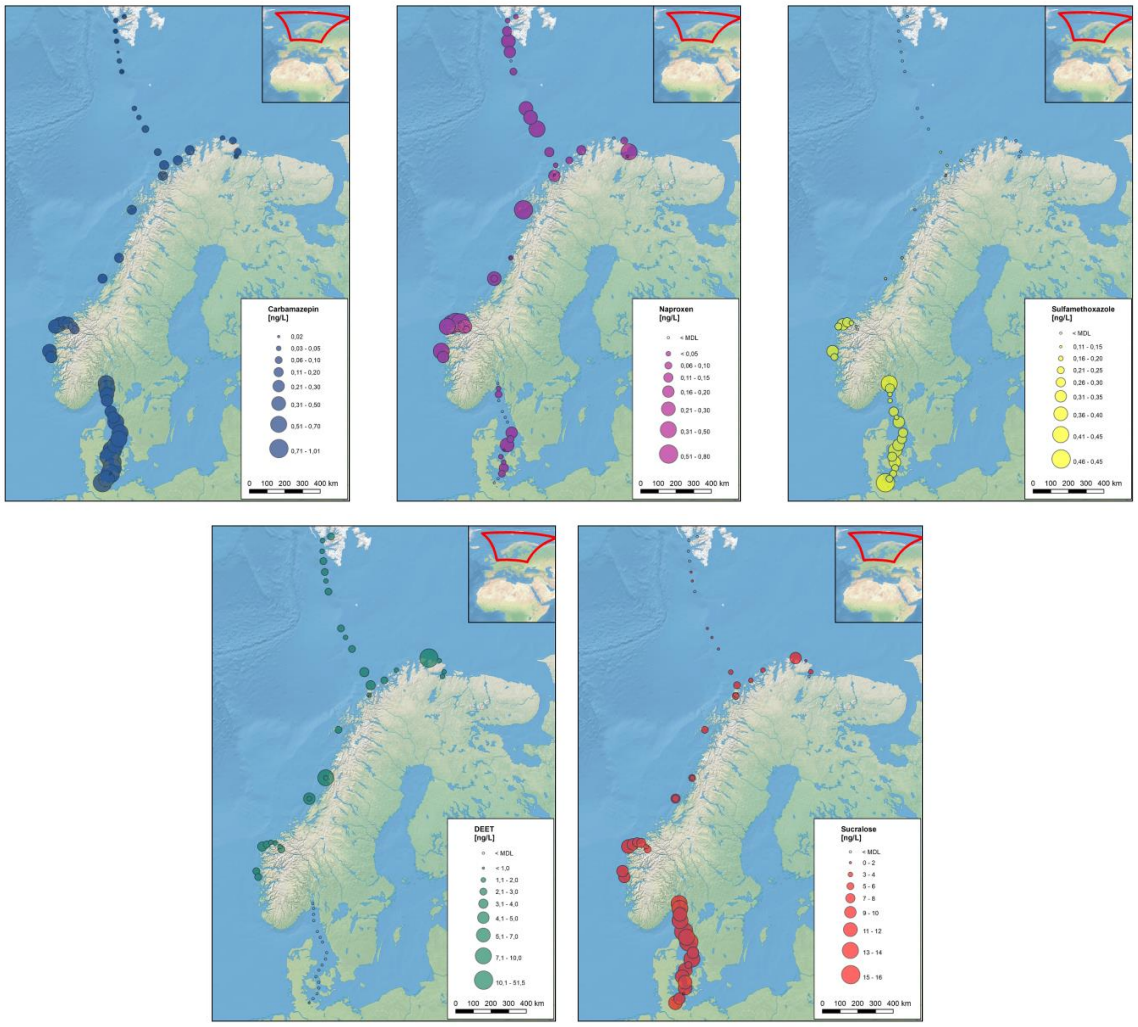

Figure 5.8: *Levels of selected PPCPs and food additives detected at >50% sites. Detected concentrations are depicted as circles at individual sampling sites.*

The antibiotic sulfamethoxazole has been previously detected in near-shore waters (Alygizakis et al., 2016; Borecka et al., 2015b; Klosterhaus et al., 2013b; Nödler et al., 2014b; Shimizu et al., 2013; Zhang et al., 2013a)(Loos et al., 2013). Three previous reports have documented the occurrence of sulfamethoxazole in the open sea (Brumovský et al., 2017b, 2016; Zhang et al., 2013b) (two of which made use of Jerico FerryBox systems). Antibiotics are designed to be toxic to bacteria at low concentrations. Despite the low detected levels, their presence in the environment and marine waters may pose a pressure to microorganisms. The present results confirm Sulfamethoxazole as a marine contaminants of broad distribution in coastal water, providing original insights and new information on its trend along a large-scale transregional gradient. Notably detection of this antibiotic was achieved even in relatively open waters of the west coast of Norway and in Northern Norway.

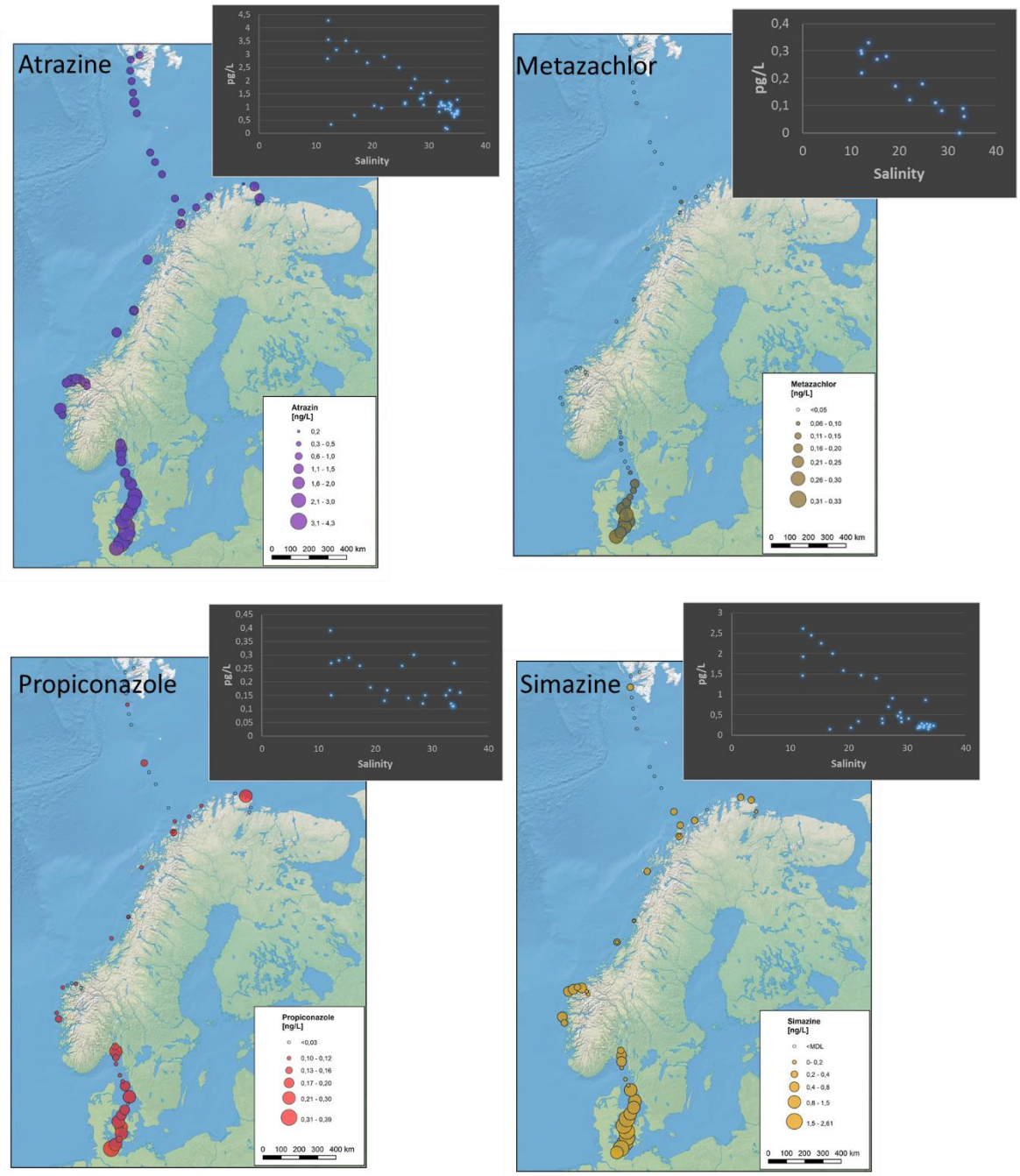

Figure 5.9: *Selected results from current-use pesticide analyses, showing the broad distribution of two photosynthesis inhibitor herbicides of high priority for environmental protection (atrazine and simazine), another herbicide never detected before in coastal waters (metazachlor) and one the fungicide propiconazole. The black chart plot show the relationships between concentrations and seawater salinity.*

Non-steroidal anti-inflammatory drugs (NSAID) are some of the most often detected CECs in coastal areas (Gaw et al., 2014). Naproxen was one of the most abundant pharmaceuticals detected during the present study with concentrations up to 0.78 ng.L^{-1}, similar to the levels detected in our previous studies in the North Sea and the Mediterranean Sea (Brumovský et al., 2017b, 2016) (as part of other Jerico monitoring activities).

The concentrations of ibuprofen observed in Action 2 were in the same order of magnitude as those reported in the Mediterranean (Brumovský et al., 2017b; Loos et al., 2013).

Diclofenac was found here only at two sampling sites at concentrations 0.30 and 0.64 ng.L^{-1}which is lower as compared to data from other coastal areas (Alygizakis et al., 2016; Nödler et al., 2014b).

The antipyretic paracetamol has been previously detected at similar levels as those observed here in the North Sea, the Adriatic Sea along the Mediterranean coast (Alygizakis et al., 2016; Brumovský et al., 2016; Nödler et al., 2014b).

Caffeine has been previously detected in coastal and offshore waters (Alygizakis et al., 2016; Brumovský et al., 2017b, 2016; Klosterhaus et al., 2013b; Loos et al., 2013; Munaron et al., 2012b; Nödler et al., 2014b; Weigel et al., 2002, 2001). The levels measured in the present study (18.62-71.81 ng.L^{-1}) are an order of magnitude higher compared to those already reported for the open North Sea (Brumovský et al., 2016). This obviously points to an important influence of local inputs to the Baltic and is consistent with higher *per capita* coffee consumption in Northern Europe.

During the present study, DEET was typically detected at higher (by a factor of 3) concentrations than in the North Sea (Brumovský et al., 2016; Weigel et al., 2002, 2001) and the Mediterranean Sea (Brumovský et al., 2017b; Loos et al., 2013).

All three investigated artificial sweeteners have been previously detected in the North Sea (Brumovský et al., 2016) with acesulfame and sucralose having 100% detection frequency. During the present study, we reported similar acesulfame and sucralose concentrations. Sucralose was the most abundant artificial sweetener whereas the lsaccharin concentrations were significantly lower (<0.95–3.01 ng.L^{-1}). In other few studies sucralose has been detected in coastal/estuarine areas in proximity to highly populated cities (Gan et al., 2013; Green et al., 2008; Mead et al., 2009; Sang et al., 2014). Saccharin and acesulfame were detected in two studies in close-to-shore waters in estuarine areas close to municipal outflow (Gan et al., 2013; Sang et al., 2014).

We elaborated a novel frame to analyse spatial distribution of anthropogenic chemical pollutants, taking advantage of the monitorin conducted in Action 2. A more sophisticated heuristic approach was introduced through the formulation of the Potential Anthropic Influence index (IPAI). This index was designed during data analyses of Action 2 as a correlator for the concentration distribution observed from the monitoring in order to support the analyses of the spatial range (SR) of individual substances. SR is a heuristic measure of the efficiency of contaminants' marine transport. The more efficiently a substance is transported away from the discharge points, the lower will be the decline of its concentrations at increasing distances from the source point. The concept of SR is obviously relevant for planning monitoring of chemical pollutants, as the SR of a substance will fundamentally correlate to the probability of finding it at a given distance from the source point. As such, it was one of the main aims of JRAP 3 to focus on approaches to derive estimates of SR for different substances and derive recommendations for future monitoring design. Figure 3.3.14 schematically illustrates this approach considering (for the sake of simplification) a unidimensional spatial transect. During its application with the field observations the method was obviously applied to the two-dimensional spatial field of environmental concentrations in surface marine waters. Briefly, the approach assumes that discharges to coastal waters of pharmaceuticals, personal care products and food additives are virtually continuous and constant over time.

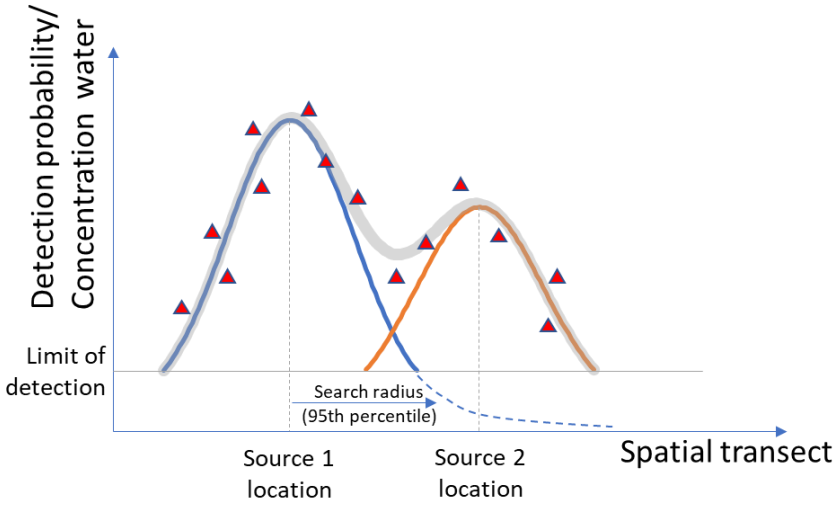

Figure 5.14: *Schematic representation of the approach for estimating SR of a given contaminant "A". The figure depicts two point-sources for A located at different places along the spatial transect (i.e. the coastline) and having different strengths. Red triangles represent hypothetical observations from monitoring along the transect. The distribution curves represent the probability (P) of detecting a substance at any given distance from source point. The grey shadowed line is the spatially aggregated probability from the two source points, that can be regarded as an Index of Potential Anthropic Influence (IPAI) from coastal emitting sources. Despite differences in emission rates the distribution curve of the two sources have the same variance as this substantially depends on contaminant specific physical chemical properties. The search radius (representing the distance along the transect from source point where P is higher than 5%) is proportional to such a variance. Different values of the SR will result in different estimates of the Index of Potential Anthropic Influence (IPAI) represented by the value of the cumulative grey curve at the location of any given sampling station. SR is then calculated as the value of the search radius that maximizes the correlation between IPAI and observed concentrations from monitoring results.*

Figure 5.14 elucidates the approach with an example. Let's consider an hypothetic substance A emitted in two locations along the coastline The mean rate of emission is different at the two sites, indicated by the pick of the concentration in proximity to the source point.. Emission rates can vary among locations, for example, because of different population sizes discharging at different points. The concentration in proximity of the source point can be also mediated by the local rate of renewal of marine water driven by currents. Assuming as a minimalistic model, that over a sufficient amount of time dilution and transport in different directions of the transect is in average similar, a normal probabilistic distribution (NPD) of detecting substance A at a given point along the transect can be drawn. If emissions sources are more than one (as depicted in Figure 3.3.14) an aggregated NPD can be derived summing the contribution from each source. As the SR of substance A is essentially determined by its physical chemical properties and the limit of the detection method, it can be assumed, in first instance, that the variance underpinning the NPD from source point 1 and 2 will be the same, despite the sources having different strength. Based on this simple premises, it is suggested that SR of a substance can be approximated by a measure of the variance of the NPD. In this case we focus on the concept of the "search radius" representing the standard deviation of the NPD. In reality, it can be expected that multiple sources will contribute simultaneously to the concentration field over a marine area. Therefore the approach to derive SR for any given substance encompasses the following two steps:

- Estimating P at any point of the spatial field (i.e. at any marine location) from drawing NPD functions from all individual sources after geolocalizing them and weighting their influence by the size of the human population served by the drain, and the level of marine water mixing expected in proximity of the discharge point.

- Identifying the value of the search radius of the NPD for which the correlation between P and the measured concentrations in surface water is maximal and significant.

This heuristic frame was conceived to enable estimation of SR based on monitoring data. It introduces an important simplification by not accounting for a detailed description of the influence of marine advection. We argue that this is an important quality of the spatial analyses presented here that can make it particularly applicable in complex coastal areas, especially when the spatial resolution of the monitoring data is high and resolution of potentially available advection models (that can imnprove the sophistication of the IPAI calculation) low. In most cases, a detailed description of hydrodynamics is hardly achievable to further constrain the assessment of SR. **Figure 5.15** maps the SR values obtained for Sucralose along the Oslo-Kiell transect by combining after finding highest correlation between IPAI and the monitoring data. **Figure 5.16** also illustrates the variation of the Spearman correlation coefficient values between IPAI and concentration data at varying research radius of the kernel density distribution.

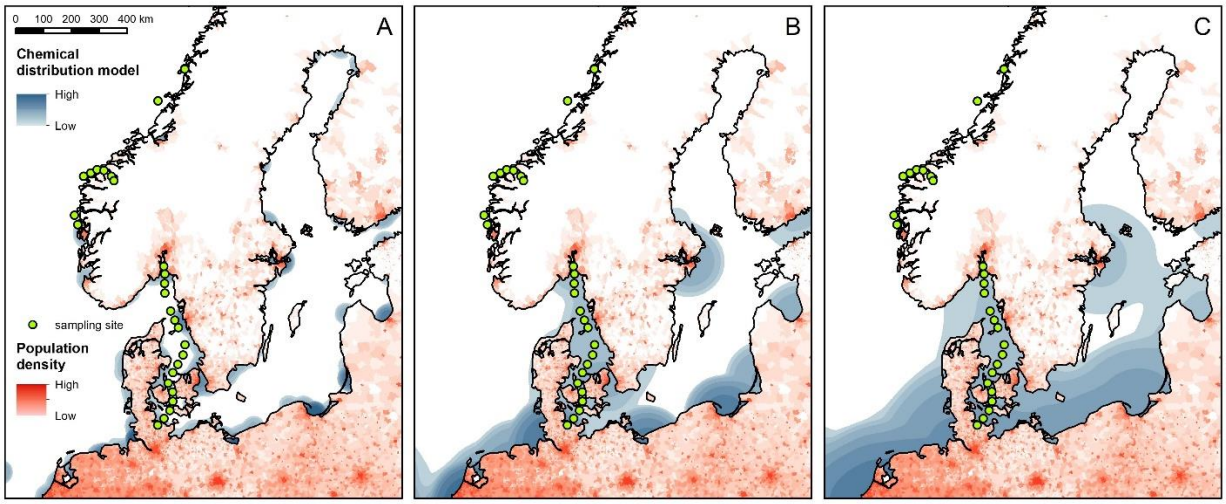

Figure 5.15: *Mapping of IPAI value from all European Coastal discharges of municipal wastewater, calculated assuming a search radius of (A) 50 km, (B) 150 km and (C) 300 km. Beyond the value of the search radius, IPAI is sensitive to the sources strength (e.g. the number of people leaving in a given discharge catchment) and the characteristic of the coast in proximity to the discharge points (e.g. a higher IPAI value is given for a source releasing in an enclosed coastal zone, such as a fjord, or a gulf, where dilution by marine advection is expectedly lower). Maps such as this can be used aspriors for the planning of spatial resolution and geographic breath of future monitoring actions in order to maximize expected variance in monitoring results.*

SR and IPAI maps can be used to rank substances based on their ability to travel away from sources, and to plan the spatial/temporal resolution of future monitoring actions using mobile research infrastructures such as FerryBox or other resources. Sucralose and saccharin represent good illustrative examples. Both these substances are artificial sweeteners with common coastal emitting sources (e.g. municipal wastewater discharge points). However, sucralose is more persistence to biochemical and fotodegradation, while saccharin is much less persistent. Saccharine appear in fact to have a lower spatial range than sucralose. In order to maximize the variability of monitoring result (e.g. given an established fix number of samples), a researcher should consider a higher spatial resolution for saccharine along a shorter transect compared to sucralose. Considering the definition of SR, in the case of sucralose (with SR = 170 km), one could reasonably anticipate that this contaminants is likely to be detected even at distances from a given source exceeding 3 times the SR (e.g. over 500 km). Sucralose is expectedly a “long-range swimmer”. As a confirmation, sucralose was detected in our campaign in most locations, including remote sampling area of the Barents Sea and the Arctic. These monitoring data highlights sucralose as one of the most abundant anthropogenic marine pollutant ever identified. **Table 5.4** shows the results for the estimation of the SR index for those compounds with detection frequency higher than 50%.

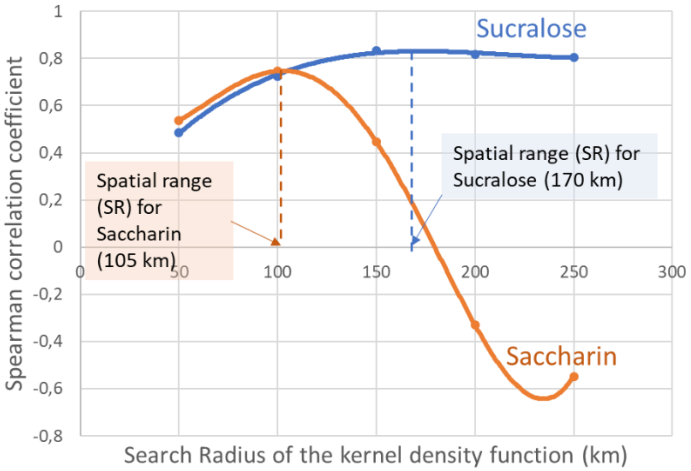

Figure 5.16: *Assessment of SR for sucralose and saccharin (as a comparison between substances with same emitting sources but contrasting spatial range). SR is the value of the probabilistic distribution P variance for which the correlation between the values of the calculate IPAI (aggregated from all emitting sources) and the concentration data from monitoring is maximal.*

Table 5.4: *Calculated SR indexes for selected compounds.*

	Calculated spatial range index (km)
Saccharine	105
Sulfamethoxazole	150
Sucralose	170
Carbamazepine	> 300
Naproxen	not applicable
DEET	not applicable

It is obvious that such a model for the estimation of the spatial range is applicable only if a significant correlation if found between IPAI and monitoring data. In this case, no correlation or inverse correlation were found between IPAI and monitoring data for some compounds. This indicated that different processes, not accounted by the IPAI model contribute to the determination of the concenbtration of those compounds in the marine environment. Through this experience we demonstrated however that for some substance, especially pharmaceuticals, personal care products and artificial food additives, such a condition is verified, at least in the selected monitored region. These results will therefore be useful to design future sampling strategy and use CRI for chemical pollution monitoring in a more efficient and focused way.

Notably, in case of the current use pesticides this approach provided interesting insights for many of them. The elaboration, had however to be reformulated, assuming only river estuaries as major sources, as these contaminants reach water ecosystems essentially through surface runoff. atrazine, diuron, propiconazole, Simazine and Tebuconazole all had calculated SR of over 250 km. These substances are indeed found in some of the remote areas of the transect. In particular, atrazine was the most ubiquitous marine contaminants identified.

Such a strong dependence on estuarine emissions makes water salinity a very good proxy of pesticides concentrations in coastal waters. Future monitoring actions for current use pesticides in coastal waters may therefore adopt a heuristic approach and use well-known salinity transects to design extension and resolution of the sampling.

Overall, data gathered during Action 2 produced important insights on the usefulness and capability of CRI such as the FerryBox fleet to address questions concerned with the identification of drivers and factors influencing the spatial distribution and the potential for long range transport of marine chemical pollutants.

5.4.3. Action 3.

PAHs were analysed along the Oslo-Kiel transect using a custom design sampling device on board of a FerryBox unit Color Fantasy. This sampling device was specifically designed to prevent contamination from on-board sources as the FerryBox laboratory in this unit is positioned in the engine room where atmosphere is enriched with PAH volatilizing from fuel and lubricant oils. The sampling device used high volume *in-situ* filtration and extraction under controlled atmosphere. A purified N pressure was applied to push the pre-collected water sample through the filter and extraction cartridge (**Figure 5.10**).

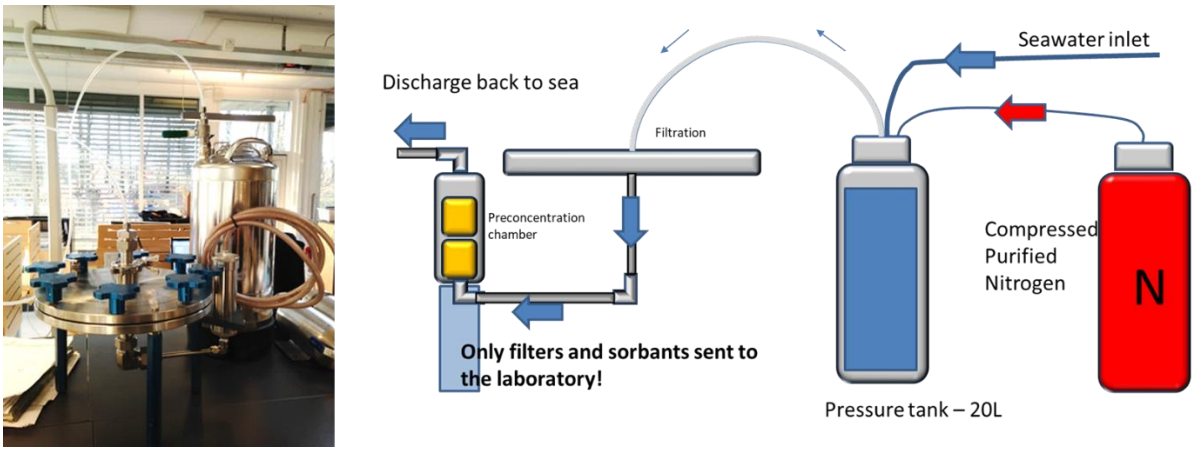

Figure 5.10: *Costum design* in situ *filtration-extraction high-volume sampler specifically developed for deployments on FerryBox units.*

Using this device, we routinely detected several PAHs across the full sampled transect. Phenanthrene, fluoranthene and pyrene, were observed at highest concentrations. Some high molecular weight PAHs were also detected in all sampling locations. These included in particular: benzo(a) anthracene, chrysene, benzo(b)fluoranthene, benzo(k)fluoranthene, triphenyl, benzo(j)fluoranthene and benzo(e)pyrene. **Figure 5.11** shows the distribution of the sum of PAH concentration along the monitored transect during the January 2017 campaign.

A significant variability in the concentration distribution was observed with the highest level measured in area of high anthropic impact, such as harbors in Oslo and Kiel, in the area of the Danish Straight and interestingly at the latitude ot the river Gøta Estuary, Station 1 being Oslo, Station 20 being Kiel (**Figure 5.11**). Sum of PAH concentrations ranged between 0.2 and 6 $ng.L^{-1}$.

Different microbial markers have been selected for the detection of pollutants in coastal seawaters, with focus on acute and chronic low-level hydrocarbon pollution and analysed using the qPCR assay: *Colwellia*, *Oleispira antartica* and AMA. *Oleispira antarctica,* a hydrocarbonoclastic bacterium, has been shown to be an important oil-degrading microorganism in cold marine environments. *Colwellia* species have been reported to be capable of degrading hydrocarbons, including during the Deepwater Horizon oil spill in 2010; these species play also a role in global carbon and nutrient cycling in cold marine environments. *Alteromonas, Marinobacter, Alcanivorax (AMA)* are typical hydrocarbonoclastic microorganisms in the marine environment.

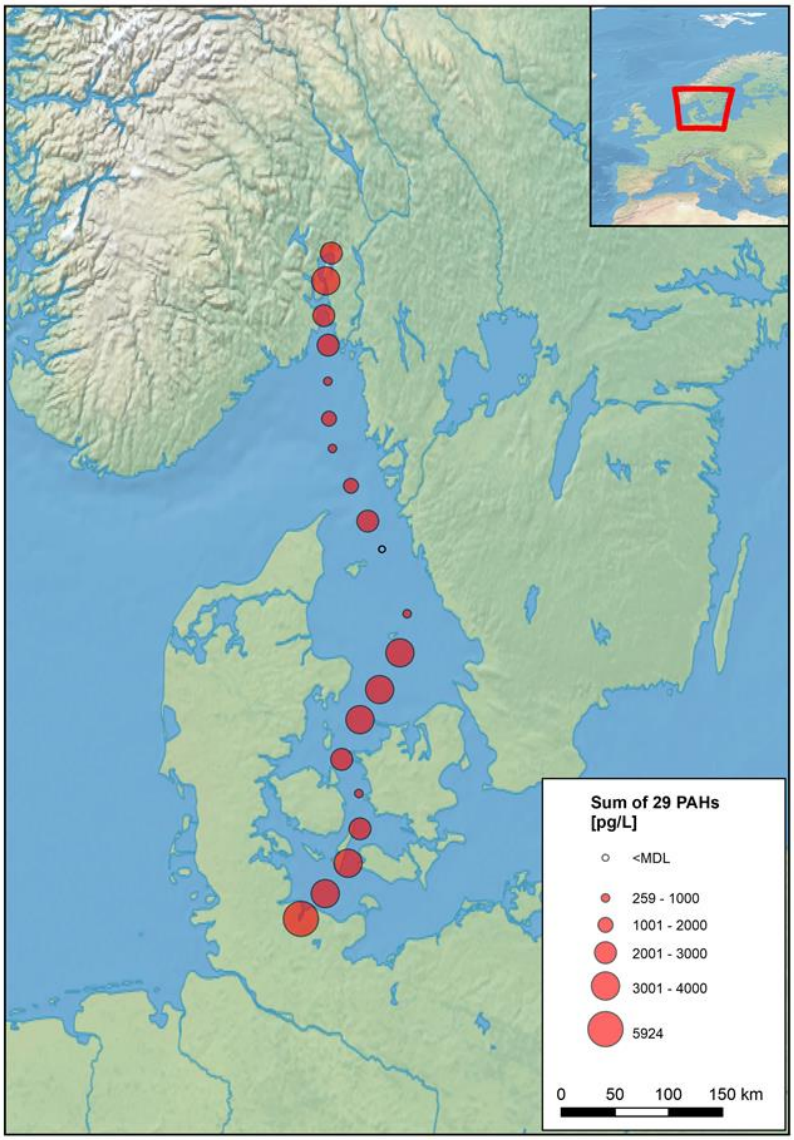

Figure 5.11: *Sum of measured PAHs along the Oslo-Kiel transect.*

Figure 5.12 shows the spatial distributions of the selected biomarkers in relation to PAH distribution. The spatial distributions of Biomarkers (especially AMA) tend to mirror the general PAH distribution pattern. However, biomarkers (especially *Colwellia*) also seemed affected by the presence of freshwater

This conclusion was confirmed by plotting the data over a temperature/salinity (T/S) diagram (**Figure 5.13**). Most stations are part of three groups, which form an overall gradient along the sampled transect. Group A represents the Skagerakk stations between Denmark, Norway and Sweden. They have less coastal characteristics, with higher temperature and salinity. Group C represents the stations in Samso and Great Belts, clearly influenced by river and surface runoff, with low salinity and low temperature. Group B is a mixed group, encompassing the stations along the Oslo fjord, and the stations in the southern part of the Kattegat which are influenced by the Baltic Sea.

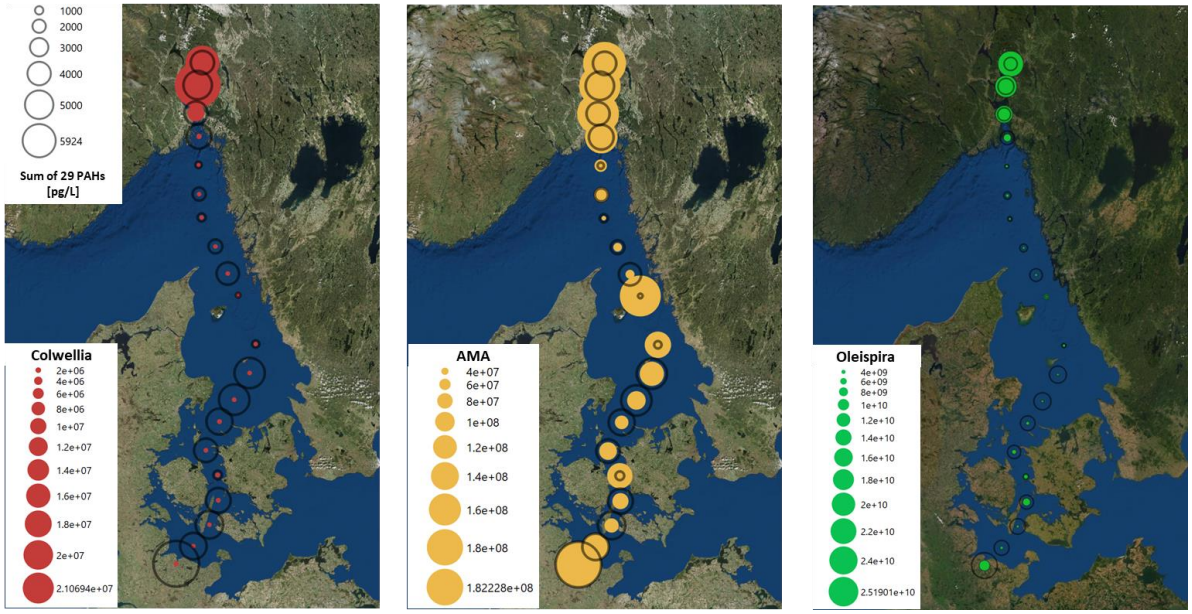

Figure 5.12: *Distribution of abundance of* Colwellia, *AMA and* Oleispira *compared with the distribution of measured PAHs along the Oslo-Kiel transect.*

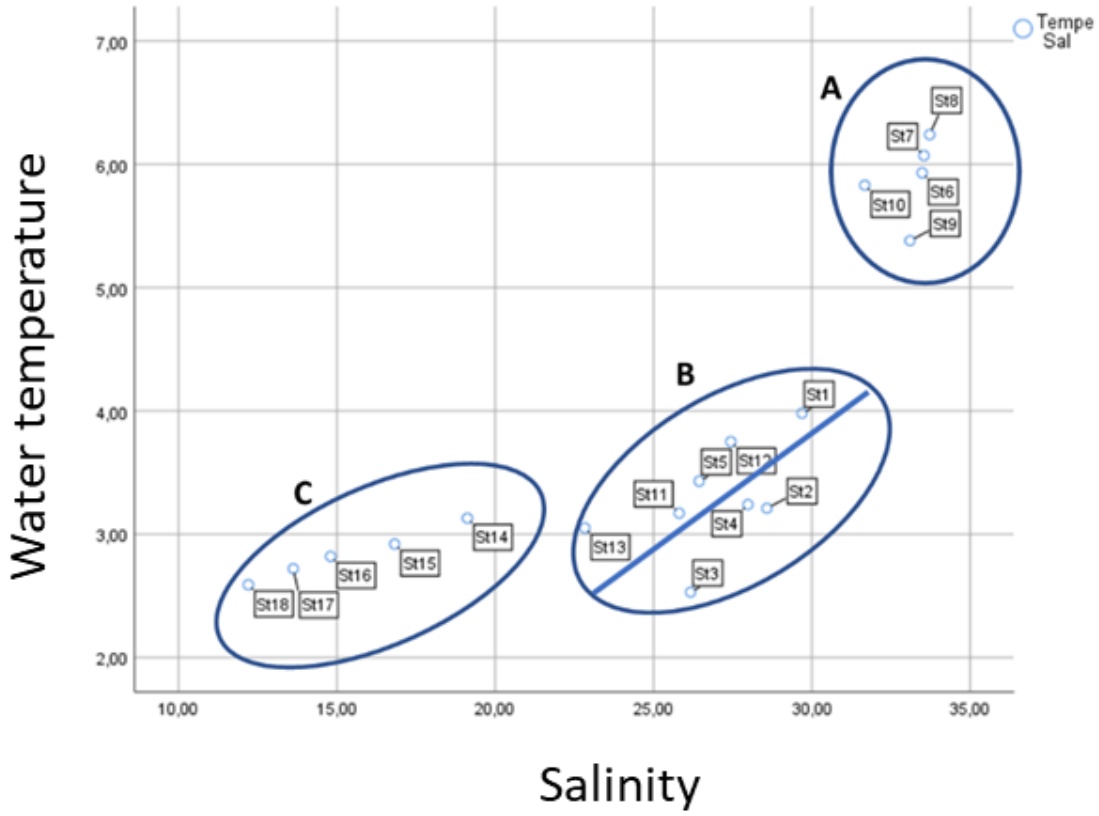

Figure 5.13: *Temperature-salinity plot of the stations sampled during Action 3.*

5.5. Main inputs relative to initial specific objectives

5.5.1. Q1: Can existing integrative sampling methods (i.e. passive samplers) be effectively used in combination with existing CRI to obtain reliable data on marine chemical pollution?

Action 1 was aiming at assessing whether collected data matched fundamental quality standards. To this regard, key challenges were: (1) the deployment and collection by CRI personnel without a specific training, (2) the maintenance of low level of contamination in blanks during complex logistics and field operations, and (3) the test of a new design of passive sampling to allow prolonged deployment time (up to one year and to facilitate field operations and logistics.

Overall, silicon passive samplers provided satisfactory results, which suggests that they can now be routinely used to address monitoring of chemical pollution in coastal areas. Large variabilities in deployment periods (e.g. from 3 months to 1 year) and environmental conditions appeared to be well handled. However, it is recommended that operators pay a particular attention to the use of field blanks, and adequate reference depuration compounds for the determination of effective sampling rates. Field blanks can be obtained, as in the present study, by bringing "dummy" sampling units to the field during the deployment of real samples, and expose them to the very same conditions experienced by "real" samples during deployment and collection. Even considering very different deployment condition and deployment times, passive samplers reported expected gradients of variability in measured concentrations. Nevertheless, precision and cross comparability can still largely be improved through an effort to allow simultaneous deployments in different regions and CRI using similar deployment times.

5.5.2. Q2: Can CRI be used to support exploratory monitoring of marine pollution to identify new chemical contaminants?

Results for quality assurance and control in the measurements obtained during Action 2 confirmed the suitability of CRI, and in particular FerryBox based sampling, to carry out monitoring of several CEC in coastal and even open sea water. Detection frequencies were high for most of the targeted analytes. Despite the presence of traces of some targeted contaminants in field blanks, detection limits were sufficiently low to detect extremely diluted substances down to the sub $ng.L^{-1}$ level. In most cases, the detection of analytes in field blanks likely resulted from the presence of analyte residues in the pre-extracted seawater used as matrix for field blanks. This water was collected 60 m deep in the Oslo Fjord and pre-processed to remove contaminant residuals. This process is, however, not 100% efficient, leading to the presence of analytes' traces in the blanks. This situation is typical and is part of the confounding factor any monitoring exercise for chemical pollution in marine water routinely faces due to the occurrence of very low concentrations. Stability tests also showed the goodness of on-board sample storage conditions, showing limited losses for some (i.e., most reactive) analytes.

Overall, results form Action 2 confirmed the benefit of using CRI and in particular FerryBox-based sampling to carry out monitoring and exploratory analysis of contaminants of emerging concern in coastal, transitional and open marine waters. To our knowledge, the data produced during Action 3 are the most extensive and resolved monitoring of emerging marine contaminants ever conducted, to date. The study is also the first to demonstrate the ubiquitous presence in coastal and open sea areas of the following substances: the artificial sweetener sucralose, the herbicide atrazine, the mosquito repellent DEET and the anti-inflammatory drug naproxen. In particular, sucralose emerges here as possibly the most abundant anthropogenic contaminants ever observed in open marine waters. Also for this type of monitoring activities, it is recommended that future studies consider a thorough use of quality assurance and control criteria, as traces of the analytes are observed in blank matrices. Measured levels are generally very low due to the large dilution operated by marine water mixing. The use of adequate blank matrices is therefore crucial. As done in the present study, the use of pre-extracted marine waters from low contamination areas is recommended as a matrix blank.

5.5.3. Q3: Can the drivers of spatial distribution of chemical contaminants in coastal waters be assessed using data from infrastructure sensors and spatial analyses?

Significant positive correlations among several frequently detected CECs, i.e., carbamazepine, sucralose and sulfamethoxazole, were observed pointing to a common source of those pollutants and common drivers in their marine fate and transport. This support the postulate of common coastal emitting sources for these substances, likely linked to municipal wastewater effluents. This is also corroborated by the significant inverse correlation between salinity and the detected levels of these contaminants reflecting the influence of riverine inputs in the southern part of the transect carrying wastewater contaminants from the in-land. The Danish straits and the Kattegat areas are receptors of the Baltic outflow conveying fresh water from rivers draining densely populated regions in Central and Northern Europe. Beyond land base sources, also the intense passenger marine traffic may represent in this region a significant local input of many of these contaminants.

Correlation between the DEET levels and the levels of three aforementioned CECs is negative, resulting in inverse correlations with salinity and latitude. A possible explanation for this finding is the effect of seasonality. DEET is a mosquito repellent mostly used in Europe in summer. Sampling was performed during Summer in the northern part of the transect, while the southern part was sampled in Winter. Hence the highest concentrations of DEET were observed in Northern Norway. This finding helps to elucidate the strong interaction between temporal and spatial drivers in determining the outcomes of monitoring results. While pharmaceutical, personal care products and food additives have prevalentely constant emissions during the year, DEET concentrations appeared to be mostly driven by the seasonality. This finding is extremely important for monitoring planning, and the characteristics and uses of different substances should be taken into consideration when monitoring coastal waters for chemical pollutants and when interpreting monitoring design.

In general, we found no correlation between the levels of detected chemicals and the distance of the sampling site to the coast. Such a simple minimalistic descriptor is therefore insufficient to draw conclusion on contaminant distribution, and should therefore not be taken into consideration when designing monitoring campaigned aimed at elucidating marine contaminant distribution and transport from sources. The mere distance from the coast, simply does not represent a good predictor of environmental concentrations for those chemicals. Instead, as described earlier an effort was placed to develop geographic descriptors that could put into relationship the distribution of marine pollutants with the distribution of active terrestrial sources. Through a spatial analysis aimed at correlating an index of anthropic impacts (i.e. the IPAI index introduced above) with concentration data we achieved an original estimation of substances spatial rabnge (SR). Through this spatial analysis we highlight strong relationships between the higher level of many detected wastewater contaminants with the area of highest human population density in the southern part of the transect. SR and the formulation of IPAI is proposed here as a tool can support the formulation of priors to pilot future regional and transregional monitoring programmes.

5.5.4. Q4: Is there a co-variance between contaminant signals and biological responses?

In Action 3, along the same transect, microbial molecular markers have been analyzed from samples taken in correspondence with PAHs samples. These markers represent microorganisms species and genes used to identify hydrocarbon pollution or high nutrient loads. The chosen markers respond better in typical marine waters with elevated salinity, less well in brackish waters as near Kiel harbour where the salinity is extremely low (around 13 PSU). Molecular markers signalling hydrocarbon contamination give the same distribution pattern as the sum of 29 PAHs (**Figure 5.17**), higher in the close proximity of the harbours and in the middle of the Kattegat area, due to intense marine traffic. This correspondence demonstrates the potential use of these markers as early warning for hydrocarbon presence. The distribution of several substances could be related to the distribution of coastal sources. In addition, for substances emitted with riverine runoff (such as mainly the currently use pesticides) seawater salinity resulted as a good proxy of distribution.

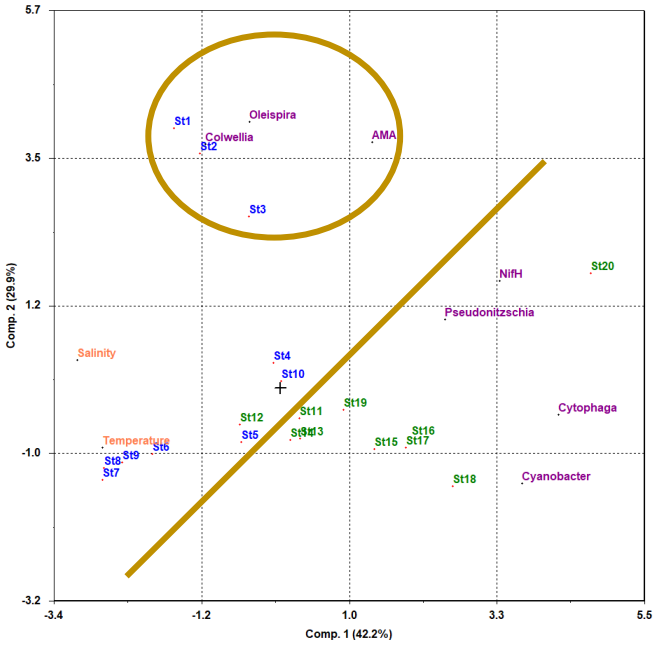

Figure 5.17: *PCA analysis including stations, temperature, salinity and molecular markers. A clear division between the first part of the transect (St1-10) from Oslo to the centre of the Kattegat (on the left of the straight line) and the stations from 11 to 20 representing the Danish straights and the Kiel Harbour. It should be noted that circa 12 hours have passed between the two semi-transects sampling (St1-10; St11-20). Station 20 in the Kiel Harbour is separated from the other because of a strong influence from the freshwater influx from the Kiel Canal. Station from 1 to 10 are clearly identified by oil-markers (*Oleispira, Colwellia *and AMA), especially station 1,2 and 3 (along the Oslo fjord), while the more "marine stations" are identified by the nutrient markers. Station 12 shows influence of both type of pollutions, being in the middle of the Kattegat (riverine influence of nutrients, heavy marine traffic).*

In conclusion, these results highlighted the possibility of using chemical and molecular biomarker to retrieve information of pollution influence on microbial community assemblages. To our knowledge this was the first time such an evidence of covariance is observed at this scale in a situation of background diffuse water contamination (in contrast to cases where hot spot pollution, such as that from oil spills or in proximity of discharge points). In order to achieve this it is stressed that adequate protocols and equipment should be deployed to avoid contamination of the samples by contaminant sources located at the infrastructure. Therefore, device that allow collection and handling of large volume water samples under conditions of protected atmosphere are strongly recommended if the operation take place on ship decks or machine rooms.

This study was of exploratory nature, and it is recommended that future use of CRI may considered extending this analysis collecting information at higher resolution or along broader spatial transects. While doing so, however, one should keep into consideration the influence of environmental factor, such as, in this case, salinity that was found to play and influential role in the distribution of biomarkers.

5.6. Analysis of the experience gained

5.6.1. Developing innovative technologies for coastal ocean observing and modelling.

Monitoring of chemical pollution in coastal waters is traditionally a complex and difficult activity. Obtaining, data with an adequate quality standard is complicated by the fact that chemical pollutants are generally present in marine waters at extremely low concentrations. Despite this, they still can pose a concern for ecosystem health as marine contaminants includes both substances that can bio-magnify in biota others, such as antibiotics and pesticides, that are instead designed to be bioactive at low concentrations. We noted that existing coastal research and monitoring infrastructures, being originally conceived for multi purpose scopes, are generally not ideally suited to support monitoring of chemical pollution at trace levels, under strict quality assurance and control standards. These

activities have been broadly relegated to dedicated cruises on research vessels rather than on permanent CRI. During JRAP 3 we have conducted significant technological improvements to expand coastal infrastructures' capacity and make them suitable to host and support marine chemical pollution monitoring activities. A major hindrance is the proneness of damaging/contaminating the samples during collection and field operation. A process that can invalidate data quality. Many environmental factors can cause such a contamination, including direct and indirect contact of sampling matrices (jars, sorbent, filter meshes) with contaminated air and surfaces during sample collection. To this regard, it is useful to mention that the access of coastal infrastructure often depends on the use of vessels and the support from staff with no specific training on the handling of samples for chemical analyses. Ships are major sources of several chemical contaminants of marine interest including oil-derived ones (such as PAHs, surfactants and plasticizers). Most of our field activities have been conducted on decks or machine rooms of vessels: certainly, the most challenging environments, from this point of view.

We have therefore dedicated the first part of the project on solving these challenges through redesigning sampling devices, redefining sampling protocols and demonstrating the lack of cross contamination by the thorough deployment of field blanks samples, and positive controls (including spike matrices assessment). As a result, we have provided a new design for passive samplers for fixed platforms that allows minimizing manipulation by operators on ship decks and reducing the time the samples are exposed to air. We have also designed an active sampling device for use on ships under "dirty" atmosphere conditions that allow sample collection and extraction on board in a fully protected atmosphere, where the exposure of sample matrices and the sample itself to the ship atmosphere is reduced to a minimum. Finally, we provided a set of recommendations to implement strict quality assurance and control measures during sampling including:

- The use of field blanks,
- The use of adequate reference depuration compounds for the determination of effective sampling rates by passive samplers
- Improving precision and cross comparability of data generated by passive sampling from fixed CRI by planning coordinated deployments in different regions and CRI using similar deployment times and periods.
- The use of adequate blank matrices when carrying out sampling of bulk waters for chemical analyses (e.g. the use of pre-extracted marine water from low contamination areas).
- Running recovery and stability test during the monitoring campaign.
- Use of devices that allow sample collection and handling under protected atmosphere in case these processes take please in particularly contaminated conditions (e.g. ship decks or machine rooms).

5.6.2. Establishing observing objectives, strategy and implementation at the regional level.

Through the spatial analysis carried out in Action 2 to tackle **Q3**, we showed that heuristic models based on the distribution of sources, a relatively simple parameterization of their contributions (e.g. based on the human population in coastal wastewater draining catchments) are sufficient in providing realistic descriptions of contaminant distributions at a regional spatial scale. Importantly, this showed that the task of building priors to define monitoring planning and strategies at the coastal regional level may prescind from the use of sophisticated hydrodynamic advection models, if sufficient information on coastal source distribution and water quality parameter data (such as temperature and salinity) are available.

Different parameterizations of heuristic spatial distribution models I however likely to be required for different zones because source characteristics, and coastal water hydrodynamism can differently affect contaminant emission and transport. For coastal applications (where the application of mechanistic hydrodynamic models might be critical), the use of heuristic approaches to produce priors for planning and optimizing regional monitoring of water contaminants appears to be viable approach. However, validating these heuristic models is a necessary step. It is recommended that future studies using CRI will keep focusing on jointly performing water contamination observation, spatial analyses of coastal sources, and analyses of covariance with water chemical-physical parameters, to validate heuristic models of contaminants distribution.

5.6.3. ***Enhancing integrated coastal ocean monitoring and interfacing with other ocean observing initiatives operating at different spatiotemporal scales.***

JRAP 3 produced important insights on the usefulness and capability of CRI such as the FerryBox fleet to address questions concerned with the identification of drivers and factors influencing the spatial distribution and the potential for long-range transport of marine chemical pollutants. Considering the large potential provided by CRI in supporting this type of monitoring (providing conditions for both high resolution and large spatial coverage) the definition of strategies for efficient monitoring designs (i.e., capable of optimizing gathered information while minimizing sampling effort) are necessary. JRAP 3 proved that knowledge of surface seawater salinity field in combination with information on the properties of targeted contaminants (and in particular their spatial ranges) can be used to derive priors of expected distribution of contaminants released with river outflows, such as, for example, pesticides. These priors can be used in particular to design optimal monitoring strategies. JRAP 3 also showed that a spatial analysis delivering information on coastal sources distribution and their estimated contributions (such as the IPAI index) in combination with knowledge on substances' spatial ranges can be used to produce priors for substances with emission not exclusively linked to riverine transport. The deployment of heuristic approaches (such as the IPAI index) is therefore recommended before starting future monitoring actions since it can help optimizing the resolution and quality of retrieved information while minimizing the costs.

5.7. Propositions for a future monitoring strategy for the topic

- Pursue with the development and test of new technologies for the assessment of of contaminants at trace levels.
- Favor the development of integrated platforms allowing for the simultaneous (semi-automated) collection of water samples under sufficiently "clean conditions".
- Adopt a regional approach to monitoring considering aspects and drivers that take adequate account of the distribution of coastal sources and anthropic presence.
- Consider the use of spatial analysis to build heuristic priors of expected contaminant distribution at regional before engaging in unnecessarily over-resolved, over-ambitious monitoring plans.
- Pay attention to the adequate use of quality assurance and control measures such as the use of field blanks, recovery test and stability tests.
- Use sampling technologies that allow preventing samples to be contaminated by infrastructure-based sources.
- Carry out validation for the use of alternative sampling and analytical techniques (i.e., less costly in terms of manpower and money) to classical grab water sampling and chemical analysis.
- Make sure samples are analyzed by chemical laboratory that offer full warranty of analysis quality. Commercial laboratories offering good service may still fail in providing adequate low limit of detections.
- When studying marine chemical pollution, favor the interaction with other initiatives in a cross-discipline approach, including joint deployment of contaminant fate and transport models and coordinated assessment of biological responses observations, e.g. through the use of biomarkers of different nature.
- Consider work aimed at expanding the inventory of known marine chemical pollutants through the use of non-target analytical chemistry approaches. However, use formulation of adequate prior expected distribution before engaging in random sample collection.
- Coordinate carefully the access to CRI with CRI operators, to make sure adequate conditions for a successful sampling and measurement quality.

5.8. References

Allan, I.J., Booij, K., Paschke, A., Vrana, B., Mills, G.A., Greenwood, R., 2009. Field Performance of Seven Passive Sampling Devices for Monitoring of Hydrophobic Substances. Environ. Sci. Technol. 43, 5383–5390. https://doi.org/10.1021/es900608w

Alygizakis, N.A., Gago-Ferrero, P., Borova, V.L., Pavlidou, A., Hatzianestis, I., Thomaidis, N.S., 2016. Occurrence and spatial distribution of 158 pharmaceuticals, drugs of abuse and related metabolites in offshore seawater. Science of The Total Environment 541, 1097–1105. https://doi.org/10.1016/j.scitotenv.2015.09.145

AMAP, 2004. AMAP Assessment 2002: Persistent Organic Pollutants in the Arctic. Arctic Monitoring and Assessment Programme (AMAP). Oslo, Norway.

Arpin-Pont, L., Bueno, M.J.M., Gomez, E., Fenet, H., 2016. Occurrence of PPCPs in the marine environment: a review. Environmental Science and Pollution Research 23, 4978–4991. https://doi.org/10.1007/s11356-014-3617-x

aus der Beek, T., Weber, F.-A., Bergmann, A., Hickmann, S., Ebert, I., Hein, A., Küster, A., 2016. Pharmaceuticals in the environment-Global occurrences and perspectives. Environmental Toxicology and Chemistry 35, 823–835. https://doi.org/10.1002/etc.3339

Borecka, M., Siedlewicz, G., Haliński, Ł.P., Sikora, K., Pazdro, K., Stepnowski, P., Białk-Bielińska, A., 2015a. Contamination of the southern Baltic Sea waters by the residues of selected pharmaceuticals: Method development and field studies. Marine Pollution Bulletin 94, 62–71. https://doi.org/10.1016/j.marpolbul.2015.03.008

Borecka, M., Siedlewicz, G., Haliński, Ł.P., Sikora, K., Pazdro, K., Stepnowski, P., Białk-Bielińska, A., 2015b. Contamination of the southern Baltic Sea waters by the residues of selected pharmaceuticals: Method development and field studies. Marine Pollution Bulletin 94, 62–71. https://doi.org/10.1016/j.marpolbul.2015.03.008

Braune, B., Chételat, J., Amyot, M., Brown, T., Clayden, M., Evans, M., Fisk, A., Gaden, A., Girard, C., Hare, A., Kirk, J., Lehnherr, I., Letcher, R., Loseto, L., Macdonald, R., Mann, E., McMeans, B., Muir, D., O'Driscoll, N., Poulain, A., Reimer, K., Stern, G., 2015. Mercury in the marine environment of the Canadian Arctic: Review of recent findings. Science of The Total Environment 509–510, 67–90. https://doi.org/10.1016/j.scitotenv.2014.05.133

Brumovský, M., Bečanová, J., Kohoutek, J., Borghini, M., Nizzetto, L., 2017a. Contaminants of emerging concern in the open sea waters of the Western Mediterranean. Environmental Pollution 229, 976–983. https://doi.org/10.1016/j.envpol.2017.07.082

Brumovský, M., Bečanová, J., Kohoutek, J., Borghini, M., Nizzetto, L., 2017b. Contaminants of emerging concern in the open sea waters of the Western Mediterranean. Environmental Pollution 229, 976–983. https://doi.org/10.1016/j.envpol.2017.07.082

Brumovsky, M., Becanova, J., Kohoutek, J., Thomas, H., Petersen, W., Sorensen, K., Sanka, O., Nizzetto, L., 2016a. Exploring the occurrence and distribution of contaminants of emerging concern through unmanned sampling from ships of opportunity in the North Sea. J. Mar. Syst. 162, 47–56. https://doi.org/10.1016/j.jmarsys.2016.03.004

Brumovský, M., Bečanová, J., Kohoutek, J., Thomas, H., Petersen, W., Sørensen, K., Sáňka, O., Nizzetto, L., 2016. Exploring the occurrence and distribution of contaminants of emerging concern through unmanned sampling from ships of opportunity in the North Sea. Journal of Marine Systems 162, 47–56. https://doi.org/10.1016/j.jmarsys.2016.03.004

Brumovsky, M., Karaskova, P., Borghini, M., Nizzetto, L., 2016b. Per- and polyfluoroalkyl substances in the Western Mediterranean Sea waters. Chemosphere 159, 308–316. https://doi.org/10.1016/j.chemosphere.2016.06.015

Dachs, J., Mejanelle, L., 2010. Organic Pollutants in Coastal Waters, Sediments, and Biota: A Relevant Driver for Ecosystems During the Anthropocene? Estuaries Coasts 33, 1–14. https://doi.org/10.1007/s12237-009-9255-

de Souza Machado, A.A., Spencer, K., Kloas, W., Toffolon, M., Zarfl, C., 2016. Metal fate and effects in estuarA review and conceptual model for better understanding of toxicity. Science of The Total Environment 541, 268–281. https://doi.org/10.1016/j.scitotenv.2015.09.045

European Comission, 2008. Directive 2008/56/EC. Official Journal of the European Union 164, 19–40.

Gan, Z., Sun, H., Feng, B., Wang, R., Zhang, Y., 2013. Occurrence of seven artificial sweeteners in the aquatic environment and precipitation of Tianjin, China. Water research 47, 4928–37. https://doi.org/10.1016/j.watres.2013.05.038

Gaw, S., Thomas, K. V., Hutchinson, T.H., 2014. Sources, impacts and trends of pharmaceuticals in the marine and coastal environment. Philosophical Transactions of the Royal Society B: Biological Sciences 369, 20130572–20130572. https://doi.org/10.1098/rstb.2013.0572

Gioia, R., Nizzetto, L., Lohmann, R., Dachs, J., Temme, C., Jones, K.C., 2008. Polychlorinated Biphenyls (PCBs) in air and seawater of the Atlantic Ocean: Sources, trends and processes. Environ. Sci. Technol. 42, 1416–1422. https://doi.org/10.1021/es071432d

Green, N., Schlabach, M., Bakke, T., Brevik, E.M., Dye, C., Herzke, D., Huber, S., Plosz, B., Remberger, M., Schoyen, M., Uggerud, H.T., Vogelsang, C., 2008. Screening of selected metals and new organic contaminants 2007, Screening.

Gros, M., Rodríguez-Mozaz, S., Barceló, D., 2012. Fast and comprehensive multi-residue analysis of a broad range of human and veterinary pharmaceuticals and some of their metabolites in surface and treated waters by ultra-high-performance liquid chromatography coupled to quadrupole-linear ion trap tandem. Journal of Chromatography A 1248, 104–121. https://doi.org/10.1016/j.chroma.2012.05.084

Hughes, S.R., Kay, P., Brown, L.E., 2013. Global Synthesis and Critical Evaluation of Pharmaceutical Data Sets Collected from River Systems. Environmental Science & Technology 47, 661–677. https://doi.org/10.1021/es3030148

Klosterhaus, S.L., Grace, R., Hamilton, M.C., Yee, D., 2013a. Method validation and reconnaissance of pharmaceuticals, personal care products, and alkylphenols in surface waters, sediments, and mussels in an urban estuary. Environment International 54, 92–99. https://doi.org/10.1016/j.envint.2013.01.009

Klosterhaus, S.L., Grace, R., Hamilton, M.C., Yee, D., 2013b. Method validation and reconnaissance of pharmaceuticals, personal care products, and alkylphenols in surface waters, sediments, and mussels in an urban estuary. Environment International 54, 92–99. https://doi.org/10.1016/j.envint.2013.01.009

Lohmann, R., Booij, K., Smedes, F., Vrana, B., 2012. Use of passive sampling devices for monitoring and compliance checking of POP concentrations in water. Environ. Sci. Pollut. Res. 19, 1885–1895. https://doi.org/10.1007/s11356-012-0748-9

Lohmann, R., Gioia, R., Jones, K.C., Nizzetto, L., Temme, C., Xie, Z., Schulz-Bull, D., Hand, I., Morgan, E., Jantunen, L., 2009. Organochlorine Pesticides and PAHs in the Surface Water and Atmosphere of the North Atlantic and Arctic Ocean. Environ. Sci. Technol. 43, 5633–5639. https://doi.org/10.1021/es901229k

Loos, R., Tavazzi, S., Paracchini, B., Canuti, E., Weissteiner, C., 2013. Analysis of polar organic contaminants in surface water of the northern Adriatic Sea by solid-phase extraction followed by ultrahigh-pressure liquid chromatography-QTRAP® MS using a hybrid triple-quadrupole linear ion trap instrument. Analytical and bioanalytical chemistry 405, 5875–85. https://doi.org/10.1007/s00216-013-6944-8

Magnér, J., Filipovic, M., Alsberg, T., 2010. Application of a novel solid-phase-extraction sampler and ultra-performance liquid chromatography quadrupole-time-of-flight mass spectrometry for determination of pharmaceutical residues in surface sea water. Chemosphere 80, 1255–1260. https://doi.org/10.1016/j.chemosphere.2010.06.065

Mead, R.N., Morgan, J.B., Avery, G.B., Kieber, R.J., Kirk, A.M., Skrabal, S. a., Willey, J.D., 2009. Occurrence of the artificial sweetener sucralose in coastal and marine waters of the United States. Marine Chemistry 116, 13–17. https://doi.org/10.1016/j.marchem.2009.09.005

Munaron, D., Tapie, N., Budzinski, H., Andral, B., Gonzalez, J.L., 2012a. Pharmaceuticals, alkylphenols and pesticides in Mediterranean coastal waters: Results from a pilot survey using passive samplers. Estuarine, Coastal and Shelf Science 114, 82–92. https://doi.org/10.1016/j.ecss.2011.09.009

Munaron, D., Tapie, N., Budzinski, H., Andral, B., Gonzalez, J.-L., 2012b. Pharmaceuticals, alkylphenols and pesticides in Mediterranean coastal waters: Results from a pilot survey using passive samplers. Estuarine, Coastal and Shelf Science 114, 82–92. https://doi.org/10.1016/j.ecss.2011.09.009

Naser, H.A., 2013. Assessment and management of heavy metal pollution in the marine environment of the Arabian Gulf: A review. Marine Pollution Bulletin 72, 6–13. https://doi.org/10.1016/j.marpolbul.2013.04.030

Nödler, K., Voutsa, D., Licha, T., 2014a. Polar organic micropollutants in the coastal environment of different marine systems. Marine Pollution Bulletin 85, 50–59. https://doi.org/10.1016/j.marpolbul.2014.06.024

Nödler, K., Voutsa, D., Licha, T., 2014b. Polar organic micropollutants in the coastal environment of different marine systems. Marine Pollution Bulletin 85, 50–59. https://doi.org/10.1016/j.marpolbul.2014.06.024

Noguera-Oviedo, K., Aga, D.S., 2016. Lessons learned from more than two decades of research on emerging contaminants in the environment. Journal of Hazardous Materials 316, 242–251. https://doi.org/10.1016/j.jhazmat.2016.04.058

Noone, K.J., Sumaila, U.R., Diaz, R.J., 2013. Managing Ocean Environments in a Changing Climate: Sustainability and Economic Perspectives, 1st ed. Elsevier.

Pan, K., Wang, W.-X., 2012. Trace metal contamination in estuarine and coastal environments in China. Science of The Total Environment 421–422, 3–16. https://doi.org/10.1016/j.scitotenv.2011.03.013

Rigét, F., Bignert, A., Braune, B., Stow, J., Wilson, S., 2010. Temporal trends of legacy POPs in Arctic biota, an update. Science of The Total Environment 408, 2874–2884. https://doi.org/10.1016/j.scitotenv.2009.07.036

Sang, Z., Jiang, Y., Tsoi, Y.-K., Leung, K.S.-Y., 2014. Evaluating the environmental impact of artificial sweeteners: a study of their distributions, photodegradation and toxicities. Water research 52, 260–74. https://doi.org/10.1016/j.watres.2013.11.002

Shimizu, A., Takada, H., Koike, T., Takeshita, A., Saha, M., Rinawati, Nakada, N., Murata, A., Suzuki, T., Suzuki, S., Chiem, N.H., Tuyen, B.C., Viet, P.H., Siringan, M.A., Kwan, C., Zakaria, M.P., Reungsang, A., 2013. Ubiquitous occurrence of sulfonamides in tropical Asian waters. Science of The Total Environment 452–453, 108–115. https://doi.org/10.1016/j.scitotenv.2013.02.027

Vidal-Dorsch, D.E., Bay, S.M., Maruya, K., Snyder, S.A., Trenholm, R.A., Vanderford, B.J., 2012. Contaminants of emerging concern in municipal wastewater effluents and marine receiving water. Environmental Toxicology and Chemistry 31, 2674–2682. https://doi.org/10.1002/etc.2004

Vrana, B., Mills, G.A., Allan, I.J., Dominiak, E., Svensson, K., Knutsson, J., Morrison, G., Greenwood, R., 2005. Passive sampling techniques for monitoring pollutants in water. Trac-Trends Anal. Chem. 24, 845–868. https://doi.org/10.1016/j.trac.2005.06.006

Wania, F., MacKay, D., 1996. Tracking the Distribution of Persistent Organic Pollutants. Environmental Science & Technology 30, 390A-396A. https://doi.org/10.1021/es962399q

Weigel, S., Berger, U., Jensen, E., Kallenborn, R., Thoresen, H., Hühnerfuss, H., 2004. Determination of selected pharmaceuticals and caffeine in sewage and seawater from Tromsø/Norway with emphasis on ibuprofen and its metabolites. Chemosphere 56, 583–592. https://doi.org/10.1016/j.chemosphere.2004.04.015

Weigel, S., Bester, K., Hühnerfuss, H., 2001. New method for rapid solid-phase extraction of large-volume water samples and its application to non-target screening of North Sea water for organic contaminants by gas chromatography–mass spectrometry. Journal of Chromatography A 912, 151–161. https://doi.org/10.1016/S0021-9673(01)00529-5

Weigel, S., Kuhlmann, J., Hühnerfuss, H., 2002. Drugs and personal care products as ubiquitous pollutants: occurrence and distribution of clofibric acid, caffeine and DEET in the North Sea. Science of The Total Environment 295, 131–141. https://doi.org/10.1016/S0048-9697(02)00064-5

Zhang, R., Tang, J., Li, J., Cheng, Z., Chaemfa, C., Liu, D., Zheng, Q., Song, M., Luo, C., Zhang, G., 2013a. Occurrence and risks of antibiotics in the coastal aquatic environment of the Yellow Sea, North China. The Science of the total environment 450–451, 197–204. https://doi.org/10.1016/j.scitotenv.2013.02.024

Zhang, R., Tang, J., Li, J., Zheng, Q., Liu, D., Chen, Y., Zou, Y., Chen, X., Luo, C., Zhang, G., 2013b. Antibiotics in the offshore waters of the Bohai Sea and the Yellow Sea in China: Occurrence, distribution and ecological risks. Environmental Pollution 174, 71–77. https://doi.org/10.1016/j.envpol.2012.11.008

5.9. Abbreviations

POP: Persistent Organic Pollutants
MSFD: Marine Strategy Framework Directive
CRI: Coastal Research Infrastructures
CEC: Contaminants of Emerging Concern
PAH: Polycyclic Aromatic Hydrocarbons
PCBs: Polychlorinated Biphenyls
PBDE: Polybrominated diphenyl Ethers
GIS: Geographical Information System
CIESIN: Center for International Earth Science Information Network
IPAI: Index of Potential Anthropic Influence
SR: spatial range
PPCP: Pharmaceuticals and Personal Care Products

6. JRAP 4: 4D characterization of trans-boundary hydrography and transport

Contributors
Anna Rubio, Ainhoa Caballero, Ivan Manso-Narvarte, Julien Mader, **AZTI, Spain**
Annalisa Griffa, Carlo Mantovani, Maristella Berta, **CNR-ISMAR, Italy**
Alejandro Orfila, Ismael Hernandez-Carrasco, **CISC-IMEDEA, Spain**
Pascal Lazure, Ivane Pairaud, Guillaume Charria, Ingrid Puillat, **IFREMER, France**
Giovanni Coppini, Stefania Angela Ciliberti; Eric Jansen, **CMCC, Italy**
Johannes Schulz-Stellenfleth, **HZG, Germany**
Pierre De Mey, **CNRS, France**
Bruno Zakardjian, Céline Quentin, **CNRS**, France

6.1. Topic and specific objectives.

Coastal areas are submitted to different natural and anthropogenic pressures that compromise the health of coastal ecosystems and associated resources. Monitoring and understanding the dynamics of coastal currents is crucial for the development of environmentally sustainable coastal activities, the preservation of marine ecosystems and the support marine and navigation safety. Oceantransport in coastal areas, which is driven by a large variety of complex processes, play a key role in the dispersal/retention of pollutants, planktonic species (potentially toxic), and more generally in cross-shelf exchanges. The need for an integrated observation and real-time monitoring of coastal areas, within the context of the Marine strategy Framework Directive, has been also the main driver for development of multiplatform operational observatories along the coast; including HF radar observations and high-resolution modelling for the continuous monitoring and forecasting of the coastal ocean currents.

Estimating ocean transport is highly challenging because it is inherently chaotic and depends on the details of the velocity field at various spatio-temporal scales. This is especially true for the surface coastal ocean, where a host of competing processes at various scales and dynamics influence transport of advected quantities. Surface transport at coastal areas is driven by a large variety of processes (tides, current instabilities, coastal jets, eddies, fronts…) acting simultaneously, in response to different forcing and over a broad spectrum of time-space scales. These processes play a key role in the dispersal/retention of pollutants, planktonic species (potentially toxic), and more generally in cross-shelf exchanges. The characterization and better predictability of these structures is critical to understand the physical/biological coupling in the coastal zone and for the effective integrated management of coastal areas (where the use of the marine space is concentrated).
In his area, HF radars play a very important role in monitoring the surface ocean and in estimating transport, thanks to their coverage (range of 30-200 km) and high resolution in time (order of 1 hour) and space (order of 1-3 km). HF radar information though is confined to the first upper meter, while ecological quantities such as larvae, planktonic organisms as well as pollutants and microplastic move also in the water column. Thus, one of the main crucial challenges that motivates JRAP 4 is the integration of HF radar data with other traditional sensors like, e.g., tide gauges, surface Lagrangian drifters or moored instruments and the combination of the observations with numerical models, which can also be used to provide forecast. In addition to understand coastal surface transport, the combination of data at the surface (as the provided by HF radars) with information on the water column, from in situ moored instruments, remote sensors or regional/coastal circulation model simulations offers further interesting possibilities for understanding the 3D coastal circulation and associated transports. Solving the 3D transports is key to ensure the application of the information gathered by the coastal observatories to biogeochemical and environmental issues, since eggs, larvae or pollutants can be located deeper in the water columns and not only follow 2D surface transport pattenrs. Another important research line is to exploit the complementarity and synergy between in-situ measurement in coastal areas and satellite remote sensing of currents at basin or global scales.

The main goal of JRAP 4 is to provide estimates of 4D transport (3D in space and time) in three pilot areas using information from Observing Systems based on HF radar for surface currents, hydrographic instrumentations (thermistors, CTD, tide gauges and gliders) for the water column, as well as the outputs of Observing System Simulation Experiments for discussing on the optimization of the existing monitoring networks.

Within this general framework, JRAP 4 was aiming at tackling the following three main questions:

- **Q1**: Can we use JERICO infrastructures to study the 4D shelf/slope circulation and transports and
- their time variability?
- **Q2**: What is the impact of the ocean transport on the distribution of floating and dissolved matter?
- **Q3**:: How can we maximize the impact of the JERICO-RI for assessing coastal transport?

6.2. Overall structuration and strategy

JRAP 4 focused on three study areas featuring different ocean dynamics (**Figure 6.1**). These were the German Bight (GB), the SE Bay of Biscay (SE BOB) and the NW Mediterranean (NW MED).

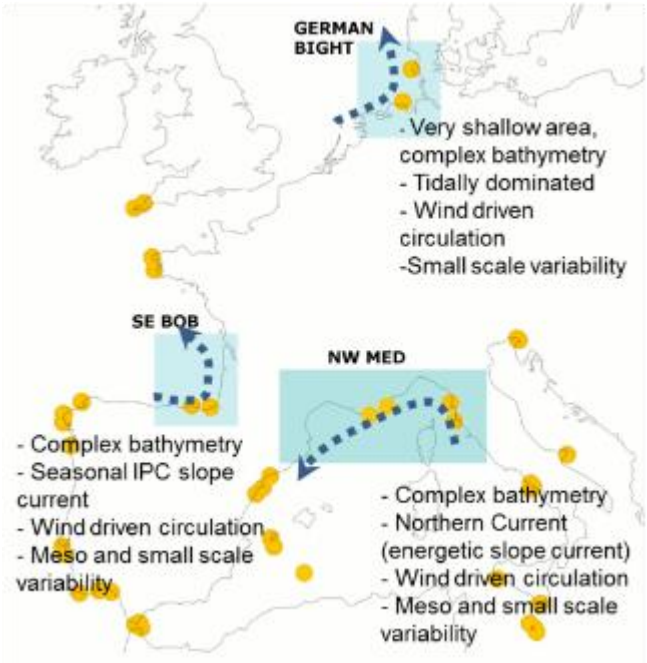

Figure 6.1: *Locations of the three study areas. Yellow dots display he location of HF radar systems available at the beginning of JRAP4.*

The three study areas are, in addition, submitted to different human pressures/activities which will, in turn, drive specific applied research activities.

The research work in JRAP 4 was based on: (i) Historical data available at each of the study areas; (ii) New observations using JERICO_NEXT infrastructure, which have allowed to improve the existing observatories to solve smaller scales and to make a step forward in the understanding of coastal ocean processes; and (iii) Observing System Simulation Experiments and Observing System Experiments (OSSE and OSE, link with Task 3.7 and JRAP 6) which were used to objectively propose optimization of existing observing networks (new HF RADAR antennas, different fixed stations position) and to test the numerical capabilities in assimilating HF radar data and evaluating transport.

The study of the 4D shelf/slope circulation and transport and their time variability in the three trans-boundary areas was performed through the joint analysis of JERICO multiplatform data of surface currents and hydrography (including data from HF radars, drifters, satellite imagery …) and information from the water column (drifters, moorings, gliders, satellite data, coastal profilers…). Additional experiments and deployments were achieved to assess the potential impact of the ocean transport on the distribution of floating and dissolved matter (plankton or other pelagic organisms, marine litter and contaminants, etc.) in line with MFSD descriptors 2, 7 and 10.

6.3. Achieved actions

The sampling plans implemented in the three pilot areas are shown below: together with lists of existing infrastructures and new (i.e., achieved within JERICO-NEXT) deployments.

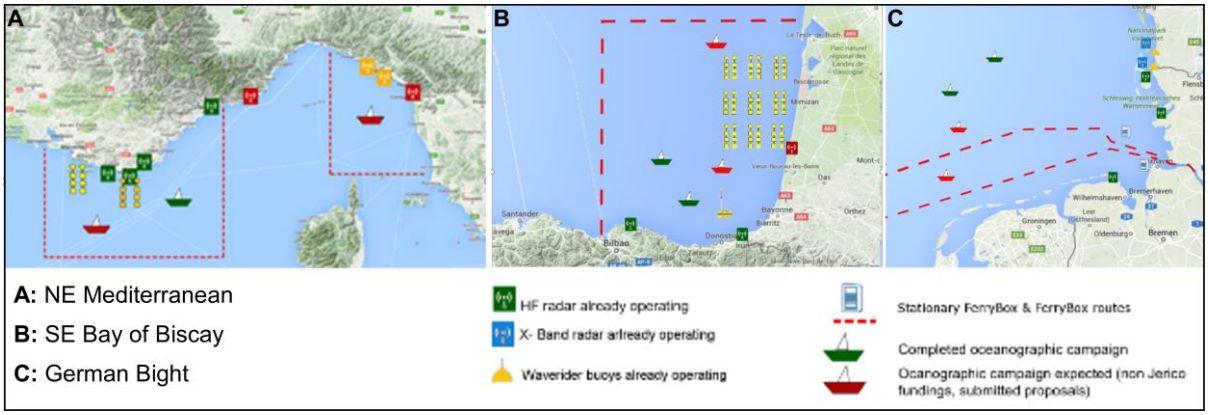

6.3.1. NW Mediterranean

Existing infrastructures:

- 4 HF CNRS-ISMAR radar systems (25MHz) hourly surface currents (35 km range,1 km spatial resolution)
- 2 HF CNRS (MIO) radar systems (16.1 - 16.2 MHz) off Toulon and of Nice producing hourly surface currents (80 km range,3 km spatial resolution)

New deployments:

- 2 HF radar antennas 25 MHz in the NW Med, installed by CNR-ISMAR (5Terre, Eastern Ligurian Sea) + additional HF radar sites in the area of Cinque Terre.
- A trial experiment was performed in February 2017 with CTD, ADCP, glider as well as plastic sampling in the radar area.
- IFREMER successfully tested the MASTODON-2D mooring lines in October 2016. A second deployment was successfully achieved in August-September 2017.

6.3.2. SE Bay of Biscay

Existing infrastructures:

- 2 HF AZTI-EUSKALMET radar systems (4.5 MHz) producing hourly surface currents (150 km range, 5 km spatial resolution)
- 1 AZTI-EUSKALMET slope mooring producing hourly TS and current measurements in the water column (surface to 150m)

New deployments:

- ETOILE campaign & MASTODON moorings (July-August 2017)
- TNA BB-TRANS glider survey

6.3.3. German Bight

Existing infrastructures:

- Current in the water column (frequency > 1 h) […]
- 3 HF radar stations providing surface ocean currents at frequencies of 20'
- (100 km range, 2 km spatial resolution)
- Tide gauges - Sea height level (frequency > 1 h)
- ADCP Ocean

New deployments:

No new deployments in this area. Work focused on the optimization of HF radar assimilation scheme for the German Bight using results presented in Schulz-Stellenfleth and Stanev (Ocean Modelling 100 (2016): 109–124).

Variables/parameters.

Variables	Sampling method	Location/area	Period	Institutes
Surface ocean currents	**HF radar**	SE BoB, NW Med, GB (every 20 min)	2009-present	CNR, AZTI, CNRS-MIO, HZG
Fixed point TS and current profiles	**Slope buoys** **MASTODON-2D**	SE BoB, hourly data SE BoB, NW Med	2006-present 07-08/2017, 08-09/2017	AZTI IFREMER
TS, ADCP current, turbidity, fluorometry and turbulence profiles	**Glider (BB-TRANS TNA)** **ETOILE SURVEY** **UPCAST SURVEY**	SE BoB, sampling depending on the sensors NW Med	15/05/2018 - 15/06/2018 07-08/2017 08-09/2017	AZTI, HZG & CNR-ISMAR IFREMER, AZTI, CNRS-LOG IFREMER, MIO
Microplastic abundances and multispectral fluorometry and phytoplankton samples	**ETOILE SURVEY**	SE BoB	07-08/2017	AZTI, IFREMER

6.3.4. Data analysis

- Analysis of temporal series of TS, currents from moorings
- Mapping (Objective analysis or others) of TS, currents, fluorometry, turbulence, turbidity profiles
- Laboratory analysis of some *in-situ* samples (e.g. phytoplankton and microplastic)
- Use of surface current fields for Lagrangian diagnostics by means of different Lagrangian models
- Use of HF radar observation operator for the assimilation in regional model covering the Ligurian Sea (Adriatic-Ionian Forecasting System)

6.4. Main results

6.4.1. NW MED - Installation /testing of new HF radars and MASTODON-2D moorings

Current circulation and transport in the Ligurian Sea were studied using data from HF radars complemented by data from gliders, drifters, and vessel-mounted instrumentation. MASTODON-2D thermistor lines were upgraded by Ifremer within JERICO-NEXT and deployed in September-October 2017 off the Provence coast (between Marseille and Toulon, **Figure 6.1**). This device is a low cost and easy to deploy autonomous system continuously monitoring the water column temperature and proved able to record an intense and long-lasting upwelling event. Surface currents and transport were computed by HF radar data, showing the complexity of variability at seasonal and synoptic scales.

The depth of the lines goes down to 120-200 m and stays 5-10 m below the surface. As shown by the results after the deployments off the Provence coast in **Figure 6.2**, they enabled the recording of an intense (up to 10 °C cooling of subsurface water) and long lasting (>10 days) upwelling event. The spatial coverage allowed capturing different behaviors in the area, with a different relaxation behavior after the upwelling event.

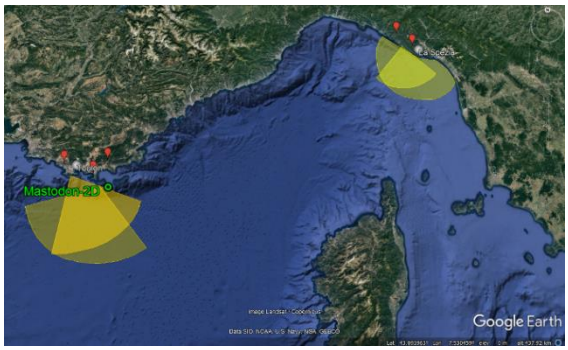

Figure 6.1: *In yellow the HF radar coverage in the Ligurian Sea presently part of JERICO-NEXT. Red pins are the HF radar antennas. In green the thermistor line Mastodon-2D upgraded by Ifremer within JERICO-NEXT.*

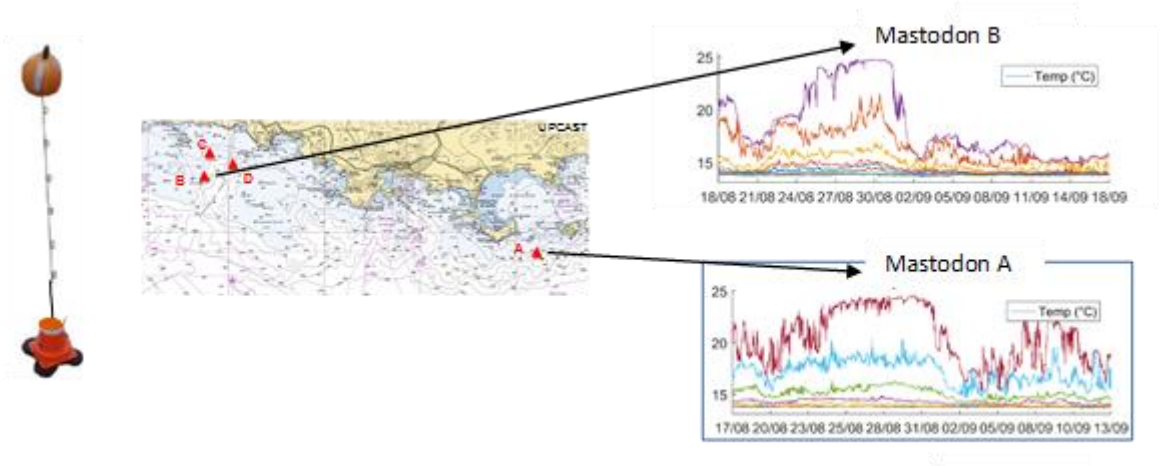

Figure 6.2: *Mastodon. In the left panel a picture of the MASTODON-2D line. In the middle panel the map showing the deployment sites and in the right panels an example of the sea surface temperature drop (purple lines) recorded by two thermistor lines during an upwelling event in 2017.*

6.4.2. NW MED - Characterization of current velocity and transport with HF radar, glider and wind data

While HF radar data can provide unprecedented spatial and temporal coverage of surface velocity, for many applications is very important to have information also on subsurface transport. This problem was approached in synergy with WP 3, methodologies to analyze and blend velocity data at the surface and in the water column have been developed and then applied to the JRAP 4 data sets. A combination of HF radar dataset and glider section near Toulon provided an example of 3D vision of the Northern Ccurrent pathway indicating the velocity, direction and vertical structure in the Ligurian Sea.

A preliminary study aiming at separating the wind induced current in the upper layers from the geostrophic current was carried out using an historical data set in the Toulon area including HF radar data at the surface and geostrophic velocities from glider data in the water column (**Figure 6.3**, Berta et al., 2018). As a further step, the blending of various velocity data set was investigated. A DCT-PLS method (Fredj et al. 2016) was tested, in collaboration with Prof. E. Fredj from the Jerusalem College of Technology using first the outputs from the GLAZUR hydrodynamic model following an OSSE approach, and then actual observations. Results are positive and encouraging in terms of reconstruction of the 3D velocity in the water column. Other methodologies were investigated in collaboration also with AZTI, as detailed further down. The blending experience proved to be also useful as a previous step to actual model data assimilation, providing sensitivity to the type of data and treatment.

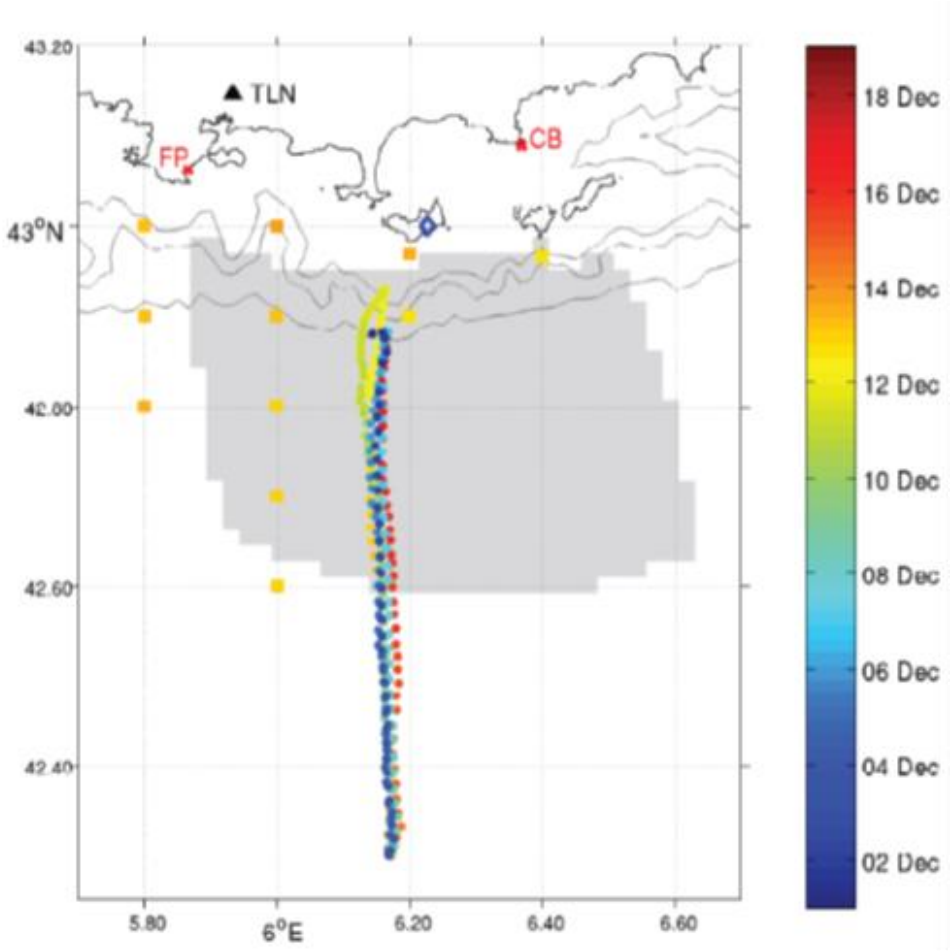

Figure 6.3*: Historical dataset in the Toulon area including HF radar data and glider transects used for the wind-geostrophic current components analysis and the data blending experiments. The gray area is the HF radar surface current field coverage, the yellow squared marks represent the CTD stations, while the dots array near 6.20_ E is the track of the repeated glider transects. CTD stations and glider tracks are colour coded in time. The blue diamond indicates Porquerolles wind station's position. Bathymetric lines at 500 m, 1000 m and 2000 m depth. The following acronyms are used: TLN: Toulon, FP: Fort Peyras, CB: Cap Bénat.*

The analysis of HF radar data in the Gulf of Manfredonia (Corgnati et al., 2018) was used by CNR-ISMAR together with drifter data and otoliths analysis (Sciascia et al., 2018) to investigate recruitment of small pelagic fishes (sardines) by the use of drifters data and the outputs of a Lagrangian model (Figure 6.4). The Gulf of Manfredonia is an important nursery area for sardines and a major question from the fishery and ecological management point of view is whether the nursery is supported by local spawning or by spawning from remote areas in the North and Central Adriatic. Radar data were used to compute retention properties inside the Gulf, while historical and targeted drifter data provided information on connectivity between the remote spawning areas and the Gulf. Results indicate that the average residence time in the Gulf of Manfredonia is relatively short (< 10 days) compared to the typical passive pelagic larval duration (30-50 days). Therefore, the larvae nursery in the Gulf of Manfredonia seems more likely supported by remote spawning areas.

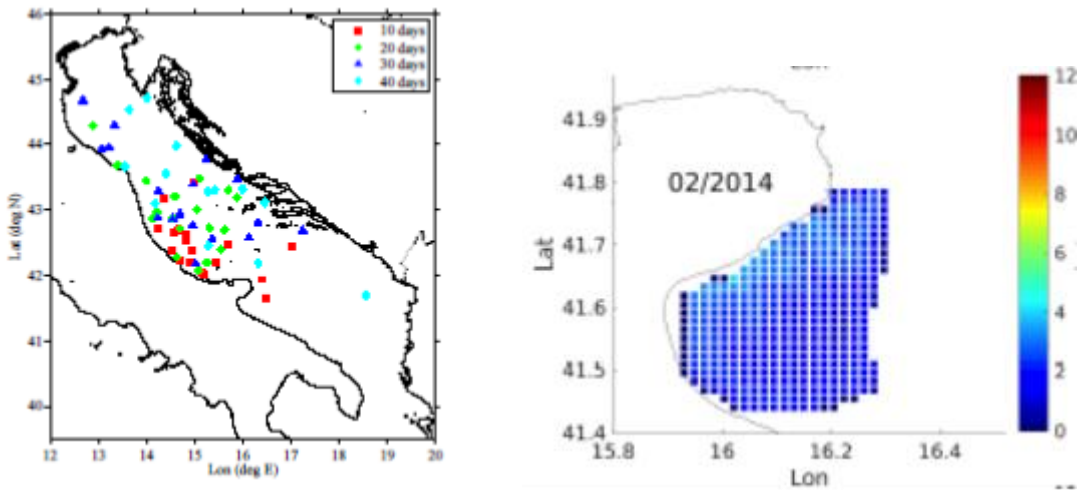

Figure 6.4: *Left panel: historical drifter locations at 10 days, 20 days, 30 days, and 40 days before entering the Gulf of Manfredonia. Right panel: bootstrap estimates of average residence times (in days) of virtual particles advected in the HF radar velocity field and released within the boundaries of the Gulf of Manfredonia (example for February).*

6.4.3. NW MED - Application of WP3 methods in NW Med.

The main objective was to test the new OSE/OSSE infrastructure demonstrating new numerical capabilities in: (1) using high resolution time/space observations (in particular the assimilation of HF radar data) to improve the quality of operational products, and (2) understanding ocean processes and dynamics in the Mediterranean Sea with focus on the Ligurian Sea coastal area. The assimilation of HF Radar data in a hydrodynamic model significantly improved the definition of the trajectory of drifting material, which demonstrated the benefits that HF radar data can brig to an operational forecasting system. **Figure 6.5** shows the results of the virtual drifter simulation for a one-week period. HF radar assimilation had a significant impact on virtual drifters, making the smoothed-out trajectories of the control run more realistic. In addition thanks to availability of high quality and high-resolution HF radar, a novel implementation of data assimilation scheme, based on Ensemble Kalman Filter approach, was developed with the aim of improving ocean forecasting. An OSE/OSSE infrastructure for the Adriatic Sea and the NW Mediterranean was tested and further applied to complex case studies such as the OSE in the Ligurian Sea and the Fishery and Oceanography Observing System in the Adriatic Sea. Results demonstrate the good ability of the Adriatic-Ionian Forecasting System coupled to Ensemble Square Root filter to improve the quality of the ocean fields and predictability (Berta et al., 2018 and Jansen et al., 2019). This represents a first step towards an operational OSE/OSSE system for designing future coastal observatories in the Mediterranean Sea and for evaluating the impact of future observations in our operational systems (from regional to coastal scales).

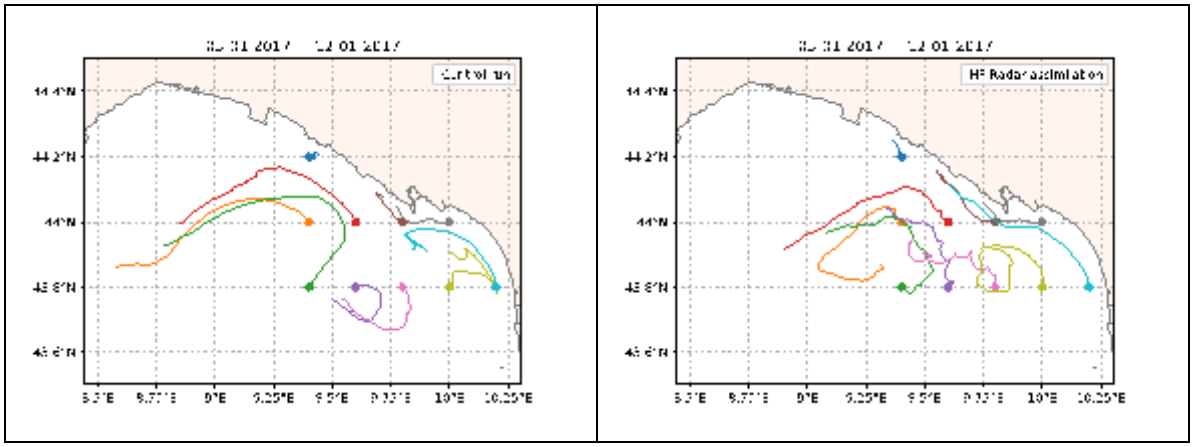

Figure 6.5: *Virtual drifter trajectories modelled by the Ensemble Kalman Filter approach with HF radar assimilation. The starting locations of the virtual drifters are indicated by the closed circles.*

6.4.4. SE BOB - Study of winter anticyclonic eddies from the analysis of historical remote sensing data.

Different remote sensing data were combined over the 2011-2014 time-period to characterize winter anticyclonic eddies in the SE BoB and to infer their effects on cross-shelf exchanges. The study focused on an anticyclonic eddy that developed in a period when typical along shelf-slope currents depicted a cyclonic pattern. While the joint analysis of available satellite data (infrared, visible and altimetry) permitted the characterization and tracking of the anticyclone properties and path, data from a coastal HF radar system enabled a quantitative analysis of the surface cross-shelf transports associated with this anticyclone (**Figure 6.6**). The warm core anticyclone had a diameter of around 50 km, maximum azimuthal velocities near 50 cm.s^{-1} and a relative vorticity of up to -0.45 f. The eddy generation occurred after the relaxation of a cyclonic wind-driven current regime over the shelf-slope; then, the eddy remained stationary for several weeks until it started to drift northwards along the shelf break. The surface signature of this eddy was observed by means of HF radar data during 20 consecutive days, providing a unique opportunity to characterize and quantify, from a Lagrangian perspective, the associated transport and its effect on Chl-*a* surface distribution. Results suggest that the eddy-induced recurrent cross-shelf export is an effective mechanism for the expansion of coastal productive waters into the adjacent oligotrophic ocean basin (See Rubio et al. 2018 for more detail).

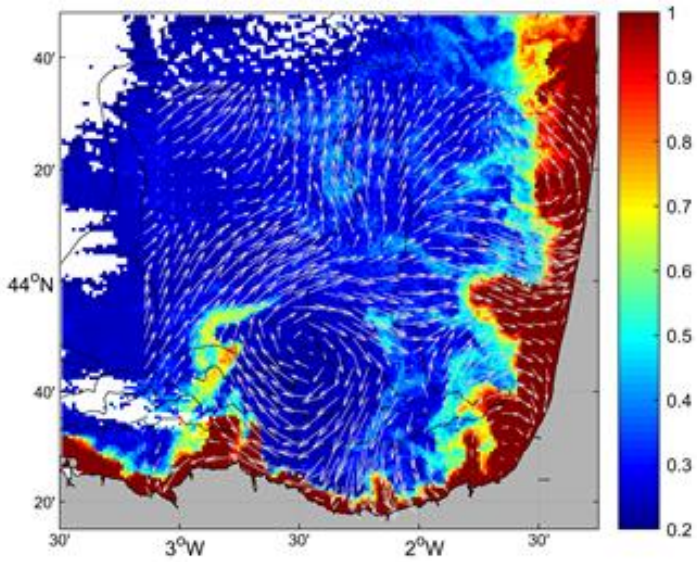

Figure 6.6: *MODIS-Aqua derived Chl-a (mg.m^{-3}) and HF radar hourly surface current vectors in the 21 December 2014 eddy cross-shelf. Chl a - rich waters export towards the open ocean can be observed. Isobaths (m): 200, 1000, 2000, 3000.*

6.4.5. SE BOB - ETOILE cruise

During summer 2017, the area covering the CapBreton Canyon (SE BoB) was surveyed in the framework of the ETOILE cruise. One objective was to observe the propagation of internal waves on the Aquitaine shelf. A network of low-cost thermistor chains (Mastodon moorings) was deployed for 3 weeks. These mooring revealed the existence of internal solitary wave (ISW) trains to depths of 50m above the bottom (**Figure 6.7**). These ISWs have been be followed from the outer shelf to the coast and their transformation from depression waves into elevation waves was also observed.

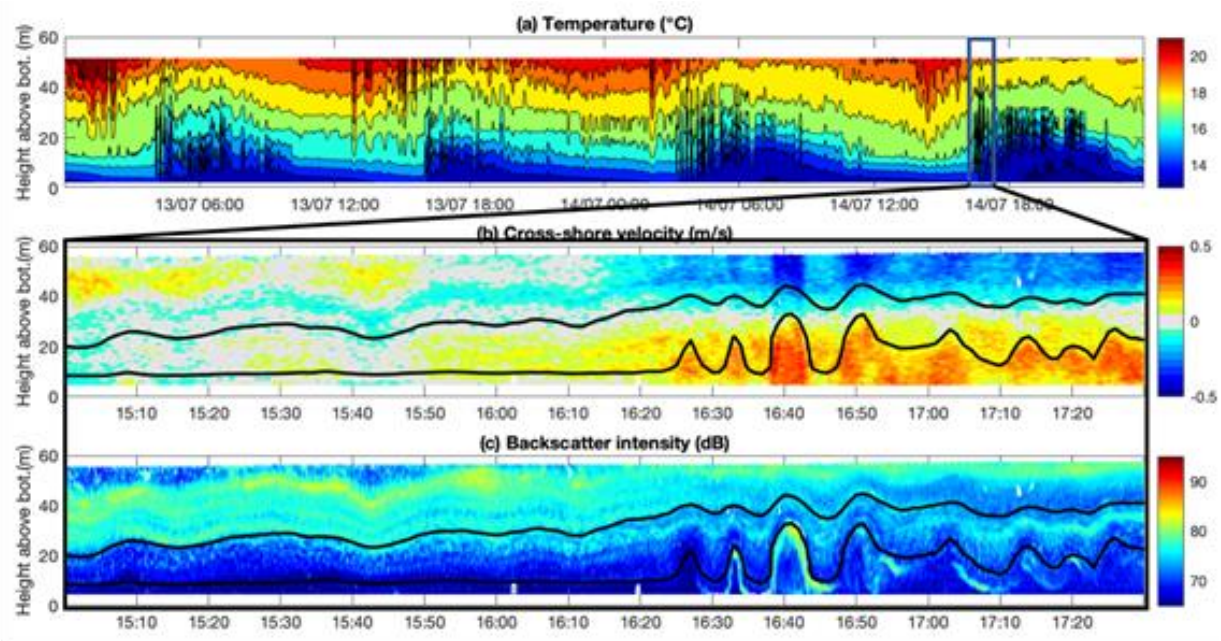

Figure 6.7*: ADCP and thermistors data during the ETOILE experiments in summer 2017. (a) Temperature profiles showing a succession of depression and elevation ISWs in the southern Bay of Biscay at 60 m depth. (b)(c) Zoom on one ISW train captured by the ADCP showing the cross-shore velocity and the backscatter intensity profiles. The black contours represent the 16 and 18 °C isotherms.*

The second part of the campaign was designed to gather hydrographic and hydrodynamic data, and to determine the spatial (3D) distribution of phytoplankton and floating marine litter. To that end *in situ* profiles of temperature and conductivity were collected using both a CTD and a Moving Vessel Profiler. Other parameters like *in vivo* chlorophyll fluorescence, multi-spectral fluorescence casts, chlorophyll *a* and particulate suspended matter concentration and marine floating litter were also collected. The effect of the observed mesoscale features in the distribution of floating marine litter and phytoplankton is discussed in detail in Dávila (2018). The distribution of marine litter seemed to be spatially correlated with positive surface relative geostrophic vorticity (not shown), with maximum concentrations at the periphery of cyclonic eddies. Concerning phytoplankton, a deep chlorophyll maximum was observed at ~50 m depth, highly dominated by Brown Algae (**Figure 6.8**). When examining the vertical distribution of brown algae it was found that their abundance correlated stonglywith negative vorticity (corresponding areas with anticyclonic rotation), while green algae vertical distributions were mainly influenced by salinity.

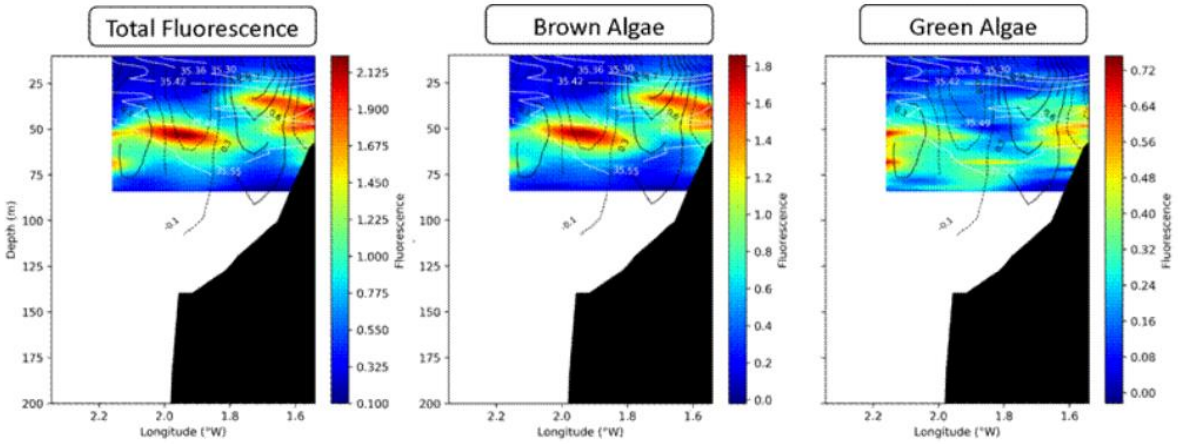

Figure 6.8: *Cross sections of multi-spectral fluorescence. Brown algae abubdances correlated with areas of negative vorticity (or anticyclonic circulation; in black lines) whereas green algae abundances seem to follow the depression of the halocline (in white lines).*

6.4.6. SE BOB - BB-TRANS TNA glider mission in HF radar area (May 2018)

The BB-TRANS mission took place from 17 May to 14 June 2018. A Slocum deep glider equipped with a CTD, ADCP, fluorescence-turbidity and MicroRide sensors, sampled the water column of the SE BoB, from the surface to at a 1000 m depth. The aim of this mission was to acquire data along the water column within the area covered by a coastal HFradar system. Moreoves, the glider sections where planned in order to mach the tracks of the two satellite altimeters crossing the area during the sampling period. These measurements allowed to: (1) test different methodologies of data blending for deriving transport in the water column together with surface currents obtained by HF radar; and (2) to evaluate the accuracy of coastal altimetry along-track data in the study area. From the analysis performed, both gliders crossed mesoscale eddies. The signature anticyclonic core around 26 May was observed in the profiles of the shallow glider (**Figure 6.9**) while the deep glider passed close to the periphery during the same days (not shown). Around this date, a down lifting of the seasonal thermocline was observed in the vertical profiles of the shallow glider (**Figure 6.9**, black rectangle). The down-lifting was more pronounced in the salinity and density profiles and had a clear impact on the fluorescence, with Deep Chlorophyll Maximum reaching deeper waters.

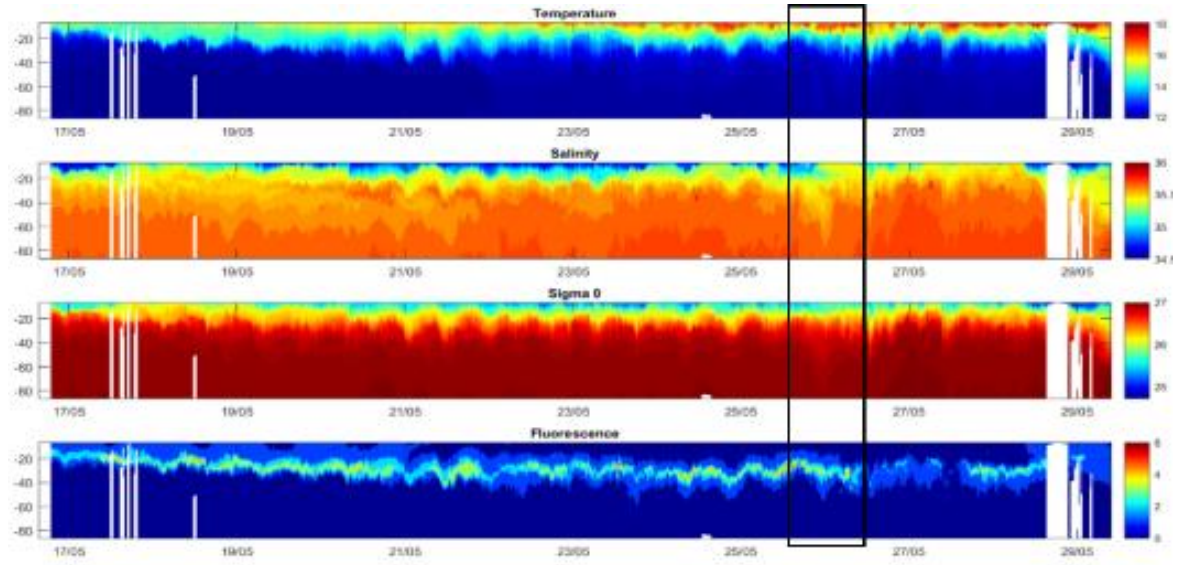

Figure 6.9: *Profiles of potential temperature, salinity, density and fluorescence (panels from top to bottom) along the shallow-glider tracks from the surface to 100 m depth. The black rectangle delimits the signal of the eddy.*

6.4.7. SE BOB - Application of WP3 methods in NW Med: SE BoB; Data blending

The combination of HF radar data with data from complementary in-situ platforms, providing information of the currents at subsurface layers (ADCP moorings), was investigated in WP3 and corresponding methodologies were then applied during JRAP 4 to reconstruct the 3D current velocity field from *in-situ* observations.. We tested two data-blending methods' skills by using pseudo-observations of currents, extracted from a numerical model, emulating the real observatory existing in the SE BOB), which includes two ADCP moorings over the upper-slope inside the footprint areas of a long-range HF radar. Reconstructed fields (outputs of the methods) were compared with 3D fields from where we extracted pseudo-observations (which are used as the synthetic reference fields). Overall, the results show satisfactory 3D reconstructions with mean errors for each depth between 2-10 $cm.s^{-1}$ (**Figure 6.10**). Errors tended to be lower in areas with high-density of observations and higher away from those areas. Although different performances were observed, both methods showed robust performances and promising skills for the computation of new operational products integrating complementary observations broadening the applications of the observational data.

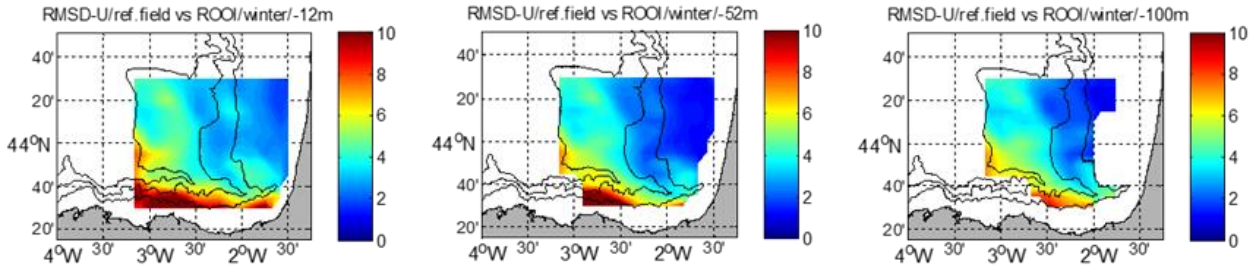

Figure 6.10: *Maps for 12, 50 and 100 m showing the errors (RMSD in cm/s) of the reconstruction for the ROOI data-blending methods (Jordà et al. 201) applied to the SE Bay of Biscay observatory. Results are shown only for the U component and winter.*

In a different exercise, the data from the SE BoBHF radar was used for the application and assessment of several methodologies to reconstruct HF radar velocity fields (Hernandez-Carrasco et al. 2018). One of them, based on self-organizing maps (SOMs) has been developed and tested in the framework of WP3. Then, a comparative analysis of this method with other available gap-filling techniques was performed, i.e., open-boundary modal analysis (OMA) and data interpolating empirical orthogonal functions (DINEOFs). The performance of each approach was quantified in the Lagrangian frame through the computation of finite-size Lyapunov exponents, Lagrangian coherent structures and residence times (not shown). We determine the limit of applicability of each method regarding four experiments based on the typical temporal and spatial gap distributions observed in HF radar systems unveiled by a K-means clustering analysis. Our results show that even when a large number of data are missing, the Lagrangian diagnoses still give an accurate description of oceanic transport properties.

6.4.8. GERMAN BIGHT -4DVAR analysis scheme to combine HF radar, tide gauges and ADCP with various choices of control variables.

The aim of the analysis concerned with transports in the German Bight was to use a combination of HF radar data, tide gauge measurements and ADCP observations (in FINO-1 platform) to optimize several uncertain parameters in the circulation model using a 4DVAR technique. HF radar data were gathered by three WERA antenna stations located at Wangerooge, Büsum and Sylt. **Figure 6.11** shows results obtained with the optimized model concerning water levels and ocean currents. It turned out that the combination of tide gauge data and HF radar measurements was very useful, in particular, when there is interest is in vertical mean transports. This is because HF radar system only provided information on surface currents and the shape of the vertical current

profiles could be complicated with nonlinear coupling of tidal and wind driven current components. The work performed in JRAP 4 constitutes an important step towards the integration of HF radars into existing coastal observing systems, which can be of high value for both operational applications and re-analyses.

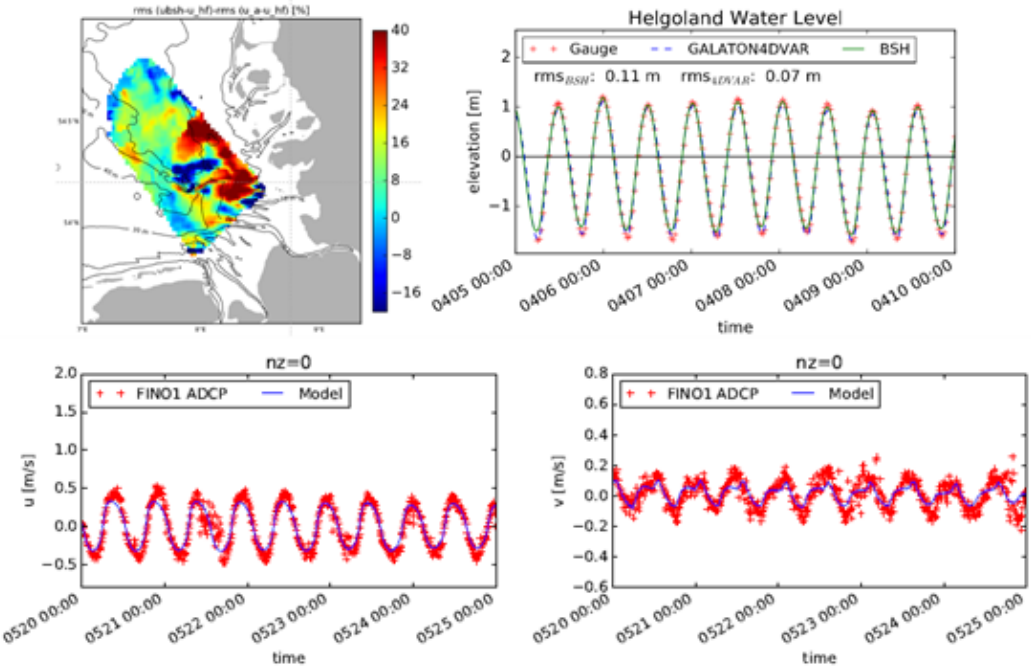

Figure 6.11: *(Top left) Relative improvement of surface currents with respect to free run. (Top right) Comparison of tuned model run with tide gauge measurements at the island of Heligoland. (Bottom left) Comparison of zonal current component of tuned model with ADCP measurements taken at the FINO-1 platform (small circle in top left panel). (Bottom right): The same for the meridional component.*

6.5. Main inputs relative to initial specific objectives

6.5.1. Q1: Can we use JERICO infrastructures to study the 4D shelf/slope circulation and transports and their time variability?

One of the main outcomes of the JRAP 4 activities was the obtention of new high-resolution observations through new deployments in two out of the three study areas: NW Med and Bay of Biscay. Some of these new deployments (like the new four radars in NW Med) were keys to upgrade current observatories. Other actions, like the deployment of MASTODON moorings and on-board surveys, helped: (1) to get additional data that solve smaller scales, and (2) to make a step forward in the understanding of coastal ocean processes and their effects of the shaping of distribution of biological parameters and pollutants (marine litter). Different methods developed for HF radar data advanced processing and analysis in WP were applied to JRAP 4 study areas and allowed to obtain: (1) gap-filled surface currents, (2) Lagrangian estimations (of transport, retention areas and times), (3) statistically forecasted currents, and (4) subsurface current maps. Several original scientific results were obtained from these advanced observational products and new potential operational products were assessed. In JRAP 4 a novel approach for the assimilation of HF radar (developed in WP3) was tested in the Adriatic. A main originality lies in the fact that this approach allows to directly assimilate radial velocity measurements of HF radar antennas without first reconstructing the Cartesian components of the surface current.

From the analysis of historical and new data the main conclusions and results concerning the characterization of coastal processes and associated partners were as follows:

- Impacts of different processes (like coastal mesoscale processes and slope current-topographic interactions, upwelling, geostrophic and wind-driven circulation) on the variability of coastal currents and transport and cross-shelf exchanges
- Observability of coastal mesoscale process (eddies, upwelling) and slope current by different measuring systems (in-situ and satellite)
- Demonstrated the benefits of the use of HF radar data combined with complementary data to obtain optimal estimates of ocean current and transports

6.5.2. Q2: What is the impact of the ocean transport on the distribution of floating and dissolved matter?

Several *ad-hoc* experiments were performed to quantify the potential impact of ocean transport on the distribution biological quantities and pollution. The analysis of the gathered multidisciplinary data was performed for different areas and time scales in relation with different ecological and environmental problematics. For this reason, no single general conclusion regarding **Q2** could be drawn. However, several interesting points can be highlighted:

- It was demonstrated that coastal eddies in the SE Bay of Biscay can be an effective mechanism for the expansion of coastal productive waters into the adjacent oligotrophic ocean basin (Rubio et al. 2018)
- During the ETOILE experiment, it was observed that the spatial distributions of marine litter and different phytoplankton groups correlated with different physical variables like salinity and vorticity and were thus controlled through different mechanisms by the presence of eddies and mesoscale frontal zones (Dávila MSC, 2018).
- The estimation of the average residence time in the Gulf of Manfredonia compared to the estimated larval lifetimes in the area supported the idea that sardine larval nursery was mainly supported by remote spawning areas (Sciascia et al., 2018)

6.5.3. Q3: How can we maximize the impact of the JERICO-RI for the assessment of coastal transport?

OSSEs were used in the SE Bay of Biscay to objectively propose an optimization of the existing observing network (additions of new HF radar antennas, changes in the positionings of fixed stations), and was pointed as a suitable method to better design the future observatories.

Additional recommendations to increase the impact of JERICO-RI for the assessment of coastal transport and impacts where also provided in relation with the results regarding **Q1** and **Q2**:

- The need to increase the multidisciplinary character of experiments, from the data acquisition
- The need of develop methodologies that allow the linking of individual and multidisciplinary observations
- The need of addressing different spatio-temporal scales and interactions between ocean compartments.

6.6. Analysis of the experience gained

6.6.1. Developing innovative technologies for coastal ocean observing and modelling.

The new observations acquired during JERICO-NEXT allowed to improve the existing observatories to solve smaller scales and to make a step forward in the understanding of coastal ocean processes. The main focus was to better characterize and understand the role that coastal mesoscale (coastal eddies, upwelling and submesoscale processes (like tides or internal waves) have in shaping coastal ocean transports. The combination of data from different platforms was key for most of the studies. The use of numerical models and advanced Lagrangian techniques in top of the combination of multiplatforma data also proved as a suited approach to tackle the main research questions raised by the JRAP4.

Besides, during JERICO_NEXT three new HF radar antennas were installed in the Eastern Ligurian Sea (NW Med), a set of Mastodon moorings where tested and deployed in the NW Med and the SE BoB, and (benefiting from a TNA actions) a glider campaign was conducted in the SE BoB. These data have provided information on the seasonality of the slope currents andthe characteristics of mesoscale and small scale (few kms) structures such as coastal eddies and jets present in the areas. They also allowed to obtain an unprecedent data set in the area for combination of multiplatform *in-situ* and remote sensing data. Indeed,several methodologies/tools from WP3 (advances QA/QC and processing, gap-filling, advances Lagrangian methods) were applied to data for the different JRAP 4 study areas, allowing an improved application of the data to different scientific questions and to fully benefit of the strong potential of in using a combination of different observation instruments.

The OSE/OSSE infrastructure developed in the frame of T3.7 for the Central Mediterranean Sea and the Southeastern Bay of Biscay (ArM method) can be used to assess new coastal observing systems with some accuracy. Main innovations that have been introduced from the modelling perspective: (i) the implementation of a novel Ensemble Square Root (EnSQR) Filter for assimilating temperature and salinity profiles and HF radar velocity. It will be exploited in the future for operational purposes; (ii) the definition of a numerical strategy for deploy high resolution ocean models for nature runs based on relocatable approach; (iii) the extend of existing methodologies (ArM method) to HF radar platforms including the use of spatial distributed observation errors. However, the benefit of observations for data assimilation depends critically on error characteristics of the respective numerical model (e.g., error sources or error correlation length both in time and space) and that of the observations. So, there is still some work to do concerning a systematic analysis and classification of these errors.

.

6.6.2. ***Establishing observing objectives, strategy and implementation at the regional level.***

The geographical extension of the JRAP 4's study areas was very different, but in all the cases the spatial scale of the three areas was less than regional. The areas were defined mainly depending on the key processes identified and the coverage of the existing observatories and/or model configurations (i.e. Ritmare, Cosyna, Euskoos). From our point of view the dimension of the three areas were satisfactory regarding the scientific questions underneath.

The thematic addressed by JRAP 4, in the case of NW Med and SE BoB, could become part of a regional observation system. The good coverage of the (large-scale) boundary currents affecting the respective shelf/slope areas support the relevance of these two observatories, in a context of a broader regional dimension. A next step could be to explore further the possibilities of collaboration with other connecting *in-situ* observatories, numerical modelling and Earth Observation communities.

In the German Bight the main scientific questions had a stronger local character, which was well covered by the observations and models running in the area.

6.6.3. ***Enhancing integrated coastal ocean monitoring and interfacing with other ocean observing initiatives operating at different spatiotemporal scales.***

There was not a true multidisciplinary component in JRAP 4, and multidisciplinary issues were only addressed when synergies inside JERICO_NEXT (with other WPs and mainly JRAPs 3 and 6) or with other projects allowed it. On example was the interfacing with the LIFE LEMA - Intelligent marine Litter removal and Management for local Authorities (LIFE15 ENV/ES/000252) project. Building on the improved HF radar surface current (advanced QA and gap-filled data from JERICO-NEXT), a numerical model and FML data (from LIFE-LEMA project) a study was undertaken to characterize the FML transport regimes in the SE BoB. The interaction was fruitful, and one paper was published (Declerck et al. 2019, JOO). Other examples of the interaction of JERICO-NEXT with other project and initiatives are listed hereafter.

From the experience gained in JRAP 4, a presequisite for integrated coastal ocean monitoring is to enabke truly multidisciplinary approaches form the planning of the actions and experiments, ensuring consistency in the temporal or spatial resolution/coverage of the observations, and the suitable tools for joint data analysis (for instance biogeoquemical numerical models).

The lack of a multidisciplinary approach in the planning of JRAP 4 and other JRAPs actions and experiments concurrent in some areas (like the installation of passive samplers in the Bay of Biscay) resulted in data sets that were not jointly exploitable. This prevented in some occasions to reach satisfactory results in the interactions between disciplines (for instance between JRAPs 1, 3 and 4). Other ad-hoc experiments (conducted with extra funds) like the ETOILE campaign (July 2017 with CTD, ADCP, multispectral fluorometry and plastic sampling in the HF radar area) or the glider mission in the SE BoB (BB-TRANSTNA, JN_CALL_2_8), or a trial experiment (February 2017 with CTD, ADCP, glider and plastic sampling within the HF radar area) and the UPCAST campaign (September 2017 with CTD, ADCP, fluorometry in the HF radar area) in the NW Med were more satisfactory.

The main aspects of the interactions between JRAP 4 and other initiatives and or projects are listed and commented herein:

- *NW Med*; IMPACT (Maritime Cross Border Cooperation Project Italy-France) (since 2017). IMPACT deals with the challenge of managing Marine Protected Areas (MPAs) on the North Western Mediterranean Sea. Linked with JERICO-NEXT JRAP 4 in terms of transport products and ecological consequences.
- RITMARE Flagship Project (until end 2016), It is the leading national marine research project in Italy, and it includes the setup of an Observation System for the Marine Environment (WP5). In particular, a network of HF radars has been set up in the Tyrrhenian and Ligurian Sea, in coordination with JERICO-NEXT.
- AMICO-NEXT (LEFE/GMMC 2016-2018). This project deals with integrated operational modeling at the coastal scale. A focus is given on the modeling of upwelling and the way to improve it, thus using the data acquired in the framework of JERICO-NEXT JRAP 4 in the NW Med (MASTODON-2D and UPCAST cruise).
- *SE BoB;* LIFE LEMA - Intelligent marine Litter removal and Management for local Authorities (LIFE15 ENV/ES/000252). Building on the improved HF radar surface current (advanced QA and gap-filled data from JERICO-NEXT), a numerical model and FML data (from LIFE-LEMA project) a study was undertaken to characterize the FML transport regimes in the SE BoB. The interaction was fruitful, and one paper was published (Declerck et al. 2019, JOO).
- COMBAT (CMEMS – SE: 2018-2020): Improve the interface between coastal monitoring and modelling systems by providing a new coastal MDT including a 7 year-long HF radar data set with advanced QC, provided by JERICO-NEXT (WP3-5 and JRAP 4).
- COCTO (Coastal Ocean Continuum in surface Topography Observations) funded by TOSCA/ROSES in the frame of SWOT altimetry mission - 2015-2018. Diagnostics developed in this project will be potentially used in the frame of JERICO-NEXT for comparisons between numerical experiments and *in situ* observations. Developments in ArM method will also benefit the COCTO project.
- ROEC (Observation network for the coastal environment in Brittany) funded by the Brittany region (based on ERDF funds) – 2016-2020. Projects aiming to develop coastal observation networks along French coasts. This development is based on future implementation of observing system. The implementation plan will be co-design based on tools (ArM methodology) co-developed in the JERICO-NEXT project.

6.7. Propositions for a future monitoring strategy for the topic

To enable a step forward in the integrated study and monitoring of coastal dynamics and transport, the future monitoring strategy for the topic developed in JRAP 4, should be focused on the following aspects of the coastal ocean are:

- Characterizing the main slope currents current three-dimensional variability and connectivity between different coastal regions under common forcing (for instance the European Atlantic marging and the IPC, the NW Med and the Northern Current), since these currents are connecting transboundary regions along the continental slope and can be an important mechanism for transport of active and passive particles (plankton, invasive species, jellyfish, pollutants, marine litter, plastics)

- Disentangling the mechanisms that drive this variability and the generation of mesoscale eddies, and submesoscale processes for improving forecasts and better understand their impacts in the coastal ocean productivity
- Addressing different spatio-temporal scales and the interactions between ocean compartments (coastal and open ocean, land sea continuum)
- Addressing the impacts of extreme weather on coastal populations, maritime traffic and coastal erosion and Climate Change effects.

Among the lessons learned from the implementation of JRAP 4 actions, one of the most important is that to conduct integrated studies we need data gathered in the same area with similar coverage and temporal scales, and models that can solve the same scales and processes. Thus, the monitoring strategy for the future should encompass the gathering of integrated observations in the coastal area through:

- The development of technology and approaches allowing truly multidisciplinary observing/sampling at the same spatio-temporal scales.
- The use of Observing System Simulation Experiments (OSSEs, Task 3.7 and JRAP 6) to assess new coastal observing systems
- The planning of additional *ad-hoc* multidisciplinary experiments tor progress in the development of new technology and approaches
- The coupling of current/waves/hydrography observation at different scales combining HF radar, moorings, and other more coastal technologies like videometry (coast-land integration and along-shelf and cross-border connectivity)
- The integration of additional sensors to the existing moorings and facilities to build a truly integrated multiplatform and multidisciplinary observing systems.
- Coupled biogeochemical modelling – DA for Physics, and progress in the use of biogeochemical data for validation/assessment
- The capitalization of established transnational collaboration in operational oceanography with neighboring observatories, other research infrastructures and communities (for instance remote sensing) and scientific projects.

One important aspect to tackle in the future will be to ensure the analysis and update of key drivers (key scientific questions, needs) and the development of tailored tools or products. For this it is key to be in contact and even work in close collaboration to the stakeholders. For instance, during the development of JRAP 4 we have obtained vet satisfactory results by using new methodologies for HF radar data processing and analysis. Some of these methodologies (to obtain gap-filled data, subsurface current maps or short-term prediction) could be applied in an operational way in the future. We need thus to keep working to progress in the TRL of the developed methods/tools for operational use. Among the products that could be further developed in the future are:

- Products related to integrated coastal management using Lagrangian approaches for particle dispersion: surface/subsurface coastal transport estimation, residence times, marine litter hotspots…
- Reanalysis of *in-situ* and satellite data tailored for the coastal zone
- Improved and geographically extended currents in collaboration with other connecting in-situ observatories, numerical modelling and Earth Observation communities.

6.8. References

Berta, M., L. Bellomo, A. Griffa, M. Magaldi, A. Molcard, C. Mantovani, G.P. Gasparini, J. Marmain, A. Vetrano, L. Béguery, M. Borghini, Y. Barbin, J. Gaggelli, and C. Quentin (2018). Wind induced variability in the Northern Current (North-Western Mediterranean Sea) as depicted by a multi-platform observing system. Ocean Sci., 14, 689-710, https://doi.org/10.5194/os-14-689-2018.

Dávila, X. (2018). Influence of (sub)mesoscale processes on the distribution of organic and inorganic particles in the SE Bay of Biscay. MsC Thesis for the Marine Environment and Resources Erasmus Mundus master degree.

Fredj, E., H. Roarty, J. Kohut, M. Smith, and S. Glenn (2016). Gap Filling of the Coastal Ocean Surface Currents from HFR Data: Application to the Mid-Atlantic Bight HFR Network. J. Atmos. Oceanic Technol., 33, 1097–1111, doi: 10.1175/JTECH-D-15-0056.1

Hernández-Carrasco, I., Solabarrieta, L., Rubio, A., Esnaola, G., Reyes, E., Orfila, A. (2018). Impact of HF radar current gap-filling methodologies on the Lagrangian assessment of coastal dynamics. Ocean Sci., 14, 827-847, https://doi.org/10.5194/os-14-827-2018, 2018

Manso-Narvarte, I., Caballero, A., Rubio, A., Dufau, C, Birol, F (2018). Joint analysis of coastal altimetry and high-frequency (HF) radar data: observability of seasonal and mesoscale ocean dynamics in the Bay of Biscay.Ocean Sci., 14, 1265-1281, https://doi.org/10.5194/os-14-1265-2018, 2018

Rubio A., Caballero A., Orfila, A.,Hernández-Carrasco, I., Ferrer L., González M., Solabarrieta, L, Mader, J. (2018) . Eddy-induced cross-shelf export of high Chl-a coastal waters in the SE Bay of Biscay. Remote Sens. Environ. 205, DOI 10.1016/j.rse.2017.10.037.

Schulz-Stellenfleth, J, and EV Stanev (2016). Analysis of the Upscaling problem–A Case Study for the Barotropic Dynamics in the North Sea and the German Bight. doi:10.1016/j.ocemod.2016.02.002

Sciascia, R., Berta, M., Carlson, D. F., Griffa, A., Panfili, M., La Mesa, M., Corgnati, L., Mantovani, C., Domenella, E., Fredj, E., Magaldi, M. G., D'Adamo, R., Pazienza, G., Zambianchi, E., and Poulain, P.-M. (2018). Linking sardine recruitment in coastal areas to ocean currents using surface drifters and HF radar. A case study in the Gulf of Manfredonia, Adriatic Sea. Ocean Sci., 14, 1461–1482.

6.9. Abbreviations

ADCP : Acoustic Dopplet Current Profiles
CODAR: Coastal Ocean Dynamics Application Radar
CTD: Conductivity Temperature Depth
DA: Data assimilation
DCT-PLS: Discrete Cosine Transform Penalized Least Square
EnSQR: Ensemble Square Root
GB: German Bight

HF: High Frequency
LPTM: Lagrangian Particle-Tracking Model
NW MED: North Western Mediterranean
OMA: Open-boundary Modal Analysis
OSE: Observing System Experiments
OSSE: Observing System Simulation Experiments
ROOI: Reduced Order Optimal Interpolation
SAR: Search and Rescue
SE BOB: South Eastern Bay of Biscay
SOM: Self Organizing Maps
WERA: WavE Radar

7. JRAP 5: Coastal carbon fluxes and biogeochemical cycling

Contributors
Lauri Laakso, Martti Honkanen, Sami Kielosto, Timo Mäkelä, Finnish Meteorological Institute, Finland
Anne-Mari Lehto, Jukka Seppälä, Pasi Ylöstalo, Timo Tamminen, Finnish Environment Institute, Finland
Yoana G. Voynova, Wilhelm Petersen, Matrina Gehrung, HZG, Germany
Carolina Cantoni, Stefania Sparnocchia, Anna Luchetta, Stefano Cozzi, CNR-Trieste, Italy
Richard Bellerby, Andrew King, Marit Norli Kai Sørensen, NIVA, Norway
Anna Willstrand Wranne and Bengt Karlson, SMHI, Sweden
Constantin Frangoulis, George Petihakis, Alkiviadis Kalampokis, Manolis Ntoumas, HCMR, Greece

7.1. Topic and specific objectives.

Coastal and continental marginal seas are among the most biologically active regions on the Earth. Although they cover only a small portion of the oceans, they contribute up to 15% of ocean primary production, are responsible for over 40% of the total oceanic carbon sequestration (Muller-Karger et al., 2005). They also sustain the vast majority of commercial fisheries (Pauly and Christensen, 1995). Due to their large influence on global carbon cycling, it is important to better quantify the role of coastal and marginal seas as sinks or sources of carbon dioxide.

Carbon fluxes in coastal seas are more complex than those in the open ocean, in part due to high spatiotemporal variability in biological activity and physical processes. For example, in the Baltic Sea, partial pressure of carbon dioxide in seawater (pCO_2) may vary between 150 and 650 µatm due to a strong seasonal cycle in phytoplankton productivity, microbial remineralization, and water column mixing (Wesslander, 2011). High spatiotemporal variability in European coastal seas also arise from the highly variable hydrography: sea surface temperature may vary from below 0°C on the coast of Spitsbergen up to 30°C in the Mediterranean Sea, while salinity varies from 0 in the Gulf of Bothnia, the Baltic Sea to more than 38 in the Mediterranean Sea.

Region-specific differences in solubility and biological carbon pumps control the carbonate system in coastal regions. Effects of physical forcing on those need to be better understood and quantified. Consequently, regional requirements for coastal observatories need to be formulated, including: (1) which variables need to be monitored, (2) what are their projected measurement ranges, and (3) what the required spatio-temporal scales for observations are. At the same time, however, the European and global aspects towards harmonized observations need to be taken into account to secure availability and comparability of data. To promote such development, JRAP 5 aimed to provide harmonized measurements of the carbonate system, together with biological and physical measurements, across different European coastal seas.

The large regional variability creates challenges when designing the harmonized sampling strategies for European coastal seas and setting technical criteria for measurement accuracy, instrument reliability and instrument maintenance. The networking activities in JRAP 5 had an aim to give recommendations of setting up a combined physical, chemical and biological measurement network for carbon cycle studies as needed for understanding the role of coastal systems in the global carbon cycles.

JRAP 5 on coastal carbon fluxes and biogeochemical cycling was planned to exemplify how coordinated carbonate system observations can address the role and responses of the European Coastal Ocean and Marginal Seas in the global C-cycle, and to provide recommendations for an integrated European C-cycle monitoring. This was done by observing sea surface pCO_2, pH, and other relevant parameters throughout European seas utilizing fixed stations and Voluntary Observing Ships (VOS). The main effort of this activity was to collect continuous measurements for one full year at all sites, and as a result, to define best practices for observations and standard operating procedures and to examine the links between biological, chemical and physical processes and pCO_2.

JRAP 5 aimed at answering 3 main scientific questions:

- **Q1:** What kind of role do European Coastal Ocean and Marginal Seas have on the marine carbon system?
- **Q2:** What is the role of biological activity on marine carbon uptake or release?
- **Q3:** How should the integrated C-cycle monitoring be organized in coastal regions?

7.2. Overall structure and strategy

JRAP 5 aimed to provide harmonized measurements of carbonate system parameters in different European coastal seas. JRAP 5 started by inventory of methods, equipment and environmental conditions and continued with harmonized measurement campaign covering the whole seasonal cycle. Data analysis followed common guidelines, as much as possible. The aim was to collect a consistent dataset from various sites, allowing for comparative analyses between regions and providing a holistic analysis of carbonate system variations across European coastal seas. The implementation of JRAP 5 is described in **Table 7.1** and **Figure 7.1**.

Table 7.1: *JRAP 5 implementation timeline.*

Time	Actions
M1-12	· Inventory of JRAP 5 partners carbonate system observing equipment (instruments, methodology, calibration and maintenance procedures etc.) · Information on typical environmental conditions (pCO_2-ranges, temperatures, salinities, chlorophyll concentrations etc.) at JRAP 5 observing sites collected.
M13-18	· Preparations for intensive observing campaign, e.g. installation of new instruments and maintenance of old, existing equipment · Meeting on Intensive sampling period observing strategy during the GA in Helsinki
M19-31	· Intensive observing campaign throughout European Seas · Additional campaigns with extended measurements at some observing sites over shorter periods, providing a more detailed picture of sea surface biogeochemistry
M32-36	· Data QC processes agreed according to ICOS-OTC and SOCAT standards · Intensive observing period, with data quality assured by the JRAP 5 partners and submitted to a joint data folder
M36	· Presenting the results in the General Assembly and discussing a joint publication
M38	· Carbonate system observing intercomparison exercise in Oslo, Norway (TNA activity INTERCARBO)
M39-48	· Analysis of INTERCARBO results

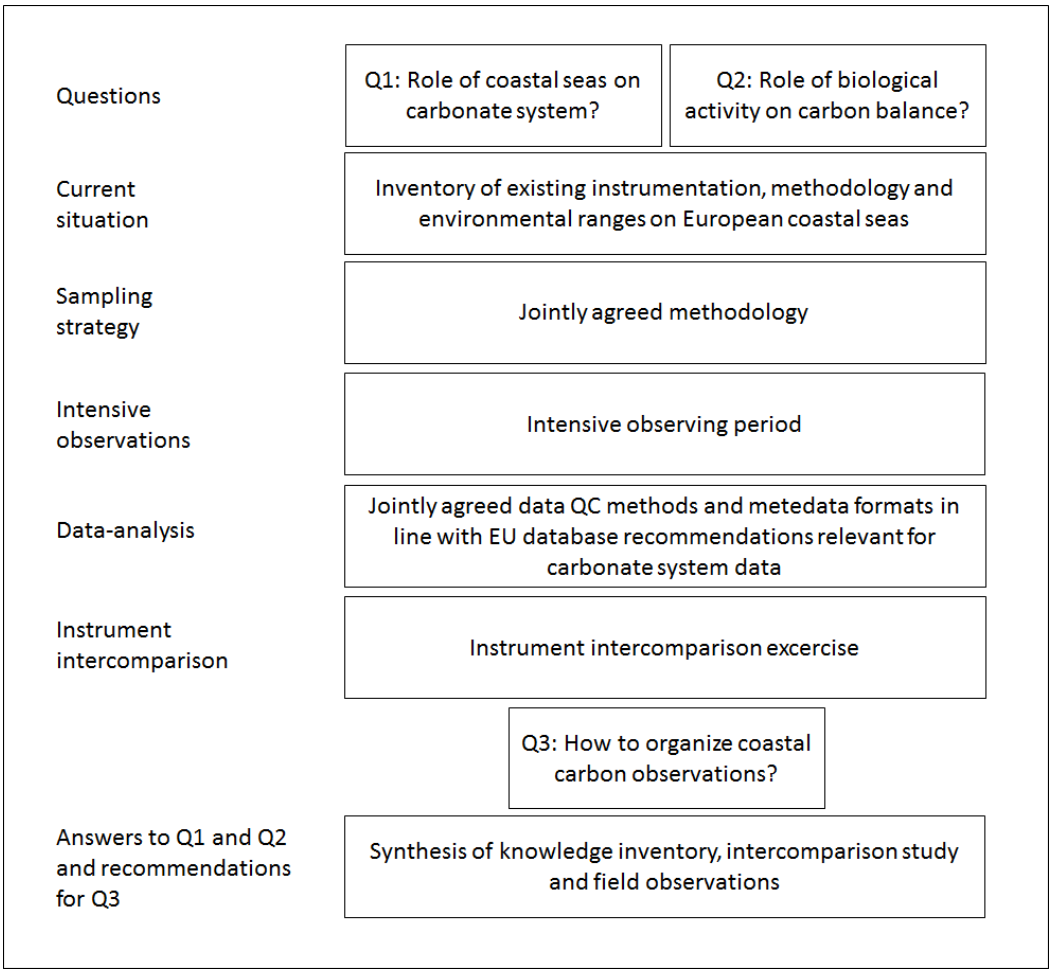

Figure 7.1: *Presentation of the overall structuration and strategy of JRAP 5.*

7.3. Achieved actions

7.3.1. Sampling plan

Following the initial plan, we had an intensive measurement period 2017/04-2018/04. Observations took place on existing fixed stations and VOS-lines, with existing instrumentation. Locations and parameters observed are listed in **Table 7.1** and **Figure 7.2**.

7.3.2. Variables/parameters

The full set of observations planned in JRAP 5 was temperature, salinity, pCO_2 *and/or* pH *and/or* total alkalinity, and chlorophyll *a*. However, as all sites did not have all variables available, the exact parameters observed varied between sites. At certain sites, variables listed above were supported by meteorological observations and short intensive measurement campaigns.

7.3.3. Data analysis.

After the intensive measurement period, data were analyzed according to a mutually agreed methodology, which was based on suitable parts of recommendations made by SOCAT and ICOS-OTC. The partners of JRAP 5 jointly agreed on the following data QA/QC processes:

- Partners read through the document "ICOS Marine Station Labelling Step 2"
- They filled in a specific metadata Excel sheet depending on the type of station: fixed or VOS line

- Partners did quality assurance of their data following the outline given in the ICOS labelling document. The instructions permitted for site and observing system specific procedures, as long as the procedures applied to the data were well documented. Thus, the partners wrote a compact but accurate readme-document which described the correction and rejection procedures they applied to the data
- Data file formats:
  - ✓ VOS-lines: each trip saved as a separate file.
  - ✓ Fixed stations: data combined in monthly or daily files.
  - ✓ Each individual data file had a header row containing the name and unit of the variable for each column.
  - ✓ Files were named based on unique identifier related to the site and date describing the measurement period.
  - ✓ Data format was ASCII, columns separated with comma ","
  - ✓ Missing values were given as -999 (no empty spaces)
  - ✓ ISO date and time format "yyyy-mm-ddTHH:MM:SS+00:00" UTC time. For decimals in seconds, "SS.S" was used.
- Data averaging: different sensors may have different time resolution (especially fixed stations). The partners selected suitable averaging times not exceeding one hour (in case of fixed station) and for VOS-line as short as possible. The choice was document in the site-specific QC-readme.
- Data from regular manual sampling of extra variables/parameters were stored in a separate file, including the specific metadata, QC description, and well-defined headers and names for the datafiles.
- As most databases require flagging of data quality, we added an extra column after each variable column with a data quality flag. For this purpose, we used CMEMS flags. 1 : good, 4 : bad, 9 : missing data
- Data together with metadata was submitted to a joint Google Drive folder for temporary storage

***Figure 7.2**: Observing sites during the JRAP 5 intensive observing campaign (M19-31). Stars indicate fixed stations and lines VOS routes. Successful observations are indicated with yellow color. Sites with limited or no carbonate system data are shown in gray color.*

7.4. Main results

The percentage of successful observations during the intensive measurement period is shown in **Table 7.2**. There were only a limited number of fixed sites or VOS lines which succeeded in combining biological and carbonate system observations for the whole period. However, this was expected prior to the intensive campaign and compensated by the large number of sites providing observations. In the results described here, the focus is on those observations with highest carbonate system data coverage, some of them including observations of biological variables. Depending on institutional traditions, slightly different notations or units for carbonate system variables are used. The differences between these are minor (1-2 orders of magnitude smaller than potential offsets between the individual instruments), and for simplicity we interchangeably use the terms pCO_2 and fCO_2 (fugacity), as well as the units µatm and ppm.

***Table 7.2**: Monthly data coverage (%) per site and variable*

Area	Location	Meteorology	CDOM	pH	Alk	pCO_2	O_2	Chl*a*	T,S
Norwegian Sea	Bergen Kirkenes	100	-	75	-	75	75	75	100
	Tromsö-Svalbard	100	-	-	-	50	100	-	100
North Sea	Oslo-Kiel	100	-	-	-	25	100	75	100
	Helgoland	-	-	-	-	-	100	100	100
	Moss-Zeebruegge-Immingham	-	100	100	-	100	100	100	100
	Cuxhaven	100	-	-	-	-	100	100	100
	Cuxhaven - Immingham	-	67	75	75	67	75	75	75
Baltic Sea	Utö	100	100	75	-	100	100	100	100
	Helsinki-Stockholm	-	75	33	-	-	67	75	75
	Kemi-Lübeck	100	92	-	-	42	42	92	92
Atlantic Ocean	Western channel Astan	100	-	-	-	25	100	100	100
	Plymouth-Roscoff	-	-	-	-	33	58	58	58
Mediterranean Sea	Paloma	92	-	-	-	92	92	-	92
	Poseidon E1-M3A	100	-	-	-	-	67	67	75
	Poseidon HBC	100	-	-	-	-	-	-	100
	Heraklion-Athens	-	-	-	-	-	42	42	42

7.4.1. Norwegian Sea - Bergen-Kirkenes.

Carbonate system observations along coastal Norway on M/S Trollfjord were made between Bergen (~60 deg N) and Kirkenes (~70 deg N) (**Figure 7.3**). They incorporated both pCO_2 (µatm) and pH (total scale) during the period July 2017-March 2018. Minimum pCO_2 and maximum pH were generally observed during summertime. The lowest pCO_2 and highest pH were observed in July/Aug 2017 where pCO_2 was measured below 200 µatm (min ~100 µatm) and pH greater than 8.1 (max 8.19) near Måløy (~62 deg N), Sandessjøen (~66 deg N), and Kirkenes (~70 deg N). The wintertime period was characterized by higher pCO_2 with maximum values of ~490 µatm and lowest pH values approaching 7.95 near Bergen (~60 deg N) in November-December 2017. Similar characteristics were estimated by Omar et al., (2016). Phytoplankton (represented here by chl *a*) was observed to be highest in April-July 2017 with values approaching 20 µg L^{-1}, with a smaller secondary bloom (up to ~2 µg chl L^{-1}) in September-October 2017. The lowest pCO_2 and highest pH observations coincided with the primary bloom in spring/summer 2017.

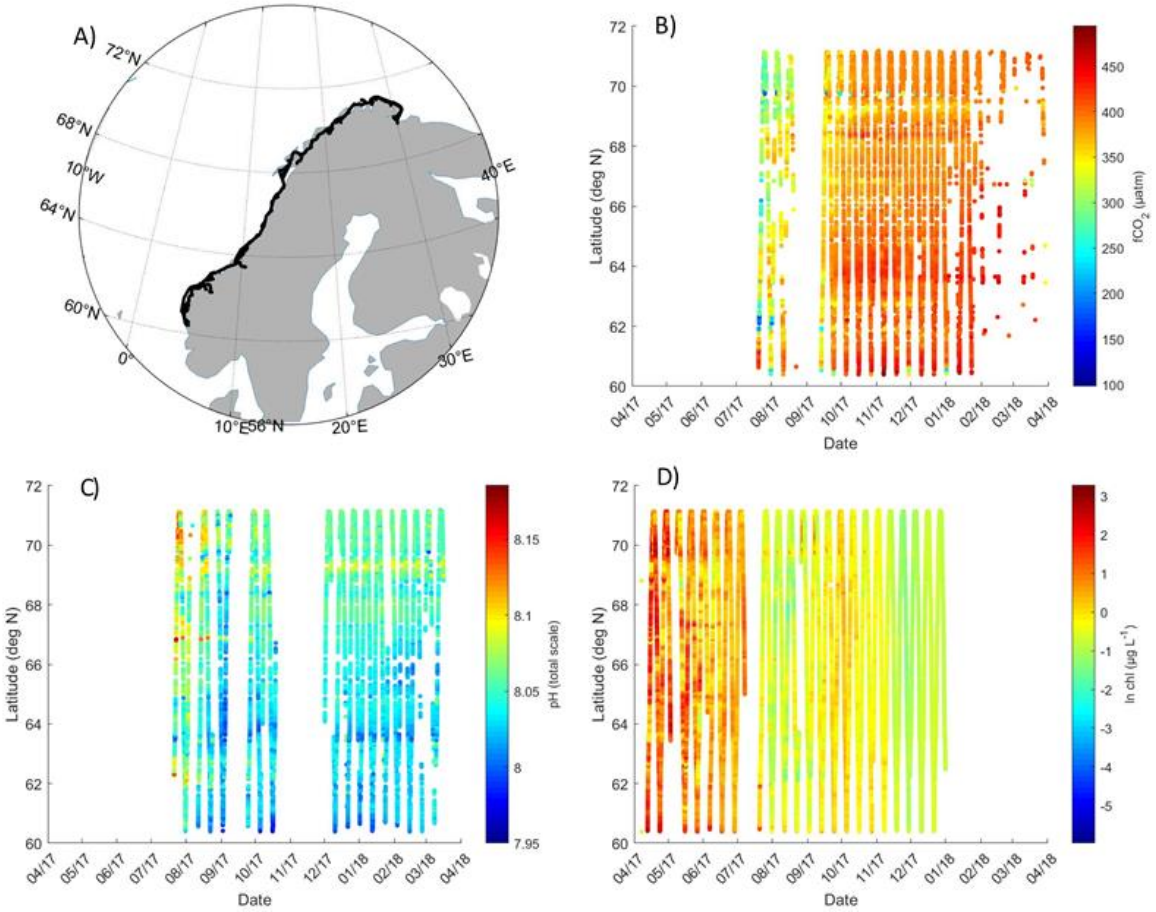

***Figure 7.3**: A) Ship track of M/S Trollfjord, B) pCO_2 (µatm), C) pHT (and D) chlorophyll a (ln µg L^{-1}) observations between April 2017-Mar 2018 from Bergen (~60 deg N) to Kirkenes (~70 deg N).*

7.4.2. Norwegian Sea - Tromsø-Svalbard.

Observations of pCO_2 were made from the container ship M/S Norbjørn which makes twice-monthly trips between Tromsø, Norway and Longyearbyen, Svalbard across the Barents Sea Opening (**Figure 7.4**). The wintertime observations that are available between November 2017 and March 2018 indicate that, in the open sea, pCO_2 ranged between 390 and 420 µatm. Highest pCO_2 was located in December and January in the central section between Tromsø and Bear Island. Undersaturation, with respect to the atmosphere, was observed in the

coastal regions with values lower than 360 µatm. In the north of the section in March, pCO_2 values were approaching a good agreement with Lauvset et al. (2013), assuming a similar $dpCO_2$ between 2006 and 2017.

These values are lower than those estimated for the Barents Sea for March by Kaltin et al. (2002) and could be indicative of an increase in primary production.

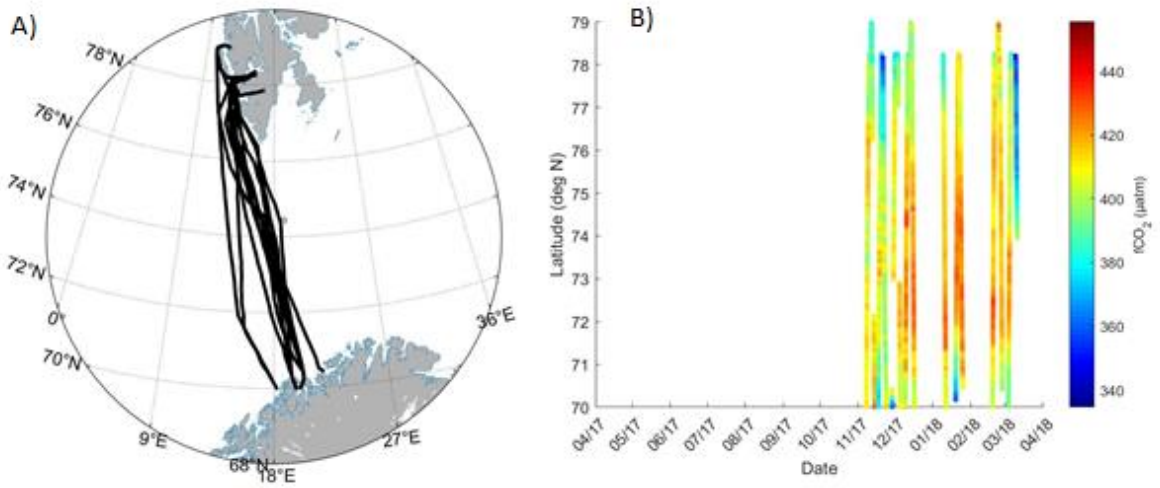

***Figure 7.4**: Ship track of M/S Norbjørn and B) pCO_2 (µatm) observations between April 2017-Mar 2018 from Tromsø (~70 deg N) to Longyearbyen, Svalbard (~78 deg N).*

7.4.3. North Sea - Norway-Belgium-England route.

The Lysbris Seaways is a cargo vessel which travels between Immingham, UK, Moss/Halden/Fredrikstad, Norway, and Zeebrugge/Ghent, Belgium. This ship has been instrumented with a FerryBox since 2009, measuring temperature, salinity, dissolved oxygen, pH, chlorophyll fluorescence, among other parameters. Since 2012, pCO_2 measurements obtained with a Contros HydroC pCO_2 sensor (Contros Kongsberg, Kiel, Germany) were added. The Lysbris moved routes slightly in mid-2010 to mid-2012, to travel to Germany and Spain, but it maintained the Immingham to Norway section of the route. For this section, we had a consistent 9-year dataset for most parameters, excluding pCO_2, which was available since mid-2012.

Figures 7.5-7.8 show the seasonal variability captured by the Lysbris between April, 2017 and March, 2018, during the JRAP#5 focus period. Temperature (**Figure 7.5**) was cold in the winter (< 8 °C) throughout the entire route, but gradually warmed up, starting south of 54 °N in the spring, to reach 14-20 °C by July. The warmest regions were near ports and south of 54 °N. In the fall, up to November, 2017, sea surface temperature was still warm (12-14 °C) south of 57 °N.

A prominent feature in the salinity records (**Figure 7.6**) is the region of the Skagerrak (salinity < 32), along the Norwegian coast, where the outflow from the Baltic Sea into the North Sea takes place (Holt and Proctor 2008; Otto et al. 1990). The geographic extent of the outflow was observed to change seasonally. During the JRAP 5 study period, its signature was most prominent in the summer, when it was observed to extent to just south of 58 °N.

Another prominent feature was observed near the UK coast, where salinity is slightly lower compared to the adjacent regions. This could be due to the river flows along the UK coast. The partial pressure of carbon dioxide (pCO_2) varied between 200 and 500 µatm (**Figure 7.7**), with the exception of the port regions, where pCO_2 was much higher, often exceeding 800 µatm.

Seasonally, pCO_2 was lowest in the spring (200-300 µatm), particularly along the Dutch and Belgian coastal regions, south of 54 °N. An exception to this is the UK coast, where pCO_2 was supersaturated. The observed pCO_2 range was much larger than the atmospheric CO_2 variations, but when the measurements were subtracted from

atmospheric CO_2 values, observed differences show that surface waters in the North Sea were largely undersaturated with very few exceptions (e.g. ports, and regions very close to land). Based on earlier observations, the pH records along the route generally vary between 7.8 and 8.5, with a pronounced seasonal and spatial variation. Dissolved oxygen (**Figure 7.8**), as a proxy for biological production was often supersaturated, with highest levels in the spring in the regions south of 54 °N, matching the low pCO_2 concentrations shown in **Figure 7.7**.

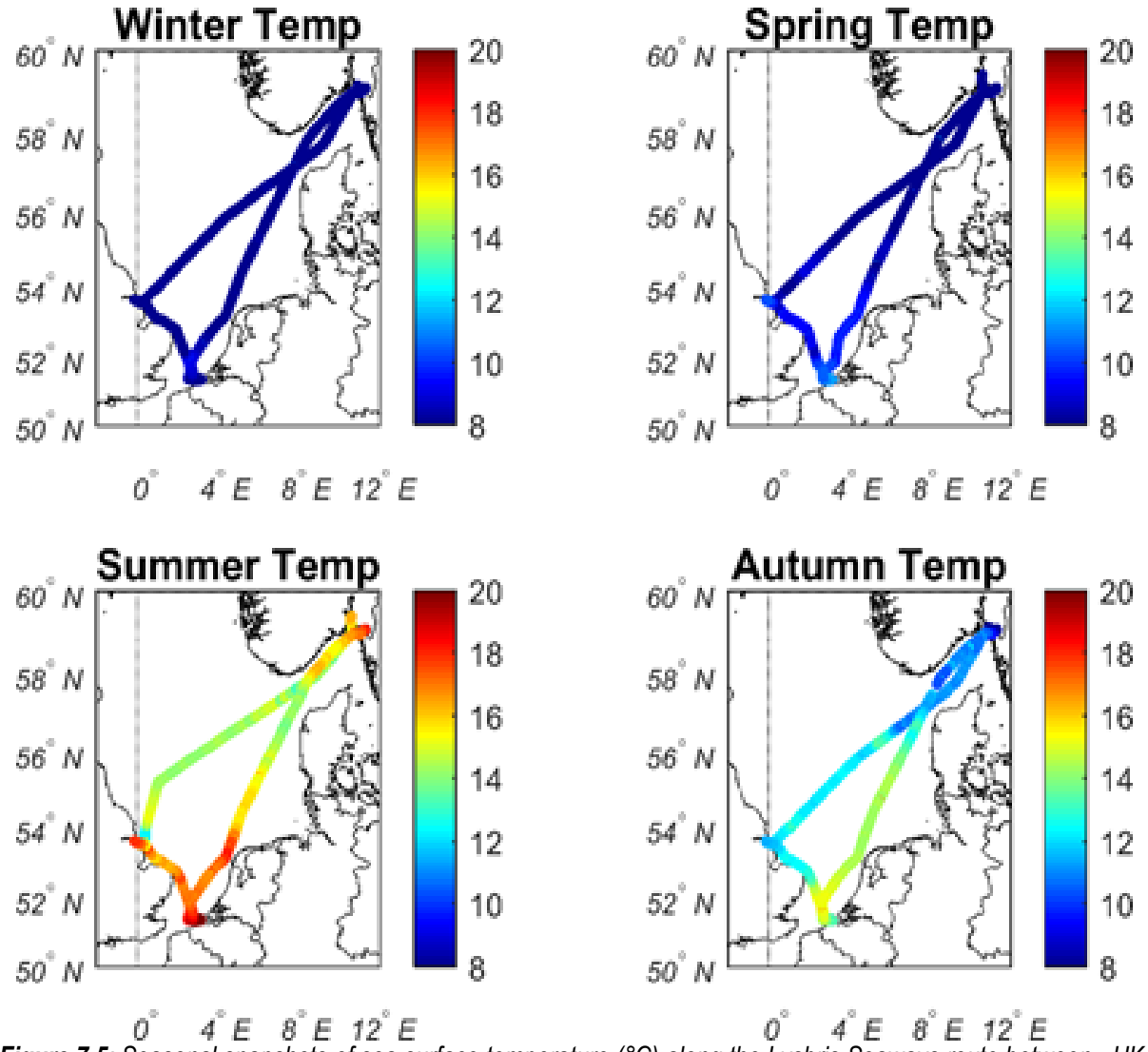

***Figure 7.5**: Seasonal snapshots of sea surface temperature (°C) along the Lysbris Seaways route between , UK, Norway and Belgium during the JRAP 5 intensive period (April 2017 - March 2018). The Greenwich meridian (0° E) is marked with a vertical line. Each panel shows a different time of year: winter (December 2017 - January 2018), spring (April 2017), summer (June-July 2017), and autumn (November 2017).*

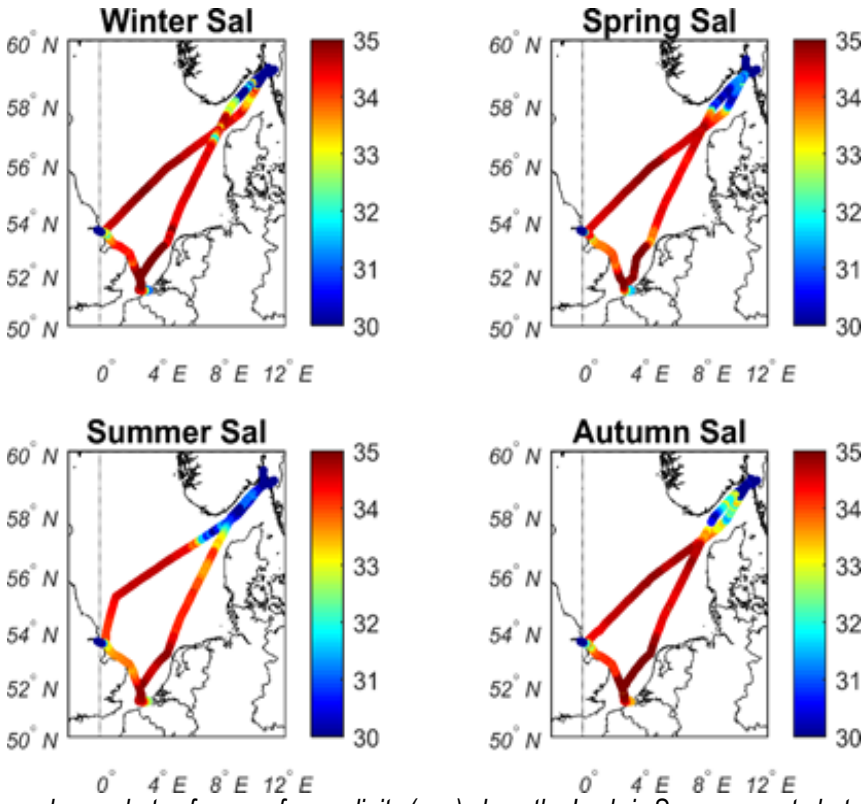

***Figure 7.6**: Seasonal snapshots of sea surface salinity (psu) along the Lysbris Seaways route between UK, Norway and Belgium during the JRAP#5 intensive period (April 2017 - March 2018). Time periods are described in **Figure 7.7**.*

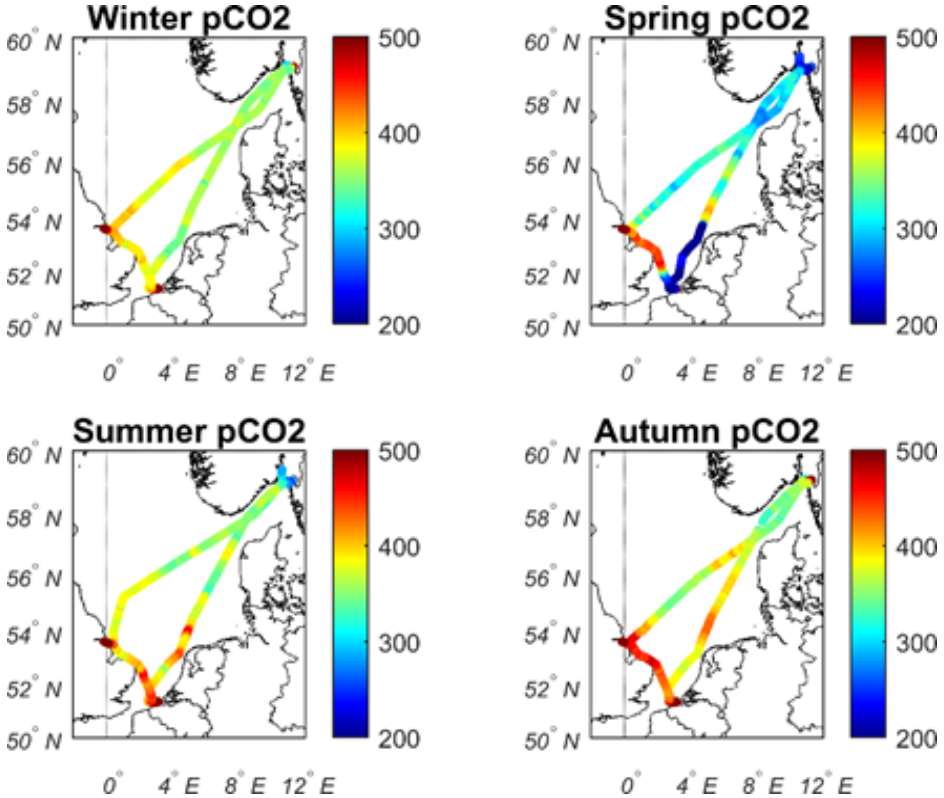

Figure 7.7**: Seasonal snapshots of sea surface pCO_2 (µatm) along the Lysbris Seaways route betweenUK, Norway and Belgium during the JRAP 5 intensive period (April 2017 - March 2018). Time-periods are described in **Figure 7.5.

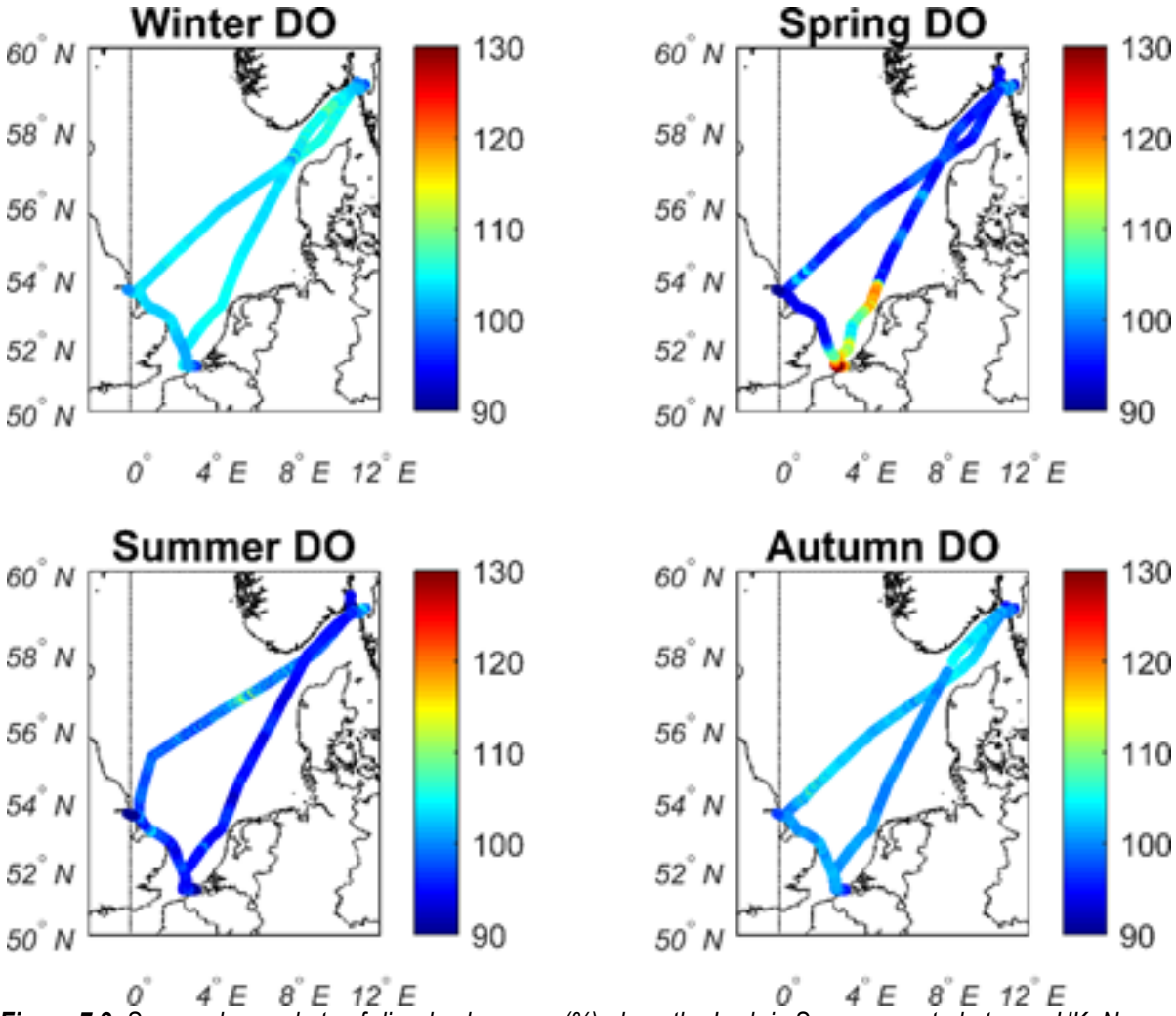

***Figure 7.8**: Seasonal snapshots of dissolved oxygen (%) along the Lysbris Seaways route between UK, Norway and Belgium during the JRAP 5 intensive period (April 2017 - March 2018). Time-periods are described in **Figure 7.5**.*

7.4.4. North Sea - Germany-England Route.

Another cargo vessel, the Hafnia Seaways, travelling between Cuxhaven, Germany and Immingham, UK, was similarly outfitted with a FerryBox and pCO_2 HydroC sensor. The ship moved to another route in 2018, but the 2017 records along this line are presented in a recent publication (Voynova et al. 2018) focused on total alkalinity measurements established in a flow-through setup in combination with the FerryBox. During the JRAP 5 intensive measurement period, the Hafnia Seaways travelled along the routes in **Figure 7.9**, and most often along the north route (light blue), or the south routes (gray and black combined). This allowed separating these two routes in **Figure 7.10**, where time series of a number of parameters is shown. For a detailed analysis of these data, we refer to Voynova et al. (2018). Briefly, the same range in pCO_2 is observed in **Figure 7.10** as in the Lysbris records (200-500 µatm), but surface waters along this route were supersaturated for much longer during the year. The time of intensive biological production was fairly short, taking place between April and July, but the biological signal was more prominent, showing up in the high DO and chlorophyll fluorescence, low pCO_2, and high pH. Interestingly, our observations were characterized by a significant seasonal increase in surface water total alkalinity, showing the importance of *in-situ* measurements of the carbonate system in coastal regions.

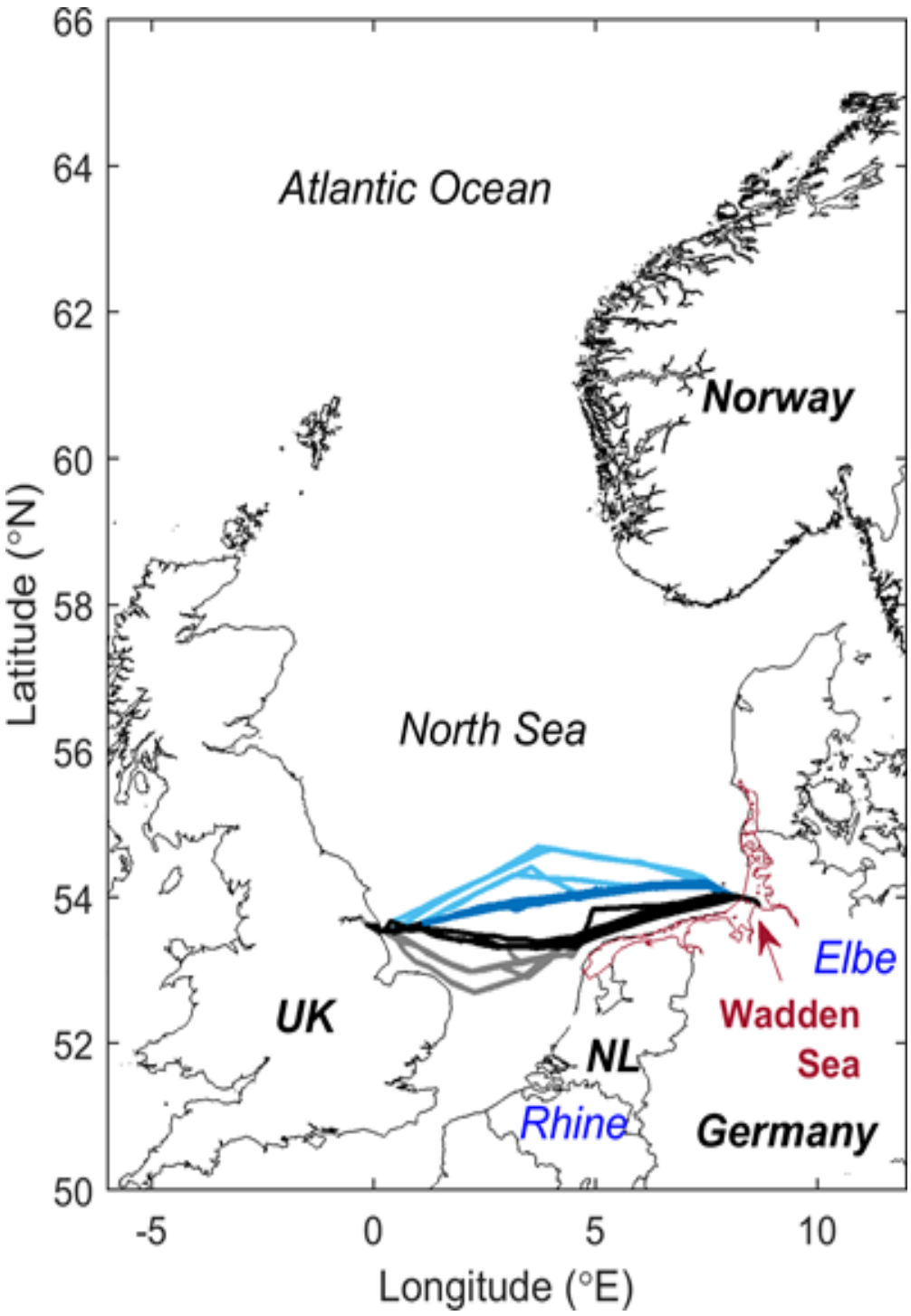

Figure 7.9: *Map of the North Sea, Wadden Sea (red line), and Hafnia seaways routes between Cuxhaven, DE and Immingham, UK during 2017.. Hafnia Seaways routes in 2017 (January 1 - October 31) are divided in north (light and dark blue) and south (black and gray) transects. Figure reproduced from Figure 1 by Voynova et al. (2018).*

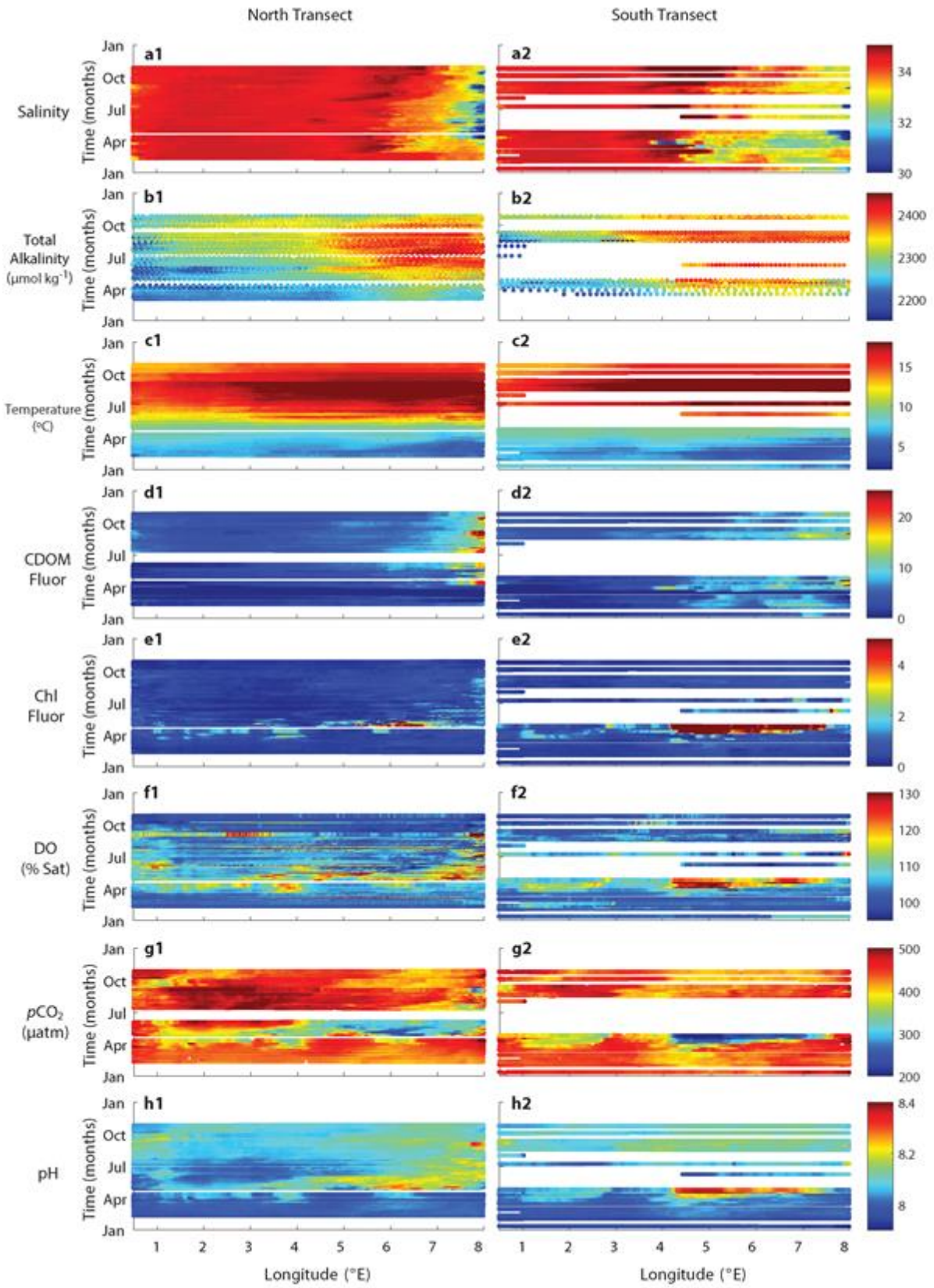

***Figure 7.10**: a. Salinity, b. TA (µmol kg^{-1}), c. temperature (°C), d. CDOM fluorescence (µg L^{-1}), e. Chl fluorescence (µg L^{-1}), f. DO (% saturation), g. (pCO_2 (µatm), h. pH measured along the North (marked with 1) and South (marked with 2) routes (Fig. 1) in 2017. Figure reproduced from Figure 4 by Voynova et al. (2018).*

7.4.5. North Sea - Oslo-Kiel.

Daily observations were made through the Skagerrak and Kattegat to the Kiel Bight between Oslo, Norway and Kiel, Germany from M/S Color Fantasy (**Figure 5.11**). Observations of pCO_2 during winter (October-December 2017 and in February 2018) indicated that pCO_2 varied between ~350-450 µatm. During this time, pCO_2 in the southern region was high (>400 µatm) possibly due to the Baltic Sea outflow and deep mixing. In March 2018, pCO_2 decreased very rapidly to <300 µatm with some values as low as ~175 µatm in the northern half of the transect. High pCO_2 was observed in March 2018, which coincided with elevated temperature and salinity which indicated an overturning event in the Oslofjord (~59.5-60 deg N).

The annual CO_2 air-sea exchange is dependent on mixed layer and water depth. Generally, deeper regions are all year-round CO_2 sinks whilst shallower regions allow for surface return of respired CO_2 (i.e. Emeis et al., 2015). The northern Skagerrak is a very strong summertime C sink with strong N-S gradients (Bozec et al., 2005). Observations in 2017 showed high chlorophyll throughout the study region between April and June with values >5 µg L^{-1} and up to ~20 µg L^{-1}. Another relatively intensive algae bloom was observed in September and October 2017. While no concomitant chlorophyll measurements are available for comparison with the 2018 pCO_2 measurements, the spring bloom in 2017 began in March/April. This timing coincides with the decline in pCO_2 during spring 2018.

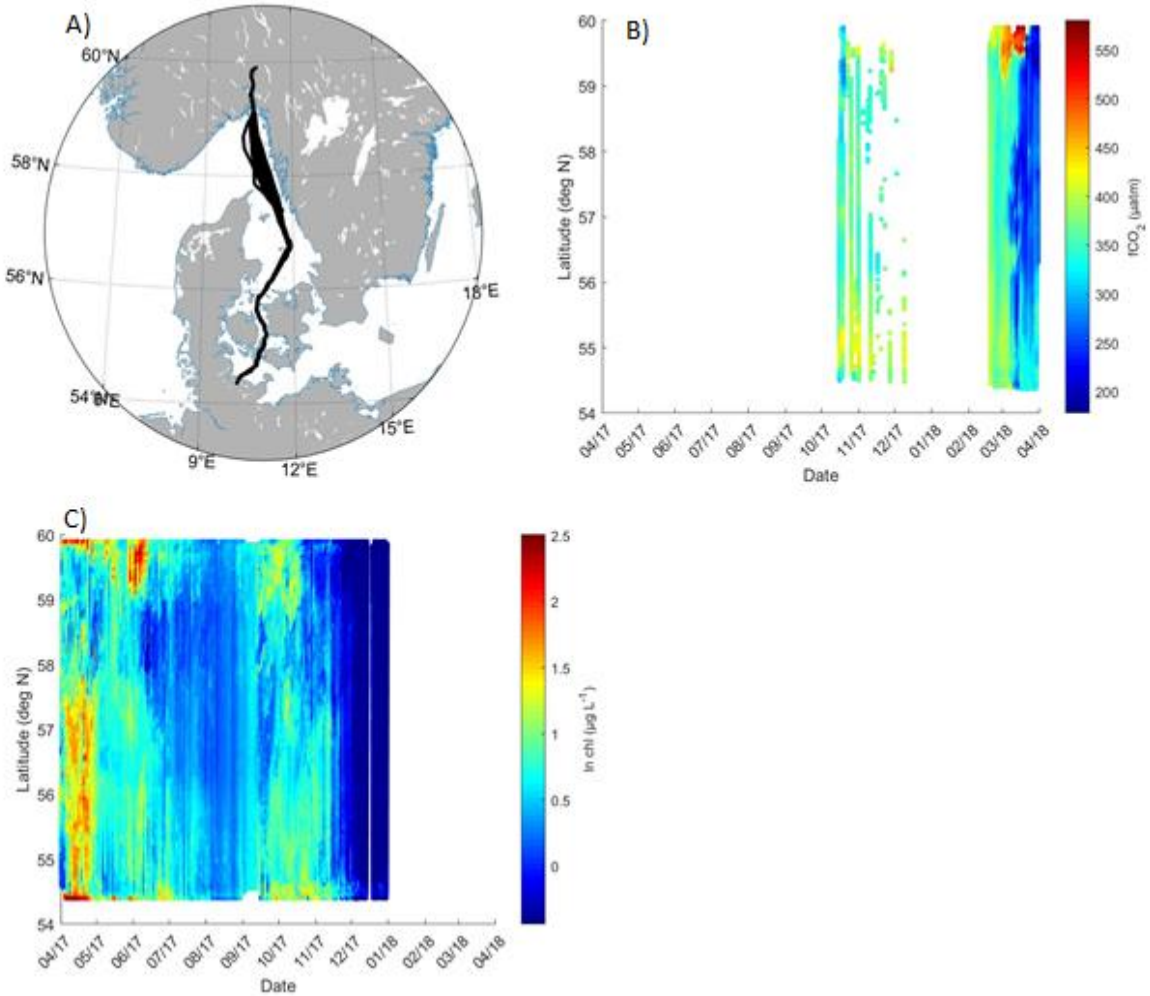

Figure 7.11: *A) Ship track of M/S Color Fantasy, B) pCO_2 (µatm), and C) chlorophyll a (µg L^{-1}) observations between April 2017-Mar 2018 from Oslo, Norway (~60 deg N) to Kiel, Germany (~54 deg N).*

7.4.6. ***The Baltic Sea - Utö Island.***

The carbonate system in the Baltic Sea is characterized by i) high inter-annual variations in pH and pCO_2 due to high biological activity, ii) relatively low total alkalinity (AT) due to low salinity, iii) recent increase in AT due to riverine loads, iv) large amounts of dissolved organic matter, and v) its mineralization to DIC. Climate change will influence all these characteristics and it is hard to predict forthcoming shifts in carbonate system. Aims of the study were to understand which two measured components of the carbonate system of the Baltic Sea are most reliably modelled and to identify how different factors (temperature, salinity, biology) influence the carbonate system.

Utö Island is located in the southern edge of the Archipelago Sea in the Baltic Sea. Observations at the Utö Atmospheric and Marine Research Station are described in Honkanen et al. (2018) and Laakso et al. (2018). Depth of the sampling station is 23 m and underwater pump provides continuous flow of sample water originating from the depth of 5 m. Seawater pHT (pH in total hydrogen scale) was measured at Utö continuously with an AFT-pH (Autonomous Flow-Thru) instrument (Sunburst Sensors) and pCO_2 was measured continuously with SuperCO2 instrument (Sunburst Sensors) equipped with two showerhead equilibration chambers. During intensive measuring campaigns, dissolved inorganic carbon (DIC) was measured from discrete water samples with DICAnalyzer AS-C3 (Apollo SciTech) and AT was determined from the same water samples with potentiometric titration (Metrohm Titrino 716). AT was calculated from the titration curve by Gran method (A_{Gran}) and ordinary least squares method using initial values from Gran method (A_{OLS}). CO_2 system calculations and modelling were performed with CO2calc software. More detailed description of the methods and results are given by Lehto (2019).

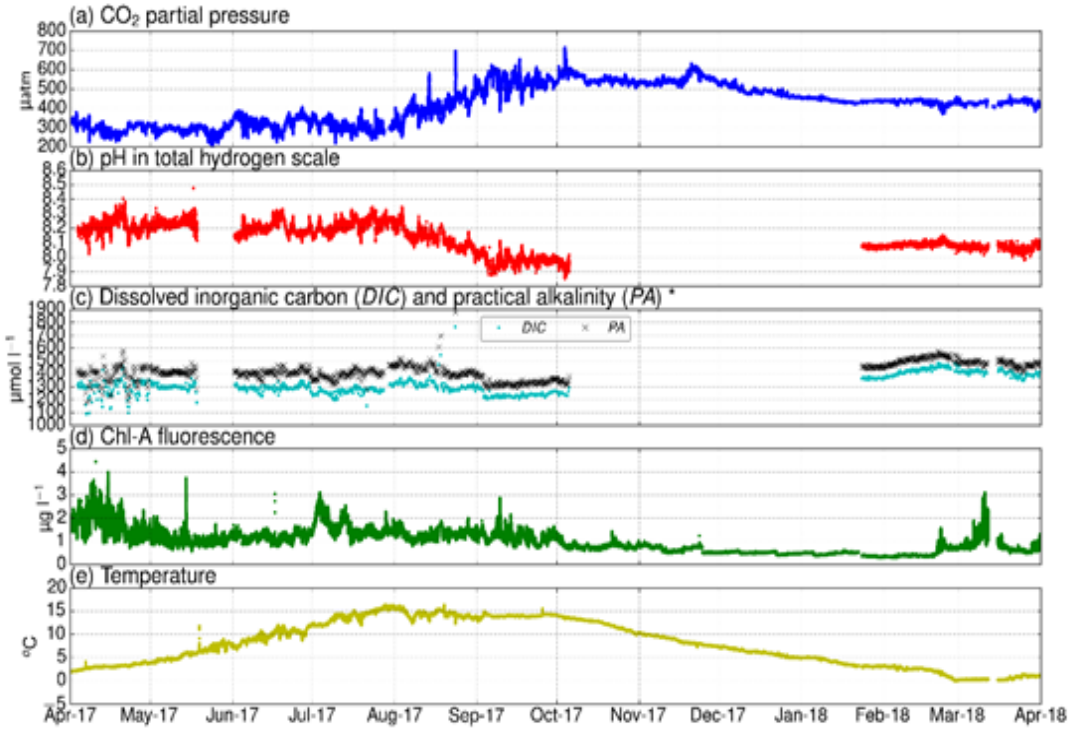

Figure 7.12*: Different flow-through measurements carried out at Utö Atmospheric and Marine Research Station during the intensive period. The sampling depth is approximately 5 m below the surface. DIC and PA are 6 h median values calculated from observed pCO_2 and pHT.*

The Baltic Sea spring bloom in 2017 was moderate as reflected in low carbon fixation: CO_2 partial pressure (pCO_2) never fell below 200 µatm (**Figure 7.12**). The lowest pCO_2 recorded was 205 µatm on 24th of May. The pHT measurement was offline during this time, when the maximum pHT was expected. On 21st of April, we

observed the pH maximum of 8.4. Chlorophyll *a* fluorescence was at a maximum in mid-April, after which it showed occasional peaks during the summer. During the spring bloom in April, the modelled DIC and practical alkalinity (PA) experienced high diurnal variability oscillating between 1000-1600 µmol L^{-1}, which might be generated by a strong vertical heterogeneity within the water column. Until August, pCO_2 of seawater stayed predominantly below atmospheric CO_2, in the range of 200-400 µatm (i.e. the sea was a sink of atmospheric CO_2).

In August, we observed pCO_2 increasing almost linearly from 300 to 500-600 µatm, where it stayed until December. At the same time, pHT decreased from approximately 8.2 to 8.0. The decrease in pHT is related to the increase in pCO_2 and to the decrease in concentration of carbonate ions. Whereas the modelled DIC stayed somewhat stable at 1300 µmol L^{-1} during August, PA decreased from approximately 1450 to 1400 µmol L^{-1}. In the case of the Northern Baltic Sea, the effect of calcium carbonate formation and dissolution on PA can be neglected due to the lack of calcifying organisms (Tyrrell et al., 2008). Thus, possible mechanisms behind the observations are mixing and biological processes. PA in the Baltic Sea is strongly related to salinity due to the geological characteristics of the drainage basins (e.g. Hjalmarsson et al., 2008). However, no significant salinity changes were observed that might indicate the effect of lateral transport. We observed a few upwelling events in autumn and early winter, when pCO_2 increased almost 200 µatm within a day. Concurrent decreases in temperature (approximately 1°C) support the conclusion of vertical mixing. During one of these events, on the 3rd of October, the pCO_2 maximum (714 µatm) and the pHT minimum (7.85) were observed. After December, pCO_2 of seawater approached slowly the pCO_2 of the atmosphere and was stable showing only small variation as biological activity had already diminished.

The interdependencies in the carbonate system variables were studied during four intensive campaigns at Utö, to complement the continuous observations of pCO_2 and pHT dynamics. During the measuring campaigns samples were taken 3 times a day at 7am, 1pm and 7pm local time. The campaign dates were: April 4th – 11th, May 4th – 11th, June 28th – July 5th and August 4th – 10th in 2017. In our measurement campaigns A_{Gran} was at highest 1630 µmol kg^{-1} in May and it declined towards the end of summer being 1520 µmol kg^{-1} at lowest. Measured A_{OLS} values were 1610 and 1490 µmol kg^{-1} respectively (**Figure 7.13**). Changes in alkalinity or salinity both are related to changes in water bodies and mixing or evaporation and precipitation. Therefore, AT and salinity usually have a linear relationship regionally (**Figure 7.14**). The trend in our DIC measurements was also descending during the summer. AT and DIC have the same main components, bicarbonate (HCO_3^-) and carbonate (CO_3^{2-}). Therefore, concentrations of DIC and AT are usually correlated and in our measurements DIC did follow the changes in alkalinity. In May DIC concentration reached 1560 µmol kg^{-1} and in August the concentration was 1455 µmol kg^{-1}. During measurement campaigns the minimum of pCO_2 was 264 ppm. Seawater pCO_2 was below atmospheric CO_2 level (390–420 ppm) during the summer until the mid-August (**Figures 7.12 and 7.13**). In other words, the seawater ecosystem is net autotrophic until the end of summer. Seawater pHT varies between 8.0 and 8.3 during the campaigns. Seawater pHT and pCO_2 show clear inverse correlation as expected (R=-0.941, p<0.001) (**Figure 7.14**).

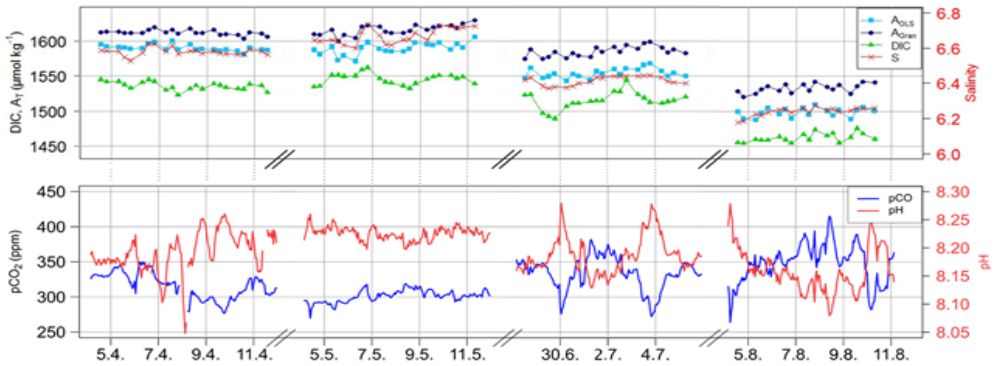

***Figure 7.13**: Inorganic Carbon System in Utö during four measurement campaigns in 2017. Gran method (blue diamonds) and ordinary least square -method (light blue squares) of alkalinity, dissolved inorganic carbon (green*

triangles) and salinity (red x-marks) are shown in the upper diagram. Down are pH (red) and pCO_2 (blue). Note the scales for salinity and pH in the right side.

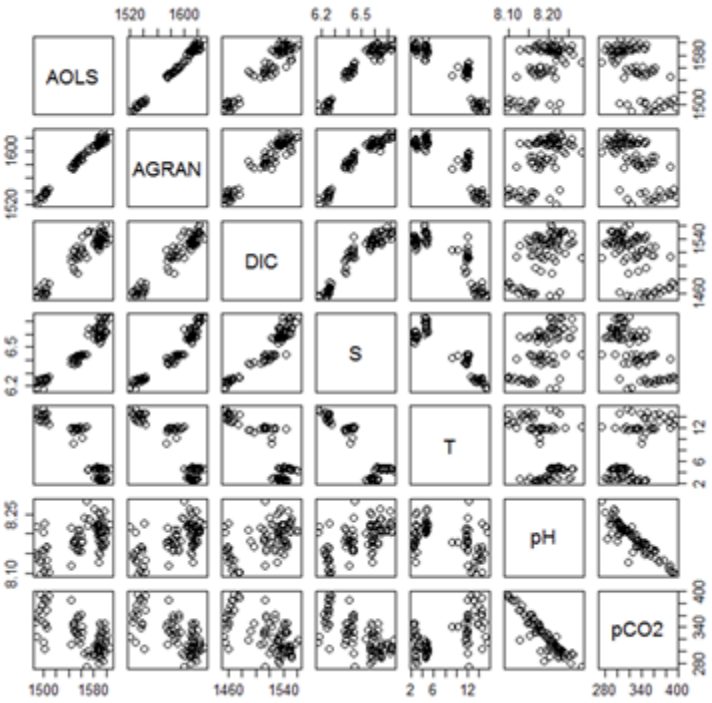

Figure 7.14: *Diagrams of correlations between different components of the inorganic carbon system.*

AT, DIC, pHT and pCO_2 were all modelled with all the combinations of two other measurable components of carbonate system (detailed results available in Lehto 2019). Modelling carbonate system with CO_2calc software (Robbins et al., 2010) gave better results when modelling was performed with one of the pair AT and DIC combined with pHT or pCO_2. Choice for dissociation constants of carbonic acid (K_1 and K_2) has a great influence on the results, whereas other options like KSO4 and total boron calculation method have an effect of under 0.02%. The effect of K_1 and K_2 on the results is largest when the seawater salinity is low like in Baltic Sea and may be several percentage points. The best modelling results for AT were obtained with DIC and pHT measurements. DIC modelling by A_{OLS} and pH fits best the measurement results. When AT or DIC was modelled using pHT and pCO_2 the results were much too large. Modelling of pHT and pCO_2 with discrete measurements AT and DIC resulted in large RMSE and bias. Results for pHT and pCO_2 were better when modelling input contains one of these. However, modelling results for pHT and pCO_2 were systematically too low compared to measured values. AT in CO_2calc model is simplified and does not contain all the possible components of the alkalinity. Dissolved organic matter (DOM) is ignored in the calculations. Due to low content of DOM in oceans it is reasonable to disregard its effect on alkalinity. By contrast, the Baltic Sea is DOM-rich basin, and organic compounds are a significant part of AT (Kuliński et al., 2014). Borates are an important component of the AT and it has been considered in the calculations of CO2calc. The problem with borates in the Baltic Sea is that the relationship between total boron concentration and salinity is not similar to that of the open ocean. CO_2calc modelling results for the Baltic Sea need to be used with caution. To get the most accurate picture of the inorganic carbon system in the Baltic Sea, it would be best to measure all the four measurable components of the system. The Baltic Sea has a large catchment area with DOM-rich river runoffs and problems with eutrophication. Added with hydrographical features and large temporal and spatial changes in circumstances, Baltic Sea is difficult to model. If it is not possible to measure all the components, modelling should be performed with AT or DIC and pHT or pCO_2 values. Model could be improved for the Baltic Sea conditions by taking account alkalinity components important in the Baltic Sea. Rivers transport a lot of organic matter to the Baltic Sea and therefore, organic component of alkalinity should be taken into account with

calculations. Also, borates cannot be estimated as reliably as in the oceans based on salinity. Improving and testing the model calls for measurements from all the components of the inorganic carbon system and from all the seasons.

7.4.7. The Baltic Sea - Baltic Proper and the Gulf of Bothnia.

In JRAP 5, SMHI observed pCO_2 on a cargo vessel M/S Tavastland traveling weekly between Lubeck, Germany, and Oulu in the north of Finland (**Figure 7.15**). The pCO_2 system from General Oceanic's was installed in 2010 and only fully operational in October 2017. The vessel Tavastland changed route between September and late November 2017 and traveled instead Gothenburg – Zeebrugge, but was back to the route in Baltic Sea in early December. During winter 2017, the FerryBox GPS broke down and generated problems with the salinity and temperature measurements, which are necessary for the calculation of pCO_2. The dataset presented covers from December to end of August 2018, and shows the effects of the large algal bloom (leading to exceptionally low summertime pCO_2 values) that occurred in the Baltic Proper during early summer months (**Figure 7.16**).

Figure 7.15: Example of weekly measurements of pCO_2 (µatm) on M/S Tavastland June 2018.

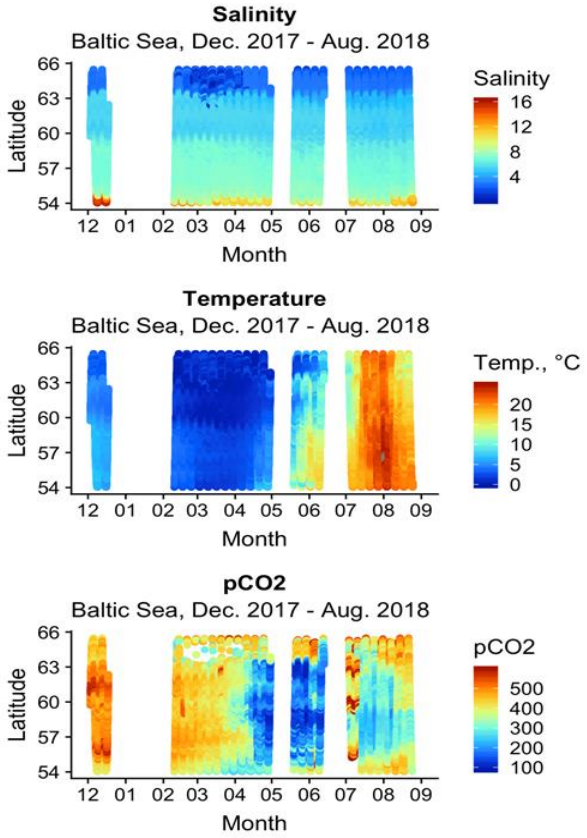

***Figure 7.16**: Salinity (psu), temperature (°C) and pCO_2 (µatm), during the period mid-May until end of August 2018.*

7.4.8. Mediterranean Sea - The Gulf of Trieste.

The Gulf of Trieste is a shallow bay (< 25 m) lying in the northernmost part of the Adriatic Sea. Meteorological conditions exhibit a pronounced seasonal cycle, which determines strong variations in seawater temperature, salinity and water column stratification during the year (Malačič and Petelin, 2001), **Figure 7.17**. During winter, the low biological activity and the low temperatures accompanied with the outbreak of strong northern winds led to a decrease in pCO_2 values and the Gulf was identified as a strong CO_2 sink with average fluxes of about -11 mmol $m^{-2}d^{-1}$ during wind events (Cantoni et. al, 2012). In summer, the high temperatures decrease CO_2 solubility leading to an increase of pCO_2 values that are scarcely balanced by photosynthetic CO_2 fixation at surface. In the lower water column, organic matter remineralization prevails and, under stable oceanographic conditions, with a strong water column stratification, it can lead to pCO_2 values as high as 1043 µatm (as recorded in Aug. 2008, Cantoni et. al, 2012). Spring and autumn are characterized by very variable conditions, strongly linked also to the spreading of riverine waters, enriched in nutrients and often also in CO_2. The presence of low salinity waters can be linked to a pCO_2 increase, due to direct riverine inputs but also to a strong pCO_2 decrease when the fertilizing effect prevails and riverine nutrients trigger intense phytoplankton blooms. However, these previous studies were based on the acquisition of discrete samples and, even if they allowed a general characterization of the area and the identification of the main drivers, they overlooked short term events.

pCO_2 (µatm) on discrete samples was calculated from pH and TA using the CO_2 speciation program CO2SYS (Pierrot et al., 2006). The offset (averaged residuals between continuous pCO_2 samples and discrete samples) was 3.33 µatm with a standard error of 1.48 µatm (n = 11). Continuous *in-situ* oxygen measurements were compared with discrete samples: the offset was -4.68 µmol L^{-1} with a standard error of 0.94 µmol L^{-1} (n = 10). The results fulfilled the ICOS requirements for a FOS (Fixed Observing Station) and PALOMA was admitted to the ICOS marine network in November 2018. Considering 400 µatm as average atmospheric concentration, the offshore area of the N. Adriatic was an atmospheric CO_2 sink from January 2017 to the end of July and from mid-November to the

beginning of April 2018. During August 2017 the area acted as a CO_2 source while in Autumn (from 15/09 to 07/11) values were mostly in equilibrium with the atmosphere (**Figure 5. 17**).

The wintry season (from 01/01 to 27/03) was characterized by low biological activity, as evidenced by the oxygen saturation mostly in equilibrium with the atmosphere (100 % ± 5 %) and the low chlorophyll values (down to 0.23 µg L^{-1}). Under these conditions, the low seawater temperature (between 10.5°C and 7.5°C) can be considered as the main driver of the low pCO_2 (down to 300 µatm) observed. In late spring –early summer (from 11/05 to 08/06) pCO_2 remained below 350 reaching the lowest annual values (283.7 µatm), even if seawater temperatures ranged between 16.4 °C and 25.2 °C. Oxygen oversaturation (up to 130 %) and higher chlorophyll concentrations (up to 1.12 µg L^{-1}) indicated the onset of intense phytoplankton blooms triggered by riverine nutrient loads (salinity down to 31 psu, NO_3 4.03 µM). Under these conditions, biological CO_2 fixation had a major role in keeping pCO_2 values low. Throughout summer (from 30/07 to 20/08) riverine nutrient loads decreased (NO_3 0.47 µM) and the slight oxygen oversaturation (100% < DO < 110%) coupled to low chlorophyll concentrations (0.51 µg L^{-1}, August 2017) indicated the lack of intense phytoplankton blooms able to strongly decrease CO_2 concentrations. Seawater temperature increased furtherly (up to 28.6 °C), leading to higher pCO_2 values that remained above 400 µatm for the whole period, reaching values as high as 471 µatm at the end of the month. During fall it is interesting to note two events on a very short time scale that were never observed with traditional sampling. On the 18/09 a decrease in salinity, coupled with an increase of oxygen saturation and decrease of CO_2 indicated the onset of a phytoplankton bloom, triggered by riverine nutrient supply. It was followed by a fast and sharp pCO_2 decline (29/09), coupled with oxygen undersaturation suggesting the break out of the summer stratification with the complete mixing of the water column and the outcropping of low oxygen bottom waters. The same dynamics, with a weaker signal, was observed the following month, between 19/10 and 22/10.

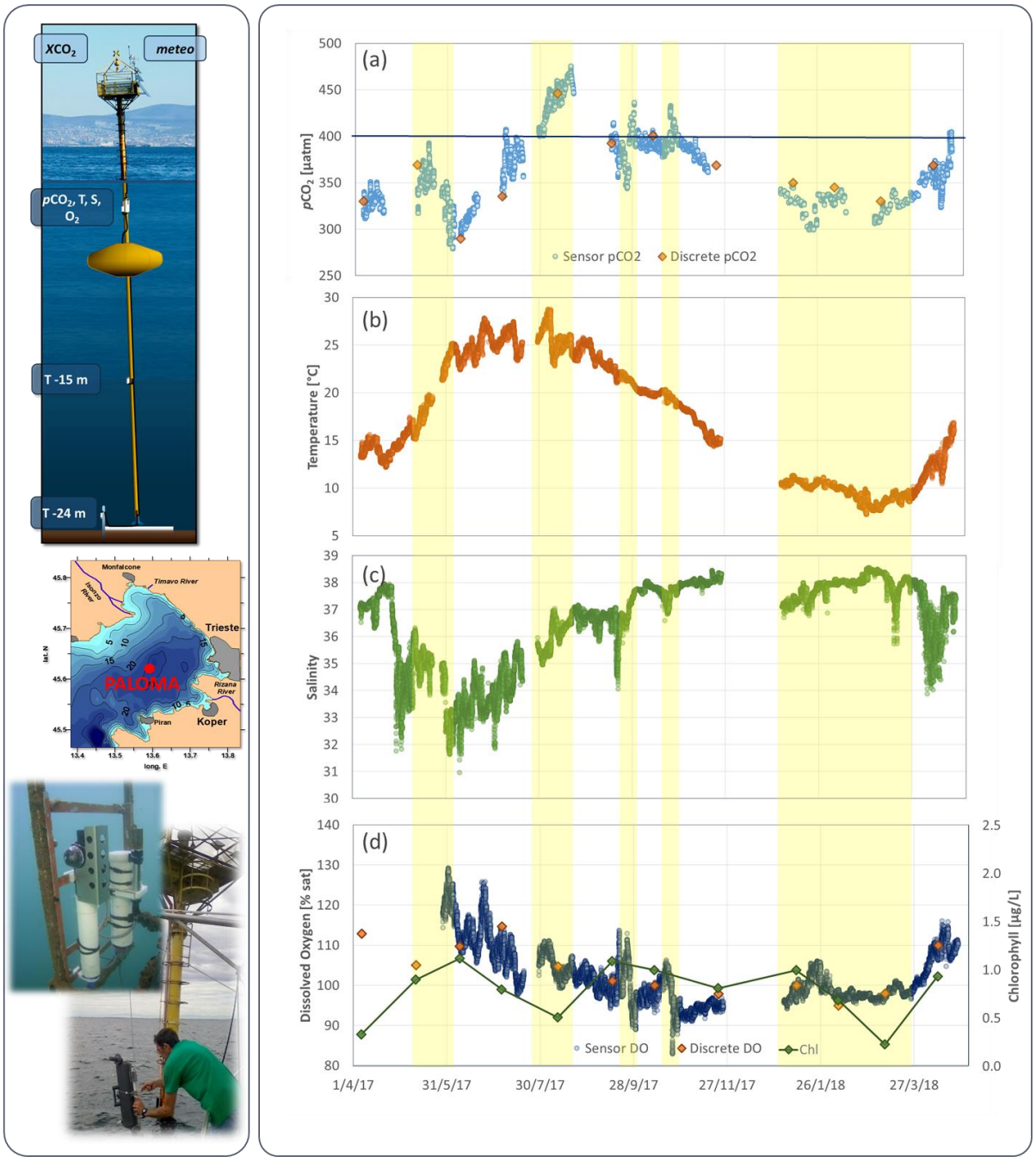

***Figure 7.17**: Data acquired at 3m avg. depth during JRAP 5 high intensity measurement activity. (a) CO_2 partial pressure (pCO_2), squares are values calculated from discrete pH and total alkalinity samples, (b) Temperature, (c) Salinity, as PSU, (d) Dissolved oxygen as % sat, squares are values calculated from discrete DO samples and Chlorophyll concentration (from fluorescence, yearly calibrated). Events discussed in the text are highlighted in yellow.*

7.5. Main inputs relative to initial specific objectives

JRAP 5 addressed three specific questions:

7.5.1. Q1: What kind of role European Coastal Ocean and Marginal Seas have on the marine carbon system?

This objective was achieved by obtaining new data and increasing understanding on pCO_2 on coastal and marginal seas. The results show high variability and regional differences. Depending on the site, results indicated the role of coastal seas as source or sink of carbon, and the respective seasonal shifts in all studied sites. It is not trustworthy to upscale our observations to get overall quantitative estimates for European coastal seas and our findings merely serve as an indicator of regional and seasonal differences. However, the results obtained may be used in the first iteration of such estimates, identifying also the gaps in observations.

7.5.2. Q2: What is the role of biological activity on marine carbon uptake or release?

There were several fixed stations and VOS routes, where pCO_2 and chlorophyll were measured simultaneously, allowing analyses of biological carbon sink on sea surface carbon balance. Based on these combined observations, biological activity was shown to have a significant role on the marine carbon balance.

7.5.3. Q3: How should the integrated C-cycle monitoring be organized in coastal regions?

An integral part of JRAP 5 was to gather information on different carbonate system instruments operated by the partners in this study, to compare different instruments in different European coastal and marginal sea conditions and create preliminary data QA/QC instructions suitable for biologically active sea areas, in line with ICOS-OTC and SOCAT requirements. The study shows the need for better coordination between coastal carbonate system observations, with frequent instrument comparisons.

7.6. Analysis of the experience gained

7.6.1. Developing innovative technologies for coastal ocean observing and modelling.

The aim of JRAP 5 was not to develop new technology, but to utilize the existing carbonate system instrumentation and evaluate their joint deployment in European coastal seas. New instruments developed in task 3.5 of WP3 were employed in VOS observations in the North Sea region. The evaluation of equipment was done through a TNA activity INTERCARBO, which was organized in Oslo in November 2018. In the INTERCARBO WS, a number of JRAP 5 partners, together with ICOS-OTC scientists and metrologists evaluated the performance and comparability of several pCO_2, pH and total alkalinity instruments in different temperature, salinity and pCO_2 conditions. The results were discussed also with instrument manufacturers and currently, a joint publication on the results is in preparation. The results show a need for regular instrument intercomparison experiments and need for continuous cooperation with instrument manufacturers.

7.6.2. Establishing observing objectives, strategy and implementation at the regional level.

On several JRAP 5 measurement sites, observed variables covered both carbonate system and basic biological variables, allowing studies of marine ecosystem carbon uptake. As the marine carbon sequestration is a function of temperature, light, available nutrients, dynamical processes like mixing, species composition and other variables, multiparameter observations of physical, chemical and biological variables are mandatory. The results support the development of multidisciplinary observing platforms with wide range of simultaneous, automated observations. If a harmonized network like this is to be built, special attention needs to be on high variability of environmental conditions and regional characteristics (**Table 7.3).**

Table 7.3: *Regional summary of observations carried out in JRAP 5. The lowest pCO_2-concentrations were found to be linked with biological activity on all regions. The ranges given above describe the observations during the intensive period only, at certain sites much higher and lower values have been recorded.*

Areas	T (C°)	S (psu)	pCO_2 (uatm)	pH	Spring	Summer	Autumn	Winter	Comments
Norwegian Sea (region)	0...18	6…34	100… 490	8.2… 8.0	Sink	Source	-	Source	Variation on open ocean relatively small compared to coastal areas
North Sea (region)	4…20	9…34	175… 500	8.5… 7.8	Sink	Sink	-	Source	Deep areas sink year round
Baltic Sea (region)	0... 25	0…20	100… 700	8.4… 7.9	Sink	Sink	Source	Source	Low salinity challenge in pH measurements
Mediterranean Sea (point)	7…29	31…38	280… 470	8.2… 8.1	Sink	Source	•	Sink	River impact significant

7.6.3. Enhancing integrated coastal ocean monitoring and interfacing with other ocean observing initiatives operating at different spatiotemporal scales.

JRAP 5 partners are linked with a large number of projects and initiatives, which partly supported our activities. For data-analysis and metadata, we utilized the published material and protocols developed by SOCAT and ICOS-OTC to study best practises in carbonate system measurements.The link with ICOS-OTC was especially close as the INTERCARBO TNA was partly organized together with ICOS-OTC members and some of the JRAP 5 observing sites (like Gulf of Trieste since November 2018) are part of ICOS-OTC network and already submit their data to ICOS. The preliminary results from the INTERCARBO TNA related to JRAP 5 were introduced to ICOS-OTC community in ICOS-OTC Monitoring Station Assembly in Southampton, UK, in March 2019. The experiences from JRAP 5 and INTERCARBO will be utilized to help ICOS-OTC to develop their instrument intercomparison test facility. Additionally, FMI and SYKE agreed to include M/S Silja Serenade VOS route between Helsinki and Stockholm to ICOS-OTC network in 2020, NIVA has also agreed through a pending proposal to include M/S Trollfjord to the ICOS-OTC network in 2020, and SMHI is in dialogue with ICOS-OTC. The ICOS-OTC community was actively involved in the 9th FerryBox workshop which took place in Genoa, Italy in April 2019. The aim is to have a closer cooperation with the ICOS-OTC community, and to exchange experiences and data between ICOS-OTC and the Euorpean FerryBox community.

In Finland and Sweden, FMI and SMHI are part of regional carbon monitoring project Bonus-Integral where the aim is to develop coordinated Baltic Sea pCO_2 monitoring network, in line with ICOS-OTC and JERICO coastal

network. FMI and SYKE also work at Utö Atmospheric and Marine Research Station closely together with ICOS-ATM, ACTRIS, HELCOM, BOOS, Finnish National Marine Research Infrastructure FINMARI and other relevant initiatives and projects.

In Norway, NIVA has a new project called Norwegian Ships of Opportunity Program for marine and atmospheric research funded by the Research Council of Norway. They will develop new carbonate system sensors on FerryBoxes. They have also a project with the Norwegian Environmental Agency where they take quarterly cruises on Oslo-Kiel and Tromsø-Svalbard FerryBoxes and collect ~15 discrete samples for carbonate chemistry measurements (total dissolved inorganic C, total alkalinity, and pH_T). pCO_2 and pH sensors are also currently being developed through this project. NIVA has recently completed an observational OA campaign in two Norwegian fjords under the Research Council of Norway ACIDCOAST project.

In Germany, HZG is working with correcting and ground-truthing the Immingham-Zeenruegge-Moss pCO_2 dataset, with and aim to submit the data set to the SOCAT database when the QC is completed.

Overall, the results of JRAP 5 emphasis the added-value of close cooperation with other research infrastructures and relevant long-term projects.

7.7. Propositions for a future monitoring strategy for the topic

JRAP 5 clearly showed the need for harmonized observing methods, frequent instrument intercomparisons, joint data-analysis methods and coordinated metadata content. This is needed for all carbonate system and biological variables. It is evident that the process takes a long time, especially since complicated biological observations are needed to understand the highly variable coastal marine carbonate system.

One clear challenge is the high variability of instruments used by partners. There are three main reasons for this:

- The installation platform characteristics often require a specific setup due to e.g. available space or other technical reasons;
- Available funding does not allow for building a new setup
- The responsible institute has several similar instruments and a set of spare parts, so adding new systems requires significant additional resources for maintenance and service, in addition to the instrumentation budgets.

It may not be realistic to require standard instrumentation, but only make sure the observations are comparable and meet the requirements (a decision made in e.g. ICOS-OTC). Based on JRAP 5 experiences and due to the high variability in the type of instruments and instrument setups used, there is a need for:

- Regular instrument intercomparisons (like INTERCARBO-TNA).
- Regular field data comparison on e.g. cross-platform comparisons such as crossing FB lines or FB lines crossing near stationary platforms
- Development of instruments together with manufacturers and/or post-processing, which can take into account different T, S, and pCO_2 conditions

7.8. References

Bozec Y., H. Thomas, K. Elkalay and H.J.W. de Baar (2005) The continental shelf pump for CO_2 in the North Sea-evidence from summer observation. Marine Chemistry, 93, 131-147.

Cantoni, C., Luchetta, A., Celio, M., Cozzi, S., Raicich, F., Catalano, G. (2012) Carbonate system variability in the Gulf of Trieste (North Adriatic Sea). Estuar. Coast. Shelf Sci. 115, 51–62. http://dx.doi.org/10.1016/j.ecss.2012.07.006

Emeis, K. C. , van Beusekom, J. , Callies, U. , Ebinghaus, R. , Kannen, A. , Kraus, G. , Kröncke, I. , Lenhart, H. , Lorkowski, I. , Matthias, V. , Möllmann, C. , Pätsch, J. , Scharfe, M., Thomas, H. , Weisse, R. and Zorita, E. (2015) The North Sea — A shelf sea in the Anthropocene. Journal of Marine Systems 141:18–33, doi: 10.1016/j.jmarsys.2014.03.012

Hjalmarsson, S., Wesslander, K., Anderson, L. G., Omstedt, A., Perttilä, M. and Mintrop, L. (2008) Distribution, long-term development and mass balance calculation of total alkalinity in the Baltic Sea. Continental Shelf Research, 28. 593-601. 10.1016/j.csr.2007.11.010

Holt, J., and R. Proctor (2008) The seasonal circulation and volume transport on the northwest European continental shelf: A fine-resolution model study. Journal of Geophysical Research 113: 1-20

Honkanen, M., Tuovinen, J.-P., Laurila, T., Mäkelä, T., Hatakka, J., Kielosto, S., and Laakso, L. (2018) Measuring turbulent CO_2 fluxes with a closed-path gas analyzer in a marine environment, Atmos. Meas. Tech., 11, 5335-5350, https://doi.org/10.5194/amt-11-5335-2018

Kaltin, S. L.G. Anderson, K. Olsson, A. Fransson, M. Chierici (2002) Uptake of atmospheric carbon dioxide in the Barents Sea J. Mar. Syst., 38, pp. 31-45

Kuliński K, Schneider B, Hammer K, Machulik U, Schulz-Bull D (2014) The influence of dissolved organic matter on the acid-base system of the Baltic Sea. Journal of Marine Systems 132, 106–115

Laakso, L., Mikkonen, S., Drebs, A., Karjalainen, A., Pirinen, P., and Alenius, P. (2018) 100 years of atmospheric and marine observations at the Finnish Utö Island in the Baltic Sea, Ocean Sci., 14, 617-632, https://doi.org/10.5194/os-14-617-2018

Lauvset S.K., M. Chierici, F. Counillon, A.M. Omar, G. Nondal, T.Johannessen, A. Olsen (2013) Annual and seasonal fCO_2 and air–sea CO_2 fluxes in the Barents Sea J. Mar. Syst., 113–114, pp. 62-74

Lehto, A-M., Modelling inorganic carbon system in Utö Baltic Sea (2019) MSc Thesis. University of Helsinki. http://urn.fi/URN:NBN:fi:hulib-201905131931

Malaćić, V., Petelin, B., Regional studies: gulf of Trieste. In: Cushman- Roisin, B., Ga_ci_c, M., Poulain, P.-M., Artegiani, A. (Eds.) (2001) Physical Oceanography of the Adriatic Sea: Past, Present and Future. Kluwer Academic Publishers, Dordrecht, pp. 167e181

Muller-Karger, F. E., R. Varela, R. Thunell, R. Luerssen, C. Hu and J. J. Walsh (2005) The importance of continental margins in the global carbon cycle, Geophysical Research Letters 32

Otto, L., J. T. E. Zimmerman, G. K. Furnes, M. Mork, R. Saetre, and G. A. Becker (1990) Review of the physical oceanography of the North Sea. Netherlands Journal of Sea Research 26: 161-238

Pauly, D., Christensen, V. (1995) Primary production required to sustain global fisheries, Nature,
374(6519): 255-257

Pierrot, D., Lewis, E., and Wallace, D. W. R. (2006) MS Excel Program Developed for CO_2 System Calculations, Tech. rep., Carbon Dioxide Inf. Anal. Cent., Oak Ridge Natl. Lab., US DOE, OakRidge, Tenn.

Robbins L, Hansen M, Kleypas J, Meylan S. (2010) CO2calc: A User Friendly Carbon Calculator for Windows, Mac OS X and iOS (iPhone). U.S. Geological Survey Open-File Report 2010–1280 17

Tyrrell, T., Schneider, B., Charalampopoulou, A., and Riebesell, U. (2008) Coccolithophores and calcite saturation state in the Baltic and Black Seas, Biogeosciences, 5, 485-494, https://doi.org/10.5194/bg-5-485-2008

Voynova, Y. G., W. Petersen, M. Gehrung, S. Aßmann, and A. L. King (2019) Intertidal regions changing coastal alkalinity: the Wadden Sea-North Sea tidally-coupled bioreactor. Limnology and Oceanography, https://doi.org/10.1002/lno.11103

Wesslander, K. (2011) "The carbon dioxide system in the Baltic Sea surface waters". Doctoral thesis. University of Gothenburg

7.9. Abbreviations

ACTRIS: European Research Infrastructure for the observation of Aerosol, Clouds and Trace Gases
BOOS: Baltic Operational Oceanographic System
HELCOM: Helsinki Commission (The Baltic Marine Environment Protection Commission)
ICOS: Integrated Carbon Observing System
ICOS-OTC: Integrated Carbon Observing System – Ocean Thematic Center
pCO_2: Partical pressure of carbon dioxide in sea water (µatm)
SOCAT: The Surface Ocean CO_2 Atlas

8. Operational oceanography and coastal forecasting

Contributors
Baptiste Mourre, Jaime Hernández-Lasheras, Mélanie Juza, Emma Reyes, Eva Aguiar, Emma Heslop, Alejandro Orfila, Joaquín Tintoré, **SOCIB, Spain**
Joao Vitorino, **IH, Portugal**
Gerasimos Korres, Leonidas Perivoliotis, Evi Mpouma, Manolis Doumas, **HCMR, Greece**
Luis Ferrer, Anna Rubio, Julien Mader, **AZTI, Spain**
Stefania Ciliberti, Eric Jansen, Giovanni Coppini, **CMCC, Italy**
Annalisa Griffa, Maristella Berta, Michela Martinelli, Pierluigi Penna, Stefania Sparnocchia, **CNR, Italy**
Lauri Laakso, Jan-Victor Björkqvist, **FMI, Finland**
Henning Wedhe, **IMR, Norway**
Bengt Karlson, Lars Axell, Lars Aneborg, **SMHI, Sweden**

8.1. Topic and specific objectives

The coastal ocean is a particularly complex system due to the wide range of processes at play driven by multiple forcing factors and characterized by small spatio-temporal scales and non-linear interactions. From a physical point of view, it is a very dynamic area where the wind-driven circulation interacts with buoyancy and tidal currents, where energetic mesoscale and sub-mesoscale processes develop under the influence of both the surrounding open ocean conditions and the details of the coastal topography. This complex hydrodynamics significantly impacts biogeochemical processes, which leads to a highly variable primary production in the coastal and shelf environments.

Numerical models are essential elements of coastal operational oceanography systems as they help: (1) understanding the complexity of the observed coastal ocean processes; (2) representing the three-dimensional coastal oceanic conditions and forecast their evolution in time; (3) integrating observations and (4) evaluating the impact of observing systems. Operational regional models (hydrodynamic, waves, biogeochemical) have been settled in a number of European coastal observatories in support of local multiplatform observing infrastructures so as to better respond to society needs and help the implementation of the Marine Strategy Framework Directive (MSFD). In particular, realistic models provide a useful support to efficiently protect the European marine environment through the characterization of the alteration of hydrographical conditions, the analysis of the dispersion of contaminants and marine litter, or the prediction of harmful algal blooms (MSFD descriptors 5, 7, 8 and 10).

However, operational ocean modelling is still highly challenging when approaching the coastal zones due to the intrinsic variability of the coastal ocean and the limitations inherent to numerical modelling. While the internal model dynamics needs to properly represent a wide range of processes, air-sea fluxes, freshwater river fluxes, deep ocean interactions, and details of the coastline and bathymetry, which are all specified as external model forcing, are also critical to achieve realistic simulations.

Data assimilation is an additional key element in most of these systems, allowing us to optimally combine model and observations and improve the realism of simulations. Data-assimilative systems provide a framework to assess the impact of observations on the model performance. This is achieved through the so-called “Observing System Experiments” (OSEs) approach when considering real measurements, and through “Observing System Simulation Experiments” (OSSEs) when optimizing future sampling strategies.

The JERICO-RI network provides a unique opportunity to evaluate the operational oceanography and coastal forecasting capabilities in the European coastal ocean, to assess existing skills, gaps and needs, and to establish a roadmap for improvements both in terms of models and observations. In this context, JRAP 6 aimed to show the importance of JERICO-RI observations for the assessment and improvement of operational regional models implemented in the coastal ocean, through the implementation of coastal model evaluation studies, OSEs and OSSEs. More specifically, JRAP 6 addressed the following questions:

- **Q1:** How accurate are our ocean models in coastal areas?
- **Q2:** How could we improve these models?

- **Q3:** What is the impact of coastal observations on the model performance after data assimilation?
- **Q4:** What would be the impact of potentially future additional observations?

While JRAP 6 focused on the assessment of physical models (hydrodynamics and waves), its results have direct implications on ecosystems given the very strong influence of coastal hydrodynamics (surface circulation, surface mixing and vertical exchanges in particular) on biogeochemical processes.

8.2. Overall structuration and strategy

JRAP 6 was planned to successively address two main objectives: first the assessment and then the improvement of operational coastal forecasting systems used for harmful algae blooms prediction, oil spill applications, drifting of gelatinous organisms, eggs and larvae dispersion or maritime search-and-rescue operations.

As part of this approach, the first task of JRAP 6 was to demonstrate that existing multiplatform coastal ocean observing infrastructures allowed an improved evaluation of the realism of the present European coastal ocean forecasting systems, considering models without data assimilation. This evaluation would allow identifying the main gaps and needs of the present European coastal forecasting systems. In a second step, data assimilation was considered, allowing incorporating measurements into the model solution with the aim to improve model results and predictions. Observing Systems Experiments (OSEs) were then conducted to evaluate the contribution of the different existing observing systems (in particular HF radar, moorings, gliders and FerryBox) in terms of model results improvement.

Finally, using numerical models and data assimilation, Observing System Simulation Experiments (OSSEs) willbe performed in three different European coastal regions to evaluate the needs for improved coastal observing systems. OSSEs allow a quantitative estimation of the impact of potential observations on the performance of ocean prediction models. This subtask was planned to specifically investigate the contribution of HF radar in the coastal ocean, bringing recommendations for the design of future coastal observing systems aiming at improving the model prediction skills.

8.3. Achieved actions

8.3.1. Sampling

Eight European coastal areas were selected (**Figure 8.1**) because of key science and societal relevance and availability of integrated observing and forecasting systems. These areas are the Southeastern Bay of Biscay, the Western Iberian Margin (area of influence of the Nazare Canyon), the Baltic Sea, the Skagerrak-Kattegat Straits area, the Norwegian coast, the Ibiza Channel in the Balearic Sea, the Adriatic Sea and the Aegean Sea. Key coastal ocean processes are present in these regions, including water mass adjustments, upwellings, shelf slope exchanges, wind-driven circulation, fjords and river plumes. More specifically, these areas present a wide panel of governing dynamical processes:

- Meridional water masses exchanges, slope current and mesoscale processes in the Balearic Sea
- Upwelling, slope current and shelf circulation under the influence of a submarine canyon along the Atlantic Iberian Margin
- Wind-driven circulation, slope current and mesoscale variability in the South Bay of Biscay
- Mesoscale to small-scale variability in the Aegean Sea
- Buoyancy-driven circulation associated with the Norwegian Fjords
- Wind-driven circulation, mesoscale and river plumes in the Adriatic Sea
- Salinity fronts and coastal currents in the Skagerrak-Kattegat area
- Wave-induced turbulence n the Baltic Sea

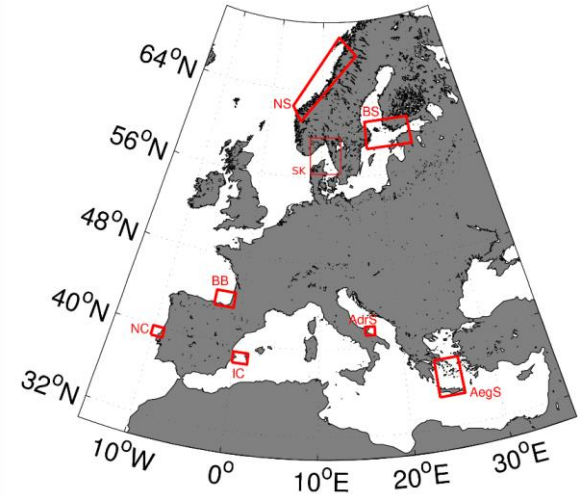

Figure 8.1: *Locations of the eight areas considered in JRAP 6. AegS: Aegean Sea; AdrS: Adriatic Sea (Gulf of Manfredonia); IC: Ibiza Channel; NC: Atlantic Iberian Margin (Nazare Canyon); BB: Southeastern Bay of Biscay; NS: Norwegian Sea; BS: Baltic Sea; SK: Skagerrak-Kattegat Straits.*

The models, data assimilation approaches and observations used in JRAP 6 are summarized in **Table 8.1**. Seven hydrodynamic models were used (Atlantic Iberian margin, South-East Bay of Biscay, Balearic Sea, Adriatic-Ionian basin, Aegean Sea, Skagerrak-Kattegat area and Norwegian coast) as well as two wave models (Baltic Sea and Atlantic Iberian margin). JERICO-NEXT multiplatform observations from fixed buoys, Ferryboxes, HF radar, underwater gliders, surface drifters and coastal research vessel CTDs were used.

Table 8.1: *Summary of the models, data assimilation approaches and components of the observing systems used in the different geographical areas covered by JRAP 6*

Partner	Study area	JERICO-NEXT observations used for model assessment / data assimilation	Other observations	Model (resolution)	Data assimilation approach
SOCIB	Ibiza Channel	Fixed stations, HF radar, glider	Satellite SLA and SST, ARGO, surface drifters	ROMS (2km)	EnOI
IH	Atantic margin (Nazare Canyon)	Fixed stations, HF radar	Satellite SST, CTDs	HOPS (0.3km)	OI
CMCC-CNR	Adriatic Sea	HF radar	Fishery & Oceanography Observing System, satellite SLA and SST, ARGO, surface drifters	NEMO (2km) / SHYFEM (unstructured)	EnKF
HCMR	Aegean Sea	Glider, FerryBox	Satellite SLA and SST, ARGO	POM (3km)	SEEK filter
AZTI	Southeastern Bay of Biscay	Fixed stations, HF radar	--	ROMS (0.67km)	--
IMR	Norwegian Sea	Fixed stations, FerryBox	CTDs	ROMS (0.8km)	--
FMI	Baltic Sea	FerryBox	--	WAM(1.8km)	--
SMHI	Skagerrak-Kattegat area	HF radar	--	NEMO(3.7km)	4D EnVar

8.3.2. *Data analysis*

High-resolution hydrodynamic models without data assimilation were first assessed. JERICO-NEXT multiplatform observations from fixed buoys, Ferryboxes, HF radar, underwater gliders, surface drifters and coastal research vessel CTDs were used for this evaluation, also including Argo floats. The assessment was focused on aspects directly related to society needs and MSFD implementation, in particular the surface circulation and the physical processes involving vertical velocities with an impact on ecosystems. In addition, the capacity of a wave model to properly represent the surface vertical mixing and its potential effect on harmful algal blooms was assessed in the Baltic Sea.

Then, the results of operational data assimilative models were evaluated using JERICO-NEXT multiplatform observations in 4 different coastal zones, namely the Ibiza Channel, Adriatic Sea, Aegean Sea and Western Iberian Margin. Observing Systems Experiments (OSEs) were conducted to evaluate the contribution of different existing observing systems in terms of model results improvement. In particular, the impact of HF radar was evaluated in the Ibiza Channel and Southern Adriatic Seas, fixed moorings were considered in the Nazare Canyon area and the impact of gliders and FerryBox were assessed in the Southern Aegean Sea.

Finally, using numerical models and data assimilation, Observing System Simulation Experiments (OSSEs) were performed in two different European coastal regions to evaluate the needs for improved coastal observing systems. Data-assimilative experiments including/excluding specific observations were used to evaluate the impact that these observations have on the model performance. This is the essence of the Observing System Experiments (OSEs) approach, which were implemented in four different areas to assess the impact of HF radar, glider, fixed platforms, FerryBox and Fishery Observing System measurements. This work led to a robust OSSE infrastructure in the Central Mediterranean sea and investigated the contribution of potentially new HF radar data in the Ibiza Channel coastal region.

8.4. Main results

The results are presented in three parts. The first part focuses on the use of coastal measurements to assess the skill of the numerical models used to simulate and forecast the evolution of ocean conditions. The second and third parts then present the results of Observing System Experiments (OSEs) and Observing System Simulation Experiments (OSSEs), respectively.

8.4.1. Numerical model assessments - Aegean Sea (POSEIDON monitoring and forecasting system).

The Aegean Sea is located to the northeast of the Ionian and to the northwest of the Levantine Sea. It is the third major sea of the Eastern Mediterranean basin. The topographical structure of the Aegean is very complicated. It is bounded to the east by the Turkish coasts (Asia Minor), to the north and west by the Greek mainland and to the south by the island of Crete. Its coastline is very irregular and hundreds of islands are scattered all over the Aegean. The water budget and the phenomenology of the Aegean Sea is largely controlled by the exchange of heat and salt with the Levantine basin to the south and the exchange of water masses with the Black Sea/Marmara Sea through the Dardanelles Straits in the North Aegean Sea.

The Aegean Sea forecasting component consists of a high resolution general circulation model of the Aegean Sea area nested within the Copernicus CMEMS with MED MFC forecasting system, a data assimilation module based on the extended Kalman filter approach that produces analyses on a weekly basis and a multivariate set of *in situ* and satellite observations used for assimilation and model validation. The Aegean Sea hydrodynamic model is based on the Princeton Ocean model (POM) and was developed as part of the Poseidon system (Korres and Lascaratos 2003; Nittis et al., 2006). The model domain covers the geographical area 19.5°E – 30°E and 30.4°N – 41°N (Fig. 2) with a horizontal resolution of 1/30° and 25 sigma layers along the vertical with a logarithmic distribution near the surface and the bottom. Boundary conditions at the western and eastern open boundaries of the Aegean Sea hydrodynamic model are provided on a daily basis (daily averaged fields) by the Copernicus CMEMS MED MFC system.

Our main focus was to assess the predictive skill of the system when run without data assimilation (model free run) and to assess a series of sensitivity runs aiming to improve the skill of the forecasting system. As such potential improvements we considered the modification of the Dardanelles open boundary condition (Dardanelles Straits inflow/outflow is a key factor for the hydrodynamics and hydrology of the North Aegean Sea), the inclusion of wave dissipated energy to the TKE of the Aegean Sea hydrodynamic model and the testing of an alternative atmospheric forcing at 1/20 horizontal resolution from a WRF model setup over the Mediterranean Sea.

Different model simulations were performed with the Aegean Sea model for the period Jan – Dec 2014 in order to assess its performance in the free run mode (EXP1), understand the impact of certain mechanisms (wave dissipated energy added to the TKE equation of the model, EXP2), assess the importance of the atmospheric forcing (EXP3) or the effects of a new open boundary condition (OBC) applied to the Dardanelles Straits (EXP4). EXP0 refers to the standard operational cycle of the POSEIDON system where a multivariate set of satellite and *in situ* observations are assimilated on a weekly basis in the Aegean Sea forecasting component.

Overall, the Root-Mean-Square-Error (RMSE) for the free run and the operational run of the model is presented in **Table 8.2**. In all cases the RMSE is higher as expected for the free run while there is an increase of error between 30-100 meters. However we have to bear in mind that error calculation below the surface layer is based on ARGO temperature profiles which do not support a regular coverage over the model domain.

Table 8.2: *Temperature RMS error for EXP0 and EXP1 at different depths over the model domain*

	Foundation SST (4m)	**5-30m**	**30-100m**	**100-300m**	**300-600m**
EXP0	**0.652 °C**	**0.672 °C**	**0.982 °C**	**0.510 °C**	**0.303 °C**
EXP1	**0.768 °C**	**0.810 °C**	**1.095 °C**	**0.629 °C**	**0.360 °C**

We assessed the ability of the Aegean Sea model to correctly represent sea surface temperature, its observed diurnal variability in terms of the diurnal range and the time of occurrence of minimum and maximum surface temperature. I**Figure 8.2** shows the distribution of SST RMSE and Bias for year 2014. Overall the model surface temperature (for depths <1m) is by 0.41°C cooler than the SEVIRI satellite observations with the exception of the area to the west of the Dardanelles Straits where the SST bias is higher than 3°C. The same situation is repeated with the SST RMSE spatial distribution where local maxima exceeding 4°C are observed next to the Dardanelles Straits. For the rest of the studied areas, the RMS error remains lower than 1°C. Considering that the inflow/outflow properties at the open boundary of Dardanelles is prescribed through climatological values these findings call for further sensitivity studies as an attempt decrease the observed RMSE and Bias.

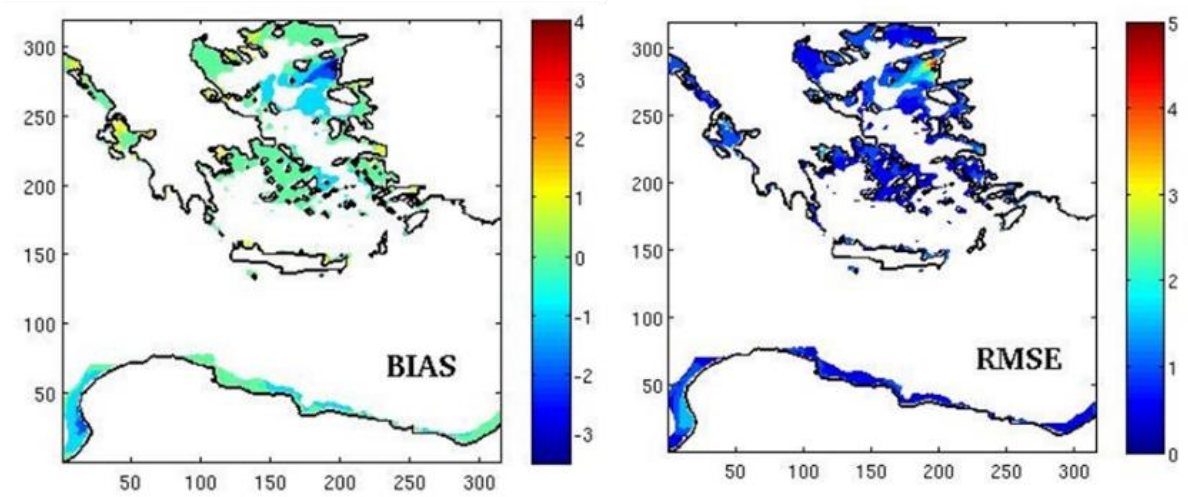

Figure 8.2: *Bias and RMS error (in °C) for model run EXP1 with respect to SEVIRI skin temperature for year 2014.*

The increased skin temperature RMSE (between 2 and 5°C) and the negative Bias in the area of Lemnos plateau west of Dardanelles Straits are clearly related to the open boundary condition applied to the Dardanelles Straits. To mitigate this effect, we tested a boundary condition based on the results of Maderich et al. (2015) that used a chain of simple linked models to simulate the seasonal and interannual variability of the Turkish Straits System. The original dataset of Maderich et al. (2015), consists of daily values, for the period 1969 - 2009, for the exchange (inflow and outflow) between Aegean Sea and the Turkish Straits system with respective values for salinity and temperature. The above data set was used to setup a daily climatology of volume inflow and outflow along with corresponding values for temperature and salinity. A further correction to the temperature of the outflowing waters to the Aegean Sea was introduced by considering foundation SST satellite measurements in the area close to Dardanelles Straits. The new boundary condition replaced the standard Dardanelles boundary condition of the Aegean Sea model (Kanarska and Maderich 2008) and the system was integrated for a one year period (2014) to test its efficacy to reduce bias and RMS errors (EXP4). Although the overall properties of the Aegean Sea model in terms of foundation SST and SSH RMS errors remained approximately the same between the two experiments (EXP1 and EXP4) there were significant changes taking place over the Lemnos Plateau area where the Black Sea brackish waters first enter into the Aegean. In **Figure 8.3** shows the skin temperature RMS error and bias to be inter-compared with **Figure 8.2** corresponding to EXP1. It is evident that the new boundary condition applied to the Dardanelles Straits drastically decreases the model bias (approximately -0.5°C for EXP4 versus -1.3°C for EXP1) and RMS error in the area over the Lemnos Plateau.

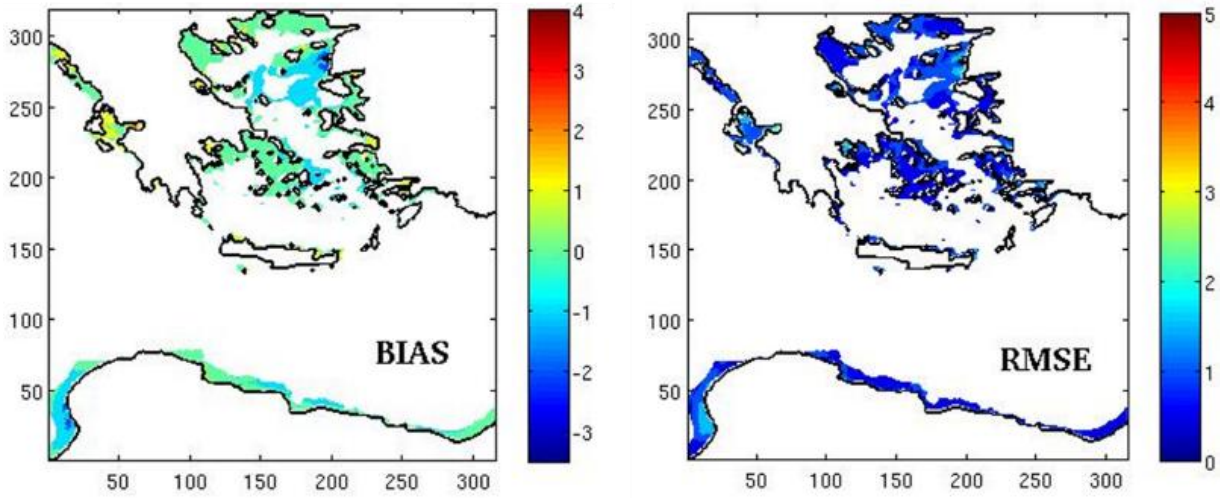

Figure 8.3: *Bias (left panel) and RMS error (in °C) for model run EXP4 with respect to SEVIRI skin temperature for year 2014.*

The above finding was also verified by inter-comparing the foundation SST RMS error time series of EXP1 with the one corresponding to EXP4 for the northeastern part of the Aegean Sea (**Figure 8.4**). It is evident that during June – September 2014 the new parameterization of the Dardanelles outflow was able to decrease the SST foundation RMS error by approximately 0.4°C while for the rest of the year the EXP4 error was lower than that of EXP1.

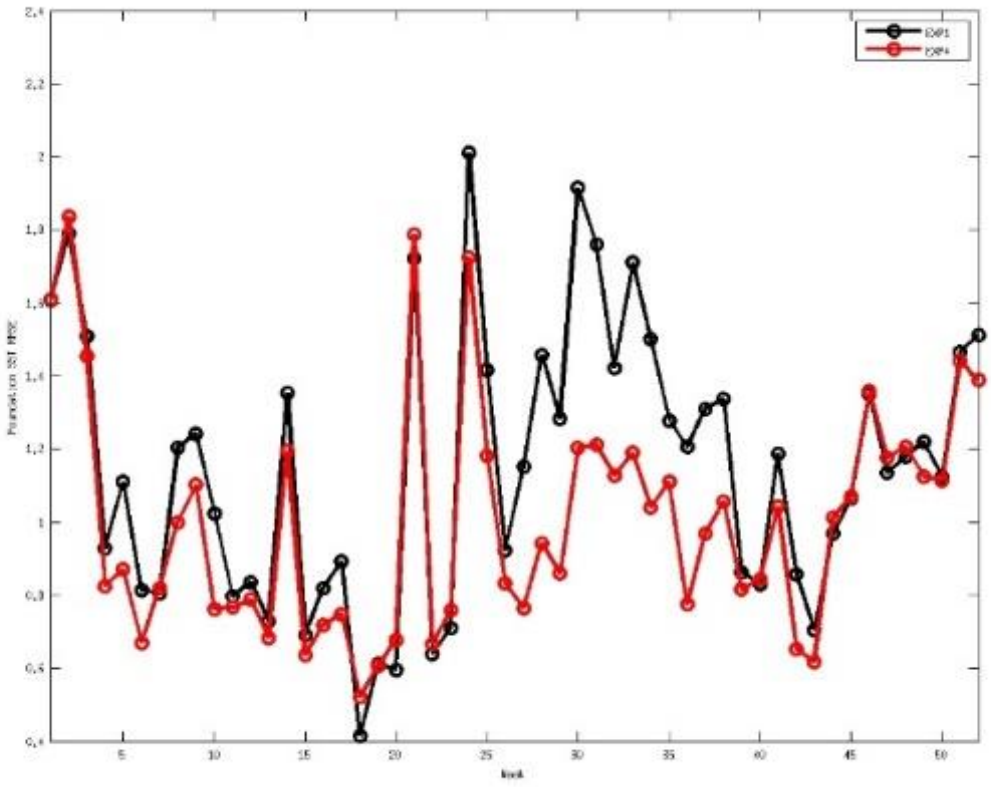

Figure 8.4: *Foundation SST RMS error for the northeast Aegean Sea (the Aegean Sea area east of 24.5°E and north of 39.3°N) corresponding to EXP1 and EXP4.*

8.4.2. Numerical model assessments - Ibiza Channel (Western Mediterranean Operational System – WMOP).

The Balearic Sea, situated in the western Mediterranean Sea, is a particularly challenging region for ocean operational forecasting systems due to the complexity of the topography and of the ocean dynamics from coastal area to open sea. In particular, the Ibiza Channel (IC) is a circulation "choke" point in the western Mediterranean, governing the meridional water mass exchanges between the adjacent sub-basins. JERICO-NEXT coastal observations from fixed mooring, HF radar and gliders in the Ibiza Channel were used to assess a regional model covering the coastal areas of the Balearic Sea and used to generate short-term operational predictions. Strengths and limitations of both the model and the observations are discussed based on this assessment.

The high resolution Western Mediterranean Operational system (WMOP) is developed at SOCIB (Juza et al., 2016). It is based on a regional configuration of ROMS (Shchepetkin and McWilliams, 2005) from Gibraltar Strait (6ºW) to Sardinia/Corsica islands (9.5ºE). The vertical grid is made of 32 stretched sigma levels. The horizontal resolution is ~1/50º. The model is run in both hindcast and forecast modes. The geographical coverage of the SOCIB observational network in the IC is shown in **Figure 8.5**. It is composed of a fixed mooring, a coastal HF radar and a glider endurance line.

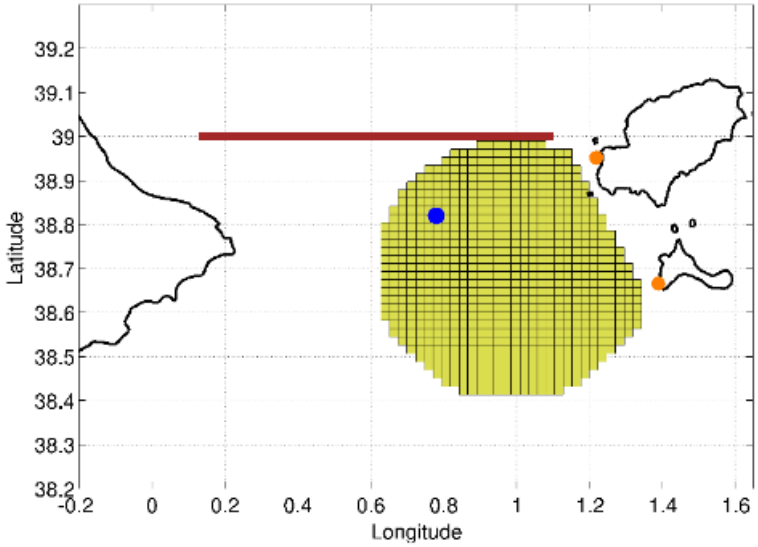

Figure 8.5: *Observational network in the Ibiza Channel: HF radar antenna locations (orange dots), HF radar coverage of the total surface current vectors grid (yellow area), glider transect (red line) and fixed mooring (blue dot).*

The temporal mean of the HF radar observations (**Figure 8.6**) shows a southeastward flow in the middle of the IC (~0.7ºE), recirculating eastwards and then flowing northwards at the east forming and joining the Balearic Current in the northern shelf of the Balearic Islands. WMOP_hindcast reproduces the observed mean circulation but with a too strong and too large northward flow. This northward meridional current dominates the mean circulation in MED-MFC in the whole eastern part of the IC.

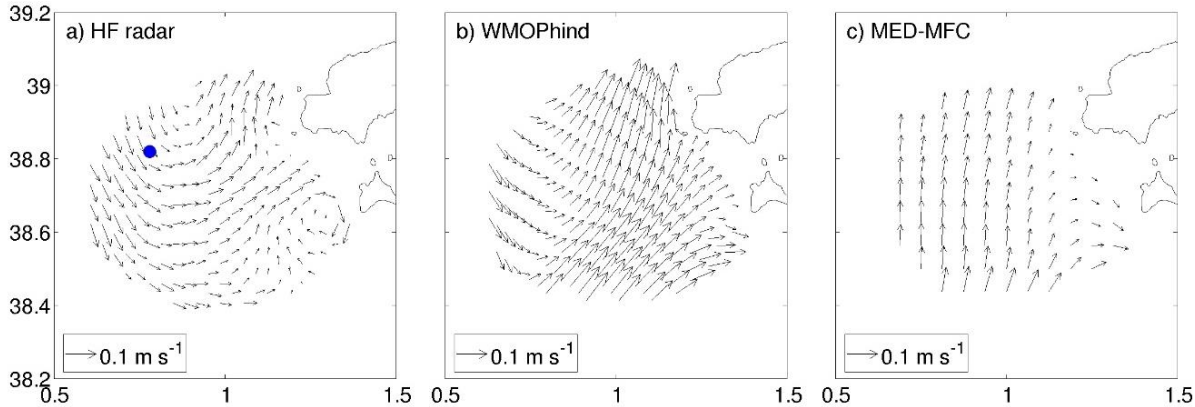

Figure 8.6: *Surface velocity means from HF radar (a), WMOP_hindcast (b) and MED-MFC (c) from June 2012 to August 2014. The fixed mooring location is indicated (blue dot).*

The Hovmöller diagrams along the zonal section at 38.7ºN (**Figure 8.7**) highlight the meridional circulation patterns across the channel and their variability at both high and low frequencies. The southward flow (negative values) to the west and the northward flow (positive values) to the east are reproduced in WMOP_hindcast, as well as strong events such as the inflow in June 2012 and the outflow in January 2015. The velocities from HF radar and WMOP_hindcast have the same order of magnitude and similar time scales of variability. WMOP_forecast has stronger velocities, is more variable and closer to the MED-MFC outputs due to the weekly restart to the MED-MFC fields. Although large discrepancies with the HF radar are found, the inflow event in fall 2016 is present in both WMOP_forecast and MED-MFC. The surface geostrophic velocities from altimetry are much less variable and represent a continuous inflow in the eastern part of the channel around 1ºE. Only the strongest events seem to be captured by the altimetry (inflow in June 2012, January and fall 2016, outflow in January 2015).

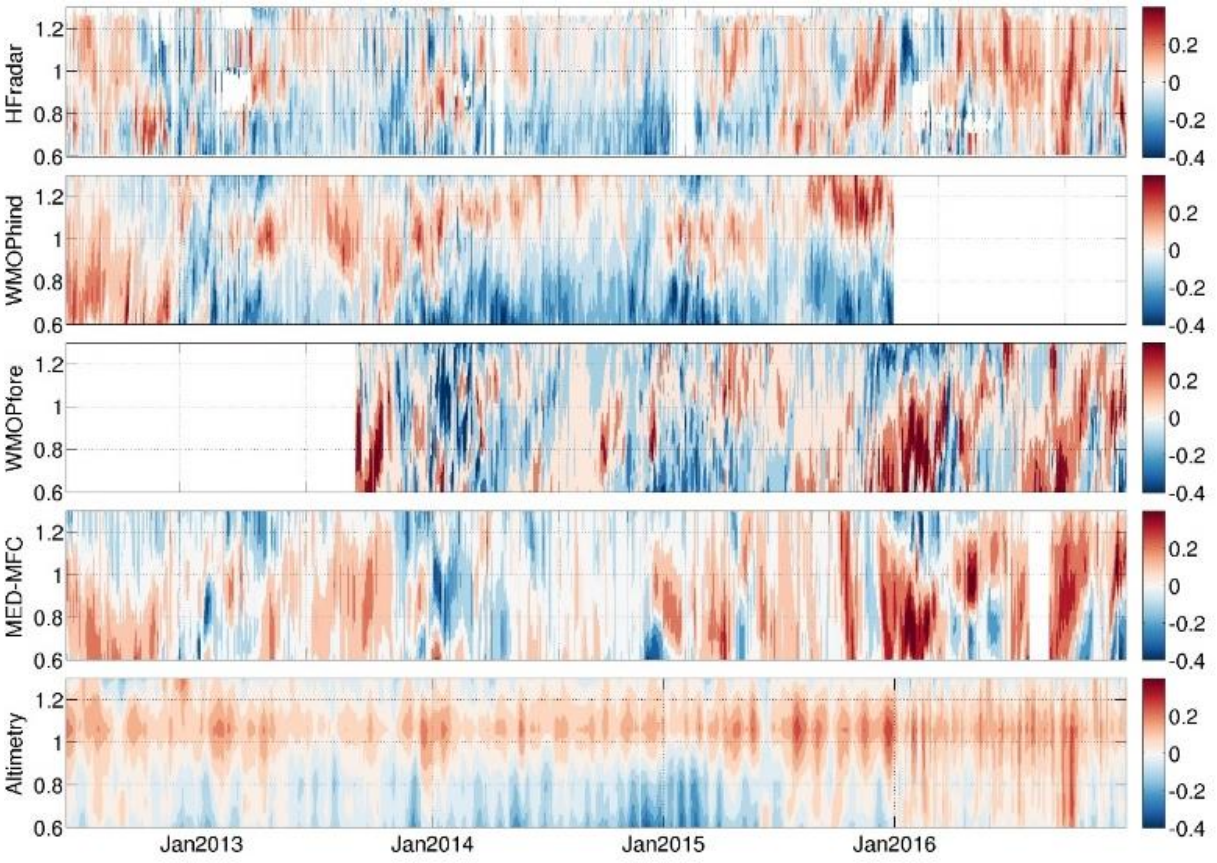

Figure 8.7: *Hovmöller diagrams of meridional velocities along the zonal section at 38.7ºN in the IC from June 2012 to December 2016 from HF radar, WMOP_hindcast, WMOP_forecast, MED-MFC and altimetry (from top to bottom panels).*

The glider monthly climatology over 2011-2015 (**Figure 8.8**) showed that the total southward transport across the IC (associated with the NC) was larger in winter and early spring (maximum of 1.2 Sv in April) while in summer, it strongly decreased until 0.5 Sv in July. The northward transport was less subject to a seasonal cycle, varying from 0.25 Sv in fall-winter to 0.45 Sv in summer. Consequently, the net flow had a marked seasonal cycle remaining negative throughout the year. WMOP_hindcast was able to reproduce the inflow and outflow variability, but the seasonal cycle of the total net transport is not well represented due to the too strong NC in summer. The MED-MFC represents the seasonal cycle of the southward transport but it reproduces a too strong northward transport leading to a positive net flow from May to December.

The observed daily/weekly transports per water mass during the glider missions from 2011 to 2015 (**Figure 8.9**) showed the typical water masses of the western Mediterranean (recent and modified surface AW, WIW, LIW and WMDW) as well as their high frequency variability transports. Although discrepancies in magnitude and phase with the observations were found, WMOP_hindcast was able to generate and propagate WIW, formed in the northwestern Mediterranean, during the winters 2011, 2012, and 2013, and to reproduce the strong outflow (NC) event in winter-spring 2015 and the important inflow of fresh AW in November-December 2015. Very few WIW quantities were found in the MED-MFC transports across the IC.

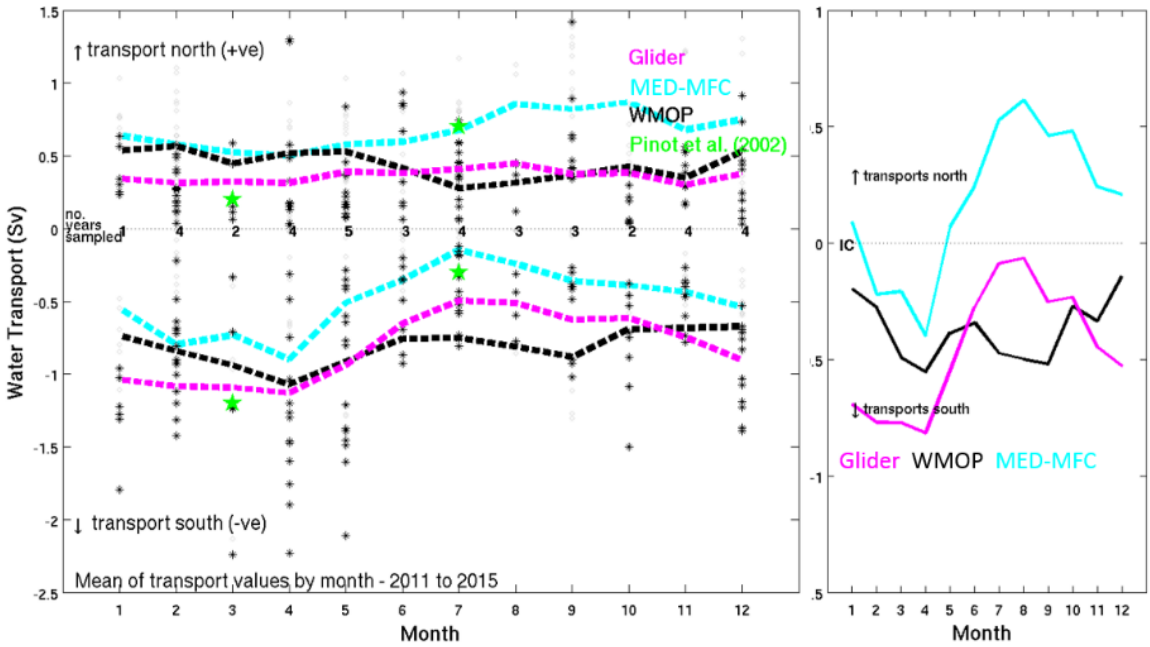

Figure 8.8: *Monthly climatology over 2011-2015 of northward (inflow) and southward (outflow) transports (left panel) and net flow (right panel) through the IC from gliders (magenta), WMOP_hindcast (black) and MED-MFC (cyan).*

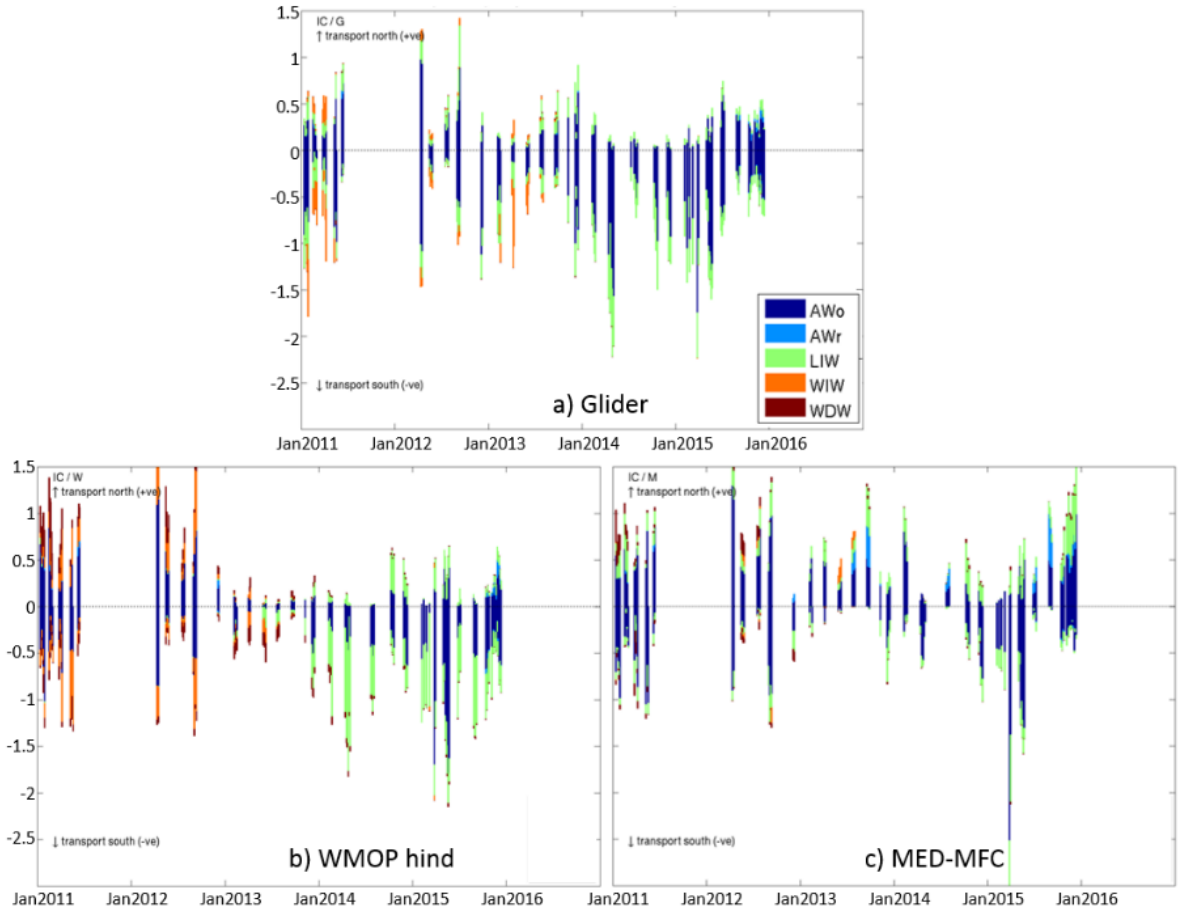

Figure 8.9: *Geostrophic velocity transport (Sv) by water mass from gliders (a), WMOP_hindcast (b) and MED-MFC (c) for the missions from 2011 to 2015 in the IC.*

As a summary, the high-resolution data from fixed mooring, HF radar and gliders allow to monitor a wide range of ocean processes in coastal area. These coastal observations are complementary to altimetry products, which are not able to provide accurate measurements in such area, as highlighted by comparisons between HF radar and altimetry. **Table 8.3** summarizes the main strnghts and limitations of observing pltforms and simulations in the Ibiza Channel case study.

Table 8.3: *Summary table of specificity / ocean process for each observation and model in the Ibiza Channel*:

Observations	Strengths	Limitations
Mooring	- Time series of SST, SSS and sub-surface currents - SST seasonal/interannual cycle - SSS magnitude and variability	- Local fixed point - Critical location to monitor specific processes (e.g. meridional exchanges) - Temporal gaps
HF radar	- Time series of 2D maps of surface currents in coastal areas - Mean surface circulation - Kinetic energy - High spatio-temporal variability	- Restricted geographical coverage (eastern IC)
Gliders	- Time series of T/S vertical section - Transport across key sections - From daily/weekly to interannual variability - Water mass transport variability	- Quasi (but not) continuous time series

Simulations	Strengths	Limitations
WMOP hindcast	- SST seasonal/interannual cycle - SSS magnitude in 2013-2014 - Mean surface circulation - Kinetic energy - Outflow seasonal cycle - Inflow/outflow strong events - Water mass (AW, WIW) propagation	- SST maxima too low - No SSS decrease in 2015 - Circulation variability (amplitude and phase) at high/low frequencies - Too strong NC in summer - Discrepancies in magnitude and phase of water mass transports
WMOP Forecast	- SST seasonal/interannual cycle - Inflow events	- Too many low salinity events - Too strong surface velocities - Too strong kinetic energy - Too strong inflow - Too strongly constrained by CMEMS MED-MFC model
MED-MFC	- SST seasonal/interannual cycle - Inflow events - Seasonal cycle of outflow transport - Water mass variability	- Too many low salinity events - Number and magnitude of inflows - Positive net flow for most of the year - Very few WIW

8.4.3. Numerical model assessments - Nazare Canyon influence area (MONICAN System).

Submarine canyons are ubiquitous features of the continental margins around the World. Large submarine canyons that intersect an important fraction of the continental slopes and shelves cause considerable impacts on the coastal ocean areas and on the ecosystems they host. The abrupt topography and short spatial scales that characterizes submarine canyons the broad variety of highly energetic processes they promote and the important area of the shelf and slope they affect all contribute to challenge the ability of numerical models to adequately hindcast or forecasts the oceanographic conditions in those areas.

Instituto Hidrografico (hereafter IH) contributed to JRAP 6 by focusing on an area of the European margin that is under the influence of a large submarine canyon and exposed to the North Atlantic conditions – the Nazare Canyon area of influence (W Portuguese margin). The Nazare Canyon (see bathymetric ma in **Figure 8.10**) is the largest submarine canyon of the Portuguese continental margin and one of the largest of the European margin. It extends for more than 200km, following a roughly zonal alignment at 39.5ºN, from abyssal waters with depths in excess of 5000m to a few hundreds of meters from the shore of Nazare. The presence of the large submarine canyon clearly plays a dominant role in shaping the response of the shelf circulation to wind forcing conditions offshore Nazare. The response to upwelling winds is intensified in the area of the canyon head and upwelling seems to persist longer in that area after the decaying of the favorable winds. During periods of downwelling, the canyon seems to channel the warm oceanic water towards the coast. Since 2009 a real-time monitoring system was installed by IH in the Nazare Canyon area in the framework of the project MONICAN (EEA Grants). The MONICAN system integrates two multiparametric buoys, two coastal tide gauge stations and one coastal meteorological station. It was introduced in the JERICO-NEXT network, contributing specifically to JRAP 6 and to WP9 (Virtual Access).

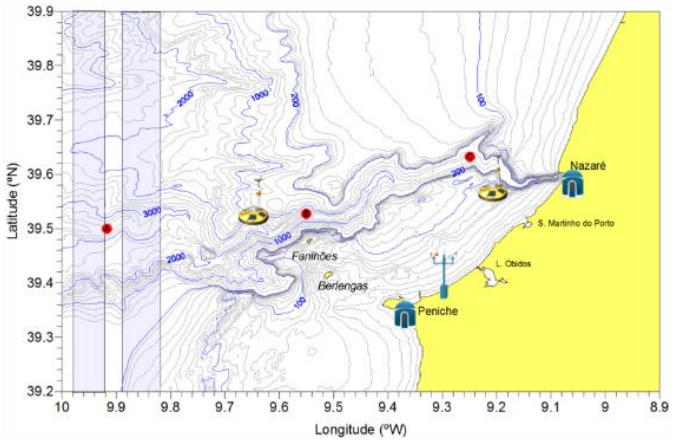

Figure 8.10: *Bathymetric map of the Nazare Canyon middle and upper sections. The different real-time components of the MONICAN system are shown. Red dots indicate the position of currentmeter moorings occupied during the previous observation programs.*

The high resolution model was based on the Harvard Ocean Prediction System (HOPS – Robinson et al., 1996; Lozano et al., 1996). In the LAM-HOPS model the horizontal discretization uses a Cartesian grid that extends between 8.903ºW and 10.027ºW in longitude and 39.202ºN to 39.898ºN in latitude with a spatial resolution of 300m in both directions. A smoothed version of the Nazare Canyon area topography was developed and implemented in the model. This retains the main aspects of the topography of the area while maintaining adequate consistency criteria (such as hydrostatic consistency). In the model the Berlengas and Farilhoes islands are not explicitly included as so but appear as very shallow areas.

Figure 8.11 shows some of the more representative examples of the results obtained for this period. For the conditions observed and modeled in the surface layers we include here the temperature and current fields at 50m depth. We have not presented the very surface layer fields since the analysis showed that mixing in LAM-HOPS model was somewhat too high. The results obtained at 50m depth, however, provide an image of how the upper layers in the area of influence of the canyon were responding to the prevailing downwelling conditions.

The observed fields at 50m (**Figure 8.11**, top) showed that the onshore penetration of warm oceanic water in response to the downwelling was channeled by the canyon, which is consistent with what is observed in the surface layer or is the SST images from MUR (not shown). Higher temperatures at 50m were observed in the canyon head and shelf area just surrounding the canyon head, reflecting generally the fact that downwelling of warm surface water was more active here. A note of caution should be made, however, for the fact that the fields built from the CTD data alone are not synoptic but reflect the fact that parts of the domain were covered during different prevailing

forcing conditions. It is here that the combination of numerical models with data assimilation and observations can lead to an improved characterization of the area, building a truly synoptic image from the non-synoptic data.

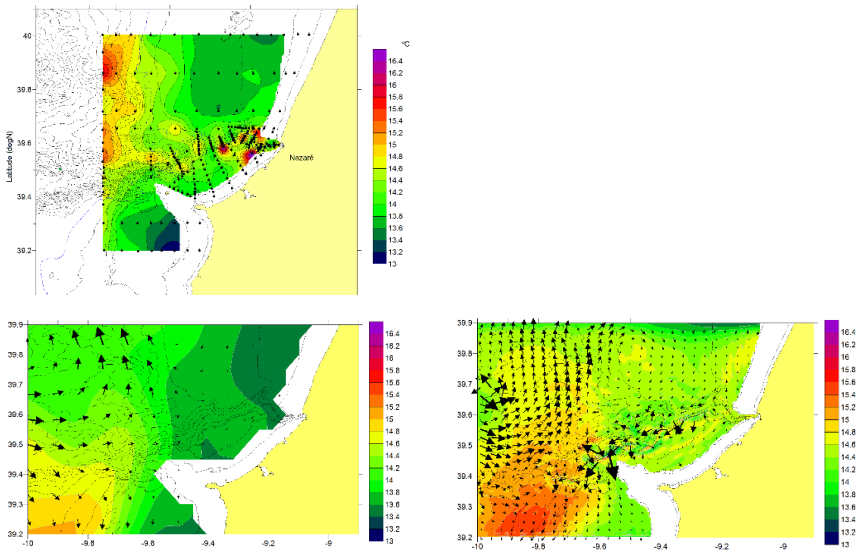

Figure 8.11: *Top panel: Temperature at 50m depth from the set of CTD stations covered between 13 and 22 June 2007 (survey1). Middle panel: Temperature and current vectors at 50m depth on the 18 June 2007 obtained with the NEMO model on the 18 June 2007. Bottom panel: Temperature and current vectors at 50m (decimated to 1point each 10 points in latitude and in longitude) on the 18 June 2007 obtained with the LAM-HOPS model.*

The temperature and current fields at 50m depth, which were obtained from the regional NEMO model on the 18 June 2007 (**Figure 8.11**, middle panel) reflects the general image of the downwelling situation, with warm oceanic water being transported in the direction of the coast along the northern flank of the canyon. This transport however seems to recirculate northward along the upper continental slope, integrating the poleward slope current. Very weak flow is observed over the shelf area at 50m depth.

The high resolution LAM-HOPS provides a richer picture of the processes that were taking place at 50m depth offshore Nazare. The results for the 18 June 2007, presented in **Figure 8.11** bottom panel, show in more detail how the onshore flow along the northern flank of the canyon (of the Estremadura Plateau) accommodate to the changing slope direction in the area of the canyon mouth and continues northwards in the form of the poleward slope current. Perhaps more importantly these results reveal that a downcanyon flow is established along the upper section of the canyon. This flow compensates the onshore transport in the surface layers that is promoted by the downwelling forcing conditions and that is also channeled by the canyon topography. The picture at 50m is complex in the canyon mouth area, where the onshore transport providing from the deep ocean area is blocked by the offshore flow channeled along the canyon. We are tempted to suggest that depending on the strength of the offshore downcanyon flow at the Nazare Canyon mouth, an so of the response of the canyon to the downwelling forcing conditions, a stronger or weaker blocking and deflection of the poleward flow occurs at the canyon mouth, “shaping” the expression of the poleward slope current that is observed northwards, along the NW Iberian slope and N Spanish slope.

8.4.4. Numerical model assessments - SE Bay of Biscay (AZTI Operational System).

The study area is located in the southeastern the Bay of Biscay. This bay extends approximately from 43.5º N to 48.5º N in latitude, and from Cape Ortegal, northwestern Spain (8º W), to the French coast (1º W). The water circulation in the Bay of Biscay is weak (~1−2 cms^{-1}) and is characterized by the frequent presence of eddies together with a persistent poleward flow . This poleward flow is also known as the slope current. Over the Basque

Country shelf, the circulation in the upper water column is mainly controlled by the wind, tides, and density currents induced by river discharges.

The Regional Ocean Modeling System (ROMS) is the hydrodynamic model used to estimate current, temperature and salinity fields in the southeastern Bay of Biscay. The ROMS domain used in the operational system covers the southeastern Bay of Biscay, extending from 43.24º N to 44º N and from 3.4º W to 1.3º W, with a mean horizontal resolution of 670 m. The ROMS simulation includes the mean freshwater discharges from the following rivers: Adour, Bidasoa, Oria and Nervión. With the aforementioned information, we obtain 96-h forecasts for the study area. At present, the forecasts of velocity, temperature and salinity fields are opened to the public, but they are still under analysis. AZTI ran three different model configurations, based on three different boundary condition options including: 1) sponge and nudging layers (with the same extension) near the open boundaries; 2) sponge layer without nudging layer; and 3) without sponge and nudging layers. Generally, option 1 and 2 provides the smoothest results, while option 3 can cause the model breaks down. Using these options, after several hours the model results begin to differentiate in a remarkable way. The recommendation is to use option 1 with an appropriate parameterization, but option 2 is also recommended in order to reduce the size of the input files. Here we show some examples of these options for the forecast between the beginning of 28 February 2018 and the end of 3 March 2018:

For the geographical area of the southeastern Bay of Biscay, high-frequency (HF) radar data were used for a first skill assessment. Due to the characteristics of these data, measured in the first 3 m depth of the water column, the main results and conclusions are related with the surface ocean circulation and the influence of the coastline on this circulation. The geographical coverage of the HF radar is shown in **Figure 8.12**.

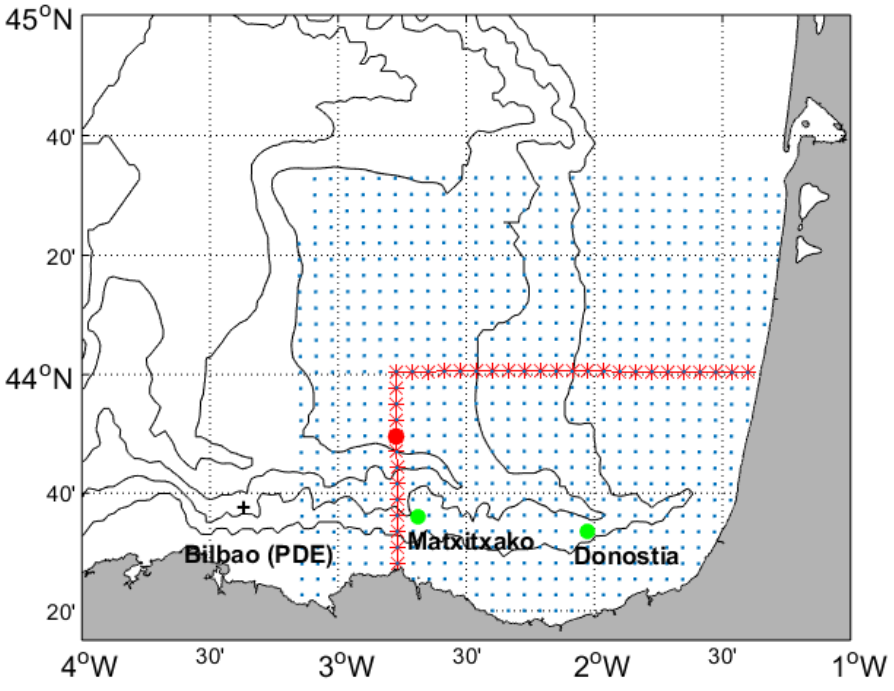

Figure 8.12. *Observational data available in the SE Bay of Biscay: HF radar coverage (blue dots), Bilbao-Vizcaya buoy (black cross) and Basque Government buoys (green dots, no data available for 2014). The red dot shows the position used to compute the spectra.*

Since 2009, the HF radar system, owned by the Directorate of Emergency Attention and Meteorology of the Basque Government Security Department, is providing information on surface currents. The daily mean simulated and observed data for the year 2014 were considered to obtain mean fields and time evolution diagrams, while the

hourly data were used to compute spectra. For technical problems with the ROMS domain with a resolution of 670 m (blow-up during several days of the simulation for the selected year), the comparison was carried out with the same ROMS domain but with a resolution of 2.2 km using as boundary conditions the IBI reanalysis data obtained with NEMO with a resolution of 6.6 km. The model outputs were interpolated into the observation positions for comparisons and analyses.

The Hovmöller diagrams along the zonal section at 44º N and one meridional section at 2.78º W highlight the main along-slope circulation patterns, which in the area are marked by a strong seasonality (**Figure 8.13**). During the winter months, the surface eastward (northward) flows dominated the shelf/slope circulation off the Spanish (French) coasts. In the summer, the flow presentet more variability and westward (southward) currents predominated. The winter eastward flow (positive values) was well reproduced by the models, as well as eastward flow events such as the one occurred at the end of April 2014, which was well observed in the two selected sections. The velocities from the HF radar and the IBI reanalysis data have the same order of magnitude and similar time scales of variability (**Figure 8.14**). There were differences in the offshore extension of the most intense jets. In particular, the model currents were found to be more confined to the shelf area.

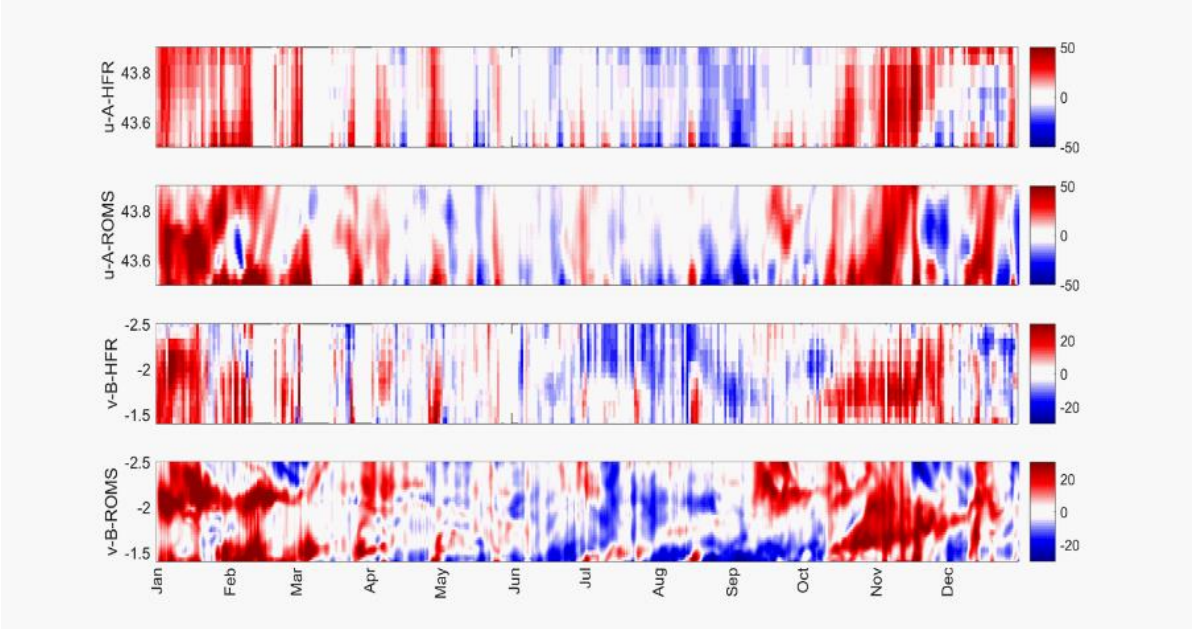

Figure 8.13: *Hovmöller diagrams for 2014 of the HF radar and daily ROMS velocities along the two sections (A and B) shown in* ***Figure 8.12****.*

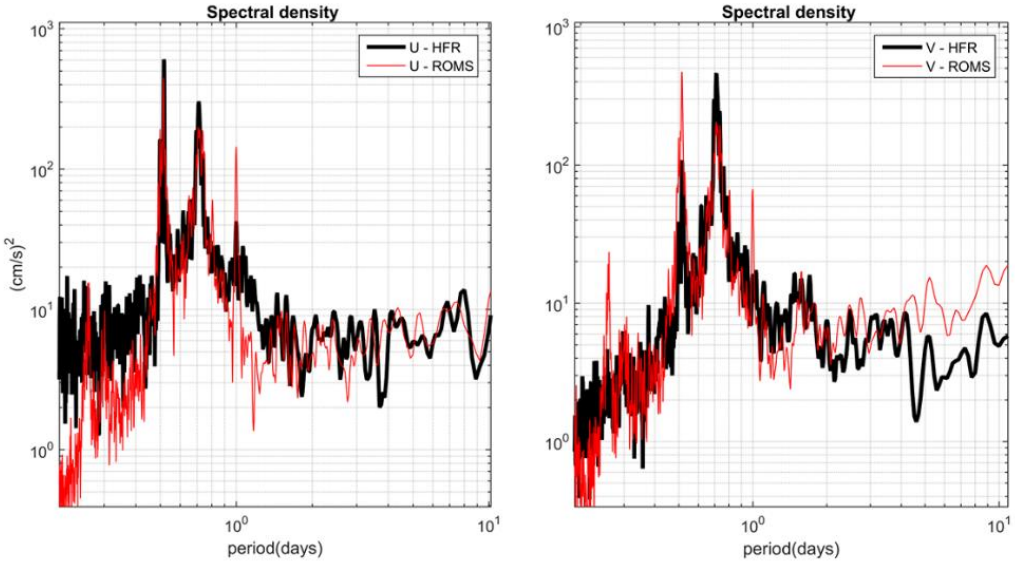

Figure 8.14: *Spectral density of the two components of the velocity extracted from the HF radar data and ROMS model at the location shown by a red dot in* ***Figure 8.12****.*

The availability of a high-frequency radar in the southeastern Bay of Biscay allowed the evaluation of model performance considering different spatio-temporal scales. Radar data were used to validate different model configurations in the southeastern Bay of Biscay for the year 2014. A marked seasonality in the surface transports paths was observed to be reproduced correctly by the models (NEMO and ROMS, with resolutions of 6.6 and 2.2 km, respectively) as well as shorter time scale intensifications of the shelf and slope currents, which in the study area are highly related to local winds. None of the models was able to reproduce an eddy observed in the footprint area in December 2014. At high-frequency scales, tidal and inertial bands showed energy signals similar to those observed by the radar system.

8.4.5. Numerical model assessments - *Baltic Sea (Alg@line System).*

We investigate here the possibility to use operative wave model results to support the VOS-line phytoplankton and algae observations. The results also help in the interpretation of remote sensing observations of algae bloom as the wave-induced mixing influences the concentrations of algae on sea surface layer (e.g., Groetsch et al., 2014). The mixing of the sea surface layer is a phenomenon driven by many different processes, such as buoyancy and momentum fluxes, and wind induced shear stress. Sea surface waves can contribute to the mixing either by directly adding turbulence to the near-surface layer when breaking, or by contributing to deeper mixing through Langmuir turbulence created by an interplay between the Stokes drift of the waves and the wind driven surface currents (Langmuir, 1938).

The complex bathymetry and irregular coastlines of the Baltic Sea add to the challenges associated with hydrodynamical modelling. The choice of a proper mixing scheme in 3D-hydrodynamical models is not straightforward, and this has been a subject of research in the Baltic Sea (Tuomi, 2014; Westerlund and Tuomi, 2016). Accounting for the role of the waves in the surface mixing processes by coupling a hydrodynamical model with a wave model has been found to increase the accuracy of model simulations. Waves also affect the mixing processes indirectly through Langmuir turbulence then the wind shear and the Stokes drift of waves create Langmuir cells.

Voluntary Observing Ship m/s Silja Serenade travels daily between Helsinki (Finland) and Stockholm (Sweden) (**Figure 8.15**) . It is part of SYKE Alg@line network in the Baltic Sea monitoring the state of the sea, including the algal blooms. Observations on m/s Silja Serenade are also part of JERICO-NEXT TNA network (WP7, TransNational Access to coastal observatories) and Finnish marine research infrastructure FINMARI.

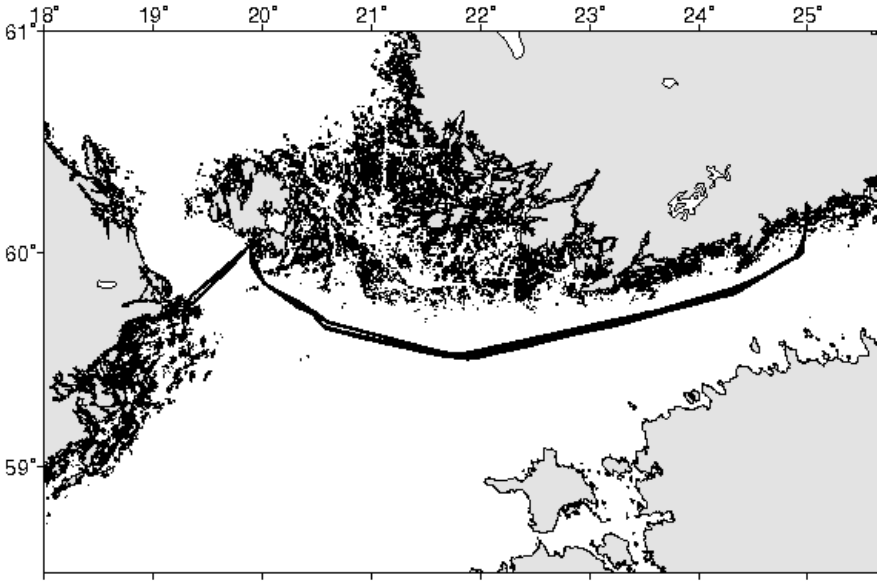

Figure 8.15: *The route of Silja Serenade in the Baltic Sea with its stop in Mariehamn in between the ports of Helsinki and Stockholm.*

Wave model data for 2015 was available from the pre-operational hindcast of the BAL MFC runs (Tuomi et al., 2017), which is based on WAM cycle 4.5.4 using a 1 nmi implementation of the entire Baltic Sea. The wave model was forced with 10 m winds from the atmospheric model HARMONIE (HIRLAM-B, 2018). The wave condition coinciding with the measured flow through data measured onboard m/s Silja Serenade was determined through interpolation in three dimensions (longitude, latitude and time). This produced time series of the significant wave height (H_s), 10-metre wind speed (U_{10}), peak wave period (T_p) and principal wave direction (θ_p). From the modelled values we could then estimate the friction velocity (u_*), the surface Stokes drift (U_{s0}), the wave induced turbulence (B_v) and the Langmuir number (L_a).

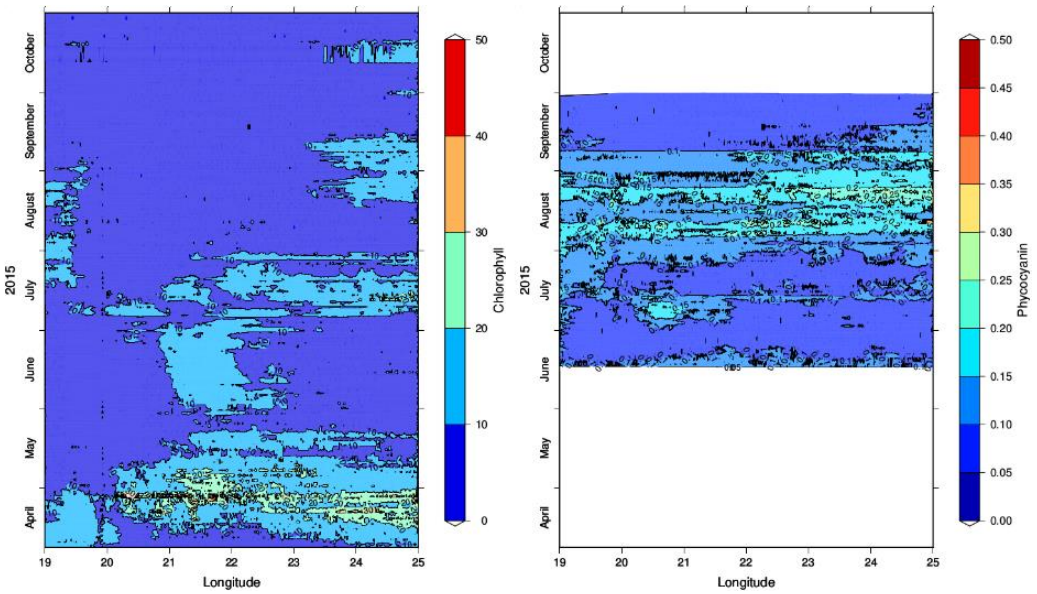

Figure 8.16: *Chlorophyll (left) and phycocyanin (right) measured by Silja Serenade.*

The measured values of temperature and salinity revealed that the temperature has a seasonal cycle, while the salinity is highest in the Baltic Proper, as expected. The spring algae bloom is clearly reflected in the chlorophyll measurements in April–May (**Figure 8.16**, left), although there is variability in the measurements both spatially and temporally also outside of this period.

The highest significant wave heights occurred in the middle of September (**Figure 8.17**).

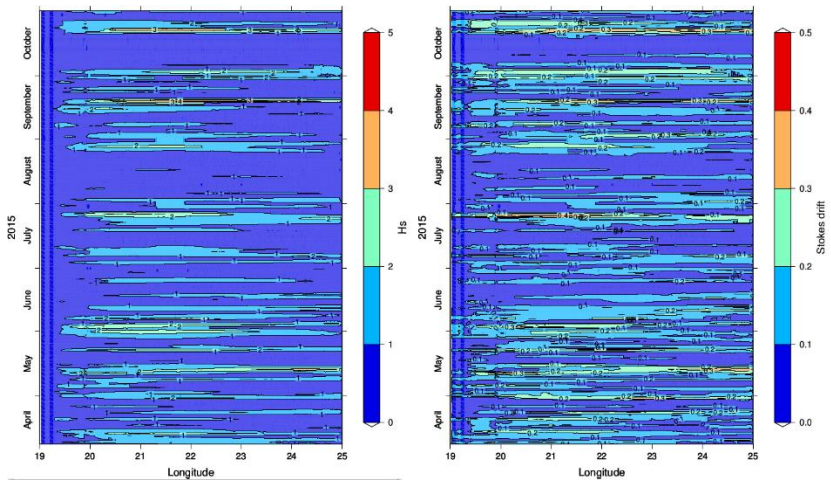

Figure 8.17: *The significant wave height (left) and surface Stokes drift (right) at the ship track of Silja Serenade from the WAM results.*

The chlorophyll (**Figure 8.16**, left) reveals no clear overall connection to the wave activity, which is probably because of the dominant role of the biological processes. There is, nevertheless, a drop in Chlorophyll in the middle of May that coincides with an increase in significant wave height. The same connection can be seen in the end of July, where the harsher wave condition coincide with decreased measured Chlorophyll.

One limiting factor in utilising the ship measurements are that they were made at a depth of about 5 metres, which is quite deep if the aim is to quantify directly the mixing caused by the turbulence of breaking waves. Moreover, the movement of ship in itself added mechanical turbulence and mixed the top layer of the sea. Nonetheless, some mixing effects seemed to be visible in the measured temperature and salinity.The presence of surface waves induce orbital motions in the water. These orbital motions decay with an increasing water depth, thus inducing an additional shear stress. This shear stress induces wave-turbulence interaction that increases the mixing in the top surface layer. We compared measurements from the Alg@line network obtained from the ferry box on board M/S Silja Serenade during the year 2015 with wave model results from the third-generation wave model WAM. The temperature, salinity and turbidity measured by the ferry box showed some variations that can reasonably be attributed to wind and wave induced mixing. The amount of chlorophyll seemed to be dominated by other factors. The estimated turbulence of braking waves at the surface was found to be highly variable, with maximum values being 25 times the mean value. The added contribution was mostly concentrated to the top layer ($z < 1$ m) of the sea. The relative contribution of the Langmuir turbulence (compared to the wind shear) was also determined, but was found to be small. This is in slight contrast to previous preliminary results by Tuomi (2014). However, there are many uncertainties involved with the estimation of the Langmuir number. Since the Langmuir turbulence is capable of enhancing the mixing deeper than turbulence by breaking surface waves, a more in-depth study into this phenomenon is recommended as future research.

8.4.6. Numerical model assessments - *Norwegian Sea.*

The Norwegian Sea covers ~1.1 million km^2 and is situated between the coast of Norway (to the east) and the Iceland and Greenland Seas (to the west/northwest). It serves as a physical and biogeochemical connection

between the North Atlantic Ocean and the Arctic Ocean. A large fraction of northward heat and biogeochemical transport from the north Atlantic into the Norwegian Sea occurs via the North Atlantic Current (NAC), passing through the Faroe-Shetland Channel. Because of this circulation, biogeochemical processes occurring in the Norwegian Sea can affect the flux of nutrients and organic matter northward to the productive regions of the Barents Sea and Arctic Ocean. On larger spatial and temporal scales, biogeochemical processes in the Norwegian Sea proper ultimately determine preformed nutrient content of North Atlantic Deep Water formation water masses in the vicinity of the Lofoten Basin, a region that accounts for over half of global deep water formation.

Aquaculture production increased from 5 million to 63 million tons during the last three decades, while capture fisheries production increased from 69 million to 93 million tons in the same time-period and is aiming for a five doubled production in the upcoming years. However, during the last five years the production has been leveled out caused by the large impact of Salmon lice impacting heavily the development of farmed fish. Main focal point for the monitoring of Norwegian coastal waters is therefore to gain knowledge on the existence and spreading of Salmon lices. The Salmon lice is not only impacting the farmed fish but also the wild fish, which after Norwegian law has to be limited to as marginal as possible. Therefore an operational Salmon lice monitoring system has been developed, including operational observations, and numerical modeling. The model system consists of the ROMS (Regional Ocean Modeling System, Shchepetkin et al., 2005) system with a coupled IBM to estimate the spreading of the Salmon lices. ROMS is a free-surface, terrain-following, hydrostatic, primitive equations ocean model. For details of the model and the set up the reader is referred to (Albretsen et al., 2011 and Sandvik et al., 2016). The ROMS model used here utilizes a one-way nested system consisting of three different resolved (4km- 800m -160 m). The salmon lice model was developed with the purpose to map the horizontal distribution of infectious salmon lice from aquaculture sites in the water masses. The release of newly hatched lice larvae (nauplii) was calculated based on number of adult female lice reported from the aquaculture sites, as described in Myksvoll et al., 2018.

The operational system implemented at IMR is taking advantage of four different data sets used for validation of the numerical model estimations. Those consists of:

- Fixed stations (8 stations along the Norwegian coast)
- Repeated hydrographical transects (1-6 times per year in Nowegian waters)
- Ferrybox (Ferrybox systems are installed on the Hurtigruten line boats MS Vesterålen and MS Trollfjord running on a 11-day roundtrip from Bergen-Kirkenes since 2006)
- Salmon lice monitoring

Observational data sets were used within the validation activity for the ROMS 800 m resolution model An overview of the obtained results is shown within the following. In **Figure 8.18** the results for the temperature (left panel) and for salinity (right panel) are displayed. For temperature we found that the cold bias reported for z layer 2 (5-25m) was primarily a result of too cold conditions in relatively cold waters with high salinities. A corresponding analysis for z layer 1 revealed that the cold bias was enhanced in the upper 5 m due to negative temperature offsets in warm, low salinity water masses. With regard to the results for salinity, there was positive salinity bias. We noted that salinity values above 35.4 were not observed in the 5–25 m z layer, while the model results included higher salinities than this value. Moreover, the model had a challenge when it comes to reproducing lowest salinities, making the range of salinity results significantly smaller in model results than in corresponding observations.

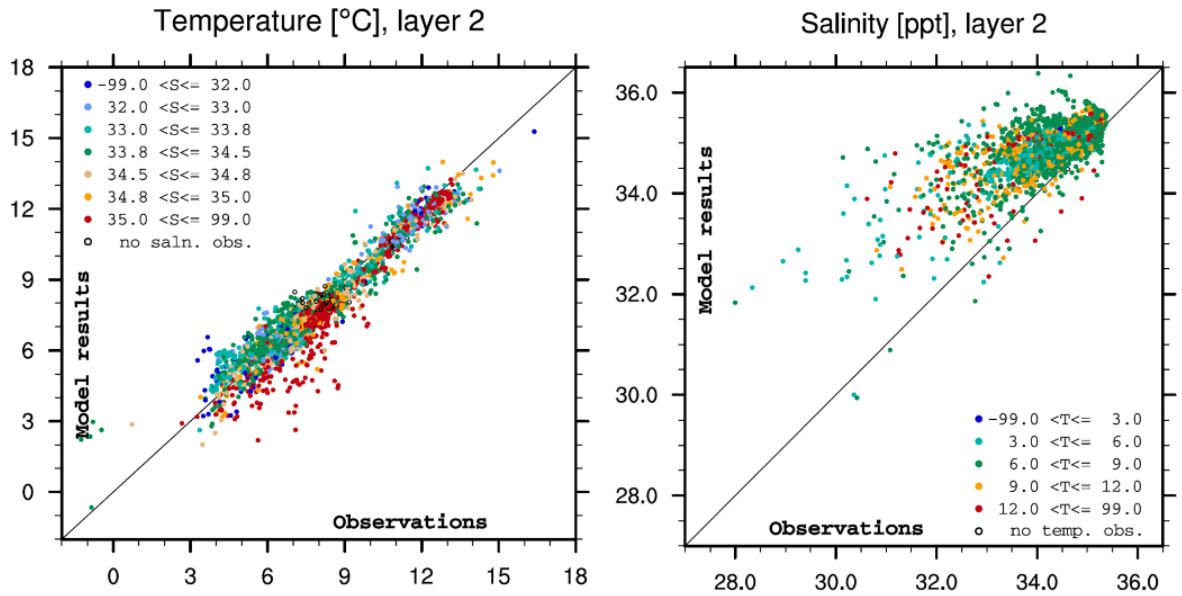

Figure 8.18: *Scatter diagrams for temperature (left panel) and salinity (right panel) from the observations in layer 2 (5-25 m). Observations and model values are given as the horizontal and vertical axes, respectively. The color coding corresponds to the observed value of the alternative variable, i.e. salinity in the left panel and temperature in the right panel. The color coding is shown by the inset graphic legends (taken from Myksvoll et al., 2018).*

Figure 8.19 shows the comparison between observed mean abundance of young stages and modeled number of copepodids from the hindcast within 15x15 grid points for all stations including both 2015 (n = 21), 2016 (n = 44) and 2017 (n = 37). The grid size 15x15 was chosen for illustration because this was the size where the strongest correlation curve (young stages in 2017) reached the first top, however the pattern shown here was very similar across all sizes above 9x9. There were no systematic differences between the three years, however low densities of lice were observed more frequently than high densities.

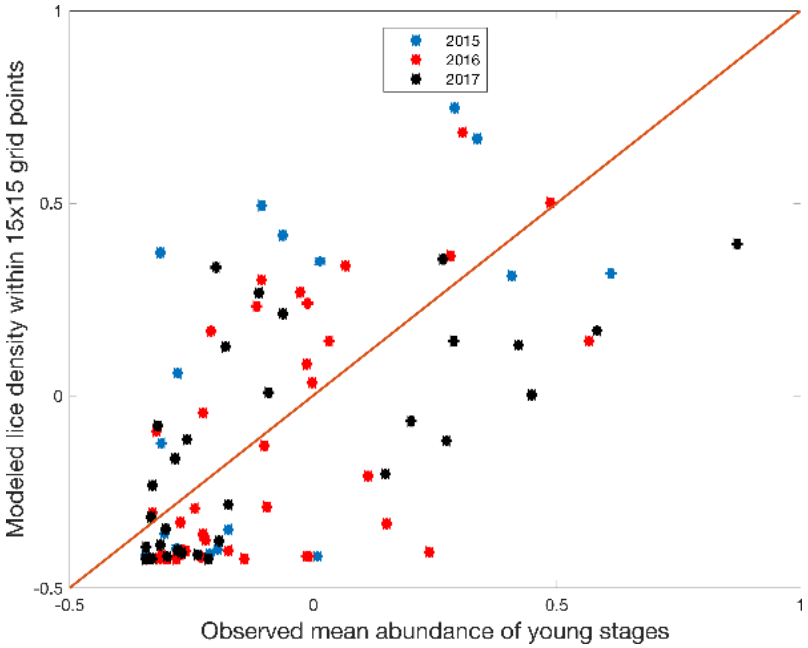

Figure 8.19: *Observed mean abundance of young stages plotted against modeled lice density within 15x15 grid points of the observations point for 2015 (blue), 2016 (red) and 2017 (black). Both variables are standardized for comparison (subtracted the mean and divided by standard deviation) and plotted on a log-log scale (taken from Myksvoll et al., 2018).*

8.4.7. ***Observing System Experiments - Aegean Sea.***

The assimilation system for the Aegean Sea hydrodynamical model is based on the SEEK filter with covariance localization and partial evolution of the correction directions. We assessed the performance of the Aegean Sea forecasting system when additional to the standard operational run observations, gliders T/S profiles and Ferrybox SST & SSS observations within the South Aegean Sea are taken into account. For that, during the period 2012 – mid July 2018 additionally to the standard data set of observations (satellite SSH, foundation SST and Argo T/S profiles) daily gliders T/S profiles within the South Cretan Sea and SST data along the ferryboat route from Piraeus to Heraklion were assimilated into the model.

Two major experiments have been performed over a 9-month period (31 Oct 2017 – 17 July 2018) with the Aegean Sea forecasting system to test the impact of the inclusion of additional *in situ* observations made on a quasi-operational basis within the South Aegean Sea in the estimation of the Aegean Sea hydrodynamic state: (1) the control run where the standard set of satellite and *in situ* observations (Argo T/S profiles) were assimilated into the model on a weekly basis; and (2) an OSE experiment where glider profiles and Ferrybox observations were taken into account on the daily scale. Vertical temperature and salinity sections are presented in **Figure 8.20**. Results show that the Aegean Sea state was best represented when the standard SSH, foundation SST and Argo T/S profiles observations, the glider data and the Ferrybox surface observations were assimilated together in the forecasting system through the use of a properly tuned localized version of the SEEK filter .

One important issue with both sets of *in situ* observations (glider underwater profiles and Ferrybox SST & SSS along the Ferryboat track observations) examined in this study is their intermittent character due to missions design (glider profiles) and/or operational problems (glider profiles and Ferrybox surface observations). Ferrybox data although regularly acquired until 21 Dec 2017 along the Ferryboat track from Piraeus to Heraklion and vice versa, became unavailable for the following months and reappeared only after the beginning of April 2018 due to Ferrybox system malfunctioning, maintenance and an accident that occurred to the Ferryboat itself. Glider profiles on the other hand were characterized by 20-30 days gaps between the four missions while between the first and the second mission the gap was quite large reaching a period of 60 days. Thus the intermittent character of both data sets did not allow for finalized conclusions about their impact on the data assimilation in the Aegean Sea forecasting system although some important results were vident. In order to reach these results apart from the control run and the OSE experiment described in previous sections another two OSE experiments (named OSE1 and OSE2) were performed using the standard set of observations plus the daily Ferrybox SST & SST observations (OSE1 experiment) or the standard set plus the glider T/S profiles (OSE2 experiment). In **Table 8.3** we summarize the results of all experiments performed in term of misfits RMS errors. It should be mentioned again that the RMS of misfits presented here represent an almost independent estimate of the quality of the estimates because it computes the difference between model simulations starting from an analysis state and observations before the observations are assimilated.

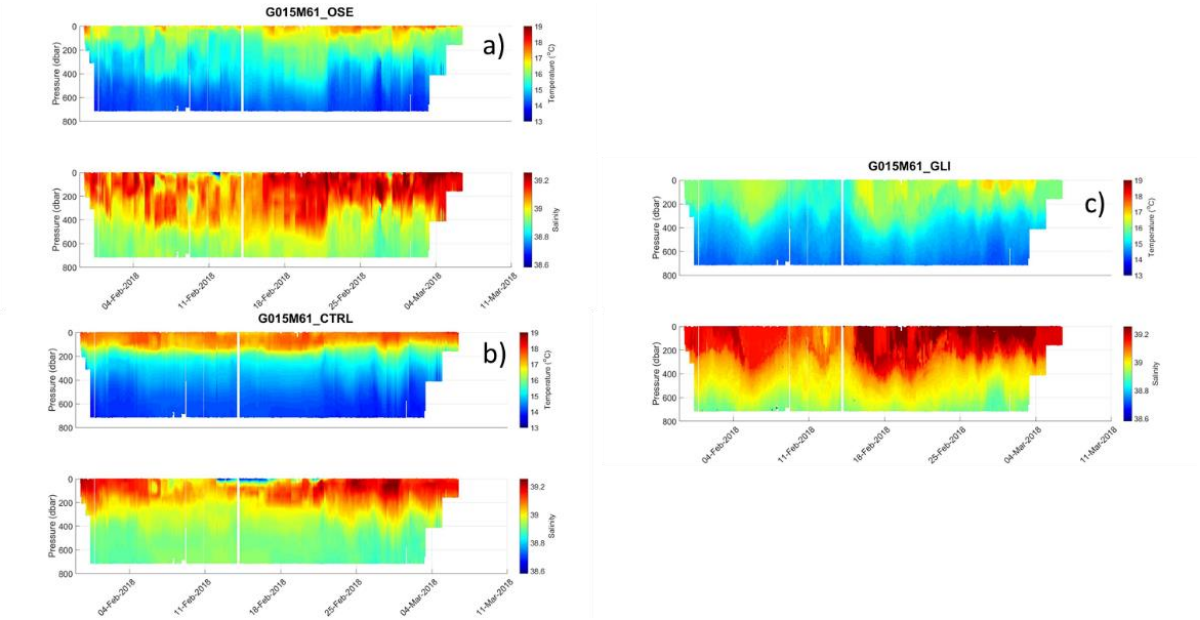

Figure 8.20: *Vertical temperature (upper) and salinity (lower panel) along the path of the glider for the period 30 Jan 2018 – 06 Mar 2018 (second mission). Temperature profiles are in °C and salinity in psu. a) profiles corresponding to the OSE run forecasts (before glider profiles are assimilated into the system) b) profiles corresponding to the model control run and c) profiles as observed by the glider.*

Table 8.3: *Average RMS errors of the four experiments (control, OSE, OSE1 & OSE2) with respect to glider T/S profiles, Argo T/S profiles, Ferrybox SST and SSS observations, sea surface height and foundation SST. For each error category If the value achieved is lower than that of the control experiment the table cell is shaded in grey.*

	CTRL	OSE	OSE1	OSE2
Glider Temperature profiles	0.661 °C	0.4 °C	0.837 °C	0.380 °C
Glider Salinity profiles	0.1 psu	0.059 psu	0.109 psu	0.060 psu
Argo Temperature profiles	0.653 °C	0.582 °C	0.6317 °C	0.569 °C
Argo Salinity profiles	0.178 psu	0.177 psu	0.178 psu	0.187 psu
Ferrybox SST	1.068 °C	0.960 °C	1.023 °C	1.109 °C
Ferrybox SSS	0.338 psu	0.264 psu	0.257 psu	0.389 psu
Sea surface height	4.0 cm	3.79 cm	3.67 cm	3.78 cm
Foundation SST	1.131 °C	1.034 °C	1.078°C	1.005°C

From the aggregated results presented in **Table 8.3** we can conclude the following:

- The OSE experiment achieved the best performance over the control run and OSE1 & OSE2 experiments with respect to all observational data set considered for estimating the RMS error misfits.
- All three OSE experiments (OSE, OSE1 & OSE2) were able to improve the satellite SSH and foundation SST error misfits with respect to the control run of the system. Improvements were higher for the analysis SSH RMS errors.
- All three OSE experiments were able to reduce the foundation SST error. The highest improvement (9%) was achieved by the OSE2 experiment.
- All three OSE experiments were able to reduce the RMS error with respect to Argo temperature profiles with OSE2 achieving the best performance

- OSE2 experiment was unable to reduce the Ferrybox SST and SSS misfits' rms error with respect to the control run. On the other hand, the combined assimilation of Ferrybox and glider observations was able to reduce the Ferrybox SST misfits RMS errors even lower than the OSE1 run.

An interesting case of how the additional assimilation of glider profiles and Ferrybox observations done in the OSE experiment was beneficial for the Aegean Sea forecasting system in terms of reducing the system biases can be seen through its effect on the sea surface salinity model bias over the south Aegean (north of Crete and south of 37°N) for the control run and the OSE experiment. During the period April – July 2018 (days 49 – 141 in **Figure 8.21**), the system control run in the south Aegean presented a significant bias with respect to Ferrybox SSS observations. This amounts to 0.238 psu (with the model being fresher than the observations) although between November – December 2017 the average bias was 0.085 psu. This result could be partially verified through the glider surface salinity observations in the south Aegean and the two buoys (E1M3A and Heraklion coastal buoy) SSS time series over the same period. We argue that this significant SSS bias after April 2018 was mainly due to meteorological forcing (decreased evaporation rates) used to drive the hydrodynamic model. In the OSE experiment the SSS bias reduced to -0.009 psu for the first period (Nov – Dec 2017) and to 0.01 psu from April 2018 until the end of the run. It is interesting to mention that the RMS error (corresponding to the OSE run) of Ferrybox SSS misfits over the south Aegean is 0.196 psu which was again lower than the figure corresponding to the control run (0.247 psu).

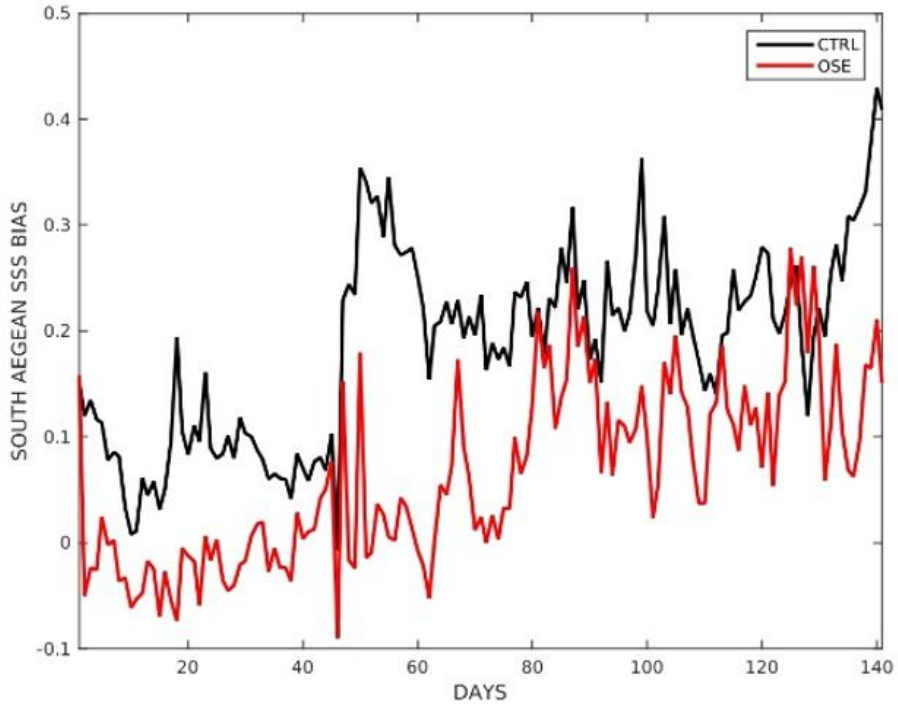

Figure 8.21: *Sea surface salinity bias (obs-model) for the south Aegean Sea corresponding to the control run (black curve) and the OSE experiment. SSS observations are due to the Ferrybox operating during the period 31 Oct 2017 – 17 Jul 2018.*

8.4.8. Observing System Experiments - Ibiza Channel.

A series of Observing Systems Experiments (OSEs) was performed to assess the capability of the WMOP model to forecast surface currents in the Ibiza channel and the impact of the assimilation of HF radar data. Since 2012, SOCIB operates a CODAR HF radar system in the Ibiza channel with two antennas, one in Ibiza Island and the other in Formentera, monitoring the channel and providing total currents with a maximum range of approximately 70 km from the coast. This implies that more than half of the Channel is continuously monitored by the HF radar system. In this context, and according to the project objectives, three one-month period simulations

were generated. Two of them assimilated data from different configurations: (1) GNR: satellite SST-SLA and Argo T-S profiles, and (2) GNR + HF radar data. The last one did not assimilate any data. Results were evaluated making use of an independent set of 14 drifters, which were deployed in the area.

A pair of different WMOP simulations using DA, with and without including HF radar observations, was run for a 1 month period during September and October 2014 and compared against a free-run simulation. Results show the ability of the WMOP DA system to correct currents in the Ibiza Channel when using assimilation. Furthermore, the improvement over the whole domain of the other variable fields (SLA, SST and temperature and salinity profiles, **Figure 8.22**) was not degraded by the assimilation of these high resolution data. Finally, the results in terms of lagrangian trajectories (**Figure 8.23**) showed that, the assimilation of HF radar improved the prediction of lagrangian trajectories based on an independent validation using surface drifters. When assimilating HF radar data, the mean separation distance was reduced by 50 % with respect to the NO ASSIM case and by 29% with respect to the GNR case for the 48-h prediction horizon.

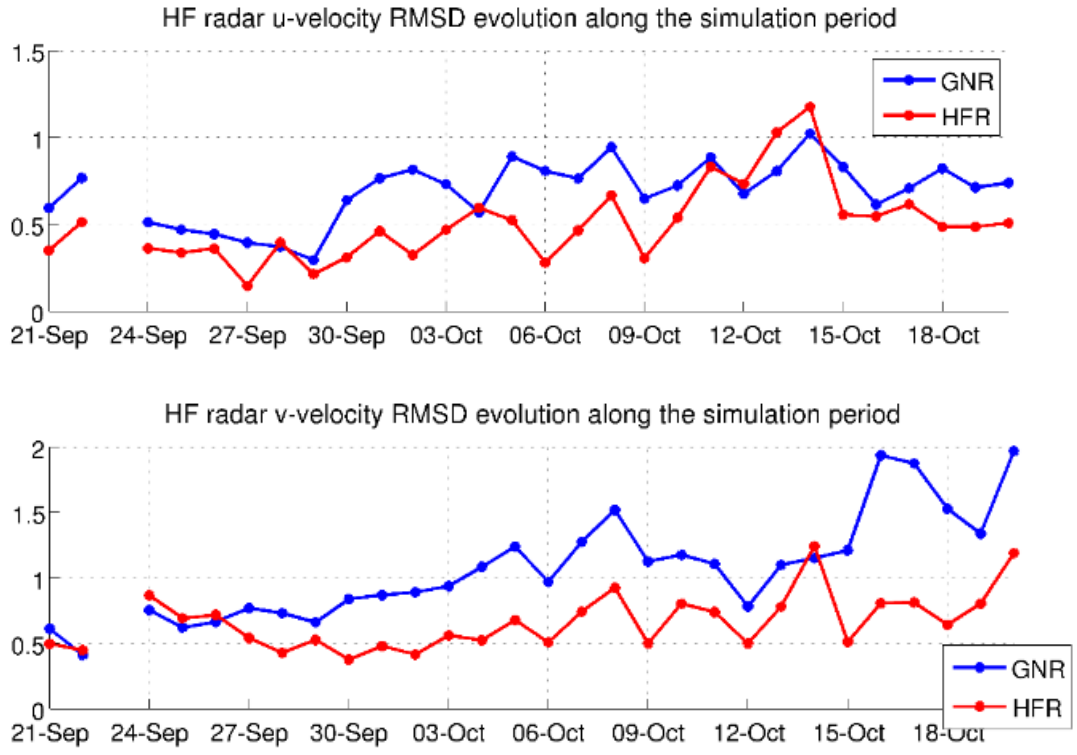

Figure 8.22: *Normalized RMSD evolution along the simulation period. Top pannel shows results against SLA observations. Bottom panel results against SST observations. Labelled days correspond to analysis date.*

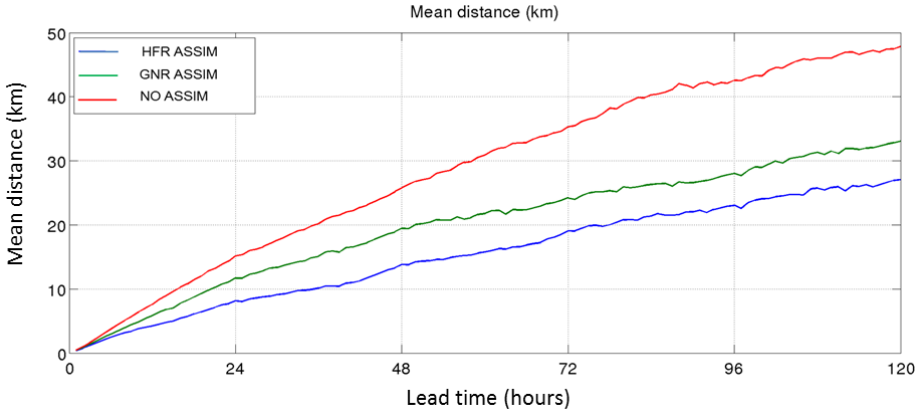

Figure 8.23: *Mean distance evolution between drifter and virtual particles over the 5 days lagrangian simulation period averaged over the 14 drifters for each simulation (NO ASSIM, GNR, HFR) and over the 8 different lagrangian simulations. Y-axis express mean distance in km, while X-axis express lead time in hours. Dashed vertical lines indicate analysis dates.*

8.4.9. Observing System Experiments - Adriatic Sea.

This section presents OSE results in the Adriatic Sea, using the Adriatic-Ionian Regional Model at a 2 km resolution coupled with the Ensemble Square Root filter method for the assimilation of HF radar data together with temperature and salinity profiles. The novel modelling approach was used for assessing observing system experiments in the Gulf of Manfredonia, using HF Radar data, and in the Northern Adriatic Sea by performing a Fishery Observing System experiment. Observation data, as illustrated in **Figure 8.24**, were made available by CNR-ISMAR.

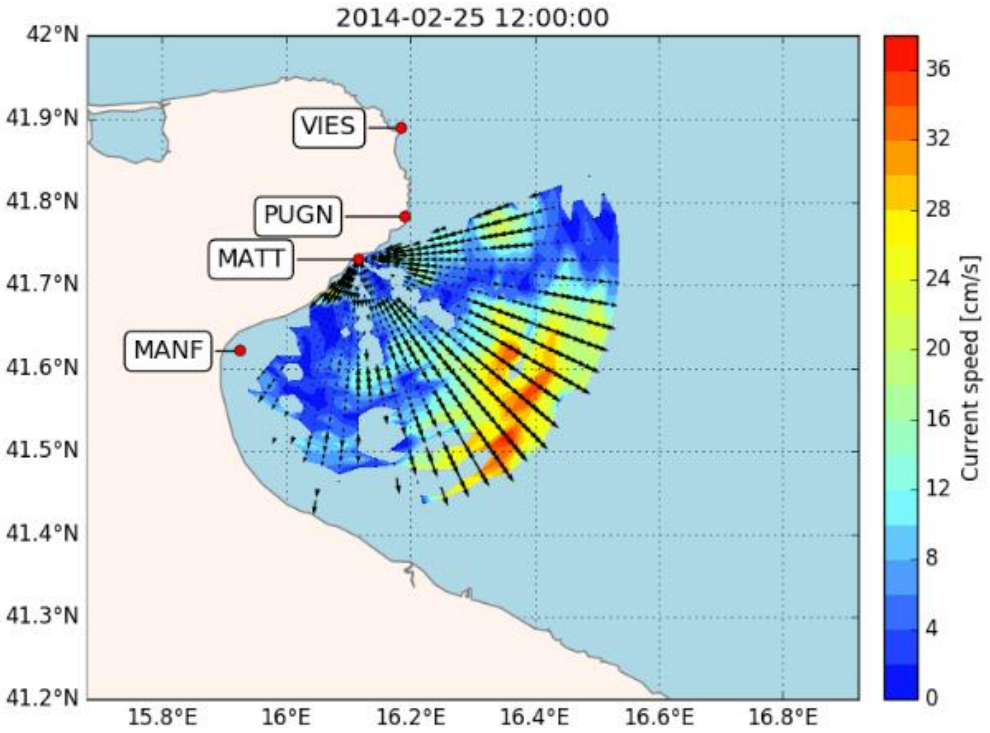

Figure 8.24: *Location of the four HF radar antennas near the Gulf of Manfredonia. The typical range of an antenna is illustrated by superimposing the data measured by the antenna in Mattinata.*

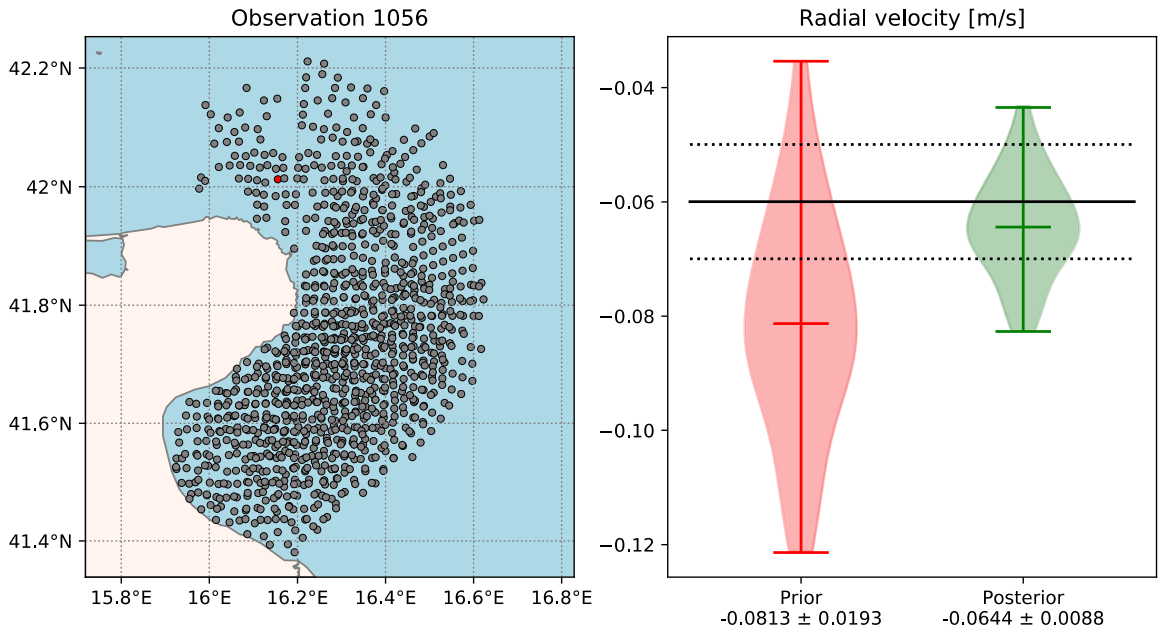

Figure 8.25: *Result of assimilating a typical radial observation into the ensemble. On the left is a map of all observations in the assimilation window, with the current observation indicated in red. On the right is the value of the observation and its uncertainty indicated in black, with the prior ensemble in red and the posterior ensemble shown in green.*

Results (**Figure 8.25**) show the capability of the novel approach, developed by CMCC, in assimilating currents, T and S to perform observing system experiments. Considering OSE in the Gulf of Manfredonia, the AIFS-EnSRF demonstrated that hourly assimilation with √R = 1cm/s shows a clear improvement over time as the assimilation progresses and also an improvement over the daily assimilation. Considering FOOS in the Northern Adriatic Sea, the AIFS-EnSRF demonstrated satisfactory capabilities in assimilating high resolution T/S samplings at the intermediate/deep levels, while the model performances at the surface seemed to be quite variable.

8.4.10. Observing System Experiments – Nazare Canyon.

The high-resolution model was used to evaluate how observation strategies and observation systems can contribute to improve the ability of a numerical model to characterize and forecasts the physical conditions prevailing in such a complex coastal ocean environment. The results presented here only regard the time period corresponding to Case Study 1 (June-July 2007) and are focused on two observation strategies, one corresponding to the collection of profiles of temperature and salinity in the area of influence of Nazare Canyon using a CTD operated onboard a ship and the second one corresponding to the use of fixed platforms for the measurement of relevant parameters at selected geographical positions and selected depths during a long period of time. A third observation strategy, the use of HF radars to provide surface current data in a large domain of the coastal ocean area, is also described.

The use of data assimilation in a high resolution model of the area of influence of Nazare Canyon led to a significant improvement in the ability of the model to reproduce fundamental features of this coastal ocean area marked by a long submarine canyon, as illustrated in **Figure 8.26**. Features like the intense closed circulation that occurs in the inshore segment of the upper section of Nazare Canyon can potentially create retention areas for phytoplankton and can eventually favor the development of HABS. In particular the improvements in the characterization of the intense circulations patterns in this area that was provided by the model with assimilation of a combination of CTD and fixed platform data are keys to understand how the Nazare Canyon affects the marine

ecosystem and economical activities and to guide mitigation measures during an eventual crisis at sea (e.g. oil spill accident) that may affect the coastal populations and the marine protected areas that are present along this coastal ocean.

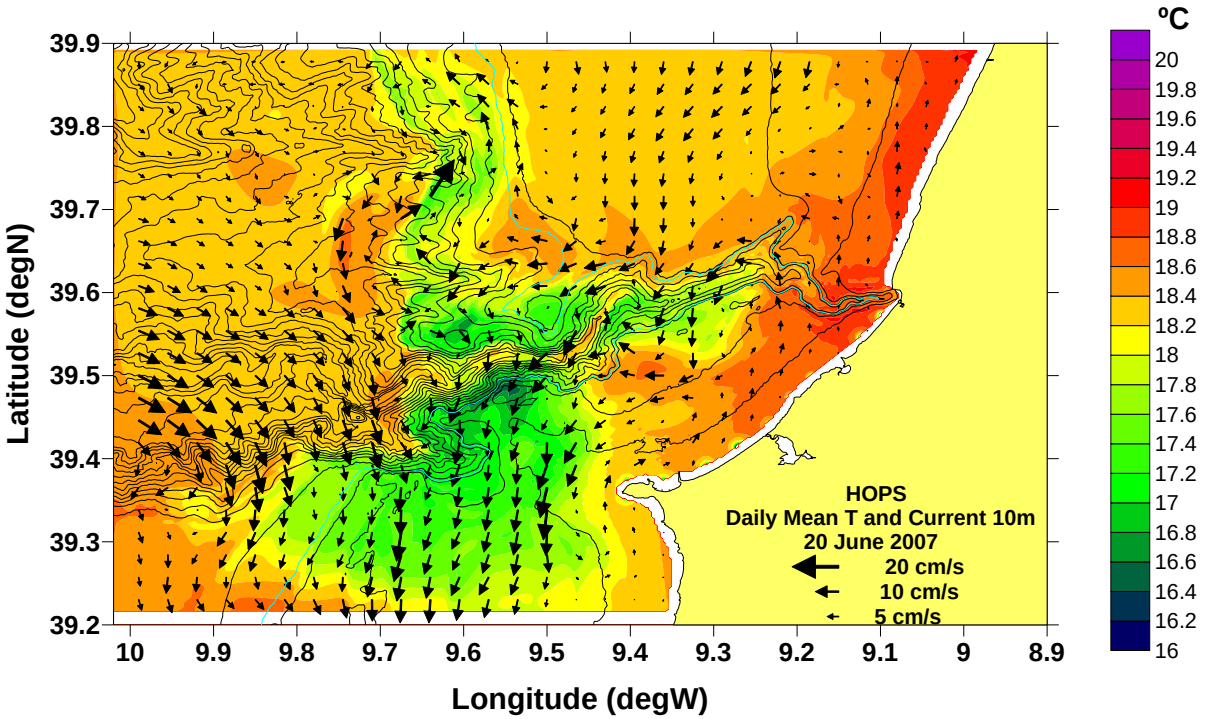

Figure 8.26: *Temperature at 10m: HOPS witouth assimilation (left) and with assimlation of TS profiles and currentmeters (right).*

8.4.11. Observing System Experiments - Skagerrak-Kattegat Straits.

The SMHI setup of the NEMO 3D model covers the Baltic Sea and the North Sea areas. It is running operationally. Two High-Frequency (HF) radars were deployed and operated on the Swedish west coast during autumn 2014 to late December 2015 (leased from CODAR). Due to a necessary change of frequency of the HF radars, the best quality from the system was acquired during the last ten months of operations (March to December 2015). Radial velocities from the two HF radar stations were used to calculate eastward and northward current components, which were subsequently assimilated into the ocean model NEMO-Nordic (Pemberton et al., 2017) which is the operational ocean forecasting model at SMHI. The data assimilation methods tested were 3D EnVar and 4D EnVar (Axell and Liu, 2016). **Figure 8.27** shows the monthly mean current for March 2015 according to (middle left) HF radar data and (right) NEMO-Nordic using 4D EnVar.

The forecast system (model plus data assimilation) was also used in 3D mode (3D EnVar) to assimilate available *in situ* standard stations of salinity and temperature, to validate against the measurements in the coastal water outside Tångesund. The validation shows a good model representation of the highly variable coastal stratification. As future extensions of this work, these model data will be used as outer boundary conditions for a coastal zone model, which will be validated against current and stratification data in Tångesund and in the fjord system inside Tångesund. This model system will be used to extend the current data for the Tångesund region, to connect the occurrence of harmful toxins in the Tångesund mussel farm with advection of water past the farm from the open sea or from the inside the fjord system.

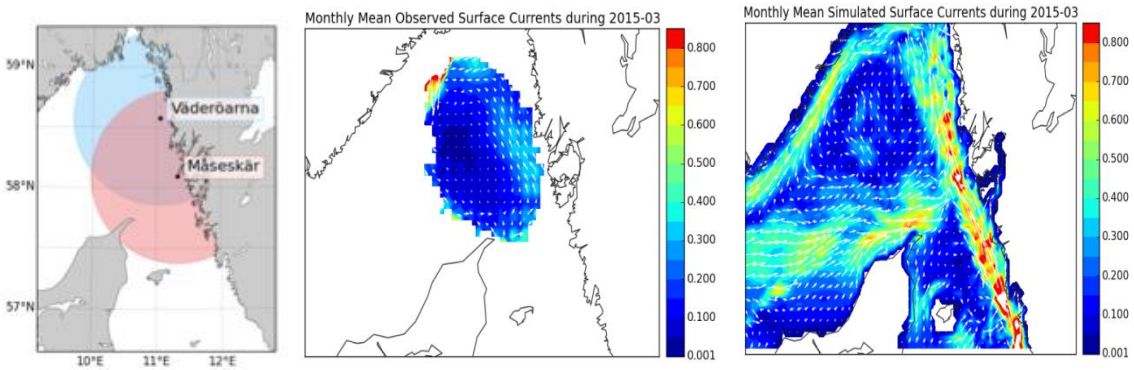

Figure 8.27: *Location of HF radar antennas (left), monthly mean current in the Skagerrak according to HF radar data (middle) and NEMO-Nordic model (right) using 4D EnVar data assimilation.*

8.4.12. Observing System Simulation Experiments – Adriatic Sea.

In order to test future instrument deployments and new observation types, an OSE/OSSE infrastructure was developed based on the AIFS model. Following the recommendations of Halliwell (2014), the AIFS-EnSRF assimilation system was paired with another NEMO-based model at very high resolution. This twin model uses the SURF relocatable model (Trotta, 2016) at 1/64° horizontal resolution to provide synthetic observations for the AIFS-EnSRF system. A scheme illustrating the different components of this system is reported in **Figure 8.28**.

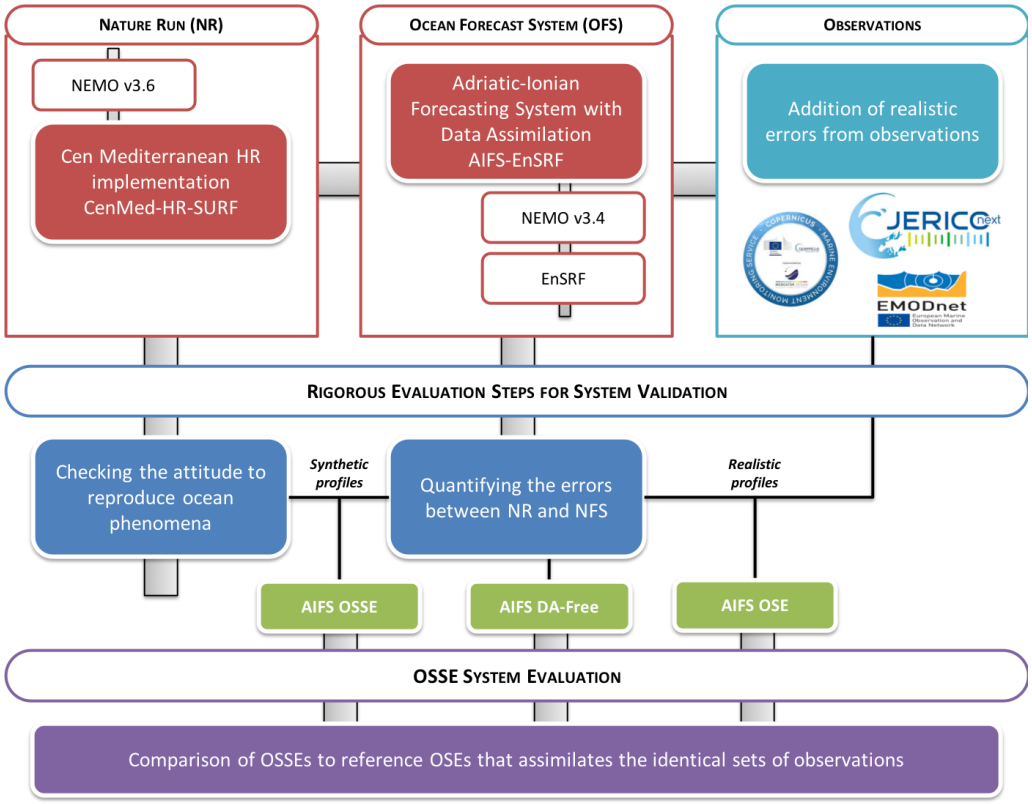

Figure 8.28: *CMCC OSE/OSSE infrastructure for the Central Mediterranean Sea.*

To validate the OSE/OSSE system, an experiment was performed over a 2-month period. During this experiment both an OSE and an OSSE were performed using NR and OFS as described above. For the OSE the observations were regular ARGO profiles of temperature and salinity for all ARGO profilers located in the Adriatic

and Ligurian Seas during this period. The OSSE assimilated the same observations, but used synthetic ARGO profiles. These synthetic ARGO profiles were extracted from the high-resolution nature run, at the same time and location as the regular ARGO profiles. Assimilating real profiles in the OSE and the corresponding synthetic profiles in the OSSE constituted the twin-experiment setup that could be used to evaluate the differences between the OSE and OSSE.

A first visual evaluation was performed by comparing the real and synthetic profiles to the model values. An example of this comparison is shown in **Figure 8.29**. In general the differences appear to be similar between the model and the two types of profiles. The higher-resolution nature model performed better overall in modelling the ARGO profile than AIFS.

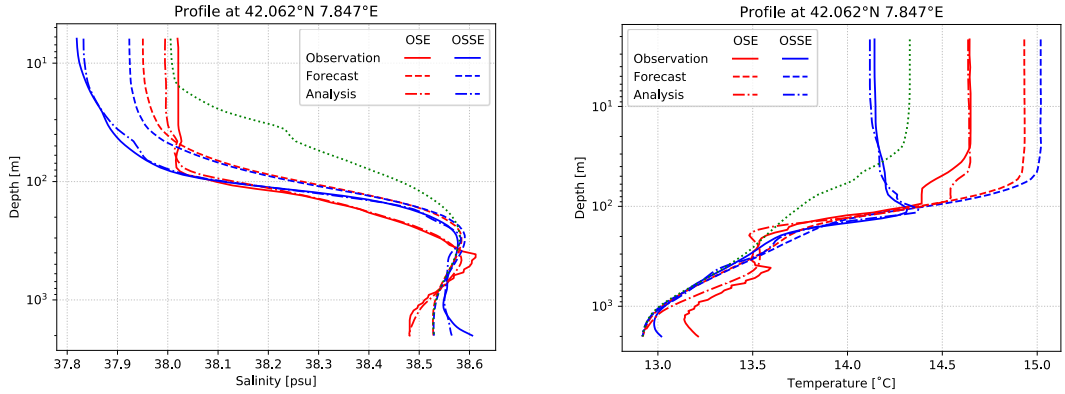

Figure 8.29: *Example of the assimilation of a profile in the OSE (red) and OSSE (blue). The initial state is indicated by the dashed line, after assimilating the observation (solid line) the analysed is the dash-dotted line. The dashed green line shows the free run of AIFS for comparison.*

The CMCC OSE/OSSE infrastructure developed in the frame of JERICO-NEXT project can be used to assess new coastal observing systems with some accuracy. The main innovations that have been introduced from the modelling perspective are:

- The implementation of a novel EnSQR Filter for assimilating temperature and salinity profiles and HF radar velocity. It will be exploited in the future for operational purposes
- The definition of a numerical strategy for deploy high resolution ocean models for nature runs based on relocatable approach
- The verification of the OSE/OSSE modeling infrastructure to be used in the future to design and assess new observing networks in the Central Mediterranean area
- The development of validation tools for assessing the quality of the AIFS-EnSQR model to be used as reference for the future upgrade of the observing systems.

8.4.13. Observing System Simulation Experiments – HF radar OSSEs in the Ibiza Channel.

Observing system simulation experiments (OSSEs) have been performed to evaluate the potential of implementing two new HF radar antennas on the western side of the Ibiza Channel, leading to a full coverage of the Channel (**Figure 8.30**).

Four different simulations were run to explore the capabilities of the new possible radar site. The first objective was to recreate the previous OSE but employing the new analogous observation datasets created from the Nature Run. According to this, three simulations were run for a 30 day period in a simulated operational basis, assimilating different sets of observations every 3-day cycle. Simulations span the period from 20 September to 20 October 2014. All three assimilated the generic observation dataset, based on SLA, SST and temperature and salinity profiles. The one called **GNR** did only assimilate this dataset. The other two simulations also assimilated HF radar observations from the actual coverage area (**HFR actual**) or from the future one (**HFR future**). A control simulation

(**NOASSIM**) was used to compare against and evaluate the effect of DA. The OSSE considering the actual HFR data coverage provided consistent results with respect to the OSE experiment assimilating real data in terms of error statistics, providing a validation of the Ibiza Channel OSE/OSSE infrastructure.

The Taylor diagrams (**Figure 8.31**) show that the employment of DA supposes an improvement in the prediction of surface currents both in terms of correlation and RMSD (centered values are represented in the diagram). Although not decreasing the centered RMSD for the u component, assimilating HF radar observations led to an improvement in terms of correlation. The HF radar future simulation gave the best results among all, outperforming by 10% the results obtained considering only the present observations.

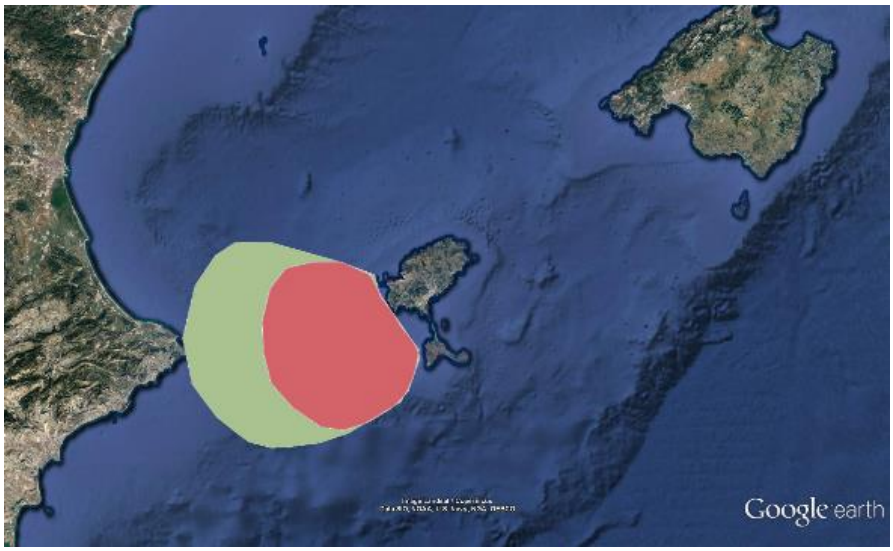

Figure 8.30: *Present (red) and potentially future (green) HF radar coverage areas.*

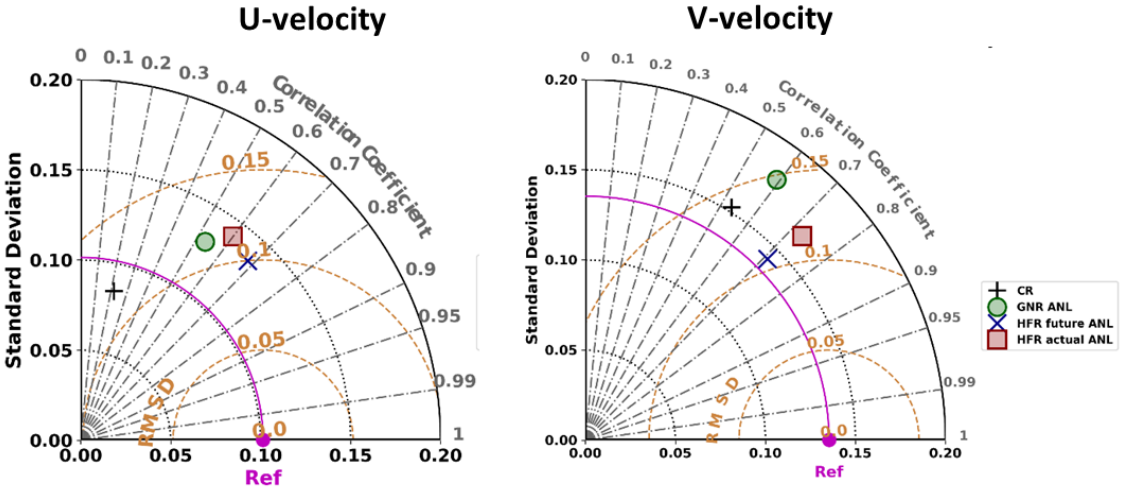

Figure 8.31: *U (left) and V (right) velocity component Taylor diagrams for the four different simulations equivalents against observations within the future radar coverage area for whole the experiment period*

The OSSE presented here to evaluate the capability of a future site for two new antennas covering the full Ibiza Channel has shown that representation of currents would be further improved in the Ibiza Channel area with respect to the present coverage. Further experiments could now allow refining the OSSE setup and better represent observation errors.

8.5. Main inputs relative to initial specific objectives

Through the implementation of coastal model assessment studies and observing system experiments in different areas of European coastal waters, the JRAP 6 has allowed to exploit the potential of JERICO-NEXT observations to better understand the performance of numerical models used for coastal forecasting and evaluate the improvement in the high-resolution simulations achieved when assimilating these data into the models. The JRAP has benefitted from the technical developments carried out in WP3 in terms of HF radar observations, HF radar data assimilation and OSE/OSSE infrastructure. Here is a brief summary of the main inputs relative to the four intitial specific questions:

8.5.1. Q1: How accurate are our ocean models in coastal areas?

HF radar, glider and fixed platforms have been demonstrated to provide high-value observations to characterize the ocean variability over a large range of scales, revealing the signature on ocean transports of mesoscale, wind events, water mass spreading or topographically-driven currents. Specifically, in the Ibiza Channel and Bay of Biscay, models have been found to be able to properly reproduce the spatio-temporal scales of sea surface current variability as observed by HF radars. In the Ibiza Channel, while the mean pattern and main modes of variability are properly captured by the model, it was also found to overestimate the magnitude of the surface velocities and associated kinetic energy. In the Bay of Biscay, the winter eastward flow is properly reproduced in the model. However, the offshore extension of the most intense jets differs between model and HF radar observations, the model currents being more confined to the shelf area. Also, some important eddy events were found to be missed in the model. In the Ibiza Channel, complementary mooring and glider observations revealed the difficulty to represent the variability of the surface salinity, but still the capability of the model to represent the variability of meridional flows across the channel, including in particular the presence of intermediate water masses formed to the north in the Gulf of Lion. The Aegean Sea case study revealed a large SST bias in the area of Dardanelles Strait, probably linked to inaccurate open boundary conditions applied to the coastal model. In the area of the Nazare Canyon, the model is found to satisfactorily depict the onshore penetration of warm oceanic water in response to downwelling, which is channeled in the canyon consistently with observations from SST and CTDs, as well as details of temperature increases close to the head of the canyon. Finally in the Norwegian Sea fixed moorings reveal that the model is affected by a cold bias, attributed to too cold conditions in relatively cold waters with high salinities, as well as a positive salinity bias depicting the difficulty to reproduce low salinities in this region.

8.5.2. Q2: How could we improve these models?

The sensitivity of model results to the horizontal resolution, model parameters, surface forcing or to the treatment of open boundary conditions was evaluated following this initial model assessment, providing solutions to improve model simulations. In the Aegean Sea, the SST error was reduced by 0.4 deg after improvement of the open boundary conditions at the strait of Dardanelles. At the same time, the addition of a realistic wave energy flux to the ocean was found to bring only a very slight improvement to the simulations. Sensitivity tests focusing on the atmospheric forcing have shown that a small improvement of the order of 0.08 deg in terms of SST error could be achieved by considering higher resolution WRF model inputs. In the Ibiza Channel, the inclusion of an explicit momentum diffusion in the model was found to reduce the level of kinetic energy to values that are in better agreement with HF radar estimates. In the area of the Nazare Canyon, the high resolution of the coastal model was found to be essential to reproduce the details of the circulation associated with the canyon and in particular the interaction with the Mediterranean water at intermediate levels.

8.5.3. Q3: What is the impact of coastal observations on the model performance after data assimilation?

In a third step, Observing System Experiments (OSEs) have allowed us to evaluate the impact of glider, FerryBox, fixed moorings and HF radar observations when assimilated in our coastal models. In particular, results have shown the ability of the modelling systems to correct surface currents through the assimilation of HF radar data, leading to an improvement of the prediction of model Lagrangian trajectories based on an independent validation using surface drifters. In the Ibiza Channel, the mean separation distance for the 48-h prediction horizon was found to be reduced by 50% when assimilating HF radar data with respect to the case without assimilation,

and by 29% with respect to the case of assimilation of satellite and Argo observations only. In the Aegean Sea, the assimilation of glider and FerryBox measurements was demonstrated to lead to a reduction of the satellite SSH, foundation SST and Argo temperature profiles errors in the model. The SSS bias related to the meteorological forcing and affecting the south Aegean Sea was for instance reduced from 0.238 to 0.01 with this combined data assimilation. Importantly, Ferrybox and glider observations were found to be complementary to reduce the Ferrybox SST misfits RMS errors. In the Adriatic Sea, the radial velocity uncertainty was found to be reduced by 50% when assimilating HF radar observations. Finally, the use of data assimilation in a high resolution model of the area of influence of the Nazare Canyon resulted in a significant improvement in the ability of the model to reproduce fundamental features of this coastal ocean area. In particular, the improvements in the characterization of the intense circulations patterns that was provided by the model with assimilation of a combination of data from CTD and fixed platforms were found to be key to understand how the Nazare Canyon affects the marine ecosystem and economical activities and to guide mitigation measures during potential emergencies.

8.5.4. Q4: What would be the impact of potentially future additional observations?

As a last step, Observing System Simulation Experiments (OSSEs) were performed to evaluate the impact of future observing systems. A robust OSE/OSSE infrastructure was developed in the framework of WP3 with calibration and validation in the Adriatic Sea and Northwestern Mediterranean Sea. This infrastructure now allows evaluating the impact of observations from multiple platforms including HF radars and could be used in the future to assess new coastal observing systems. In the Ibiza Channel, OSSEs have been implemented to evaluate the potential of two new antennas leading to a full coverage of the Ibiza Channel. Results indicate that the installation of these two new antennas would lead to an error reduction of about 10% in terms of meridional surface velocities in the model compared to the present situation. Overall, and considering the specificities of coastal situations in European waters, JRAP6 has been able to demonstrate the usefulness of JERICO-NEXT coastal observations in distinct environments, leading to an improvement of the understanding and of the performance of high-resolution numerical models implemented in the coastal European ocean. This constitutes an essential step towards the achievement of better model predictions, which are today required to respond to emergencies and manage the environment and ecosystems in the very dynamic coastal environment.

8.6. Analyzis of the experience gained

8.6.1. Developing innovative technologies for coastal ocean observing and modelling.

The JRAP6 has evaluated a) the contribution of the existing coastal observing systems in terms of assessment of numerical model simulations and predictions; and b) the impacts of these observing systems (both present and future) in terms of model performance after data assimilation. Given the numerical framework of this JRAP, the technological developments were not focused on the observations but on the modelling, model evaluation and data assimilation methodologies. In particular, new data assimilation schemes were developed to assimilate HF radar data in high-resolution coastal models, considering both measured radial and reconstructed total velocities. New CMCC and SOCIB ensemble data assimilations schemes were found to be able to successfully incorporate HF radar surface velocity information into their respective models after a careful tuning of observation errors and assimilation frequency. In the Aegean Sea, the SEEK filter was adapted to assimilate glider data and Ferrybox observations into the model, leading to a significant correction of salinity errors. Important developments were achieved in terms of Observing System Simulation Experiments (OSSEs) infrastructure, with the implementation of calibrated experiments following standards inherited from the meteorological community. In terms of model evaluation, multi-platform measurements were used to assess the performance of wave and ocean circulation models, as well as atmospheric model predictions. The usefulness of HF radar, fixed moorings and glider observations was demonstrated in several areas. Finally, the comparison of wave model outputs to Voluntary Observing Ship phytoplankton and algae observations in the Baltic Sea provided an innovative approach to investigate the impact of surface wave mixing on the observed variations of chlorophyll. Due to the ambitious objectives of JRAP 6 with respect to the allowed resources, these experiments generally provided the initial results that should pave the way for further studies.

8.6.2. *Establishing observing objectives, strategy and implementation at the regional level.*

The numerical experiments carried out in this JRAP were conducted in a range of coastal ocean environments that may be assumed as representative of many areas found along the European margin. The processes present in these environments included wind forced upwelling and downwelling, along-slope current, inter-basin water mass exchanges through a narrow channel, coastal mesoscale activity, flows under the influence of a marked submarine canyon, river plumes or wind-induced circulation and turbulence. The spatial scales of these processes ranged from a few km to 100-200 km. Given the fundamental specificities of these single coastal environments, the multi-regional approach proved satisfactory, allowing providing model assessment and data assimilation performance results in these multiple situations.

8.6.3. *Enhancing integrated coastal ocean monitoring and interfacing with other ocean observing initiatives operating at different spatiotemporal scales*

JRAP 6 was articulated around local observatory initiatives (MONICAN system in the area of influence of the Nazare canyon, SOCIB in the Balearic Sea, POSEIDON in the Aegean Sea, Alg@line in the Baltic Sea, Euskoos in the Bay of Biscay, CNR-ISMAR in Adriatic Sea), complemented by coastal modelling components. These observatories were clearly essential to provide the necessary coastal observing-modelling capacities for this JRAP. Moreover, on the international side, JRAP 6 was linked to the European Copernicus Marine Environment Monitoring Service (CMEMS). The models used in this JRAP were for a large majority downscaled from larger scale CMEMS models, adding value through refined resolution and coastal data assimilation, and so playing the role of "intermediate users" with the potential to link CMEMS with coastal end-users and applications.Finally, some of the results of the JRAP were discussed during yearly GODAE coastal and shelf seas task team meetings (an international forum for the development and improvement of coastal ocean forecasting systems).

8.7. Proposition of a future monitoring strategy for the topic

The studies carried out in this JRAP have led to specific recommendations in each of the study areas. They have for instance pointed out the importance of open boundary conditions, atmospheric forcing, model resolution or model mixing parameters in the modelling setup. They have allowed to quantify the impact of observations (both real and potentially future) on the model performance after data assimilation, which provides a very useful input to help guiding future monitoring strategies and optimize investments. Provided the results obtained within JRAP6, we strongly recommend keeping considering models as essential components of coastal observatories. They offer a unique capacity to integrate multidisciplinary and multivariate observations, which is one of the main challenges to be addressed in the JERICO-RI. This model-data integration provides not only improved descriptions of coastal dynamics, but also a framework to objectively evaluate the impact of observations through the calibrated OSEs/OSSEs infrastructure. While high-resolution modelling setups and data assimilation systems will need to be further consolidated in the future, additional modelling developments addressing the physical-biogeochemical coupling would also be beneficial to better exploit the whole range of multidisciplinary JERICO-RI observations.

8.8. References

Albretsen, j., A.K. Sperrevik, A. Staalstrøm, A.D. Sandvik, F. Vikebø and L. Asplin, 2011, NorKyst-800 Report No. 1, User Manual and Technical Descriptions, Fisken og Havet 2/2011, Havforskningsinstituttet. https://www.imr.no/filarkiv/2011/07/fh_2-2011_til_web.pdf/nb-no

Axell, L.B. and Liu, Y., Application of 3-D ensemble variational data assimilation to a Baltic Sea reanalysis 1989–2013, Tellus 68, doi: 10.3402/tellusa.v68.24220, 2016.

Halliwell Jr, GR, A Srinivasan, V Kourafalou, H Yang, D Willey, M Le Hénaff, and R Atlas. "Rigorous Evaluation of a Fraternal Twin Ocean OSSE System for the Open Gulf of Mexico." Journal of Atmospheric and Oceanic Technology 31, no. 1 (2014): 105–130.

HIRLAM-B: HIRLAM system documentation, http://hirlam.org, 2018.

Juza, M., Mourre, B., Renault, L., Gómara, S., Sebastián, K., Lora, S., Beltran, J.P., Frontera, B., Garau, B., Troupin, C., Torner, M., Heslop, E., Casas, B., Escudier, R., Vizoso, G., Tintoré, J. (2016). SOCIB operational ocean

forecasting system and multi-platform validation in the Western Mediterranean Sea. Journal of Operational Oceanography, 9, s155-s166.
Kanarska, Y. and Maderich, V., 2008. Modelling of seasonal exchange flows through the Dardanelles Strait. Estuar. Coast. Shelf S., 79: 449-458.
Korres G. and A.Lascaratos, 2003. A one-way nested eddy resolving model of the Aegean and Levantine basins: Implementation and climatological runs. Analles Geophysicae, MFSPP – Part I Special Issue, 21, 205-220.
Maderich, V., Ilyin, Y., Lemeshko, E., 2015. Seasonal and interannual variability of the water exchange in the turkish straits system estimated by modelling. Mediterranean Marine Science 16
Myksvoll, M.S., A.D. Sandvik, J. Albretsen, L. Asplin, I.A. Johnsen, Ø. Karlsen, N.M. Kristensen, A. Melsom, J. Skarðhamar, and B. Ådlandsvik, 2018, Evaluation of a national operational salmon lice monitoring system—From physics to fish, PLoS ONE, 13, e0201338
Nittis, K., L. Perivoliotis, G. Korres, C. Tziavos and I. Thanos, 2006. Operational monitoring and forecasting for marine environmental applications in the Aegean Sea. Environmental Modelling and Software, 21, 243-257.
Pemberton, P., Löptien, U., Hordoir, R., Höglund, A., Schimanke, S., Axell, L., and Haapala, J.: Sea-ice evaluation of NEMO-Nordic 1.0: a NEMO–LIM3.6-based ocean–sea-ice model setup for the North Sea and Baltic Sea, Geosci. Model Dev., 10, 3105-3123, https://doi.org/10.5194/gmd-10-3105-2017, 2017.
Sandvik, A.D., P.A. Bjørn, B. Ådlandsvik, L. Asplin, J. Skarðhamar, I.A. Johnsen, M. Myksvoll, and M.D. Skogen, 2016, Toward a model-based prediction system for salmon lice infestation pressure, Aquacult Environ Interact, 8, 527–542.
Shchepetkin, A.F., McWilliams, J.C., 2005. The regional oceanic modeling system (ROMS): A split-explicit, free-surface, topography-following-coordinate oceanic model. Ocean Model. 9 (4), 347-404.
Tuomi, L.: On Modelling Surface Waves and Vertical Mixing in the Baltic Sea, Laura Tuomi, Ph.D. thesis, 2014.
Tuomi, L., Vähä-Piikkiö, O., and Alari, V.: Baltic Sea Wave Analysis and Forecasting Product BALTIC_SEA_ANALYSIS_FORECAST_WAV_003_010, Tech. rep., 2017.
Westerlund, A. and Tuomi, L.: Vertical temperature dynamics in the Northern Baltic Sea based on 3D modelling and data from shallow-water Argo floats, Journal of Marine Systems, https://doi.org/10.1016/j.jmarsys.2016.01.006, 2016.

8.9. Abbreviations

CMEMS: Copernicus Marine Environment Monitoring Service
EnOI: Ensemble Optimal Interpolation
EnKF: Ensemble Kalman Filter
KE: Kinetic Energy
MONICAN: MONItoring Nazare Canyon
NEMO: Nucleus for European Modelling of the Ocean
OSEs: Observing System Experiments
OSSEs: Observing System Simulation Experiments
POM: Princetown Ocean Model
ROMS: Regional Ocean Modelling System
RMSE: Root-Mean-Square-Error
SEEK: Singular Evolutive Extended Kalman filter
SEVIRI: Spinning Enhanced Visible and Infrared Imager
SLA: Sea Level Anomaly
SSH: Sea Surface Height
SST: Sea Surface Temperature
WMOP: Western Mediterranean Operational system

9. Synthesis

Through the gain of experience generated within its six JRAPs, WP4 contributed to the JERICO-RI scientific strategy elaborated within JERICO-NEXT. This overall strategy is detailed in Deliverable **D1.2**. It is based on five main pillars (**Figure 9.1**), namely:

- **Pillar 1:** Developping innovative technologies for Coastal Ocean Observing and modelling
- **Pillar 2:** Enhancing integrated Coastal Ocean Monitoring
- **Pillar 3:** Interfacing with other ocean observing initiatives operating at different spatiotemporal scales
- **Pillar 4:** Fostering societal impact for a larger community of stakeholders
- **Pillar 5:** Establishing observing objectives, strategy and implementation at the regional level

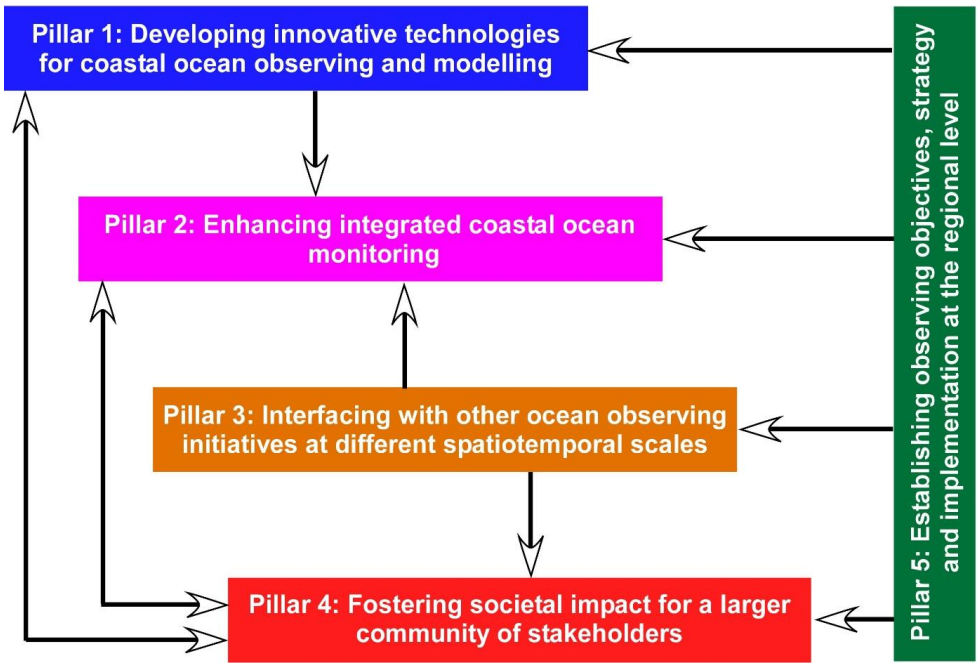

***Figure 9.1**: General structuration of JERICO-RI science strategy showing its five main pillars together with their main interactions.(Taken from JERICO-NEXT **D1.2**).*

The following sections present the main contributions of WP4, as a whole, to each of these pillars.

9.1. Developping innovative technologies for Coastal Ocean Observing and modelling

9.1.1. Technology: a major issue for Costal Ocean Observing

All six JRAPs addressed specific technological issues (for most of them in relation with the developments achieved within JERICO-NEXT WP3), which clearly confirms that the development of innovative technologies constitutes a major key point for the future of Coastal Ocean Observing. Overall, all tested procedures and/or developments achieved within the different JRAPs resulted in significant improvements and therefore proved either operational or promising. However, gaps, were also clearly identified regarding both data acquisition/delivery to databases (JRAP 1) and processing through modelling (JRAPs 3, 4 and 6). In this sense, the results of JERICO-NEXT JRAPs clearly identify the continuation of technological innovation as a major priority for Coastal Ocean Observing.

9.1.2. Discrepancies in Technology Readiness Levels between disciplines

Addressed technological issues clearly differed between JRAPs, which were mostly discipline oriented. JRAPs 1 and 2 were both dedicated to biological (i.e., pelagic and benthic) observations. Their technological components both dealt with the testing of (semi-) automated *in-situ* sensors/equipments for the observation of biodiversity and/or ecosystem functional characteristics. JRAP 5 dealt with the observation of coastal carbon fluxes with a technological component mostly consisting in intercalibrations to overcome the heterogeneity of the equipments operated by the different partners. JRAP 3 was dedicated to the assessment of chemical contaminants. Its technological component first focussed on the test of the suitability of innovative sampling designs (e.g. passive samplers and Ferry Boxes). JRAP 3 also developed a new data handling (modelling) procedure to better address the relationship between potential sources and observed contamination levels. JRAPs 4 and 6 both dealt with physical/operational oceanography with a strong emphasis on the use and development of physical modelling (e.g. through innovative assimilation procedures and Observation System Simulation Experiments). Current technological issues associated with biological observation were therefore mostly related with data acquisition *per se*. Conversely, issues related to physical observations were mostly related to data processing and to the optimization of observing systems both through modelling. The situation of "biogeochemical observations" was somehow intermediate as exemplified by the actions (i.e., regarding sampling and data analysis procedures) achieved within JRAP 3. More generally, these discrepancies are indicative of Technology Readiness Levels between disciplines, which clearly complicates the implementation of multidisciplinary observation platforms (see section **9.1.3**). A way forward clearly consists in carrying out specific developments for better balancing the disciplinary scope of (semi)automated observations.

9.1.3. Data acquisition: the importance of developing multidisciplinary platforms

As stated above, JRAPs were clearly discipline oriented, which is also the case of most current national, regional and European ocean observation monitoring initiatives. This situation results from, but also contributes to, the scarcity of platforms encompassing large sets of sensors allowing for integrative multidisciplinary observations. Moreover, during some JERICO-NEXT JRAPs, there were clear difficulties in the implementation of initially planned multidisciplinary observations as exemplified by JRAP 5 during which biological observations were achieved only at a restricted number of sites. Overall, this underlines the necessity of developing multidisciplinary platforms, which refers both to observation acquisition *per se* and to the processing of the large heterogeneous data sets generated by such platforms.

9.1.4. The major importance of modelling and of developping coupled models

Modelling was a major component of the two JRAPs dedicated to physical oceanography (i.e., JRAP 4 and 6). The work achieved within these two JRAPs clearly supports the major importance of modelling in addressing the spatial heterogeneity and temporal dynamics of physical processes taking place in the Coastal Ocean. Furthermore, JRAP 6 stressed that, although developed for they own purpose, physical models are of use for other communities including biologists and biogeochemists. This was confirmed by the fact that JRAP 2 (i.e., through the planned use of an hydro-sedimentary model) also included a modelling component. JRAP6 initially planned to use coupled physical-biogeochemical models, which could finally not be achieved due to delays in the development of such models. This situation is somehow similar to the one described for observation acquisition in section **9.1.2**. Here again, it could be overcomed by putting a focus on the development of biological/biogeochemical models and on their coupling with physical models. This is certainly not an easy task, which nevertheless could benefit from the production of multidisciplinary data sets resulting from the technological developments proposed in sections **9.1.2** and **9.1.3**. Such data sets would indeed provide ground truth for the modeling of time series combining environmental, physical, biogeochemical and biological data.

9.2. Enhancing integrated coastal ocean monitoring

9.2.1. Harmonization and regional specificities

A major issue regarding Coastal Ocean Observing consists in enhancing the harmonization of observations achieved by different operators at various locations so that they become fully comparable. A way forward consists in defining best practices procedures allowing reaching satisfactory quality standards. Harmonization was a key component of JRAP 5, which focussed on the assessment of carbon cycling at a pan-European scale. Interestingly, this JRAP also showed the practical impossibility to fully homogenize the equipment at all sites. Instead, JRAP 5

stressed the necessity of frequent intercalibration and cross validation. At a more general level, the sampling plan of most, if not all, JRAPs involved the selection of several sites representative of different environmental characteristics and potential scientific and socio-economical issues. Here again this pleaded for the definition of an optimal threshold between homogenization and the consideration of regional specificities while designing a future European Coastal Ocean Observing infrastructure. The experience gained within the different JRAPs also showed that this optimal balance is clearly depending on the nature and more specifically the spatial scale of tackled (environmental) issues. As stated above, it was clearly essential for JRAP 5 but almost not considered, except for data processing, in JRAP 2, which consisted in a juxtaposition of actions aiming at assessing local effects of different anthropogenic disturbances on benthic ecosystems.

9.2.2. Multidisciplinarity

Almost all JRAPs included multidisciplinartity to some extent in their initial planning. This corresponded to interactions between: (1) physics and biology (JRAPs 1, 2 and 4), (2) physics and biogeochemistry (JRAP 6), (3) physics and chemistry (JRAP 3), (4) biogeochemistry and biology (JRAPs 2 and 4). Some of these interactions led to the elaboration of JRAPs' joint actions such as the one achieved in the Southern Bay of Biscay by JRAPs 1, 3 and 4. The implementation of multidisciplinarity within WP4 first consisted in coordinated data acquisition (JRAP 5) but most often also included a modelling component (all other interactions). In spite of significant progress, the implementation of multidisciplinarity within the different JRAPs was overall considered as unsatisfactory due to gaps in biological data acquisition (JRAP 5) or failure in hydrosedimentary model availability (JRAP 2), and to the lack of maturity of current biogeochemical model, which himpered the development of sound physical-biogechemical coupling in the complex systems constitutive of the coastal ocean (JRAP 6). There are clearly several ways to overcome this situation. As far as data acquisition is concerned, Most JRAPs underline the interest in developing new multidisciplinary platforms allowing for high frequency data acquisition (see also section **9.1.3**). JRAPs 3 and 4 also stressed the importance of an *a priori* optimization of monitoring strategies (see also section **9.2.3**). JRAP 4 specifically underlined the interest of Observing System Simulation Experiments in this particular context by organizing a common set of field physical-biological measurements together with JRAP 1. Biological and biogeochemical processes are clearly under the (partial) control of physical ones. They are also taking place over a wide range of spatiotemporal scales, which makes the efficient coupling of physical, biological and biogeochemical far from casual.

9.2.3. Monitoring strategies

JRAP 4 stressed the fact that the implementation of multidisciplinary observations should benefit from an *a priori* optimization of the overall monitoring strategy. This question was tackled by JRAPs 3, 4 and 6 at the JRAP (i.e., disciplinar) level. JRAP 3 for example preconized the use of qualitative models linking sources and contaminant concentrations to optimize future sampling plans in view of assessing the level of contamination of the European Coastal Ocean. JRAP 4 and 6 recommanded the use of OSSEs to optimize the implementation of future coastal observatories. As stated above, JRAPs were mostly discipline oriented and some of them (e.g. JRAP 4) clearly stated that this need for *a priori* optimization would be even reinforced in the case of multidisciplinary observatories because of the heterogeneity in the spatiotemporal scales and dynamics associated with physical, biogeochemical and biological processes. Here again the development of coupled models (see also section **9.2.2**) certainly constitutes a key point for the optimization of the sampling design of a future Coastal Ocean Observing infrastructure. JRAP 3 also clearly put forward the fact that a future Coastal Ocean Observing infrastructure should also be designed to handle uncertainty (i.e., the possibility to detect non a *priori* planned contaminants). This necessity is likely more evident for biology and biogeochemistry since all key controlling processes are not necessarily fully unravelled or even yet *a priori* identified. This was also apparent in the inputs from JRAP 2. One of its four actions was indeed designed to assess the effect of river inputs on the structuration and functioning of a prodeltaic benthic system; whereas it turned out that the main controlling factor was in fact ocean hydrodynamics. Overall, it appears that a threshold should be reached between an *a priori* optimization (which is necessary based on current knowledge) and a certain degree of ability to detect the impact of non-foreseen changes/processes when designing future monitoring strategies.

9.3. Interfacing with other ocean observing initiatives operating at different spatiotemporal scales

All JRAPs involved tight interactions with other observing initiatives consisting in observing infrastructures and/or research projects. JRAP 2 provided a good example of this duality through its cooperation with the MAGEST network for data acquisition on the Gironde River, and the French national research program AMORAD for the implementation of an hydrosedimentary model. The interactions with other observing infrastructures developed by each JRAP proved satisfactory. However, it should be stressed that those interactions were facilitated by the (small) spatiotemporal scales addressed by most JRAPs and it is anticipated that interactions at larger scales (see section **9.5**) will imply a coordination of the monitoring strategies of the entities involved. The interactions with research projects sometimes proved odd. This was the case for JRAP 2 since the hydrodynamical model was not delivered by AMORAD within the timeframe of JERICO-NEXT, which underlines the interest of setting up this kind of interactions over the long-term as well.

9.4. Fostering societal impact for a larger community of stakeholders

The nature of addressed topics clearly varied both within and between JRAPs. This heterogeneity refers both to the nature (i.e., fundamental vs applied) and the spatial scale (i.e., from the local to the pan-european level). JRAP 5 was dealing with the assessment of coastal carbon fluxes; a fundamental question, which was tackled at the pan-european level through a network of monitoring stations. Conversely, JRAP 2 provided a good example of the diversity of the issues tackled within a single JRAP with the coexistence of fundamental academic questions (e.g., the functional consequences of changes in biodiversity) and applied ones (e.g., the assessment of the effect of clam dredging on the benthic diversity hosted by maerl beds in the Bay of Brest). This duality was also appearent in JRAP 4, which made use of academic physical models to tackle the question of sardine, recruitment in the Gulf of Manfredonia. Overall, the diversity of topics/issues addressed within WP4 is indicative of the (much larger) diversity of potential stakeholders of Coastal Ocean Observing. Such diversity should clearly be taken in consideration while designing a future pan-European Coastal Ocean Observing infrastructure. JRAP 4 also exemplified the fact that the use of physical models to tackle (larger) environmental issues question would greatly benefit from the inclusion of current knowledge. This certainly includes fundamental scientific knowledge (e.g. the swimming capacity/behaviour of young sardines as for one of the actions achieved by JRAP 4). It also suggests that stakeholders should be deeper involved in the definition of the products derived from Coastal Ocean Observing so that they become better suited in tackling their concerns.

9.5. Regional Establishing observing objectives, strategy and implementation at the regional level

Except for JRAP 5, and due to the nature of the questions they addressed, all JRAPs were implemented at a sub regional spatial scale. Furthermore, the design of all JRAPs, including JRAP 5, mostly consisted in complementary actions achieved at different sites representative of a large set of environmental conditions and issues. Overall, this structuration was found satisfactory within the context of JERICO-NEXT. It, however, also showed clear limitation relative to the implementation of the first four pillars of the JERICO-RI strategies (JERICO-NEXT **D1.2**, see also sections **9.1**–**9.4**). JRAP 4 for example explicitely stated that the systems and tools developed within JERICO-NEXT could become part of (a) regional systems and most JRAPs therefore recommended the design and implementation of a future Coastal Ocean Observing insfrastructure as a network of regional observatories. This constitutes the pillar 5 of the JERICO-RI science strategy. This pillar is transversal and clearly essential to the implementation of the other four pillars constitutive of this strategy (**Figure 9.1**). The following section is briefly listing the main advantages of such a structuration relative to some of the JRAPs inputs to the first four pillars of the JERICO-RI science strategy.

All JRAPs stressed the major importance of technological innovation and several of them pinpointed the interest in achieving cross-validation experiments (i.e., simultaneous field measurements carried out with different pieces of equipment, including reference approaches) in view of homogenizing data acquisition and testing equipment complementarity. This will clearly benefit from the implementation of Augmented Regional Coastal Observatories consisting of spatially dense networks of multidisciplinary observing platforms. More generally, the experience gained from the different JRAPs resulted in the identification of three main components that could contribute to the better integration of Coastal Ocean Observing, namely: (1) the enhancement of observation homogenization, (2)

the development of multidisciplinary observations, and (3) the optimization of monitoring strategies. The implementation of Augmented Regional Coastal Observatories will clearly contribute to these objectives by: (1) identifting privilegied areas for intercalibration experiments as well as for the development and test of innovative multidisciplinary platforms and best practices, and (2) enhancing the definition of optimized monitoring strategies in relation with the main environmental specificities of regional systems including the interactions between their different components. All JRAPs stressed the necessity of developing interactions with other observing initiatives, while defining monitoring strategies. They also underlined the diversity of such initiatives especially relative to the spatiotemporal scales at which they are operating. Augmented Regional Coastal Observatories will also operate over a large range of nested spatiotemporal scales, which will clearly enhance interactions. This will also facilitate the identification of and the interactions with a larger set of stakeholders since their concerns are alsoassociated with a large set of spatiotemporal scales.